From leaf to crop:

quantifying photosynthesis responses of two flower crops

Ningyi Zhang

Propositions

1. Under canopy shade, the adaptive significance of plant responses to low light depends on responses to light quality.
   (this thesis)

2. Far-red light reflected upwards by lower parts of the plant increases canopy performance.
   (this thesis)

3. The chaperone effect in scientific publishing (Sekara et al., 2018, PNAS, 115, 12603-7) makes fame in our science more about who we are than what we do.

4. Artificial intelligence will increase the level of thinking by human beings.

5. Human beings are less plastic than plants in living with their neighbours.

6. The existence of social classes is largely driven by the resource inheritance between generations.

7. The methodology of writing a scientific paper is the same as that of writing a novel, in the sense that a good scientist should always be a good storyteller.

Propositions belonging to the thesis, entitled

From leaf to crop: quantifying photosynthesis responses of two flower crops

Ningyi Zhang

Wageningen, 24 June 2019

From leaf to crop:

quantifying photosynthesis responses of two flower crops

Ningyi Zhang

Thesis committee

Promotors

Prof. Dr Leo F.M. Marcelis

Professor of Horticulture and Product Physiology

Wageningen University & Research

Prof. Dr Niels P.R. Anten

Professor of Crop and Weed Ecology

Wageningen University & Research

Co-promotor

Dr Jochem B. Evers

Associate Professor, Centre for Crop System Analysis

Wageningen University & Research

Other members

Prof. Dr Martin K. van Ittersum, Wageningen University & Research

Prof. Dr Xin-Guang Zhu, Chinese Academy of Sciences

Dr Heidrun Huber, Radboud University Nijmegen

Dr Pieter H.B. de Visser, Wageningen University & Research

This research was conducted under the auspices of the C.T. de Wit Graduate School for Production Ecology and Research Conservation

From leaf to crop:

quantifying photosynthesis responses of two flower crops

Ningyi Zhang

Thesis

submitted in fulfilment of the requirements for the degree of doctor
at Wageningen University
by the authority of the Rector Magnificus,
Prof. Dr A.P.J. Mol,
in the presence of the
Thesis Committee appointed by the Academic Board
to be defended in public
on Monday 24 June 2019
at 1:30 p.m. in the Aula

Ningyi Zhang
From leaf to crop: quantifying photosynthesis responses of two flower crops,
196 pages.

PhD thesis, Wageningen University, Wageningen, the Netherlands (2019)
With references, with summary in English

ISBN 978-94-6343-971-8
DOI https://doi.org/10.18174/476977

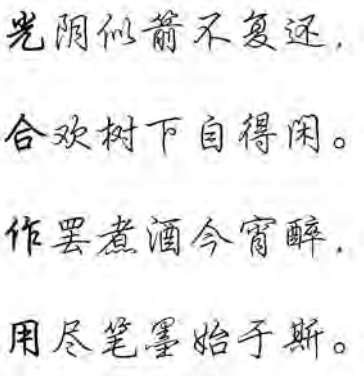

This is a Chinese poem (七言绝句) I wrote to describe my time in Wageningen. 七言绝句 (Qi Yan Jue Ju) is a typical format of traditional Chinese poem. This type of poem always contains four lines, with each line has seven characters. In the present poem, putting the first character (the character in bold) of each line together makes a word 光合作用, which means photosynthesis in Chinese. This word is also a keyword of my thesis. Below is the meaning of each line.

Time flies and never come back.

Although doing a PhD sometimes can be stressful, I had a nice time in this journey.

Today I finish my thesis and let's drink lots of wine.

Finishing my PhD is not an ending but only a starting point of my research career.

Abstract

Variations in environment factors, e.g., light intensity, light spectrum, water and nutrient level, and crop structure manipulations may occur in the greenhouse. Changes in these factors could affect ornamental crop production in the greenhouse through affecting plant photosynthesis at different levels, e.g., leaf, plant and crop level. The aim of this thesis was to quantify photosynthesis responses to (i) combined changes in photosynthetically active radiation (PAR) and red to far-red ratio (R:FR), (ii) water and nitrogen stress combinations and (iii) crop structure manipulations at different levels for two ornamental crops: lily and rose.

Using the photosynthesis model of Farquhar, von Caemmerer and Berry (the FvCB model) and the stomatal conductance model of Ball, Woodrow and Berry (the BWB model), leaf photosynthesis responses to water and nitrogen stress combinations were quantified for lily. The changes of the FvCB model parameters due to variations of water and nitrogen conditions were linearly correlated with the changes of leaf nitrogen per unit leaf area. Most of the BWB model parameters did not depend on the nitrogen level. Using a functional-structural plant model, photosynthesis responses to changes in PAR and R:FR, and the presence of bent shoots were quantified at plant and crop level for rose. At mild shade, plant responses to low R:FR were more important for plant photosynthesis, while with the increase of shade level, plant responses to low PAR became more important. Moreover, the consequences of responses to changes in PAR and R:FR for plant photosynthesis tended to mitigate each other. The presence of bent shoots increased flower shoots dry weight, which was entirely due to the contribution of extra photosynthesis by bent shoots. In addition, bent shoots reflected relatively more far-red than red light, which lowered the R:FR in light reflected upwards that can be received by flower shoots. The low R:FR from below was associated with a steeper leaf angle in flower shoots, which increased canopy photosynthesis by allowing more light to penetrate to the lower plant parts.

Overall this thesis illustrates the importance of considering the interactions of multiple factors when quantifying photosynthesis responses to environmental variations. A functional-structural plant model is a useful tool to upscale photosynthesis responses from leaf to crop level.

Table of contents

Chapter 1

General introduction

The importance of quantifying photosynthesis responses to multiple greenhouse conditions for ornamental crop production

The global population is expected to be 9.5 billion by 2050, which is an increase of 35% compared to today's population (Long *et al.*, 2015). This will lead to an increase in the demand for crop production not only in food crops, but also in ornamental crops. Unlike food crops which are generally harvested for biomass (fresh or dry weight), ornamental crops are generally evaluated based on quality attributes (e.g., morphological quality traits like stem length and flower size, and vase life). This makes that studies on plant biomass production have received much more attention in food crops (e.g., Centritto *et al.*, 2009; Evers *et al.*, 2010; Pallas *et al.*, 2010; Chen *et al.*, 2014) than in ornamental crops (e.g., Gutierrez Colomer *et al.*, 2006; Lin *et al.*, 2011). However, plant biomass is essential for guaranteeing many quality traits of ornamental crops. For example, stem length and diameter are positively affected by assimilate supply in rose (Marcelis-van Acker, 1994), flower number is positively correlated with plant dry weight in chrysanthemum (Carvalho & Heuvelink, 2003), and the tepal carbohydrate content is important for flower longevity in lily (Van der Meulen-Muisers *et al.*, 2001). Therefore, to increase ornamental crop production while keeping product quality, biomass production needs to be optimized.

Plant biomass production is largely driven by photosynthesis, which is strongly affected by environmental factors, e.g., light, temperature, water and nutrient conditions. These environmental variables affect photosynthesis at both leaf, plant and crop (i.e., the population of crop plants) level. For instance, photosynthesis responses to light environment occur at leaf level, being that not only leaf photosynthetic rate is affected by instantaneous light environment, but also photosynthetic capacity of individual leaves could acclimate to a specific light intensity (Oguchi *et al.*, 2003, 2005); responses also occur at plant and crop level, being that the distribution of light energy in the canopy drives the distribution of leaf nitrogen, which further determines the distribution of leaf photosynthetic capacity in the canopy and affects canopy photosynthesis (Hikosaka *et al.*, 2016a). Therefore, to optimize plant biomass production, a crucial step is understanding photosynthesis responses to environmental variables at both leaf, plant and crop level.

As highly economically valuable products, ornamental crops are largely growing in the greenhouse, which is the most controlled and interfered production system used on a large

scale by growers. For instance, the glasshouse area in the Netherlands is ca 9300 hectare (Vermeulen, 2016); in China, the greenhouse area has reached ca 0.3 million hectare in 2016 (National Bureau of Statistics of China, 2017). Since greenhouse environments can be highly controlled, greenhouses provide the opportunities to grow crops at optimal environmental conditions and to achieve high level of photosynthesis. However, in reality, environmental fluctuations and unfavourable growth conditions may occur in the greenhouse, which affect plant photosynthesis.

First, light levels in the greenhouse are typically at lower levels than outside because a significant fraction (ca 25% to 40%) of solar radiation is intercepted by glass and greenhouse construction frames (Hemming *et al.*, 2008; Kempkes *et al.*, 2012). Supplementary lighting is frequently used to improve light conditions in the greenhouse. The assimilation lamps normally provide light that has a different spectral composition comparing with the sunlight spectrum. For instance, high-pressure sodium (HPS) lamps normally provide light with wavelength between 550 and 700 nm, red light emitting diodes (LED) normally provide light with wavelength between 600 and 700 nm, and blue LEDs normally provide light with wavelength between 400 and 500 nm. The use of supplementary lighting, on the one hand, increases the amount of light that can be used for plant photosynthesis; on the other hand, it changes the light spectrum which is different from the sunlight. The change of light spectrum could affect plant architectural development. This is because plants typically exhibit photomorphogenic responses to light quality (van Ieperen, 2012, and see section "Photosynthesis responses to light intensity and spectrum"). These responses can strongly affect plant light interception and photosynthesis. Second, water and nutrient supplies may not always be optimal and stable in the greenhouse. In developing countries, low-tech greenhouses are widely used, in which irrigation and fertilization may not always be kept at optimal levels due to lack of resources or knowledge (Dai *et al.*, 2011; Lin *et al.*, 2011). Thus in low-tech greenhouses, crops are frequently growing with sub-optimal and fluctuating supplies of water and nutrients, which may hamper plant photosynthesis. Third, crop structure manipulations (e.g., pruning and shoot bending) are regularly done in the greenhouse (as well as in many field crops and trees) to optimize e.g. canopy structure and source-sink relations for yield production (Kim & Lieth, 2004; Han *et al.*, 2007; Lopez *et al.*, 2014). The manipulation of plant structure, on the one hand, directly changes canopy structure and affects the associated canopy light interception. On the other hand, structure manipulations entail e.g. losses of

branches and leaves (due to pruning) and local buckling of the stem tissue (due to bending), which may induce plant plastic responses such as activations of dormant buds and acclimations in leaf photosynthetic capacities (Anten *et al.*, 2003). All these effects following crop structure manipulations could in turn affect plant photosynthesis.

To optimize photosynthesis of greenhouse crops, photosynthesis responses to the aforementioned greenhouse conditions need to be quantified. Thus, the overall goal of this thesis is to quantify photosynthesis responses to multiple environmental variables (light, water and nitrogen) and crop structure manipulations at different levels (leaf, plant and crop level) for two flower crops (lily and rose) growing in the greenhouse. In the remaining part of this general introduction, I will give background information of current knowledge of photosynthesis responses to variations in light, water and nitrogen conditions and changes in crop structure.

Photosynthesis responses to light intensity and spectrum

The effects of light on photosynthesis include effects of both light intensity and light spectral composition. Being the source of energy, light intensity on the one hand directly drives the rate of photosynthesis. On the other hand, plant architecture and leaf photosynthetic traits can adapt to different growth irradiances. Plants adapt their canopy structure due to different functioning purpose at high light (avoiding excessive radiation) and low light (maximizing light capture) environments (Pearcy *et al.*, 2005). Plants also adapt their leaf photosynthetic characteristics to light environments. Leaves growing at high light normally have higher photosynthetic capacity than leaves growing at low light (Hirose & Werger, 1987a; Murchie & Horton, 1997; Evans & Poorter, 2001). The acclimation of leaf photosynthetic capacity to growth irradiance relies on the plasticity in leaf thickness and tissue mass density (these two together gives the leaf mass per unit area, LMA), changes in leaf anatomy and changes in leaf chemical compounds. Lower photosynthetic capacity in low-light leaves is associated with a lower LMA of these leaves (Evans & Poorter, 2001). In mature leaves with fixed leaf thickness, photosynthetic capacity can adapt to changes in light intensities by adjusting the size and distribution of chloroplasts in the leaf tissue (Oguchi *et al.*, 2003, 2005) or through changes in leaf nitrogen and the ratio between light harvest pigments and Rubisco (Murchie & Horton, 1997; Meir *et al.*, 2002; Dai *et al.*, 2009). The low photosynthetic capacity in low-light leaves is also associated with reductions in respiration rate of these leaves (Sims & Pearcy, 1991;

Niinemets *et al.*, 1998). This is an important strategy for plants growing under low light, where reducing carbon loss is more beneficial for plants than maximizing carbon gain (Walters & Reich, 2000).

The effects of light spectral composition on photosynthesis occur at multiple levels. At plant level, light spectrum could affect plant architectural development, which further affects plant light absorption. For example, low red to far-red ratio (R:FR) induces longer internodes and steeper leaf inclination angles in some species (Ballaré & Pierik, 2017). As plants preferentially absorb red light (R) and reflect far-red (FR), light reflected from plants has a lower R:FR than natural sunlight. Thus within dense vegetation there is also a gradient in R:FR. Low R:FR is considered to be a cue for neighbour plant presence. The responses to low R:FR are important in light competition as they help plants to position their leaves above those of their neighbours (Dudley & Schmitt, 1996; Pantazopoulou *et al.*, 2017). At least in some plant species, the R:FR gradient in the canopy also appears to drive the distribution of their leaf nitrogen among leaves (Pons *et al.*, 1993; Pons & De Jong-Van Berkel, 2004). This affects the distribution of leaf photosynthetic capacity in the canopy, which further affects canopy photosynthesis. At leaf level, leaf anatomy is affected by the spectral distribution of light which may directly affect leaf photosynthesis. For instance, adding blue to red light increases the thickness of palisade and spongy parenchyma and the number of chloroplasts per palisade mesophyll cell in pepper plants (Schuerger *et al.*, 1997); blue light also induces chloroplast movements in *Arabidopsis* (Jarillo *et al.*, 2001); ultraviolet-B radiation decreases the thickness of both palisade and mesophyll tissue in cotton plants (Kakani *et al.*, 2003). At the chloroplast level, plants acclimate their photosystem composition to their growth light spectrum. Plants growing under enriched far-red light, which is preferentially absorbed by photosystem I (PSI), increase the relative size of photosystem II (PSII) (resulting in an increased PSII/PSI ratio) (Chow *et al.*, 1990). By contrast, plants growing under blue light, which is preferentially absorbed by PSII, decrease their PSII/PSI ratio (Hogewoning *et al.*, 2012). The adjustment of photosystem stoichiometry is important to ensure an efficient flow of electrons from one photosystem to the other, thereby optimizing electron transport and improving photosynthetic efficiency under changes in light spectrum, especially when light is limiting (Walters, 2005).

Specific combinations of light intensity and spectrum usually indicate specific environments in natural ecosystems. For example, as noted low photosynthetically active radiation (PAR)

together with low R:FR normally occurs when plants are shaded by surrounding vegetation. However, the use of artificial lighting in the greenhouse may create new combinations of light intensity and spectrum that do not exist in natural environments. Ancestors of these greenhouse crop plants may have never experienced such light combinations during natural selection. In greenhouse conditions, changes in different light factors (i.e., light intensity and spectrum) occur simultaneously, while different light factors may entail changes in different traits (e.g., plant architectural traits and leaf photosynthetic traits). Therefore, quantifying photosynthesis responses to such conditions requires (i) separately quantifying plant responses to each light factor, (ii) separately quantifying the effects of individual plant traits induced by each light factor on plant photosynthesis, and (iii) quantifying how these individual trait responses interact in determining plant photosynthesis. Knowledge of these three aspects is crucial for understanding crop photosynthesis responses to light conditions in the greenhouse.

Photosynthesis responses to water and nitrogen

Photosynthesis responses to water stress are affected by changes in both diffusional processes and biochemical processes (see reviews in Chaves *et al.*, 2002, 2009; Lawlor & Cornic, 2002; Flexas *et al.*, 2004; Pinheiro & Chaves, 2011). Effects of drought on diffusional processes include decreases in both stomatal conductance (g_s) and mesophyll conductance (g_m). Plants close their stomata (i.e., decrease g_s) in response to both scarce water in the soil and dry air. This may directly decrease the amount of CO_2 that goes into the leaf tissue through stomata (i.e., decreases the intercellular CO_2 concentration C_i). Stomatal closure can be caused by the decrease of leaf turgor, the increase of vapour pressure deficit (VPD) in the air and root signalling (Chaves *et al.*, 2009). For example, drought induces an increased production of abscisic acid (ABA) in roots, which is transported to leaves and causes stomatal closure (Schachtman & Goodger, 2008). After CO_2 travelling from air to the intercellular space in the leaf tissue, intercellular CO_2 needs to diffuse to the chloroplast where the carbon assimilation takes place. This process is limited by the mesophyll resistance (equal to $1/g_m$). g_m may be reduced by drought stress, resulting in that CO_2 concentration in the chloroplast (C_c) decreases to a larger extent than the decrease of C_i (Renou *et al.*, 1990). The decrease of g_m may result from changes in leaf anatomic traits due to leaf shrinkage (Lawlor & Cornic, 2002). g_m responses may also be regulated by biochemical signalling processes as rapid responses of g_m (within few minutes) are found after cutting leaf petiole (Flexas *et al.*, 2006). In addition, CO_2

can laterally travel in the mesophyll tissue (Morison *et al.*, 2007). This could be important for maintaining photosynthesis under drought, as drought could induce patchy stomatal closure and lateral CO_2 diffusion allows CO_2 travelling in the mesophyll between positions under open stomata and closed stomata (Sharkey & Seemann, 1989; Chaves *et al.*, 2009).

The biochemical limitation to photosynthesis under drought is generally estimated to be smaller than the diffusional limitation (Galmés *et al.*, 2007a). Under mild water stress, down-regulation of photosynthesis in response to the decreasing of C_i could be achieved through thermal dissipation to prevent excessive energy impairing photosystem (Demmig-Adams & Adams, 1996; García-Plazaola *et al.*, 2003). Biochemical limitation generally happens at severe drought when maximum g_s is below a certain threshold (Flexas *et al.*, 2004). The impairment of photosynthetic metabolism is mainly caused by a decrease of Rubisco activity (mostly due to reduced Rubisco content and less due to decreased activation state), the impairment of RuBP regeneration capacity, and the breakdown of other metabolic proteins such as chlorophyll (Flexas *et al.*, 2004).

Apart from diffusional and biochemical limitations that affect photosynthesis under drought, the respiratory response to drought is important to determine plant net carbon gain together with photosynthesis. The effects of water stress on leaf respiration rates are inconsistent in different species, ranging from decreasing, maintaining and increasing respiration rate under drought (Galmés *et al.*, 2007b; Gratani *et al.*, 2007; Gimeno *et al.*, 2010). However, changes observed in respiration rates under drought are generally smaller than decreases in photosynthesis, resulting in the net carbon uptake being even more limited under water stress as the proportion of respiration to photosynthesis increases (Pinheiro & Chaves, 2011).

The positive correlation between leaf nitrogen content and photosynthetic capacity is well established in many species (Field & Mooney, 1986; Evans, 1989; Reich *et al.*, 1994, 1995; Hikosaka, 2004). Most nitrogen in the leaf is used to build photosynthesis relevant proteins such as RuBP carboxylase and thylakoid proteins (Evans, 1989; Makino & Osmond, 1991). Changes in leaf nitrogen content, which may be caused by variations in nitrogen supply in the soil or leaf senescence, therefore lead to changes in leaf photosynthesis (Grassi *et al.*, 2002; Kitajima & Hogan, 2003; Dordas & Sioulas, 2008). The effects of nitrogen on photosynthesis, however, can be strongly linked with photosynthesis responses to water stress. On the one hand, nitrogen transformation processes, such as mineralization and nitrification, are closely

dependent on water and its mobility in the soil (Gonzalez-dugo *et al.*, 2010). Less water uptake may also accompany with less mass transport in the soil, resulting in less nitrogen transporting to roots. Thus drought stress could affect nitrogen availability in the soil and affect plant nitrogen uptake (White *et al.*, 2004). On the other hand, responses of CO_2 diffusional processes (i.e., g_s and g_m responses) to water stress can be affected by leaf nitrogen, though the reported combined effects of water and nitrogen on g_s are not consistent. The sensitivity of g_s to water stress is found to increase or decrease with the increase of nitrogen supply (Radin & Ackerson, 1981; Green & Mitchell, 1992; Liu & Dickmann, 1996). In general, g_m is found to positively correlate with leaf nitrogen content (Evans, 1989; Lauteri *et al.*, 1997).

Since irrigation and fertilization are usually applied together in the greenhouse, variations in water and nitrogen levels occur simultaneously during crop growth, especially in low-tech greenhouses in which irrigation and fertilization may not always be optimized. Although the separate effects of water and nitrogen on photosynthesis have been extensively studied (e.g., Tenhunen *et al.*, 1990; Grassi *et al.*, 2002; Cechin & de Fátima Fumis, 2004; Misson *et al.*, 2004; Gu *et al.*, 2012), the combined effects of water and nitrogen on photosynthesis have received less attention (e.g., Shangguan *et al.*, 2000). Quantifying photosynthesis responses to water and nitrogen stress combinations is an important step towards understanding and optimizing crop photosynthesis in low-tech greenhouses.

Photosynthesis responses to changes in plant structure

Plant structure can be physically changed by many external factors during plant growth. In natural environments, plants endure loss of leaf area (i.e., partial defoliation) due to herbivore feeding and physical damage. While losses of leaves and branches reduce leaf area, the reduction in plant growth could be partly alleviated by plant compensatory responses. Defoliated plants often show an increased leaf photosynthesis mainly through increasing their leaf photosynthetic capacity (A_{max}) and improving light penetration in the canopy (Anten & Ackerly, 2001). The increase in A_{max} upon defoliation is associated with several factors including improved leaf nitrogen availability (Lavigne *et al.*, 2001; Ozaki *et al.*, 2004), increased stomatal conductance (Ozaki *et al.*, 2004), increased availability of water, nutrient and hormones (Mc Naughton, 1983), delayed leaf senescence and increased soluble protein concentrations (Nowak & Caldwell, 1984), increased specific activity of Rubisco (Turnbull *et al.*, 2007), and decreased source:sink ratio at whole-plant level (Eyles *et al.*, 2013). Besides,

after certain period following defoliation, the increased A_{max} in defoliated plants decreases to the level similar to that of non-defoliated plants (Turnbull *et al.*, 2007). Furthermore, remaining parts of the defoliated plants could adapt their architecture to optimize light interception. Defoliated plants could alter their pattern of resource allocation to favour leaf area production (Pinkard & Beadle, 1998; Anten *et al.*, 2003; Cooper *et al.*, 2003; Eyles *et al.*, 2009). In addition, other plant architectural traits (e.g., leaf inclination angle) relevant to light interception may also change in defoliated plants, since light environment around the remaining plant parts changes following defoliation.

Branch pruning and shoot bending are two types of structure manipulations often used in crop production to optimize plant architecture and source-sink relations to achieve a better yield and product quality (Medhurst *et al.*, 2003; Kim & Lieth, 2004). In general, plant responses to branch pruning are similar to responses to partial defoliation, except that pruning also results in losses of stems in addition to leaves. This may affect compensatory responses such as leaf area production due to changes in source-sink relations, as stem can be a storage organ for assimilates. Branch pruning also stimulates axillary bud break because of the removal of correlative inhibition and the increase of light intensity at the positions of axillary buds due to branch removal (Wubs *et al.*, 2013). Shoot bending is normally applied in some woody species crops (e.g., rose) and fruit trees (e.g., apple and pear) (Ito *et al.*, 1999; Kim & Lieth, 2004; Han *et al.*, 2007; Liu & Chang, 2011; Lopez *et al.*, 2014). In cut-rose production, weak and non-flowering shoots are bent downwards such that they do not shade the flower shoots while producing assimilates that can be used for flower shoot growth to improve their ornamental quality (e.g., stem length and thickness) (Kool & Lenssen, 1997; Särkkä & Eriksson, 2003; Kim *et al.*, 2004). Bending away some upwardly growing shoots reduces self-shading in the remaining upright shoots, which may increase upright shoot light interception and photosynthesis. On the other hand, bent shoots are located below upright shoots where light intensity is relatively low. Leaves on bent shoots could acclimate to the shade environment, resulting in low photosynthetic capacity of these leaves (González-Real *et al.*, 2007). Bent shoots could also endure local buckling of the stem, which decreases xylem transectional area and hydraulic conductance, and thus reduce leaf photosynthesis (Schubert *et al.*, 1995; Kim *et al.*, 2004).

To analyse photosynthesis responses to crop structure manipulations, we need to (i) quantify the instantaneous effects of changes in plant architecture on plant light absorption and photosynthesis, (ii) quantify the acclimation responses of plant architectural development and leaf photosynthesis following crop structure manipulations, and (iii) quantify the effects of these acclimation responses on plant photosynthesis. Knowledge of the three aspects is important for optimizing photosynthesis responses to crop structure manipulations in greenhouse crop production.

Experimental systems and research approaches used in this thesis

In this thesis, I aim to quantify photosynthesis responses (at leaf, plant and crop level) to multiple greenhouse conditions, including variations in PAR and R:FR levels, water and nitrogen conditions, and crop structure manipulations. To this end, a combination of experimentation and modelling is applied, taking lily and rose crops growing in the greenhouse as examples.

To study photosynthesis responses at leaf level, I choose lily crop (*Lilium auratum* × *speciosum*) that is subjected to water and nitrogen stress combinations as the experimental system. This choice is made because of the following three reasons. (i) Water and nitrogen are two factors that may have strong interactive effects on photosynthesis at leaf level (see section "Photosynthesis responses to water and nitrogen"). (ii) Lily is an important cut-flower crop worldwide. In particular, this crop is widely growing in low-tech greenhouses in China, in which fluctuations in water and nitrogen levels frequently occur (Dai *et al.*, 2011; Lin *et al.*, 2011). As a result, lily plants are frequently subjected to different combinations of water and nitrogen stress. (iii) Lily is a monocotyledonous herbaceous species which has a single-stemmed growth form, resulting in a relatively simple plant architecture. As the focus of photosynthesis responses to water and nitrogen stress combinations in lily crop is at the leaf level, the simple plant architecture of lily is favourable for excluding effects occurring at plant and crop level to some extent. Subsequently, to quantify the leaf-level photosynthesis responses, I use a combination of the biochemical photosynthesis model of Farquhar, von Caemmerer and Berry (the FvCB model) (Farquhar *et al.*, 1980) and the stomatal conductance model of Ball, Woodrow and Berry (the BWB model) (Ball *et al.*, 1987), which is revised by Leuning (1995) and Yin & Struik (2009a). The FvCB model and BWB model respectively describe photosynthetic processes and CO_2 diffusional processes at leaf level.

To study photosynthesis responses at plant and crop level, I choose rose crop (*Rosa hybrida*) that is subjected to combined reductions in PAR and R:FR, and shoot bending as the experimental system. This choice is made because of the following three reasons. (i) PAR and R:FR are two factors that are known to strongly affect leaf photosynthetic and plant architectural traits (see section "Photosynthesis responses to light intensity and spectrum"). Bending part of the shoots in plants not only directly changes the canopy structure, which affects plant light interception and photosynthesis, but also may induce photosynthesis responses at the leaf level (see section "Photosynthesis responses to changes in plant structure"). Therefore, the combined reductions in PAR and R:FR, and shoot bending entail strong photosynthesis responses at both leaf, plant and crop level. (ii) Rose is widely grown in modern greenhouses worldwide, in which artificial lighting is frequently applied. In addition, shoot bending is largely used in cut-rose production to improve flower shoot quality. As a result, rose plants are frequently subjected to simultaneous changes of PAR and R:FR, and shoot bending treatment. (iii) Rose is a dicotyledonous woody species whose structure is mainly determined by the branching pattern and its manipulation. Thus plant architecture of rose crop is relatively variable and is favourable to entail photosynthesis responses at both leaf, plant and crop level. Subsequently, to quantify photosynthesis responses at plant and crop level, a functional-structural plant (FSP) model is used. The FSP model simulates plant light absorption and photosynthesis of individual organs and considers plant architectural development in three-dimension (3D) (Vos *et al.*, 2010). Thus the FSP model is suitable for upscaling photosynthesis from leaf to plant and crop level without specific assumptions for the canopy constitutes (e.g., homogeneous canopies with a uniform light distribution among individual leaves). By contrast, most canopy photosynthesis models (e.g., multi-layer, big-leaf, or sun-shade models) assume a homogeneous canopy, in which a strong light gradient only occurs at the vertical direction in the canopy (Hikosaka *et al.*, 2016b). This assumption, however, does not hold for heterogeneous canopies in which light gradients could occur at both vertical and horizontal directions, such as the rose canopy in Chapters 4 and 5.

Outline of this thesis

From the background and questions introduced in this general introduction (Chapter 1), four research chapters are defined (Figure 1.1) as outlined below.

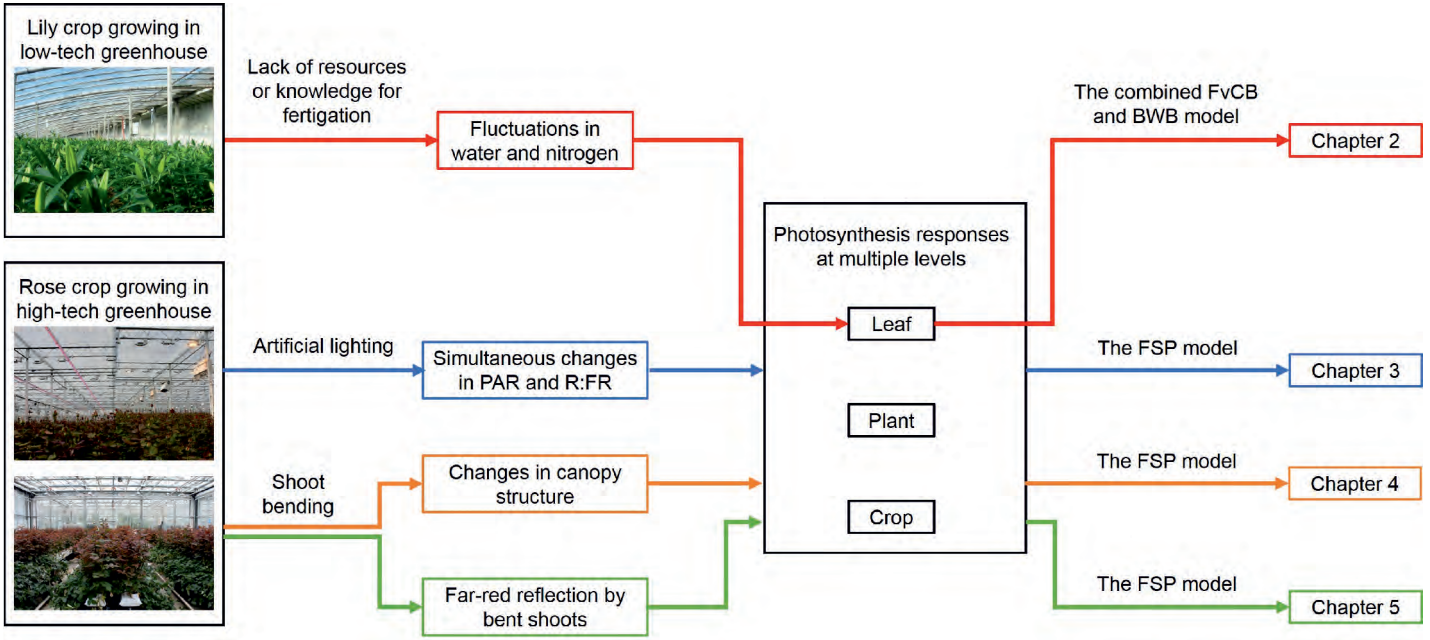

Figure 1.1. Schematic representation of the set-up of this thesis. Photosynthesis at leaf level is quantified in Chapter 2 using a combined leaf photosynthesis and stomatal conductance model. To this end, lily plants were subjected to different combinations of water and nitrogen stress, of which the effects on leaf photosynthesis were measured. Photosynthesis at leaf, plant and crop level is quantified in Chapters 3-5 using a functional-structural plant (FSP) model. To this end, rose plants were subjected to different combinations of photosynthetically active radiation (PAR) and red to far-red ratio (R:FR) level, and shoot bending treatments, of which their effects on leaf photosynthetic and plant architectural traits were measured.

In Chapter 2, I quantify leaf photosynthesis responses to water and nitrogen stress combinations (Figure 1.1). First, I conduct an experiment in which lily plants are subjected to different water and nitrogen treatments. Then, I parameterize the FvCB model and the BWB model and estimate the mesophyll conductance for each water and nitrogen treatments. Finally, I investigate whether or not changes of these parameters with water and nitrogen stress combinations can be correlated with changes in leaf nitrogen content. The relationships between these parameters and leaf nitrogen content are incorporated into the combined FvCB and BWB model to explore leaf photosynthesis responses to different water and nitrogen stress combinations.

In Chapter 3, I quantify plant photosynthesis responses to combined reductions in PAR and R:FR (Figure 1.1). First, I conduct an experiment in which rose plants are subjected to different combinations of PAR and R:FR levels by applying neutral shading screen and far-red LED on top of the plants. From the experiment, individual plant trait responses (including leaf photosynthetic responses and plant architectural responses) to PAR and R:FR levels are separately quantified. Then, an FSP model of rose is used to quantify the effects of each individual trait responses on plant light absorption and photosynthesis, and to explore the interactions between individual trait responses to PAR and to R:FR levels on plant photosynthesis.

In Chapter 4, I quantify the contribution of bent shoots to plant photosynthesis in a heterogeneous rose canopy (Figure 1.1). In cut-rose production, weak and non-flowering shoots are bent downwards, resulting in the rose plants consisting of vertically growing flower shoots (i.e., upright shoots) and horizontally growing bent shoots. First, I conduct an experiment in which rose plants are subjected to different numbers of bent shoots (0, 1 or 3). From the experiment, the effects of bent shoot presence on upright shoot architectural development and leaf photosynthesis are quantified. Then, an FSP model is used to separately quantify the contribution of upright shoots and bent shoots to photosynthesis of the whole canopy.

As leaves mostly absorb red light and reflect a large fraction of far-red light, the presence of bent shoots may also entail a low R:FR signal in light reflected upwards, which may affect upright shoot architecture. In Chapter 5, I tested whether and how reflection of far-red light by bent shoots may induce upright shoot responses and how this in turn indirectly affects plant

photosynthesis (Figure 1.1). First, I conduct an experiment in which rose plants, with or without bent shoots, were grown with neighbour rose plants with or without bent shoots. From the experiment, I quantify the relationships between the presence of bent shoots and the R:FR ratio (in both incident light, side-reflected light and light reflected upwards) distributions in upright shoots, as well as the upright shoot architectural responses. Then, an FSP model is used to evaluate the consequences of responses to R:FR signals in light reflected from below for plant performance in terms of light absorption and photosynthesis.

Results in Chapters 2-5 are further discussed in a broader context in the general discussion (Chapter 6). Specifically, I discuss three main themes, inducing the combination of multiple factors affecting plant performance, the upscaling of photosynthesis from leaf to canopy, and the applications of FSP models, in the broader perspective of crop production. First I discuss the importance of studying plant responses to combinations of multiple environmental factors. Then I discuss the relevance of upscaling from responses of individual functional traits to performance at plant and crop levels. Following this part, I discuss how FSP models can be useful tools to do the upscaling, and discuss the potential strength of combining FSP models with other modelling approaches. Finally, I discuss the implications of the three main themes for crop breeding and cultivation in the greenhouse and field.

Chapter 2

Can the responses of photosynthesis and stomatal conductance to water and nitrogen stress combinations be modelled using a single set of parameters?

Ningyi Zhang[1,2,3,#], Gang Li[1,#], Shanxiang Yu[1,#], Dongsheng An[1], Qian Sun[1], Weihong Luo[1], Xinyou Yin[2]

[1] College of Agriculture, Nanjing Agricultural University, Nanjing, China

[2] Centre for Crop Systems Analysis, Wageningen University & Research, Wageningen, The Netherlands

[3] Horticulture and Product Physiology Group, Wageningen University & Research, Wageningen, The Netherlands

[#] These authors contributed equally to the work

This chapter has been published as Zhang *et al*., 2017, Frontiers in plant science, 8, 328.

Abstract

Accurately predicting photosynthesis in response to water and nitrogen stress is the first step towards predicting crop growth, yield and many quality traits under fluctuating environmental conditions. While mechanistic models are capable of predicting photosynthesis under fluctuating environmental conditions, simplifying the parameterisation procedure is important towards a wide range of model applications. In this study, the biochemical photosynthesis model of Farquhar, von Caemmerer and Berry (the FvCB model) and the stomatal conductance model of Ball, Woodrow and Berry which was revised by Leuning and Yin (the BWB-Leuning-Yin model) were parameterised for *Lilium* (*L. auratum* × *speciosum* 'Sorbonne') grown under different water and nitrogen conditions. Linear relationships were found between biochemical parameters of the FvCB model and leaf nitrogen content per unit leaf area (N_a), and between mesophyll conductance and N_a under different water and nitrogen conditions. By incorporating these N_a-dependent linear relationships, the FvCB model was able to predict the net photosynthetic rate (A_n) in response to all water and nitrogen conditions. In contrast, stomatal conductance (g_s) can be accurately predicted if parameters in the BWB-Leuning-Yin model were adjusted specifically to water conditions; otherwise g_s was underestimated by 9% under well-watered conditions and was overestimated by 13% under water-deficit conditions. However, the 13% overestimation of g_s under water-deficit conditions led to only 9% overestimation of A_n by the coupled FvCB and BWB-Leuning-Yin model whereas the 9% underestimation of g_s under well-watered conditions affected little the prediction of A_n. Our results indicate that to accurately predict A_n and g_s under different water and nitrogen conditions, only a few parameters in the BWB-Leuning-Yin model need to be adjusted according to water conditions whereas all other parameters are either conservative or can be adjusted according to their linear relationships with N_a. Our study exemplifies a simplified procedure of parameterising the coupled FvCB and g_s model that is widely used for various modelling purposes.

Keywords: mesophyll conductance; model; nitrogen; photosynthesis; stomatal conductance; water

Introduction

In the past decades, many crop models have been developed for predicting yield in response to changing environments. Some studies evaluated the performance of different crop models under different growth conditions such as different temperature, water supply and soil fertility (Jamieson *et al.*, 1998; Adam *et al.*, 2011; Palosuo *et al.*, 2011). Surprisingly, when testing these models under a large land scale or long time span, the yield predictions in most models turned out to be an artefact of the balance between incorrect predictions of assimilation and leaf area index (Jamieson *et al.*, 1998) or between biomass production and harvest index (Palosuo *et al.*, 2011). The radiation-use efficiency approach that was taken in many crop models may over-simplify underlying processes and a more detailed approach, based on quantitative functional relationships for underlying processes, is needed in order to capture the effects of high temperature and high radiation intensities on crop growth under changing environments (Adam *et al*., 2011; Challinor *et al*., 2009). While detailed models usually require more effort in terms of model parameterisation, some parameters and functional relationships are found to change very little (i.e. are conservative) among crop types (von Caemmerer *et al*., 2009) and environmental conditions (Yin, 2013). Therefore, it is important to test the conservative level of commonly used functional relationships, so as to balance between the level of detail in these models and the efforts needed for model parameterisation.

Photosynthesis is the primary physiological process that drives crop growth and productivity and influences many plant quality traits, and is strongly affected by environmental factors. Accurately predicting photosynthesis is the first step towards predicting crop growth, yield and quality in response to environmental changes. Water and nitrogen variations frequently occur in crop fields. The effects of water and nitrogen on photosynthesis have been extensively and separately studied (Grassi *et al.*, 2002; Xu & Baldocchi, 2003; Gu *et al.*, 2012). The combined effect of water and nitrogen on photosynthesis, however, has received less attention.

Previous modelling studies have shown that the use of empirical factors to capture the effect of stresses, does not model photosynthesis reliably in many cases (Jamieson *et al.*, 1998). The effects of environmental factors on leaf photosynthesis can be best investigated by use of the biochemical model of Farquhar, von Caemmerer and Berry (the FvCB model hereafter) (Farquhar *et al.*, 1980) combined with diffusion models. The FvCB model has been widely used to describe photosynthesis in response to multiple environmental changes (Harley *et al.*,

1992; Grassi *et al.*, 2002; Xu & Baldocchi, 2003; Monti, 2006; Qian *et al.*, 2012). The model describes photosynthesis as the minimum of the Rubisco-limited rate and the electron transport-limited rate. Major parameters in this model are the maximum Rubisco carboxylation rate (V_{cmax}, definitions of all model variables hereafter are listed in Table 2.1), the maximum electron transport rate (J_{max}) and the mitochondrial day respiration (R_d). These biochemical parameters have been found to be linearly correlated with leaf nitrogen content per unit leaf area (N_a) under environmental changes such as various nitrogen supply (Grassi *et al.*, 2002; Yin *et al.*, 2009) and elevated CO_2 (Harley *et al*., 1992; Yin 2013), as well as seasonal changes (Zhu *et al.*, 2011). However, whether or not the linear relationships between these biochemical parameters and N_a exist under drought is debatable, mainly due to inconsistent effect of drought on N_a (Díaz-Espejo *et al.*, 2006; Damour *et al.*, 2008, 2009).

The FvCB model itself requires the CO_2 concentration in the chloroplast (C_c) as an input variable. To this end, estimating stomatal conductance (g_s) and mesophyll conductance (g_m) is necessary to enable the FvCB model to predict photosynthesis using the atmospheric CO_2 level (C_a) as input. The stomatal conductance model of Ball, Woodrow and Berry (1987) (the BWB-type model hereafter), as one of the most commonly used models of g_s, is often coupled with the FvCB model (Harley *et al.*, 1992; Kosugi *et al.*, 2003). In the BWB-type model, g_s responds to net photosynthetic rate, relative humidity and CO_2 concentration at the leaf surface. Although it is phenomenological, the BWB-type model is widely used to model g_s at leaf level (e.g. Leuning, 1995) and is the most feasible yet biologically robust tool for extrapolating g_s at the field or forest stand level (Misson *et al.*, 2002; Alton *et al.*, 2007). The original BWB-type model does not capture stomatal responses to soil water status, thus some efforts were made towards modifying the BWB-type model to predict g_s under drought. Either the slope used in the BWB-type model (describing the response of g_s to photosynthetic rate, relative humidity or vapour pressure deficit and CO_2 concentration) (Tuzet *et al.*, 2003; Maseyk *et al.*, 2008; Héroult *et al.*, 2013) or the residual stomatal conductance (the value of g_s when irradiance approaches to zero) (Misson *et al.*, 2004) was reported to decrease under drought, and was related to soil moisture or leaf water potential (Baldocchi, 1997; Misson *et al*., 2004; Keenan *et al*., 2010; Egea *et al*., 2011; Li *et al*., 2012; Müller *et al*., 2014; Wang and Leuning, 1998; Zhou *et al*., 2013). In another study, however, neither of these two parameters was affected by drought (Xu & Baldocchi, 2003). So far, there is no consensus as to how to adjust the BWB-type model parameters to properly model g_s under drought. Moreover, there are very

few studies that investigated the responses of these parameters to nitrogen supply and to the combination of water and nitrogen supply.

g_m has been considered as infinite in most early studies, in which intercellular CO_2 concentration (C_i) was used to substitute C_c in the FvCB model (Harley *et al.*, 1992; Kosugi *et al.*, 2003). However, this assumption has later been proved not true since C_c is lower than C_i (Warren, 2004). Ignoring g_m leads to the underestimation of V_{cmax}, especially under stress conditions such as drought (Monti, 2006). g_m has been found to decrease under water-deficit conditions and low nitrogen availability in many previous studies (reviewed in Flexas *et al*., 2008). There have been only a few attempts to incorporate the effect of drought on g_m in the photosynthesis model by using a dependence of g_m on g_s (Cai *et al.*, 2008) based on the observation of a close correlation between g_s and g_m in response to water-deficit conditions (Flexas *et al.*, 2002; Warren, 2008; Perez-Martin *et al.*, 2009) or by including an empirical soil moisture dependent function for g_m (Keenan *et al.*, 2010). Given that so far no consensus exists, more investigations are needed to incorporate the responses of g_m to water and nitrogen variations into the photosynthesis model.

When applying the combined FvCB, g_s and g_m model for predicting photosynthetic responses to fluctuating environmental variables, inevitably many parameters need to be quantified. Information about which parameters are conservative and which are variable depending on the treatment is extremely useful for predicting photosynthesis under diverse environmental conditions. Given the previous experience that the FvCB model parameters, once expressed as a function of N_a, are not altered by environmental variables such as elevated [CO_2] (Yin 2013), we are particularly interested in examining whether the responses of FvCB, g_s and g_m model parameters to water and nitrogen stress can be modelled using a single set of parameters when they are related to leaf nitrogen content. The objectives of this study are (i) to test whether or not water and nitrogen stress combinations change the linear relationships between photosynthetic biochemical parameters and leaf nitrogen content, and (ii) to investigate the responses of stomatal conductance model parameters and mesophyll conductance to different water and nitrogen conditions and to quantify these responses for the purpose of model simplicity. To this end, we used *Lilium* (*L. auratum* × *speciosum* 'Sorbonne') as the test plant, as this plant is commonly grown under low-investment greenhouses where plants are frequently subject to different water and nitrogen regimes.

Table 2.1. List of model variables and their definitions and units.

Variable	Definition	Unit
A_c	Rubisco carboxylation-limited photosynthetic rate	μmol CO_2 m^{-2} s^{-1}
A_j	Electron transport-limited photosynthetic rate	μmol CO_2 m^{-2} s^{-1}
A_n	Net photosynthetic rate	μmol CO_2 m^{-2} s^{-1}
a_1	Ratio of C_i to C_a for vapour saturated air	--
b_1	Decreasing slope of C_i/C_a ratio with the increase of VPD	kPa^{-1}
C_a	Ambient CO_2 level	μbar
C_c	CO_2 level in the chloroplast	μbar
C_i	Intercellular CO_2 level	μbar
C_{i*}	C_i-based CO_2 compensation point in the absence of R_d	μbar
D_{Jmax}	Deactivation energy of J_{max}	J mol^{-1}
D_{gm}	Deactivation energy of g_m	J mol^{-1}
E_{gm}	Activation energy of g_m	J mol^{-1}
E_{Jmax}	Activation energy of J_{max}	J mol^{-1}
E_{KmC}	Activation energy of K_{mC}	J mol^{-1}
E_{KmO}	Activation energy of K_{mO}	J mol^{-1}
E_{Rd}	Activation energy of R_d	J mol^{-1}
E_{Vcmax}	Activation energy of V_{cmax}	J mol^{-1}
f_{cyc}	Fraction of electrons at PSI following the cyclic transport around PSI	--
f_{pseudo}	Fraction of electrons at PSI following the pseudocyclic transport	--
F'_m	Maximum fluorescence	--
F_s	Steady-state fluorescence	--
g_m	Mesophyll conductance	mol m^{-2} s^{-1} bar^{-1}
g_{m25}	Value of g_m when leaf temperature is 25 °C	mol m^{-2} s^{-1} bar^{-1}
g_s	Stomatal conductance for CO_2 diffusion	mol m^{-2} s^{-1}
g_0	Residual stomatal conductance when the irradiance approaches to zero	mol m^{-2} s^{-1}
I_{inc}	Incident irradiance	μmol photon m^{-2} s^{-1}
J	PSII electron transport rate that is used for CO_2 fixation and photorespiration	μmol e^- m^{-2} s^{-1}
J_{max}	Maximum value of J under saturating irradiance	μmol e^- m^{-2} s^{-1}
J_{max25}	Value of J_{max} when leaf temperature is 25 °C	μmol e^- m^{-2} s^{-1}
K_{mC}	Michaelis-Menten coefficients of Rubisco for CO_2	μbar
K_{mC25}	Value of K_{mC} when leaf temperature is 25 °C	μbar
K_{mO}	Michaelis-Menten coefficients of Rubisco for O_2	mbar
K_{mO25}	Value of K_{mO} when leaf temperature is 25 °C	mbar
LMA	Leaf mass per area	g m^{-2}
N_a	Leaf nitrogen content per unit leaf area	g N m^{-2} leaf
N_b	Base leaf nitrogen content at or below which A_n is zero	g N m^{-2} leaf
O	Partial pressures of O_2 in the chloroplast	mbar
R	Universal gas constant (=8.314)	J K^{-1} mol^{-1}
R_d	Mitochondrial day respiration	μmol CO_2 m^{-2} s^{-1}

Variable	Definition	Unit
R_{d25}	Value of R_d when leaf temperature is 25 °C	μmol CO_2 m^{-2} s^{-1}
s	Factor used to calculate electron transport rate from chlorophyll fluorescence	--
S_{Jmax}	Entropy term of J_{max}	J K^{-1} mol^{-1}
S_{gm}	Entropy term of g_m	J K^{-1} mol^{-1}
T	Leaf temperature	°C
V_{cmax}	Maximum Rubisco carboxylation rate	μmol CO_2 m^{-2} s^{-1}
V_{cmax25}	Value of V_{cmax} when leaf temperature is 25 °C	μmol CO_2 m^{-2} s^{-1}
VPD	Vapour pressure deficit	kPa
X_J	Slope of the linear relationship between J_{max25} and N_a	μmol e^- $(g\ N)^{-1}$ s^{-1}
X_V	Slope of the linear relationship between V_{cmax25} and N_a	μmol CO_2 $(g\ N)^{-1}$ s^{-1}
Φ_2	Apparent operating efficiency of PSII photochemistry	mol e^- $(mol\ photon)^{-1}$
Γ^*	CO_2 compensation point in the absence of R_d	μbar
κ_{2LL}	Conversion efficiency of incident light into J at strictly limiting light	mol e^- $(mol\ photon)^{-1}$
θ	Convexity factor for response of J to I_{inc}	--
β	Absorptance of light by leaf photosynthetic pigments	--
ρ_2	Proportion of absorbed light partitioned to PSII	--

PSI: photosystem I; PSII: photosystem II.

Materials and methods

Plant materials and experimental design

Four experiments with the same type of water and nitrogen treatments were conducted in different growth seasons in a plastic greenhouse located at Nanjing, China (32°N, 118°E) during 2009 to 2011 (Table 2.2). The greenhouse, covered by anti-drop polyvinyl chloride film, was composed of two spans and east-west oriented with a length of 28 m, span width of 8 m, gutter height of 3 m and arch height of 5 m. Heating pipes were installed during winter season. During summer season, the greenhouse was cooled through natural ventilation and an inner shading screen installed at the position with a distance of 1.0–1.4 m to the top. Temperature, vapour pressure deficit and photosynthetically active radiation are shown in the supporting information (Figures S2.1, S2.2, S2.3). No CO_2 enrichment was applied, and standard cultivation practices for disease and pest control were used as is common for commercial *Lilium* production in China. *Lilium* bulbs, with a circumference of 14–16 cm, were planted in plastic pots filled with substrates of sand, turf and soil (3:1:1). The physicochemical properties

of the substrate are shown in Table 2.2. The pots, with a depth of 14 cm, upper diameter of 18 cm and bottom diameter of 12 cm, were put on seedling beds ($l \times w \times h$ = 25.0 m × 1.7 m × 1.0 m) and arranged at a density of 36 plants m^{-2}.

Two water levels were used: well-watered conditions, with a soil water potential (SWP) of −4 to −15 kPa according to Li *et al*. (2012), and water-deficit conditions, with a SWP of −20 to −40 kPa. The SWP at 0.1 m below the soil surface was monitored using tensiometers (SWP-100, Institute of Soil Science, Chinese Academy of Sciences) with three replicates per water level. When the SWP reached its designed lower limit value, plants were irrigated until it reached the designed upper limit value. The SWP at 0.1 m below the soil surface and the corresponding gravimetric soil water content were measured to establish calibration curves. These curves were then used to determine the amount of water required for irrigation. The dates of starting water treatment in the four experiments are shown in Table 2.2.

At each water level, there were four levels of nitrogen supply: 25, 45, 65 and 85 mg available nitrogen per kg substrate (hereafter N25, N45, N65 and N85, respectively). Nitrogen was added in the substrate as urea taking into account that urea can be converted into nitrate within one or two days (Harper, 1984). The amount of urea needed was calculated based on the targeted treatment level and the amount of available nitrogen in the substrate (Table 2.2), and urea was directly spread in the substrate, with the dates shown in Table 2.2. According to Sun (2013), 65 mg available nitrogen per kg substrate is the optimal level of nitrogen supply in commercial *Lilium* production for the cultivar used in this study. Treatments, with a plot area of 2.0 ×1.5 m^2 and three replicates per treatment, were arranged in a split-plot design with water level assigned to the main plots and nitrogen level to the sub-plots.

Table 2.2. Detailed information of experimental treatment conditions, physicochemical properties of the growth substrate and measurements.

	Exp. 1[a]	Exp. 2[b]	Exp. 3[b]	Exp. 4[b]
Experimental treatment conditions				
Planting date (dd-mm-yyyy)	27-09-2009	29-11-2009	09-09-2010	05-12-2010
Date of starting water treatment (dd-mm-yyyy)	20-10-2009	25-12-2009	20-10-2010	15-02-2011
Date of starting nitrogen treatment (dd-mm-yyyy)	18-10-2009	12-01-2010	21-10-2010	09-02-2011
Harvesting date (dd-mm-yyyy)	22-01-2010	25-04-2010	02-01-2011	02-05-2011
Physicochemical properties of the growth substrate				
Total N (%)	0.03	0.03	0.02	0.02
Organic C (%)	2.08	2.08	2.24	2.24
Available N (mg kg^{-1})	10.10	10.10	9.67	9.67
Available P (mg kg^{-1})	15.75	15.75	11.42	11.42
Available K (mg kg^{-1})	36.97	36.97	40.38	40.38
Bulk density (g cm^{-3})	1.08	1.08	1.12	1.12
EC (mS cm^{-1})	0.18	0.18	0.20	0.20
pH	6.22	6.22	6.01	6.01

[a] In Exp.1, light response curve, CO_2 response curve and chlorophyll fluorescence were measured, and the combined measurement of photosynthesis and chlorophyll fluorescence under non-photorespiratory conditions was conducted.

[b] In Exps.2-4, light response curve and chlorophyll fluorescence were measured.

Gas exchange and chlorophyll fluorescence measurements

Gas exchange was measured on newly fully expanded leaf (the 4th leaf counting from the top downward) at flower bud visible stage using the LI-6400 Portable Photosynthesis System (Li-Cor BioScience, Lincoln, NE, USA) under 21% O_2. In Exp. 1, both light response curves and C_i response curves were measured in order to identify any differences in photosynthesis parameter estimation by using these two types of curves. For light response curves, incident irradiance (I_{inc}) in the leaf cuvette was decreased in the series of 1500, 1200, 1000, 600, 400, 200, 100, 50, 20 and 0 μmol m^{-2} s^{-1}, while keeping C_a at 370 μmol mol^{-1}. For C_i response curves, C_a was increased stepwise: 50, 100, 150, 200, 250, 380, 650, 1000 and 1500, while keeping I_{inc} at 800 μmol m^{-2} s^{-1}. The microclimate conditions in the leaf chamber were automatically controlled. The CO_2 concentration and water vapour between leaf and the reference chamber were automatically matched before data were recorded. We found that photosynthesis parameters estimated from A_n-I_{inc} curves and A_n-C_i curves were similar (see Results). Therefore, in Exps. 2, 3 and 4, only A_n-I_{inc} curves were measured, as measurement of A_n-C_i curves inevitably involves the problem of CO_2 leakage into and out of the leaf cuvette, which would require additional measurements to correct for.

Chlorophyll fluorescence was simultaneously measured using FMS2 (Hansatech Instruments Ltd, UK) at a similar position on the leaf where gas exchange was measured. The steady-state fluorescence (F_s) was measured under natural radiation level (ranged from 0 to 1200 μmol m^{-2} s^{-1}) and saturating I_{inc} (at 1500 μmol m^{-2} s^{-1}) after 3 to 5 mins light adaptation, followed by applying a light pulse > 7000 μmol m^{-2} s^{-1} for < 1 s to measure maximum fluorescence F'_m. The apparent operating efficiency of photosystem II photochemistry (Φ_2) was calculated as $\Phi_2 = 1 - F_s/F'_m$ (Genty *et al.*, 1989).

Due to inadequate environmental control in the low-investment greenhouse, air temperature and vapour pressure deficit (VPD) hardly stayed constant although they were kept within the range suitable for *Lilium* growth (Figures S2.1 & S2.2). Therefore, all gas exchange and chlorophyll fluorescence measurements in the four experiments were subjected to variations of temperature and VPD.

In order to convert chlorophyll fluorescence data on Φ_2 into electron transport rate, combined measurement of gas exchange and chlorophyll fluorescence was conducted using the LI-

6400XT Portable Photosynthesis System (Li-Cor BioScience, Lincoln, NE, USA) at low oxygen using a gas blend of 2% O_2 and 98% N_2 in the leaf chamber at flower bud visible stage (Exp. 1). A_n–I_{inc} curves were measured while keeping C_a at 1000 μmol mol^{-1}, to create non-photorespiratory conditions. A_n at high C_a levels (i.e. 650, 1000 and 1500 μmol mol^{-1}) at 2% O_2 was also measured while keeping I_{inc} at 800 μmol m^{-2} s^{-1}. Φ_2 was assessed using the same procedure as described above. In order to establish the correlation of estimating R_d using different methods, combined measurement of gas exchange and chlorophyll fluorescence for A_n–I_{inc} curves (under 21% O_2, keeping C_a at 370 μmol mol^{-1}) was also conducted in Exp. 1. All gas exchange data wherever the set-point C_a differed from the ambient CO_2 level were corrected for CO_2 leakage from measurements using thermally killed leaves.

Leaf characteristics

After gas exchange and chlorophyll fluorescence measurements, the leaves were cut, and leaf area was measured before being put in the oven at 105°C for 30 min and subsequently at 80°C until constant weight. Leaf nitrogen concentration (for organic nitrogen) was measured by using the Kjeldahl digestion method (Sun, 2013). Briefly, leaf dry samples were ground, and a 0.5 g of ground sample was digested with 30% hydrogen peroxide and 5 mL of concentrated sulphuric acid at 340 °C. 10 mL of 10 mol L^{-1} sodium hydroxide was then added for distilling the digested solution. The distillate was titrated using 0.02 mol L^{-1} sulfuric acid, and bromocresol green-methyl red was used as the indicator. Leaf nitrogen content per unit leaf area (N_a, g m^{-2}) was calculated based on leaf nitrogen concentration, leaf dry weight and leaf area.

Estimation of photosynthetic model parameters

The FvCB model (Farquhar *et al.*, 1980) predicts net photosynthetic rate (A_n) as the minimum of the Rubisco carboxylation-limited rate (A_c) and the electron transport-limited rate (A_j):

$$A_n = \min(A_c, A_j) \tag{2.1}$$

$$A_c = \frac{(C_c - \Gamma_*)V_{cmax}}{C_c + K_{mC}(1 + O/K_{mO})} - R_d \tag{2.2}$$

$$A_j = \frac{(C_c - \Gamma_*)J}{4C_c + 8\Gamma_*} - R_d \tag{2.3}$$

where C_c and O are the chloroplast partial pressures of CO_2 and O_2, respectively; K_{mC} and K_{mO} are the Michaelis-Menten coefficients of Rubisco for CO_2 and O_2, respectively; R_d is day respiration; Γ^* is the CO_2 compensation point in the absence of R_d and was calculated as $0.5O\frac{K_{mC}}{K_{mO}}[\exp(-3.3801+\frac{5220}{298R(T+273)})]$ (Yin *et al*. 2004), derived from the parameter values of Bernacchi *et al*. (2001); J is the photosystem II electron transport rate that is used for CO_2 fixation and photorespiration.

R_d was firstly estimated as the y-axis intercepts of the linear regression plots of A_n against I_{inc} (the Kok method hereafter) (Sharp *et al.*, 1984). The Kok method tends to underestimate R_d (Sharp *et al.*, 1984; Yin *et al.*, 2011). Therefore, R_d was also estimated from the linear regression of A_n against ($I_{inc}\,\Phi_2/4$) (the Yin method hereafter) (Yin *et al*., 2009; 2011) using data available from the combined measurement of gas exchange and chlorophyll fluorescence, in order to establish the calibration relationship between values of R_d estimated by the two methods. As combined gas exchange and chlorophyll fluorescence data were used only in part of our measurements, all the R_d estimated based on the Kok method was then corrected according to the established calibration relationship to obtain R_d estimates for all treatments.

The calculation of A_c or A_j in the FvCB model requires C_c, which is unknown beforehand. Therefore, A_j relevant parameters were estimated based on Yin *et al*. (2009) using chlorophyll fluorescence data. To convert fluorescence-based data on Φ_2 into electron transport rate J, a calibration needs to be made for each water and nitrogen treatment. This was done by linear regression plot of A_j against ($I_{inc}\,\Phi_2/4$), using data obtained under non-photorespiratory conditions from low light levels of the A_n–I_{inc} curve and three high CO_2 levels. The slope s of this linear regression was used as a calibration factor to calculate values of electron transport rate under all conditions: $J = sI_{inc}\,\Phi_2$ (Yin *et al.*, 2009). The obtained J was then fitted to the following equation to obtain electron transport parameters of the FvCB model:

$$J=\frac{\kappa_{2LL}I_{inc}+J_{max}-\sqrt{(\kappa_{2LL}I_{inc}+J_{max})^2-4\theta J_{max}\,k_{2LL}I_{inc}}}{2\theta} \quad (2.4)$$

where κ_{2LL} is the conversion efficiency of incident light into J at strictly limiting light; J_{max} is the asymptotic maximum value of J when I_{inc} approaches to saturating level; θ is a convexity factor for response of J to I_{inc}, and was assumed to have a constant value of 0.8 (Yin & Struik, 2015). Since chlorophyll fluorescence measurement was conducted under fluctuating

temperature, the value of J_{max} at 25 °C (J_{max25}) and κ_{2LL} were calculated by combining Eq. 2.4 with Eq. 2.7 (see later) that describes the temperature response of J_{max}.

With J_{max25} and κ_{2LL} calculated as described above, J_{max} for each A_n–I_{inc} curve from gas exchange measurement was derived according to the temperature level during each measurement using Eq. 2.7 (see later). J at each light level in the A_n–I_{inc} curve was then derived using Eq. 2.4 based on J_{max} and κ_{2LL} calculated before.

With J and R_d calculated, g_m was then estimated assuming that g_m was constant across the entire light response curve. Whether or not g_m is constant across light or CO_2 levels remains debatable, but this assumption allows the identification of any differences among water and nitrogen treatments in the actual average g_m. For that purpose, a relatively less measurement error-sensitive method, the NRH-A method (Yin and Struik, 2009a), was used to estimate the value of g_m as constant, by fitting the following non-rectangular hyperbolic (NRH) equation for the A_j part of the C_i-based FvCB model:

$$A = 0.5\left\{x_1 - R_d + g_m(C_i + x_2) - \sqrt{\begin{matrix}[x_1 - R_d + g_m(C_i + x_2)]^2 - \\ 4g_m[(C_i - \Gamma_*)x_1 - R_d(C_i + x_2)]\end{matrix}}\right\} \quad (2.5)$$

where $x_1 = J/4$ and $x_2 = 2\Gamma_*$; C_i is the intercellular CO_2 level. According to our experimental data, A_j-limitation in a light response curve of *Lilium* usually occurred at or below 1000 μmol m^{-2} s^{-1}, as a good linear relationship between A_n and J was observed within this range (Figure S2.4). The advantages of the NRH-A method over other existing methods including the most widely used variable-J method in deriving the average g_m was fully illustrated by Yin and Struik (2009a).

Eq. 2.5 can also be applied to calculate A_c by setting: $x_1 = V_{cmax}$ and $x_2 = K_{mC}(1 + O/K_{mO})$. V_{cmax} was then estimated by fitting the combined Eqs. 2.1, 2.4 and 2.5 to the entire light response curve or C_i response curve using the already estimated values of J_{max}, κ_{2LL}, R_d and g_m as input.

Temperature responses of photosynthesis parameters

To account for the effect of the varying temperature during measurement, temperature response functions were introduced so that the estimation of key parameters could be adjusted to the same reference temperature for the comparison among treatments. The temperature responses of R_d and Rubisco kinetic properties (V_{cmax}, K_{mC} and K_{mO}) were described by an Arrhenius function Eq. 2.6, and the temperature responses of J_{max} and g_m were described by a peaked Arrhenius function Eq. 2.7, normalized with respect to their values at 25 °C:

$$X = X_{25} e^{(T-25)E_X/[298R(T+273)]} \tag{2.6}$$

$$X = X_{25} e^{(T-25)E_X/[298R(T+273)]} \left[\frac{1+e^{(298S_X-D_X)/298R}}{1+e^{[(T+273)S_X-D_X]/[R(T+273)]}}\right] \tag{2.7}$$

where X stands for each parameter; X_{25} is the value of each parameter at 25 °C (R_{d25}, V_{cmax25}, K_{mC25}, K_{mO25}, J_{max25} and g_{m25}); E_x is the activation energy of each parameter (E_{Rd}, E_{Vcmax}, E_{KmC}, E_{KmO}, E_{Jmax} and E_{gm}); S_x and D_x are the entropy term and the deactivation energy, respectively (applying to J_{max} and g_m); T is the leaf temperature; R is the universal gas constant. Since Rubisco kinetic properties are generally assumed conserved among C_3 species (von Caemmerer *et al.*, 2009), values of K_{mC25}, K_{mO25}, E_{KmC} and E_{KmO} were fixed at 272.4 μbar, 165.8 mbar, 80990 J mol^{-1} and 23720 J mol^{-1}, respectively, according to Bernacchi *et al*. (2002). To avoid over-parameterisation, E_{Rd} was fixed at 46390 J mol^{-1} (Bernacchi *et al.*, 2001); S_{Jmax} and D_{Jmax} were fixed at 650 J K^{-1} mol^{-1} (Harley *et al.*, 1992) and 200000 J mol^{-1} (Medlyn *et al.*, 2002), respectively; E_{gm}, S_{gm} and D_{gm} were fixed at 49600 J mol^{-1}, 1400 J K^{-1} mol^{-1} and 437400 J mol^{-1}, respectively (Bernacchi *et al.*, 2002).

The relationships between biochemical parameters and leaf nitrogen content

The photosynthetic capacity parameters V_{cmax25} and J_{max25} are linearly related to N_a (Harley *et al.*, 1992; Braune *et al.*, 2009):

$$V_{cmax25} = \chi_V(N_a - N_b) \tag{2.8}$$

$$J_{max25} = \chi_J(N_a - N_b) \tag{2.9}$$

where N_b is the base leaf nitrogen content at or below which A_n is zero, and a value of 0.35 g N (m^2 leaf)$^{-1}$ was used in this study (Archontoulis *et al.*, 2012); X_V is the slope of V_{cmax25} against N_a, and X_J is the slope of J_{max25} against N_a.

Parameterisation of the stomatal conductance model

A phenomenological model for stomatal conductance for CO_2 transfer was first described by Ball *et al*. (1987), revised by Leuning (1995), and further revised by Yin and Struik (2009b). Li *et al*. (2012) called this model the BWB-Leuning-Yin model. In the model, stomatal conductance was described by:

$$g_s = g_0 + \frac{A+R_d}{C_i - C_{i*}} f_{vpd} \tag{2.10}$$

where g_0 is the residual stomatal conductance when the irradiance approaches to zero; C_{i*} is the C_i-based CO_2 compensation point in the absence of R_d and was calculated as ($\Gamma_* - R_d/g_m$) using Γ_*, R_d and g_m calculated before as input; f_{vpd} is a function describing the effect of VPD, which is not yet understood sufficiently and may be described empirically as (Yin and Struik, 2009b):

$$f_{vpd} = \frac{1}{1/(a_1 - b_1 VPD) - 1} \tag{2.11}$$

where a_1 represents the ratio of C_i to C_a for vapour saturated air, and b_1 represents the decreasing slope of this ratio with increasing VPD, if g_0 approaches to zero. Because of this obvious meaning of a_1 and b_1, we chose Eq. 2.11, instead of the equation of Leuning (1995), for our analysis of the effect of VPD on g_s. Combining Eqs. 2.10 and 2.11, g_0, a_1 and b_1 can be estimated by using the data of A_n, C_i and VPD obtained from gas exchange measurement. For that, measured stomatal conductance for water vapour transfer was divided by a factor 1.6 to convert it to g_s for CO_2 transfer that is required for Eq. 2.10.

Statistical and model analyses

Using a non-linear regression with the GAUSS method in PROC NLIN of SAS (SAS Institute Inc., Cary, NC, USA), FvCB model parameters (V_{cmax25}, J_{max25}, κ_{2LL}, R_{d25}, g_{m25}, E_{Vcmax} and E_{Jmax}) and BWB-Leuning-Yin model parameters (g_0, a_1 and b_1) were estimated. Whether or

not the treatment effect on each estimated parameter was significant was tested using an F test. Following that, conserved parameter values across treatment classes were also estimated.

With these estimated parameters available, we aimed to test to what extent conserved parameter values could be used to predict A_n and g_s under water and nitrogen stress combinations, for the purpose of simplifying model parameterisation. For such, a step-wise procedure was followed. First, we analysed whether or not water and nitrogen stress combinations change the linear relationships between biochemical parameters and N_a, and tested to what extent conserved parameter values in the C_i-based FvCB model (Eq. 2.5) could be used to predict A_n under different water and nitrogen conditions. Second, we tested to what extent conserved parameter values could be used in the BWB-Leuning-Yin model to predict g_s under different water and nitrogen conditions. Third, we explored the coupled FvCB and BWB-Leuning-Yin model (for the analytical solution for this coupled model, see Yin and Struik, 2009b), which allows using C_a as input to predict A_n. We used this coupled model to assess to what extent conserved parameter values in both the FvCB model and the BWB-Leuning-Yin model could be used to predict A_n (using C_a as input) across various water and nitrogen treatment regimes.

Results

Model parameterisation

Data of A_n–I_{inc} curves showed that both water-deficit conditions and low nitrogen supply decreased A_n (Figure 2.1). The initial linear part of these curves was explored to estimate R_d. Values of R_d estimated by the Kok method were generally lower than those estimated by the Yin method (Figure 2.2). The linear correlation between values of R_d estimated by the two methods (Figure 2.2) was used to correct all R_d estimated by the Kok method.

The plot of A_j against ($I_{inc}\,\Phi_2/4$) using data obtained under low O_2 condition from low light levels of the A_n–I_{inc} curves and three high CO_2 levels was essentially linear (Figure 2.3). Both water and nitrogen conditions affected the value of the linear slope s, the calibration factor used to convert Φ_2 into J. The factor decreased by low nitrogen supply and by water-deficit conditions.

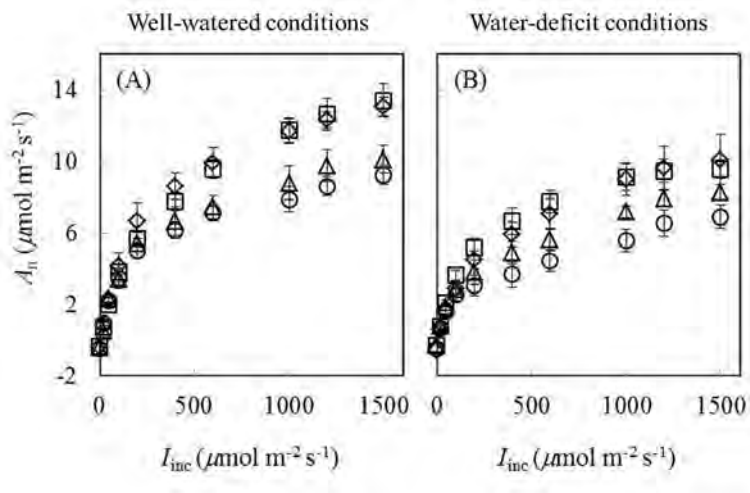

Figure 2.1. Response curves of net CO_2-assimilation rate (A_n) to incident irradiance (I_{inc}). (A) Curves obtained under well-watered conditions. (B) Curves obtained under water-deficit conditions. N85: diamond; N65: square; N45: triangle; N25: circle. Mean ± standard error of 6 replicated plants. Leaf temperature during measurement = 20±2°C.

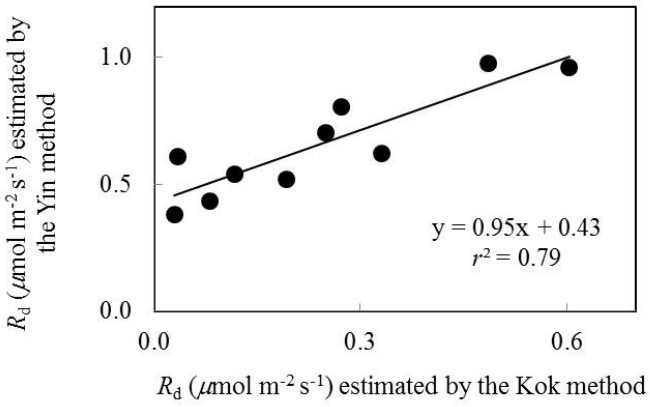

Figure 2.2. The relationship between values of day respiration (R_d) estimated by Kok and Yin methods. Each point represents the estimate of R_d using the same A_n-I_{inc} curve.

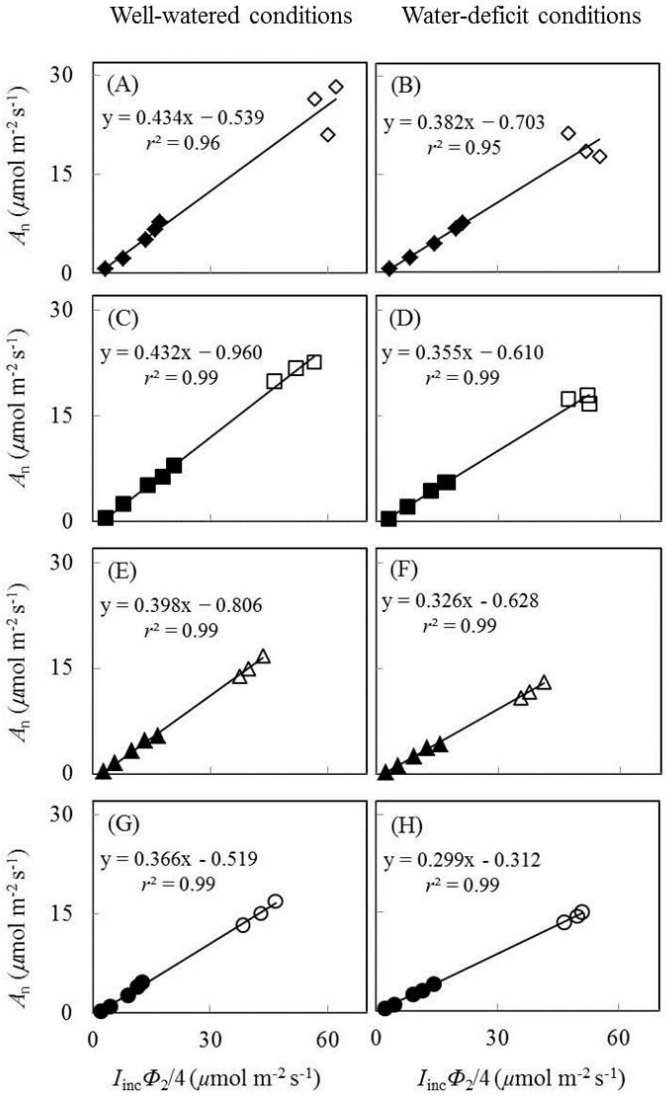

Figure 2.3. Net CO_2-assimialtion rate (A_n), measured under a non-photorespiratory condition, as a function of $I_{inc}\Phi_2/4$. Measurements were conducted under well-watered conditions (A,C,E,G) and water-deficit conditions (B,D,F,H). N85: A,B; N65: C,D; N45: E,F; N25: G,H. Closed symbols are from low light levels of the A_n-I_{inc} curves; open symbols are from three high CO_2 levels at the same I_{inc} of 800 μmol m^{-2} s^{-1}; data for open symbols and closed symbols in the same panel were measured on the same leaf; see the text.

V_{cmax} estimated from A_n-I_{inc} curves and from available A_n-C_i curves under the same measurement conditions were very similar when using the same input values of J_{max}, κ_{2LL}, R_d and g_m (Figure 2.4). This suggested the reliability of using A_n-I_{inc} curves to estimate V_{cmax}. The estimated parameter values of the FvCB model for each treatment are listed in Table 2.3, and those of the BWB-Leuning-Yin model and g_m are listed in Table 2.4. All parameters were reliably estimated, as the standard error values of the estimates were relatively small (Tables 2.3 and 2.4).

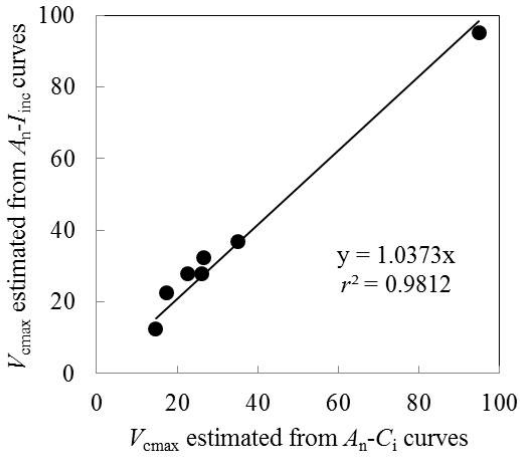

Figure 2.4. Comparison of V_{cmax} estimated from A_n-I_{inc} curves and A_n-C_i curves. Estimations were conducted using the same input values of J_{max}, κ_{2LL}, R_d and g_m. Each point represents value of V_{cmax} estimated from A_n-I_{inc} curve or A_n-C_i curve measured on the same leaf.

Table 2.3. List of parameter values estimated for the FvCB model under different water and nitrogen treatments. Values in brackets are standard errors of estimates. Different letters following the data in the same column indicate significant difference ($P<0.05$).

Treatment	κ_{2LL} (mol mol^{-1})	J_{max25} (μmol m^{-2} s^{-1})	V_{cmax25} (μmol m^{-2} s^{-1})	R_{d25} (μmol m^{-2} s^{-1})
Well-watered conditions				
N85	0.242 (0.017) c	150 (6) a	109 (8) a	0.867 (0.18) a
N65	0.309 (0.020) a	141 (4) b	96 (5) b	0.696 (0.15) abc
N45	0.238 (0.013) cd	130 (5) c	90 (5) b	0.740 (0.12) ab
N25	0.251 (0.026) c	118 (6) d	77 (5) cd	0.492 (0.10) cd
Water-deficit conditions				
N85	0.218 (0.016) d	137 (8) bc	88 (6) bc	0.514 (0.17) bcd
N65	0.265 (0.017) bc	126 (3) cd	80 (5) c	0.448 (0.10) cd
N45	0.212 (0.029) d	103 (7) e	68 (4) d	0.412 (0.16) d
N25	0.172 (0.019) e	96 (7) e	58 (4) e	0.409 (0.14) d

Table 2.4. List of parameter values estimated for parameters in the BWB-Leuning-Yin model of stomatal conductance (g_s) and for mesophyll conductance (g_m). Values in brackets are standard errors of estimates. Different letters following the data in the same column indicate significant difference (P<0.05).

Treatment	g_s			g_m
	g_0 (mol m^{-2} s^{-1})	a_1 (-)	b_1 (kPa^{-1})	g_{m25} (mol m^{-2} s^{-1} bar^{-1})
Well-watered conditions				
N85	0.021 (0.002) a	0.575 (0.029) b	0.203 (0.027) c	0.236 (0.017) a
N65	0.019 (0.002) a	0.671 (0.026) a	0.275 (0.021) b	0.197 (0.023) b
N45	0.014 (0.002) b	0.690 (0.033) a	0.321 (0.030) a	0.172 (0.032) bc
N25	0.011 (0.001) cd	0.688 (0.021) a	0.291 (0.021) ab	0.161 (0.035) bc
Water-deficit conditions				
N85	0.011 (0.001) cde	0.300 (0.041) c	0.013 (0.025) e	0.126 (0.014) cd
N65	0.009 (0.001) de	0.284 (0.039) c	0.007 (0.022) e	0.155 (0.025) c
N45	0.008 (0.001) e	0.308 (0.037) c	0.023 (0.024) e	0.103 (0.023) d
N25	0.012 (0.001) c	0.317 (0.034) c	0.086 (0.023) d	0.041 (0.013) e
Estimation of overall a_1 and b_1				
Well-watered conditions	--	0.661 (0.013)	0.270 (0.012)	--
Water-deficit conditions	--	0.262 (0.019)	0.013 (0.012)	--
All treatments	--	0.558 (0.012)	0.197 (0.010)	--

The response of estimated parameter values to water and nitrogen treatments

Water-deficit conditions significantly decreased V_{cmax25}, J_{max25}, κ_{2LL} and R_{d25} at all nitrogen levels (Table 2.3). V_{cmax25}, J_{max25} and R_{d25} decreased with decreasing of nitrogen availability whereas κ_{2LL} showed such a response to a much less clear extent under both water-deficit conditions and well-watered conditions (Table 2.3). V_{cmax25}, J_{max25} and κ_{2LL} were significantly lower in the combined water deficit and low nitrogen availability treatments than in other treatments (Table 2.3). Neither E_{Jmax} nor E_{Vcmax} was significantly affected by water and nitrogen treatments (Table S2.1).

Water-deficit conditions significantly decreased g_0, a_1, b_1 and g_{m25} at all nitrogen levels (Table 2.4). g_0 and g_{m25} decreased with decreasing nitrogen availability whereas a_1 and b_1 responded little to nitrogen treatments under both water-deficit conditions and well-watered conditions (Table 2.4). g_{m25} was significantly lower under the combined water deficit and the lowest nitrogen availability treatment than in other treatments (Table 2.4).

The relationships between estimated parameter values and leaf nitrogen content

Under both water-deficit conditions and well-watered conditions, V_{cmax25}, J_{max25}, κ_{2LL}, R_{d25}, g_{m25} and g_0 linearly increased with increasing N_a (Figure 2.5). X_V and X_J were determined as 62 μmol (g N)$^{-1}$ s^{-1} and 93 μmol (g N)$^{-1}$ s^{-1}, respectively (Figure 2.5A,C). The N_a-dependent relationship was relatively less clear for other parameters (Figure 2.5B,D−F), but an F test revealed that water and nitrogen treatments did not significantly alter the linear relationships in all the six parameters. Linear relationship existed between V_{cmax25} and J_{max25} with a slope of 1.49 under different water and nitrogen treatments (Figure 2.6).

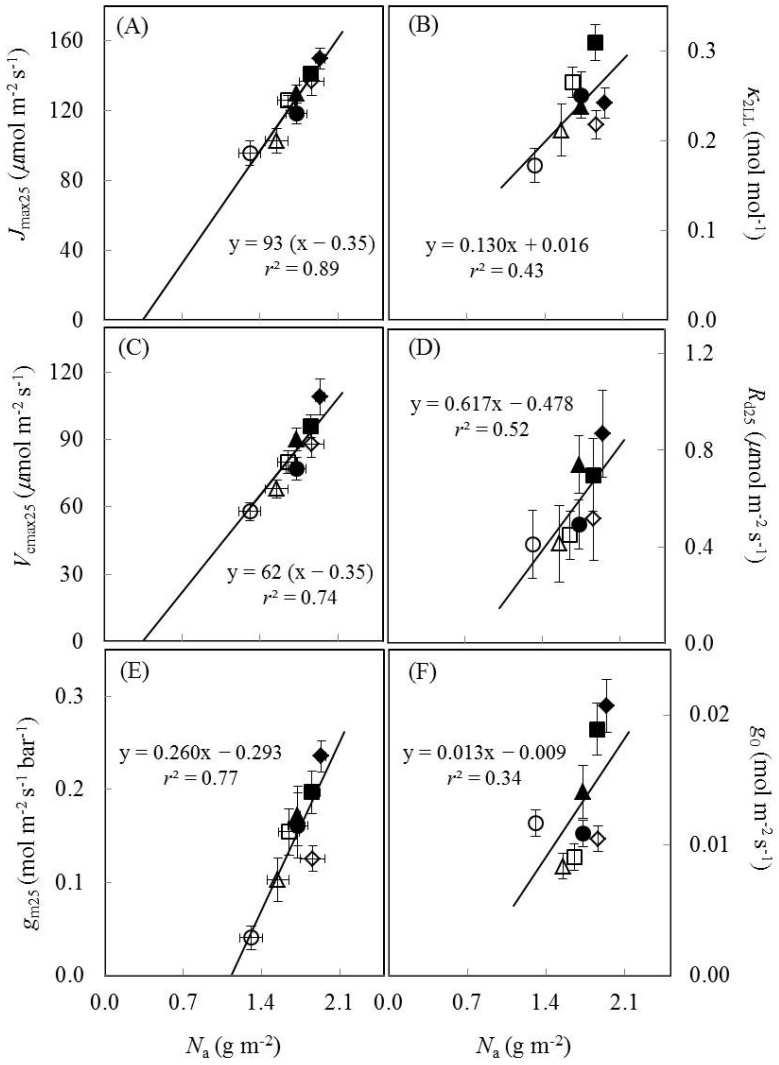

Figure 2.5. The estimated parameter values as a function of leaf nitrogen content (N_a) under different water and nitrogen treatments. The estimated parameters include: (A) the maximum electron transport rate (J_{max25}), (B) the conversion efficiency of limiting incident light into linear electron transport of photosystem II (κ_{2LL}), (C) the maximum Rubisco carboxylation rate (V_{cmax25}), (D) day respiration (R_{d25}), (E) mesophyll conductance (g_{m25}), and (F) residual stomatal conductance when the irradiance approaches to zero (g_0). Well-watered conditions: closed symbols; water-deficit conditions: open symbols. N85: diamond; N65: square; N45: triangle; N25: circle. Vertical error bar indicates standard error of estimate; horizontal error bar indicates standard error of the mean measured value.

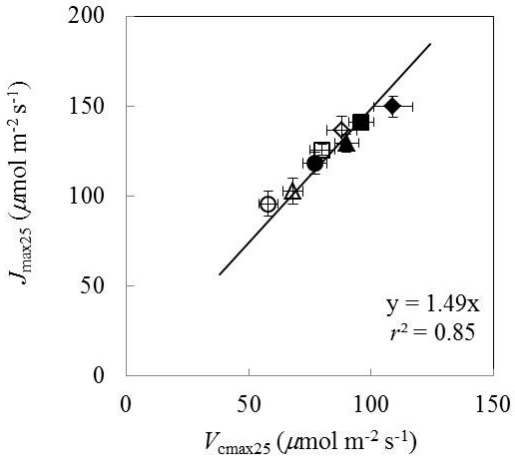

Figure 2.6. The relationship between the maximum Rubisco carboxylation rate (V_{cmax25}) and the maximum electron transport rate (J_{max25}) under different water and nitrogen treatments. Well-watered conditions: closed symbols; water-deficit conditions: open symbols. N85: diamond; N65: square; N45: triangle; N25: circle. Error bars indicate standard error of estimate.

Comparison between model predictions and measured values for A_n and g_s

Since the linear relationships between biochemical parameters and N_a were found to exist under different treatment combinations (Figure 2.5), we further tested to what extent conserved parameter values could be used in the FvCB model to predict A_n under different water and nitrogen conditions. Two sets of comparisons between the measured A_n and the predicted A_n were conducted, (i) using treatment-specific parameter values (i.e. using specific parameter values obtained under each treatment) (Figure 2.7A,B), and (ii) using shared parameter values (i.e. incorporating the N_a-dependent linear relationships and using overall E_{Jmax} and E_{Vcmax} values) (Figure 2.7C,D). For this second set of comparison, the overall values of E_{Jmax} and E_{Vcmax} for all treatments were estimated (Table S2.1) by incorporating the linear relationships between parameters (V_{cmax25}, J_{max25}, κ_{2LL}, R_{d25} and g_{m25}) and N_a. The coefficient of determination (r^2) between estimated and measured A_n in both comparisons ranged from 0.85 to 0.94 (Figure 2.7).

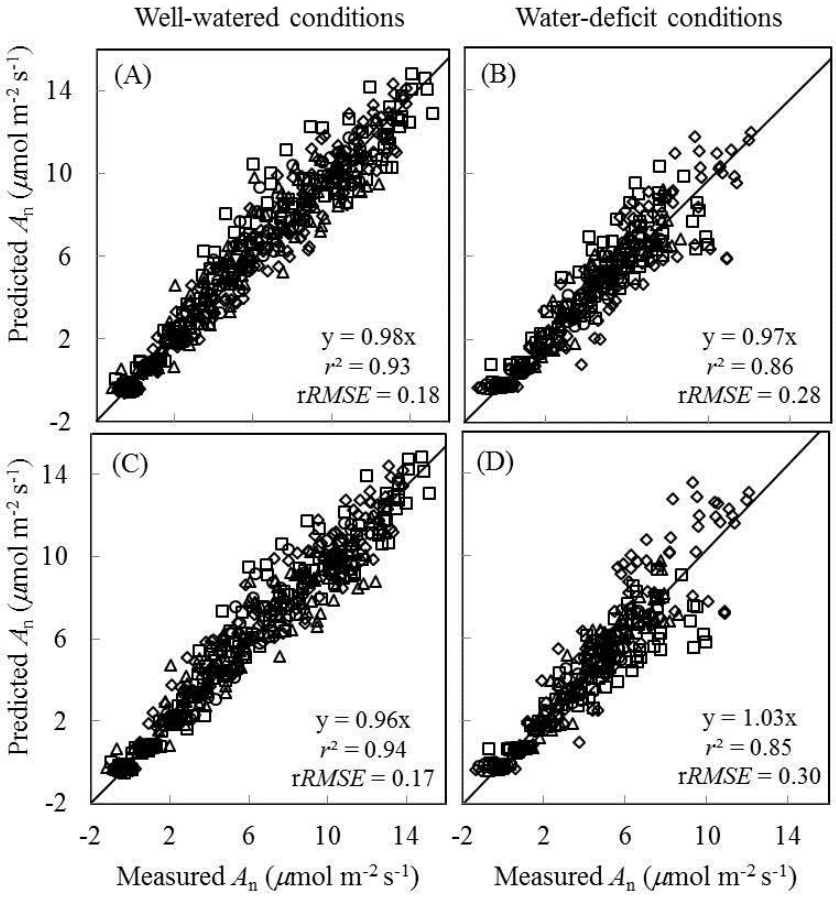

Figure 2.7. Comparisons between the measured net CO_2-assimilation rate (A_n) and the predicted A_n. A_n was predicted by the C_i-based FvCB model either using treatment-specific parameter values (A,B), or using shared parameter values (C,D). Well-watered conditions: A,C; water-deficit conditions: B,D. N85: diamond; N65: square; N45: triangle; N25: circle. The equation in each panel represents the linear regression of predicted (y) versus measured values (x) by forcing the line through the origin, r^2 is the determination coefficient of the regression, and r*RMSE* is the relative root-mean-square error ($=\frac{1}{\bar{x}}\sqrt{\frac{\sum_{i=1}^{n}(y_i-x_i)^2}{n}}$, where n is the number of data points, and $\bar{x}$ is the mean of the measured values).

We also tested to what extent conserved parameter values could be used in the BWB-Leuning-Yin model (Eqs. 2.10 and 2.11) to predict g_s under different water and nitrogen conditions. Since nitrogen had been found to have little effect on a_1 and b_1 (Table 2.4) and g_0 could be linearly correlated with N_a under both well-watered conditions and water-deficit conditions (Figure 2.5F), we tested to what extent conserved values of a_1, b_1 and g_0 can be used. For this purpose, we incorporated the linear relationships between model parameters (g_0 and g_{m25}) and N_a, and estimated overall values of a_1 and b_1 for all treatments (Table 2.4). Three sets of comparisons between the measured g_s and the predicted g_s were conducted, (i) using treatment-specific parameter values (Figure 2.8A,B), (ii) using shared parameter values for each water treatment (i.e. incorporating the N_a-dependent linear relationships and using overall values of a_1 and b_1 for each water treatment group given in Table 2.4) (Figure 2.8C,D), and (iii) using shared parameter values for all treatments (i.e. incorporating the N_a-dependent linear relationships and using overall values of a_1 and b_1 for all treatments given Table 2.4) (Figure 2.8E,F). Using treatment-specific parameter values in the BWB-Leuning-Yin model, the r^2 between estimated and measured g_s was 0.61 under well-watered conditions and 0.57 under a water deficit (Figure 2.8A,B); using shared parameter values for each water treatment, the r^2 was 0.55 for well-watered plants and 0.43 under a water deficit (Figure 2.8C,D). When shared parameters were used for all treatments, g_s was appreciably underestimated under well-watered conditions (Figure 2.8E), but overestimated under a water deficit (Figure 2.8F).This third set of predictions of g_s, when compared with the first set of predictions, underestimated g_s by 9% under well-watered conditions and overestimated g_s by 13% under water-deficit conditions.

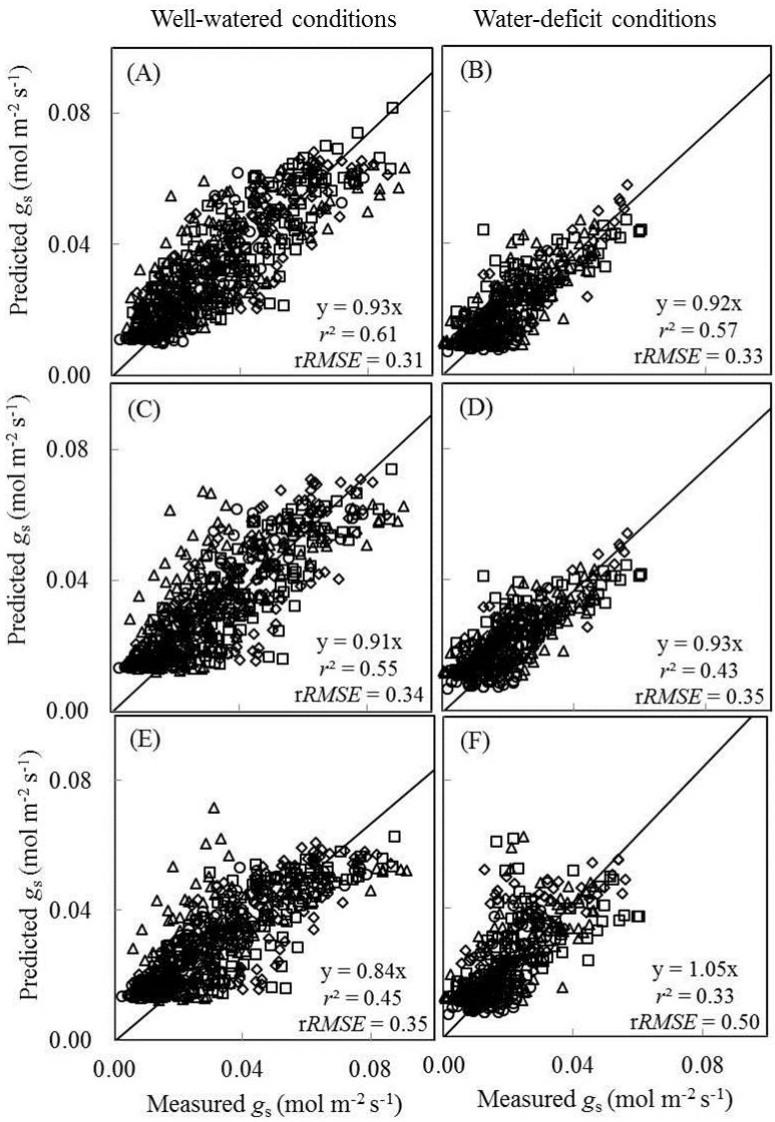

Figure 2.8. Comparisons between the measured stomatal conductance for CO_2 diffusion (g_s) and the predicted g_s. g_s was predicted by the BWB-Leuning-Yin model either using treatment-specific parameter values (A,B), or using shared parameter values for each water treatment (C,D), or using shared parameter values for all treatments (E,F). Well-watered conditions: A,C,E; water-deficit conditions: B,D,F. N85: diamond; N65: square; N45: triangle; N25: circle. For further details, see Figure 2.6.

As g_s was either underestimated or overestimated by the BWB-Leuning-Yin model using shared parameter values for all treatments (Figure 2.8E,F), we further assessed the impact of this inaccurate estimation of g_s on the prediction of A_n. Two sets of comparisons between the measured A_n and the predicted A_n were conducted. In the first comparison, shared values of the FvCB model parameters for all treatments and shared values of the BWB-Leuning-Yin model parameters for each water treatment were used in the coupled model; the r^2 between estimated and measured A_n was 0.89 under well-watered conditions and 0.80 under water-deficit conditions (Figure 2.9A,B). In the second comparison, shared values of both the FvCB model parameters and the BWB-Leuning-Yin model parameters for all treatments were used; the r^2 was 0.89 under well-watered conditions (Figure 2.9C), but A_n was overestimated by 9% under water-deficit conditions (Figure 2.9D).

Discussion

Methodology to estimate photosynthetic parameters

In our study, all model parameters were estimated based on the A_n-I_{inc} curves, instead of A_n-C_i curves, for estimating the FvCB parameters. We tested that the estimated V_{cmax} values by using these two types of curves were quite similar (Figure 2.4), as also shown in a previous study (Archontoulis *et al.*, 2012). The approach of using A_n-I_{inc} curves provides an alternative to the prevailing approach of using A_n-C_i curves and has its own advantages. First, the FvCB model is commonly used to predict leaf photosynthesis in canopies under field conditions, where it is the light level, not the CO_2 level, that fluctuates most significantly in space and in time. This suggests that the FvCB parameters estimated from A_n-I_{inc} curves should more closely represent field situations, relative to those based on A_n-C_i curves. Second, using A_n-C_i curve is known to have problems of CO_2 leakage and down-regulation of Rubisco at the low level of CO_2 during the measurement. The A_n-I_{inc} curve-based approach avoids these problems since the whole response curve is measured under ambient CO_2 level. However, using A_n-I_{inc} curves also tends to have problems. First, V_{cmax} cannot always be estimated from A_n-I_{inc} curves since the entire A_n-I_{inc} curve can be A_j limited sometimes (Archontoulis *et al*., 2012), especially for field crops that have high light saturating point (e.g. cotton, Wise *et al*., 2004). Second, the rate of TPU (triose phosphate utilization), if exerting a limitation on photosynthesis, cannot be estimated using A_n-I_{inc} curves since like Rubisco limitation, any TPU limitation on A_n-I_{inc} curves also happens at high irradiance levels (Archontoulis *et al*., 2012). Nevertheless, our limited data

(Figure 2.4) show the evidence in support of using A_n-I_{inc} curves as an alternative approach to estimate V_{cmax}. More comparisons between the two approaches using A_n-I_{inc} and using A_n-C_i curves are needed for different crop types and environments.

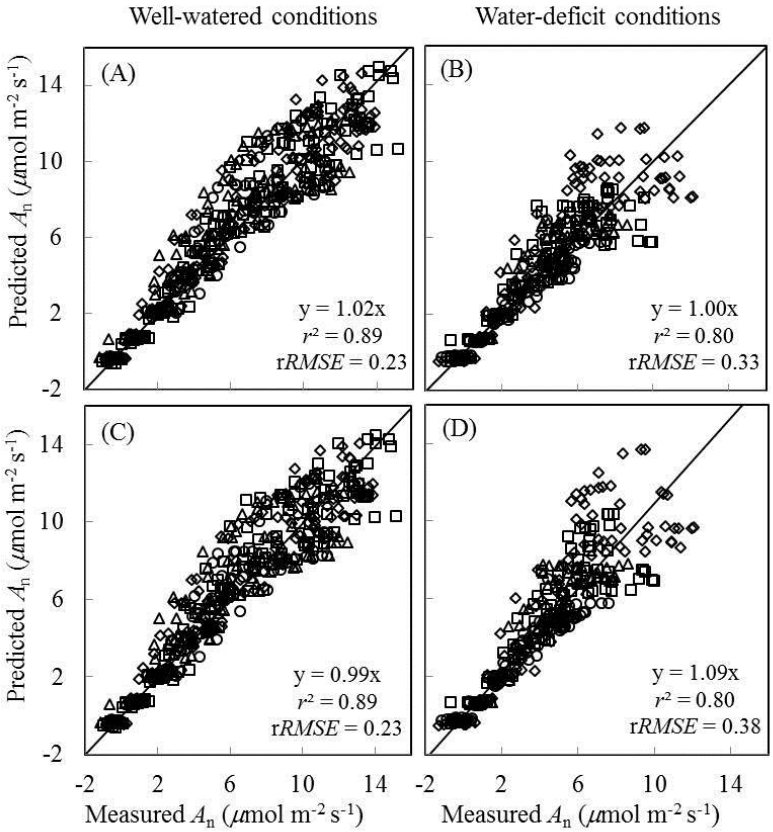

Figure 2.9. Comparisons between the measured net CO_2-assimilation rate (A_n) and the predicted A_n. A_n was predicted by the coupled FvCB and BWB-Leuning-Yin model using shared values of the FvCB model parameters for all treatments combined either with shared values of the BWB-Leuning-Yin model parameters for each water treatment (A,B), or with shared values of the BWB-Leuning-Yin model parameters for all treatments (C,D). Well-watered conditions: A,C; water-deficit conditions: B,D. N85: diamond; N65: square; N45: triangle; N25: circle. For further details, see Figure 2.6.

We adopted some parameter values from the literature as input to avoid over-parameterisation of the FvCB model. First, θ (the convexity factor for response of electron transport rate to incident light) was set to a constant value of 0.8 according to Yin and Struik (2015). It is worthy to notice that the actual value of θ could vary across species and environments. In our experiment, θ may be affected by different water and nitrogen treatments, as well as different light environment caused by different growth season. Initial analyses showed that letting θ be fitted as well resulted in enormous unrealistic variation of the estimated J_{max} and κ_{2LL}. Since the biological meaning of θ is less obvious than that of J_{max} and κ_{2LL}, we decided to set θ as a constant value to avoid biased estimations of J_{max} and κ_{2LL}. Eq. 2.4 with θ of 0.8 generates a very similar light response shape as given by the other widely used quadratic equation initially used by Harley *et al*. (1992). Second, in line with some previous studies (Xu & Baldocchi, 2003; Li *et al.*, 2012), we adopted the activation energy of R_d (E_{Rd}) and g_m (E_{gm}), the deactivation energy of J_{max} (D_{Jmax}) and g_m (D_{gm}), and the entropy term of J_{max} (S_{Jmax}) and g_m (S_{gm}) from literature (Bernacchi *et al*. 2001; Bernacchi *et al*. 2002). Whether or not these temperature response parameters change with water and nitrogen conditions is still not clear and further studies are needed. Third, Rubisco kinetic properties (K_{mC25}, K_{mO25}, E_{KmC} and E_{KmO}) were adopted from Bernacchi *et al*. (2002). Despite the generally assumption that Rubisco kinetic properties are conserved among C_3 species (von Caemmerer *et al*., 2009), values of these constants reported in the literature are different (Bernacchi *et al*., 2001; Bernacchi *et al*., 2002; Dreyer *et al*., 2001). The choice of Rubisco parameters also affected our FvCB parameter estimation. Since all parameters in the FvCB model are interrelated with each other, potential errors in our parameter estimation exist if parameter values we adopted from the literature were not applicable in our study.

Photosynthetic biochemical parameters in response to water and nitrogen conditions

Our study showed that a long-term mild water deficit and water and nitrogen stress combinations did not have significant effects on the linear relationships between biochemical parameters of the FvCB model (i.e. J_{max25}, κ_{2LL}, V_{cmax25}) and leaf nitrogen content per unit area (N_a) (Figure 2.5). Previous studies showed that a short-term water deficit did not change the linear relationships between biochemical parameters and N_a (Díaz-Espejo *et al.*, 2006; Gu *et al.*, 2012), whereas under long-term drought, either the slopes of the relationships between biochemical parameters and N_a were changed (Wilson *et al.*, 2000; Díaz-Espejo *et al.*, 2006)

or considering the effect of leaf mass per area (LMA) in the linear regressions was needed (Xu & Baldocchi, 2003). A few other studies (Damour *et al*., 2008; Damour *et al*., 2009) found that drought totally modified the fundamental relationships between J_{max} and N_a since N_a was either increasing (Damour *et al.*, 2008) or not affected (Damour *et al.*, 2009) under drought whereas J_{max} decreased. The discrepancy of the response of N_a to drought found in different studies may be caused by different species. Damour *et al*. (2008) worked with lychee tree and Damour *et al*. (2009) worked with mango tree, whereas we focused on herbaceous species *Lilium* and Gu *et al*. (2012) worked with rice. Besides, different approaches used to estimate FvCB parameters could also affect the results in different studies. First, as stated earlier, we used A_n-I_{inc} curves to parameterize the FvCB model. Whether or not the approach of using A_n-I_{inc} curves and the approach of using A_n-C_i curves yield similar results under drought still requires more comparisons. Second, early studies tend to ignore s (the calibration factor for converting fluorescence-based efficiency of photosystem II photochemistry Φ_2 into electron transport rate J) and g_m (mesophyll conductance) during the estimation of biochemical parameters. This could lead to inaccurate estimation of biochemical parameters since both s (Figure 2.3) and g_m (Table 2.4; also reviewed in Flexas *et al*., 2008) decreased under drought.

The calibration factor s used to convert Φ_2 into J is actually a lumped physiological parameter ($s = \rho_2\beta[1-f_{pseudo}/(1-f_{cyc})]$) that includes the absorptance of light by leaf photosynthetic pigments (β), the proportion of absorbed light partitioned to photosystem (PS) II (ρ_2), and the fraction of electrons at PSI following the cyclic transport around PSI (f_{cyc}) and following the pseudocyclic transport (f_{pseudo}) (Yin *et al*. 2009; Yin and Struik, 2009b). s was found to decrease by low nitrogen supply in previous study (Yin *et al.*, 2009), which is also found in our study (Figure 2.3). This decrease may be explained by the decreasing of β as a result of the decreased photosynthetic pigments in low-nitrogen leaves (Evans & Terashima, 1987). Interestingly, we found that s was smaller under water-deficit conditions compared to that under well-watered conditions despite the similar N_a (e.g. s in N65 under well-watered conditions compared with s in N85 under water-deficit conditions). It has been reported that drought did not change the partitioning of electrons between PSI and PSII (Genty *et al.*, 1987). However, stomatal closure caused by drought results in the decreasing of CO_2 concentration in the leaf, and consequently the amount of electrons used for CO_2 fixation decreases (Cornic & Briantais, 1991). Excessive electrons need to be consumed by other sinks apart from CO_2 fixation by following pseudo-cyclic electron transport (Cornic & Briantais, 1991; Biehler & Fock, 1996), or electrons need

to follow cyclic flow around PSI (Kohzuma *et al.*, 2009). Our results for the decreased s under water-deficit conditions independent on N_a suggest that drought induced an increase of f_{pseudo} or f_{cyc} or both in our experimental conditions.

Associated with estimating the factor s, mitochondrial day respiration (R_d) was estimated. Water-deficit conditions did not affect R_d in all N treatments, and there were non-significant effects of nitrogen on R_d under both well-watered conditions and water-deficit conditions (Table 2.3). Nevertheless, water-deficit conditions significantly decreased R_d in N85 and N45 treatments and generally there was a trend showing that drought and decreasing of nitrogen level decreased R_d (Table 2.3), as also revealed in some previous studies (González-Meler *et al.*, 1997; Huang & Fu, 2000). Therefore, we established an N_a-dependent relationship of R_d (Figure 2.5F) and applied this relationship to capture the changes of R_d under different water and nitrogen conditions. The linear relationship between respiration rate and leaf nitrogen content was also found under different light conditions (Ryan, 1995) and growth locations (Reich *et al.*, 1998).

A relatively stable J_{max25}/V_{cmax25} ratio among different water and nitrogen treatments was found in our study (Figure 2.6), in line with some previous studies (Makino *et al.*, 1992; Walcroft *et al.*, 1997; Díaz-Espejo *et al.*, 2006). Some studies simplified the parameterisation of the FvCB model by using a fixed value for either the J_{max}/V_{cmax} ratio (Kosugi *et al.*, 2003) or the J_{max25}/V_{cmax25} ratio (Müller *et al.*, 2005). However, care needs to be taken in setting a constant J_{max}/V_{cmax} ratio. First, when temperature varies, this ratio cannot be constant because J_{max} and V_{cmax} have different temperature response curves. In fact, the J_{max}/V_{cmax} ratio was found to decrease with temperature increase (Walcroft *et al.*, 1997; Medlyn *et al.*, 2002; Díaz-Espejo *et al.*, 2006). When scaled to a common temperature, a better correlation between J_{max} and V_{cmax} was found (Leuning, 1997). Second, g_m has a strong influence on this J_{max}/V_{cmax} ratio. In early studies (Grassi *et al.*, 2002) when g_m was not considered, a J_{max}/V_{cmax} ratio of ca 2.0 was obtained (Leuning, 1997), which is higher than our estimate where g_m was considered (ca 1.5, Figure 2.6). Finally, some studies found that water and nitrogen conditions also affected the J_{max}/V_{cmax} ratio (Grassi *et al.*, 2002; Gu *et al.*, 2012). Therefore, the approach using a fixed value for the J_{max}/V_{cmax} ratio to parameterise the FvCB model should receive critical reservation (Xu & Baldocchi, 2003; Archontoulis *et al.*, 2012).

In short, our study suggested that it is feasible to incorporate linear relationships between biochemical parameters and N_a in the FvCB model to predict photosynthesis under different water and nitrogen conditions, since the FvCB model using shared parameter values for all treatments gave satisfactory predictions of A_n under different water and nitrogen conditions (Figure 2.7C,D).

Stomatal conductance parameters and mesophyll conductance in response to water and nitrogen conditions

Accurately modelling stomatal conductance (g_s) and mesophyll conductance (g_m) are necessary steps towards predicting A_n under changing environments. The BWB-type model of g_s takes into account the effects of both environments and plant physiological status on g_s, and has been widely tested able to satisfactorily predict g_s for well-watered plants (Leuning, 1995; Li *et al.*, 2012). Some efforts have been devoted to predict g_s under drought conditions using the BWB-type model by introducing proper approaches to adjust parameter values used in the model. In general, most studies kept g_0 (residual stomatal conductance when the irradiance approaches to zero) as a fixed value and adjusted the value for the slope (roughly represents a_1 and b_1 in the BWB-Leuning-Yin model used in our study) by introducing a modifying factor of soil moisture (Egea *et al.*, 2011; Li *et al.*, 2012), or precipitation and evaporation (Baldocchi, 1997), or predawn xylem water potential (Sala & Tenhunen, 1996), or leaf nitrogen content and leaf water potential (Müller *et al.*, 2014). Leuning (1995) suggested that the BWB-type model should be able to predict g_s under water-deficit conditions by only adjusting the value for a_1. We found that both a_1 and b_1 decreased with the decreasing of soil water potential (Table 2.4), and without considering these decreases, g_s was overestimated under water-deficit conditions (Figure 2.8F). Further estimation of a_1 under water-deficit conditions by using the value for b_1 obtained under well-watered conditions resulted in a value of 0.586 for a_1, which is much larger than the original value of 0.262 obtained under water-deficit conditions (Table 2.4). Therefore, values for both a_1 and b_1 need to be adjusted to properly predict g_s under water-deficit conditions. However, a_1 and b_1 were little affected by nitrogen availability (Table 2.4) and no correlation between a_1 and N_a, nor between b_1 and N_a, under different water and nitrogen conditions was found in our study. The approach introducing a modifying factor of leaf nitrogen content on the slope (Müller *et al.*, 2014) is able to predict g_s in response to drought, and this could merely be due to similar responses of leaf nitrogen content and the slope to soil

water condition rather than because a functional relationship exists between the slope and leaf nitrogen content. Our study did not present a quantitative relationship of a_1 and b_1 with water supply conditions since there were only two water-level treatments. Further studies including more water levels would be needed to quantify changes of a_1 and b_1 under different water and nitrogen conditions.

g_0 was affected by both water conditions and nitrogen availability (Table 2.4), and a linear relationship between g_0 and N_a (Figure 2.5F) was used in our study to take into account the changes of g_0 under different water and nitrogen conditions. Although this linear relationship is less clear compared to linear relationships between N_a and biochemical parameters (e.g. J_{max25} and V_{cmax25}) (Figure 2.5), an F test showed that there is no significant difference between using a conserved linear relationship and using separate relationships to describe the N_a dependence of g_0 in response to water-deficit conditions. Under drought, plants tend to reserve water by reducing water loss, which makes it unlikely that g_0 is unaffected by water-deficit conditions. However, few modelling studies considered the change of g_0 under drought condition (Misson *et al.*, 2004; Keenan *et al.*, 2010). The reason for using a fixed value for g_0 in previous studies could be that changing the value of g_0 should not affect the prediction of g_s very much for plants with relatively high g_s since the value of g_0 itself is normally very small and approaches to zero. However, this may not hold true for plants with low g_s, as is the case in our study, since the value of g_0 may have relatively larger impact on predicting g_s.

g_m has received growing attentions in modelling photosynthesis (Niinemets *et al*., 2009), since g_m has been found to be finite and vary greatly among environments (Flexas *et al*., 2008; Yin *et al*., 2009). Previous studies found that g_m decreased under drought and low nitrogen availability (reviewed in Flexas *et al*., 2008). We found that g_m was enhanced by high nitrogen level and strongly decreased by the combination of water deficit and low nitrogen availability (Table 2.4). A relatively strong linear correlation between g_m and N_a was found in our study (Figure 2.5E), as also found in previous studies (von Caemmerer & Evans, 1991; Warren, 2004). Such a correlation may be explained by the surface area of the chloroplasts facing the cell walls, an anatomical determinant of g_m (von Caemmerer & Evans, 1991; Evans *et al.*, 1994), which depends on N_a.

Our results showed that the relation between g_m and N_a was hardly changed by water-deficit conditions (Figure 2.5E). In contrast, Gu *et al*., (2012) found that the change of g_m by water-

deficit conditions was not explained by the change of N_a but was negatively correlated with LMA. Nevertheless, LMA is generally considered as setting a limitation for the maximum g_m (Flexas *et al.*, 2008; Perez-Martin *et al.*, 2009) rather than is used to model g_m in response to environments, mainly because the change of LMA results from the long-term environmental adaptation of the plants (Poorter *et al.*, 2009) whereas g_m can vary quickly in response to environmental changes (Flexas *et al.*, 2006). This is supported by our result of using the N_a-dependent linear relationship to take into account the effects of water and nitrogen on g_m. Together with the incorporation of other N_a-dependent relationships of biochemical parameters, the model yielded similar results of A_n prediction compared to those using treatment-specific parameter values (Figure 2.7).

Some studies incorporated a dependence of g_m on g_s in the photosynthesis model (Cai *et al.*, 2008) as a close correlation between g_s and g_m in response to soil water deficit was commonly observed (Flexas *et al.*, 2002; Warren, 2008; Perez-Martin *et al.*, 2009). An approach incorporating the dependence of g_m on g_s was shown to give better prediction of A_n of different genotypes than the one incorporating the dependence of g_m on leaf nitrogen (Ohsumi *et al.*, 2007). However, the approach has been criticized as having no physiological justification (Niinemets *et al.*, 2009) since g_m and g_s respond differently to other environmental factors such as VPD (Warren, 2008; Perez-Martin *et al.*, 2009). As there is not yet sufficient physiological knowledge to reliably quantify the variability of g_m, some studies merely used a modifying factor of soil water conditions to take into account the effect of water deficit on g_m (Keenan *et al.*, 2010; Egea *et al.*, 2011). Whether or not the linear relationship between g_m and N_a could be a promising step towards modelling the variation of g_m needs to be further tested.

The effect of g_s estimation on the prediction of A_n

The coupled FvCB and BWB model has been increasingly used to model photosynthesis in response to environmental changes such as elevated CO_2 (Harley *et al.*, 1992) and drought stress (Keenan *et al.*, 2010; Müller *et al.*, 2014) and seasonal changes (Kosugi *et al.*, 2003). Normally in those previous studies, values of the biochemical parameters were related to the leaf nitrogen content and values of the stomatal conductance model parameters were changed according to the CO_2 level (Harley *et al.*, 1992), leaf water potential (Müller *et al.*, 2014), or growth season (Kosugi *et al.*, 2003).

Our study showed that considering the decreases of the stomatal conductance model parameters (a_1 and b_1) by drought was needed, otherwise, the coupled FvCB and BWB-Leuning-Yin model overestimated A_n under drought (Figure 2.9D) due to an overestimation of g_s (Figure 2.8F). The strong decrease of a_1 by drought (Table 2.4) indicates the decreasing of C_i/C_a ratio for vapour saturated air. The decrease of b_1 by drought (Table 2.4) suggests a negligible control of VPD on g_s under drought condition. These results are in line with previous studies that under drought condition, g_s at vapour nearly saturated air tended to be lower and g_s was less sensitive to VPD (Forseth & Ehleringer, 1983; Perez-Martin *et al.*, 2009). However, an exceptional case, which g_s showed much stronger sensitivity to VPD under drought, was also found in the previous study without an explanation provided (Perez-Martin *et al.*, 2009).

The BWB-Leuning-Yin model without considering the effect of water level on a_1 and b_1 also underestimated g_s under well-watered conditions (Figure 2.8E). But the subsequent prediction of A_n was not affected much (Figure 2.9C). This is probably explained by that under well-watered conditions, C_i is generally high and changing C_i at its high level only slightly affects A_n according to the diminishing-return relationship of A_n versus C_i. Therefore, as shown in Figure 2.9, the estimation of g_s had more effect on the prediction of A_n under water-deficit conditions than under well-watered conditions.

Concluding remarks

A previous analysis (Yin 2013) showed that the relationship of many crop model parameters (including those FvCB biochemical parameters) as a function of plant nitrogen status was little altered by elevated CO_2 concentration. Our present study examined whether this assertion could be extended for the water and nitrogen stress combinations. We showed that the N_a dependence of biochemical parameters of the FvCB model, g_0 of the BWB-Leuning-Yin model and the g_m value were little altered by water and nitrogen stress combinations (Figure 2.5). By incorporating these N_a-dependent relationships with the FvCB model and BWB-Leuning-Yin model, parameterisation of these models could be simplified while maintaining satisfactory predictions. The obvious exception is parameters a_1 and b_1 of the BWB-Leuning-Yin model, which depended little on nitrogen treatments but greatly on water treatments (Table 2.4). This is probably because the BWB-Leuning-Yin model is largely phenomenological, and its related conclusions are only valid for the specific species and conditions examined in this study. While the variation of parameters a_1 and b_1 had a great impact on the prediction of

stomatal conductance, it had a considerably lower impact on the prediction of leaf photosynthesis. Nevertheless, a further study is needed to quantify how these two parameters vary with water-deficit conditions, as they have a stronger bearing on modelling leaf transpiration.

Supporting information

Table S2.1. Activation energy of J_{max} and V_{cmax} estimated for each water and nitrogen treatments and their shared values for all treatments. Values in brackets are standard errors of estimates. Different letters following the data in the same column indicate significant difference (P<0.05).

Treatment	E_{Jmax} (J mol^{-1})	E_{Vcmax} (J mol^{-1})
Well-watered conditions		
N85	54618 (6862) ab	57874 (8377) a
N65	57737 (3539) a	47231 (6745) ab
N45	48441 (4122) b	41964 (5920) b
N25	46384 (5581) b	41749 (6870) b
Water-deficit conditions		
N85	51658 (6275) ab	48296 (9459) ab
N65	49017 (2519) b	43407 (8421) ab
N45	49854 (6782) b	42842 (7082) ab
N25	47369 (6782) b	46310 (8884) ab
Estimation of overall E_{Jmax} and E_{Vcmax} shared for all treatments		
--	52083 (1040)	45909 (2291)

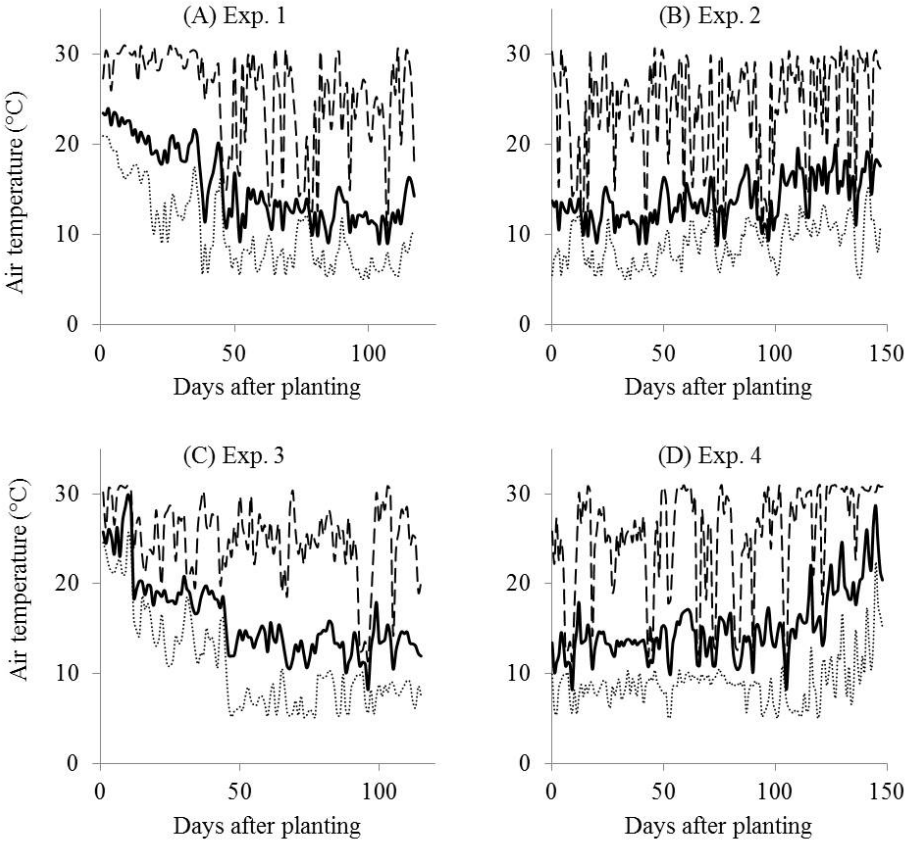

Figure S2.1. Daily mean, maximal and minimal air temperature. Measurements were conducted at the height of 1.5 m above ground inside the greenhouse during (A) Exp. 1, (B) Exp. 2, (C) Exp. 3, and (D) Exp. 4. Solid curve is daily mean air temperature, dashed curve on top is the daily maximal air temperature, dotted curve at bottom is the daily minimal air temperature.

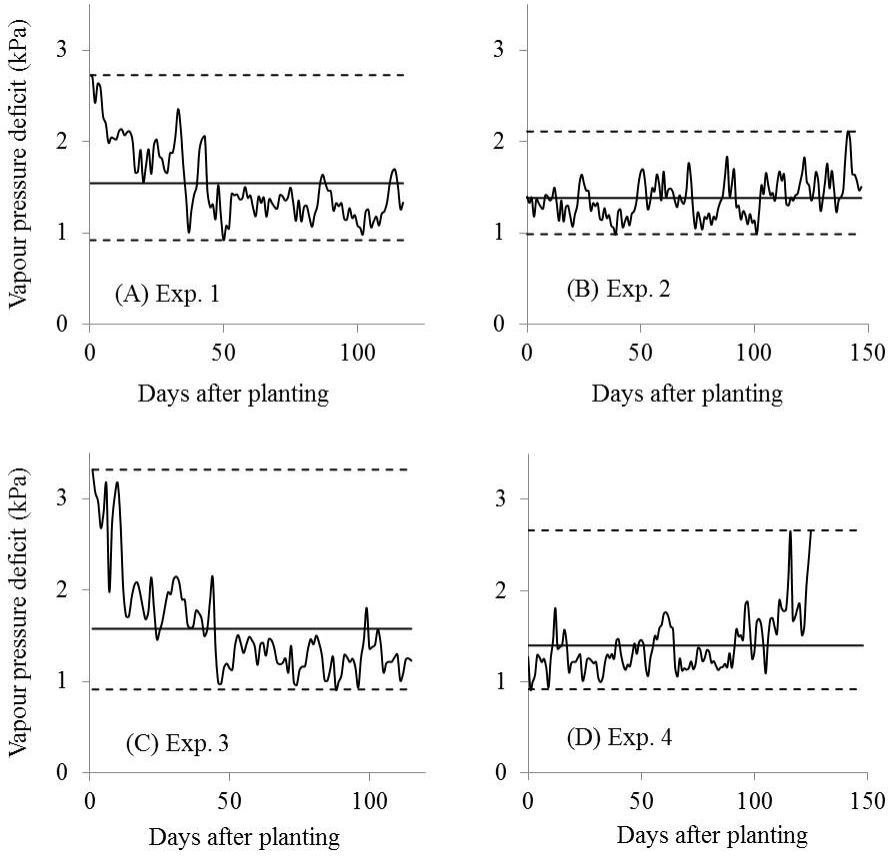

Figure S2.2. Vapour pressure deficit (VPD). Measurements were conducted at the height of 1.5 m above ground inside the greenhouse during (A) Exp. 1, (B) Exp. 2, (C) Exp. 3, and (D) Exp. 4. Curve is daily mean VPD, solid line is the average daily mean VPD during the whole growth period, and dashed lines are the maximal and minimal daily mean VPD during the whole growth period, respectively.

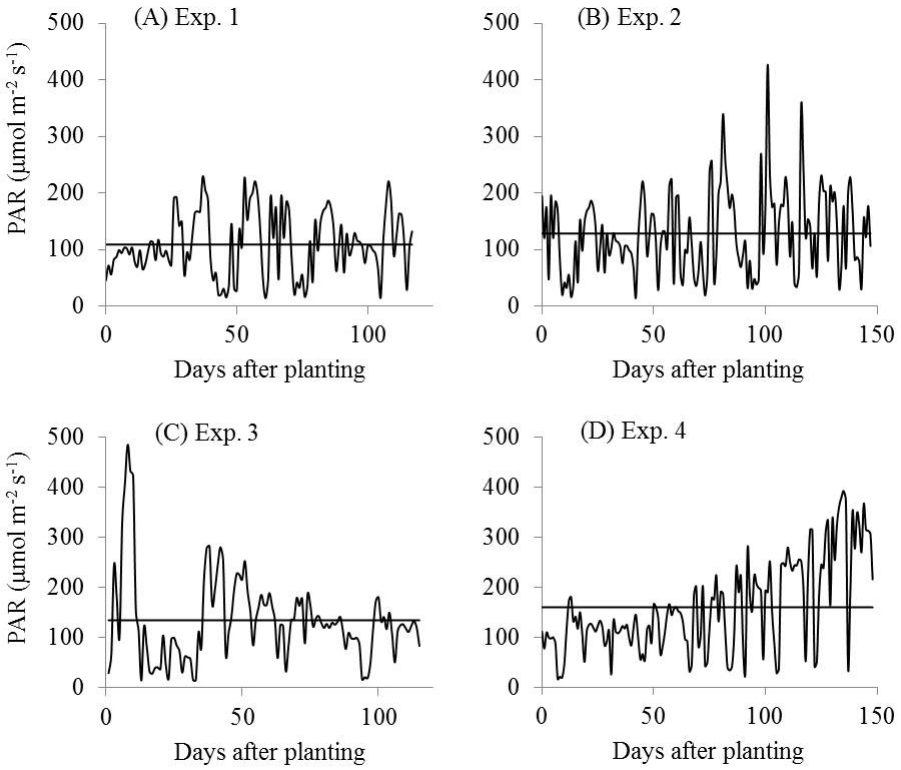

Figure S2.3. Daily mean photosynthetically active radiation (PAR). Measurements were conducted above crop canopy inside the greenhouse during (A) Exp. 1, (B) Exp. 2, (C) Exp. 3, and (D) Exp. 4. Curve is daily mean PAR, and line is the average daily mean PAR during the whole growth period.

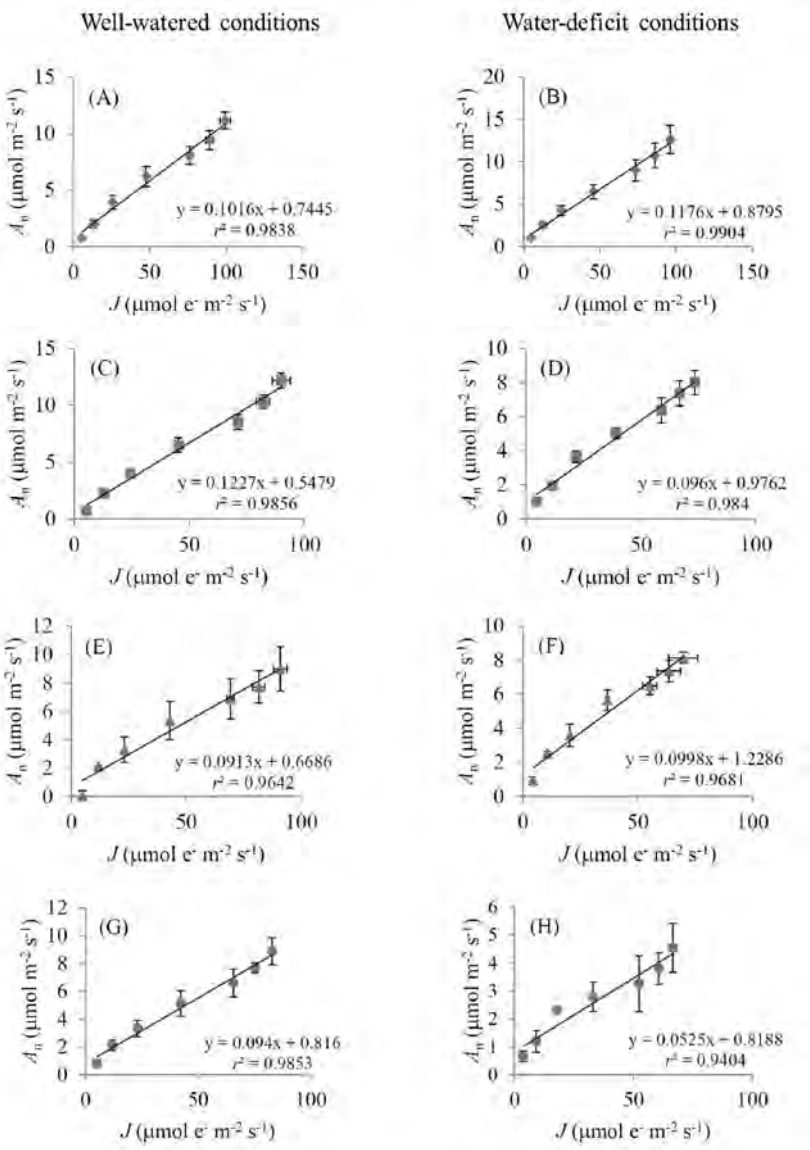

Figure S2.4. Relationships between A_n and J under well-watered conditions (A,C,E,G) and water-deficit conditions (B,D,F,H). N85: A,B; N65: C,D; N45: E,F; N25: G,H. All data points were chosen from light levels at or below 1000 μmol m^{-2} s^{-1} and leaf temperature at 20 ± 2 ℃. Vertical error bar indicates standard error of measured A_n; horizontal error bar indicates standard error of calculated J.

Chapter 3

Are shade responses beneficial to plant photosynthesis? A simulation study using a functional-structural plant model

Ningyi Zhang[1,2], Arian van Westreenen[1,2], Niels P.R. Anten[2], Jochem B. Evers[2], Leo F.M. Marcelis[1]

[1] Horticulture and Product Physiology Group, Wageningen University, Wageningen, The Netherlands

[2] Centre for Crop Systems Analysis, Wageningen University, Wageningen, The Netherlands

Abstract

Background and Aims Understanding plant phenotypic plasticity to shading by leaves in vegetation stands and its consequences for plant performance needs separate analysis of plant responses to reductions in both photosynthetically active radiation (PAR) and red to far-red ratio (R:FR) of light.

Method We measured plasticity in leaf photosynthesis and canopy architecture separately to reductions in PAR, R:FR and to a combination of the two in woody perennial rose (*Rosa hybrida*). Using a functional-structural plant model, we mimicked these plastic responses, separately quantified their effects on plant photosynthesis, and evaluated the relative importance of these plastic responses for plant photosynthesis at different shade levels.

Key Results Observed plastic responses to reduced PAR (e.g., reduced leaf photosynthetic capacity) were clearly different from responses to reduced R:FR (e.g., increased internode length and leaf angle). At mild shading levels, simulated plant photosynthesis was affected most by plastic responses to reduced R:FR, while at heavy shading, the effects of plastic responses to reduced PAR became dominant. Plasticity in leaf physiological traits had larger effects on plant photosynthesis than plasticity in architectural traits, even at mild shading when plasticity to low R:FR (typically inducing plant architectural responses relevant to shade avoidance) was dominant. The effects of low-R:FR responses and low-PAR responses on plant photosynthesis tended to mitigate each other.

Conclusions Phenotypic plasticity to shading in vegetation stands entails both plant physiological and architectural responses to different factors (reduced PAR and reduced R:FR). The relative importance of individual plastic responses to these shading factors for plant photosynthesis changes with shade levels. The adaptive significance of plasticity to one shading factor depends on the other.

Keywords: canopy architecture; functional-structural plant model; light interception; phenotypic plasticity; photosynthesis; red to far-red ratio; rose (*Rosa hybrida*); shade

Introduction

Plants have the ability (i.e., phenotypic plasticity) to change their phenotype according to the environmental conditions they grow in (Bradshaw, 1965; Schlichting, 1986; Sultan, 2000). The assumption that phenotypic plasticity helps plants to optimize their performance under certain environments is often accepted while less tested by experiments (Dorn *et al.*, 2000; van Kleunen & Fischer, 2005; Richards *et al.*, 2006; Weijschedé *et al.*, 2006; Liu *et al.*, 2016). Analysing plant phenotypically plastic responses to environmental conditions and their subsequent effects on plant performance is complicated, particularly because (i) phenotypic plasticity often includes changes in multiple interacting functional traits, and (ii) changes in environmental conditions typically include changes in multiple factors that can induce different phenotypic responses and thus influence plant performance in different ways (Callaway *et al.*, 2003; Anten *et al.*, 2010).

A typical example is analysing the effects of phenotypic plasticity to shading caused by leaves (i.e., canopy shading) on plant photosynthesis, which is an important plant performance measure. Plants grow in dynamic vegetation stands with other growing plants where they shade one another creating a light environment that varies considerably in time and space. This canopy shading entails multiple factors including reductions in photosynthetically active radiation (PAR) and changes in spectral composition especially reductions in the red (655-665 nm) to far-red (725-735 nm) ratio (R:FR) in addition to other spectral changes (Smith, 1982). The reductions in PAR and R:FR occur simultaneously but in different magnitudes with the increasing level of canopy shading. The reductions in PAR and R:FR also induce different plant plastic responses. Reductions in PAR on one hand directly decrease plant photosynthesis due to reductions in light as a resource. On the other hand, reductions in PAR induce plastic responses such as decreasing leaf photosynthetic capacity and respiration rate, changing leaf anatomy, increasing leaf photosynthetic nitrogen partitioning to light harvesting, increasing specific leaf area, and increasing the fraction of assimilates partitioned to the leaf (Gulmon & Chu, 1981; Lichtenthaler *et al.*, 1981; Sims & Pearcy, 1991; Walters *et al.*, 1993; Evans & Poorter, 2001; Oguchi *et al.*, 2005; Baird *et al.*, 2017). Reductions in R:FR by contrast induce plastic responses of plant morphogenesis including increased elongation of hypocotyls, internodes, petioles, leaf sheaths and blades, increased leaf inclination angle, reduced branching and tillering, and early flowering (Franklin, 2008; Casal, 2012; Pierik & De Wit,

2014). These plastic responses to reductions in PAR and R:FR may affect plant photosynthesis in different directions (i.e., positive and negative) and magnitudes. Moreover, the effects of individual plastic responses on plant photosynthesis may interact with each other. For instance, plant photosynthesis can be affected by both responses in plant architecture (affecting plant light capture) and leaf photosynthetic traits (affecting plant light use); these responses interact as effects of changes in leaf photosynthetic traits depend on the amount of light that the leaf receives.

To fully understand the effect of phenotypic plasticity on plant photosynthesis under canopy shading, we need to (i) determine individual trait responses to each factor (reduced PAR and reduced R:FR) separately, (ii) determine how these trait effects change with shading levels and (iii) quantify how the syndrome of trait responses to these shading factors in coherence determine plant photosynthesis. Several studies have quantified the effects of some plastic responses of individual traits (e.g., longer petiole length and larger specific leaf area) on plant performance under low PAR or low R:FR (Weijschedé *et al.*, 2006; Liu *et al.*, 2016). However, hardly any study has separately quantified the effects of multiple plastic trait responses induced by low PAR and low R:FR and compared their relative importance for plant photosynthesis under canopy shading. These analyses cannot be done by experiments alone, because it is impossible to induce each plastic trait response independently while preventing the expressions of other traits in real plants. Creating virtual plants by models can be very helpful in addition to experiments, since models allow to combine any trait in virtual phenotypes. Functional-structural plant (FSP) models simulate plant growth in response to environmental changes taking into account both plant architecture in three dimensions and physiological processes such as photosynthesis, respiration and biomass allocation (Vos *et al.*, 2010). Thus FSP models can be used to disentangle individual plastic trait responses to canopy shading and to separately quantify the effects of individual plastic trait responses on plant photosynthesis. By creating virtual phenotypes that include one plastic trait response at a time, the effect of each plastic trait on plant photosynthesis can be assessed separately (Bongers *et al.*, 2014). Subsequently the interactive effects of several plastic trait responses on plant photosynthesis can be quantified.

The objective of this study is to quantify the extent to which plastic responses to different shading factors interact in determining plant photosynthesis under canopy shading. First the

separate phenotypically plastic responses to two main factors of canopy shading (reduced PAR and reduced R:FR) were assessed experimentally. Then, an FSP model was applied to quantify the effects of individual plastic responses and the consequences of their interactions for plant photosynthesis. To this end, a greenhouse experiment was conducted in which plants of the woody perennial (shrub) rose (*Rosa hybrida*) were subjected to different light treatments: reductions in only PAR and R:FR, and combinations of the two, to evaluate plant plastic responses of plant architecture and leaf photosynthesis to reduced PAR and reduced R:FR. We chose rose as an experimental system as it is a crop whereby both lighting and plant architecture are often intensely manipulated to optimize production (Gonzalez-Real & Baille, 2000). An FSP model of rose was then developed and validated using the experimental data, and the model was used to conduct simulation studies to quantify the effect of each plastic trait response on light interception and plant photosynthesis.

Materials and methods

Plant materials and growth conditions

The experiment was conducted in two compartments (8 m × 8 m) of a Venlo-type glasshouse located in Wageningen, the Netherlands (52° N, 6° E). In each compartment, there were four rolling growth tables (1.70 m × 3.25 m). Rose plants (*Rosa hybrida* cv. 'Red Naomi!') with one-node cuttings bearing a shoot were grown in rockwool cubes (0.1 m × 0.1 m × 0.1 m). On April 5, 2016, plants were placed on growth tables with a distance of 0.15 m between each plant. When on average one flower bud had just appeared per plant, the shoots were pruned just above the 3rd 5-leaflet leaf and this leaf was removed to stimulate axillary bud break, as rose growers commonly do in practice. We started the light treatments one week after pruning, when the axillary buds were broken (average shoot length of 1cm). The experiment lasted for 6 weeks and finished by end of May 2016.

In total six light treatments (Table S3.1) were established as a randomized block design with four blocks, with 100 plants in each treatment plot (1.7 m × 1.6 m). In each plot, two rows of plants at each side of the plot were used as border plants that were not included in measurements. Light treatments included reductions in photosynthetically active radiation (PAR) and reductions in red to far-red ratio (R:FR), and a combination of the two. Reductions in PAR were achieved by adding neutral shading screen (50% transmissivity) at a distance of

20 cm above the canopy. One layer of neutral shading screen was added in treatment of 'medium PAR' and two layers of neutral shading screen were added in treatment of 'low PAR'. Reductions in R:FR were achieved by adding additional far-red light-emitting diode (LED) modules (GreenPower far-red production modules, Philips, Eindhoven, The Netherlands) at a distance of 50 cm above the canopy. This allowed us to manipulate R:FR independent of PAR. Two LED modules per plot were added in treatment of 'medium R:FR', resulting in an additional 50 μmol m^{-2} s^{-1} far-red light intensity from LED modules at the canopy level. Four LED modules per plot were added in treatment of 'low R:FR', resulting in an additional 100 μmol m^{-2} s^{-1} far-red light intensity from LED modules at the canopy level. When there were less than four LED modules in a plot, we added fake modules to ensure similar shading by the frame of LED modules for all treatments. Each treatment plot was surrounded by plastic film (with white colour facing the plot and black colour facing outside) with 20 cm depth from the top of LED frames to minimize light treatments affecting each other. The actual levels of PAR and R:FR achieved in different treatments are given in Table S3.1.

Assimilation lighting (high-pressure sodium lamps, Philips, Eindhoven, The Netherlands) was only used to prevent that assimilation lighting of neighbouring compartments disturb the treatments and to prevent gradients within the compartments. During the experimental period, the assimilation lighting was on for approximately six hours per day with an intensity of 150 μmol m^{-2} s^{-1}. Set points of day and night temperature were 22°C and 17°C respectively, and the average realized day and night temperatures during the experiment were 24°C and 18°C respectively. Set point of relative humidity was 65% during day and night, and the average realized day and night relative humidities during the experiment were 65% and 75%, respectively. CO_2 was not controlled. Watering (EC = 1.6 mS cm^{-1}; pH = 6) was done with an ebb and flood system four times a day.

Measurements

Plant architecture measurements. In each plot, five plants were randomly chosen to measure plant architectural traits when flower buds started to open. Internode length, leaf area and leaf inclination angle were measured for every second internode or leaf on the plant. Plant height, total leaf area, peduncle length and flower bud diameter were also measured. Length measurements were conducted using a ruler. Leaf inclination angle was measured as the insertion angle of the leaf compared with the horizontal level using a protractor. Leaf area was

measured using a leaf area meter (LICOR-3100, Lincoln, NE, USA). Flower bud diameter was measured using a caliper.

Leaf gas exchange measurements. In four treatments (high PAR + high R:FR, medium PAR + high R:FR, high PAR + low R:FR, medium PAR + low R:FR), two plants in each plot were randomly chosen at the flower bud visible stage to perform a combined measurement of gas exchange and chlorophyll fluorescence using the LI-6400XT Portable Photosynthesis System (Li-Cor BioScience, Lincoln, NE, USA) on leaves at the upper, middle and lower level of the canopy. The measurement was conducted on the terminal leaflet of each leaf. Light response curves of photosynthesis were made by decreasing incident light in the leaf cuvette in the series of 1500, 1200, 1000, 750, 550, 350, 200, 150, 100, 50, 20 and 0 μmol m^{-2} s^{-1}, while keeping ambient CO_2 at 400 μmol mol^{-1}, leaf temperature at 25 °C, and leaf-to-air vapour pressure difference at 1~1.6 kPa. The steady-state fluorescence (F_s) was measured simultaneously with the gas exchange measurement after 3 to 5 minutes light adaptation, followed by applying a light pulse > 8000 μmol m^{-2} s^{-1} for less than one second to measure maximum fluorescence $F_m^{'}$.

Estimation of photosynthetic parameters

Leaf photosynthetic parameters were estimated by stepwise fitting the combined measurements to a non-rectangular hyperbola (Eq. 3.1) (Marshall & Biscoe, 1980):

$$A = \frac{\Phi_{CO2LL(inc)} I_{inc} + A_{max} - \sqrt{(\Phi_{CO2LL(inc)} I_{inc} + A_{max})^2 - 4\theta A_{max} \Phi_{CO2LL(inc)} I_{inc}}}{2\theta} - R_d \quad (3.1)$$

where A (μmol CO_2 m^{-2} s^{-1}) is the net leaf photosynthetic rate; $\Phi_{CO2LL(inc)}$ (mol CO_2 mol^{-1} photon) is the quantum yield of CO_2 assimilation on the basis of incident light; I_{inc} (μmol m^{-2} s^{-1}) is the incident irradiance; A_{max} (μmol CO_2 m^{-2} s^{-1}) is the maximum leaf photosynthetic rate at saturating incident irradiance; θ is the curvature factor of the light response curve; R_d (μmol CO_2 m^{-2} s^{-1}) is the dark respiration rate. Details on procedure of estimating $\Phi_{CO2LL(inc)}$, A_{max}, θ and R_d can be found in supporting information (Method S3.1).

R_d was assumed to be linearly related to A_{max} and this linear relationship was quantified by curve fitting Eq. 3.2 (Hikosaka *et al.*, 2016b) using the estimates of A_{max} and R_d (in Eq. 3.1) for top, middle and low leaves in the canopy.

$$R_d = a \times A_{max} \tag{3.2}$$

The coefficient a is the R_d to A_{max} ratio, which is an input parameter of the model (see descriptions in *Model development*).

To quantify the relationship between light gradient and A_{max} gradient in the canopy, light level at top, middle and bottom of the canopy was measured on a cloudy day at flowering stage using a line quantum sensor (Li-Cor BioScience, Lincoln, NE, USA). Using estimated A_{max} values and measured light level for top, middle and low leaves in the canopy, the relationship between light gradient and A_{max} gradient was quantified by fitting Eq. 3.3 (Niinemets & Anten, 2009):

$$A_{max,0}/A_{max,top} = (Q_0/Q_{top})^b \tag{3.3}$$

where Q_0 (μmol m^{-2} s^{-1}) is the light intensity at middle or low level of the canopy; Q_{top} (μmol m^{-2} s^{-1}) is the light intensity on top of the canopy; $A_{max,0}$ (μmol CO_2 m^{-2} s^{-1}) is the estimated A_{max} for the middle or low leaf in the canopy; $A_{max,top}$ (μmol CO_2 m^{-2} s^{-1}) is the estimated A_{max} for the top leaf in the canopy; b is the coefficient describing the relationship between light gradient and A_{max} gradient in the canopy. $A_{max,top}$ and b are input parameters of the model (see descriptions in *Model development*).

Quantifying the effect of plastic trait responses on light interception and plant photosynthesis

Model development. A functional-structural plant (FSP) model of rose was developed to quantify the effect of plastic trait responses to low PAR and low R:FR on light interception and plant photosynthesis under canopy shading. The model was constructed in the plant modelling software GroIMP (Hemmerling *et al.*, 2008). The model includes (i) a static representation of the three-dimensional (3D) architecture of rose plants in a canopy at flowering stage, (ii) a radiation model to simulate light capture of individual organs, and (iii) a photosynthesis model to calculate net daily photosynthesis of the whole plant.

(i) The 3D rose plants. The plant 3D architecture was represented using a repetition of basic units (i.e., phytomers), which consist of an internode and a compound leaf. Each phytomer was sequentially placed along the growth axis of the plant. The size of the phytomer and the number of leaflets of the compound leaf were determined by actual plant architectural measurements, with the assumption that the phytomer size between every second phytomer can be linearly interpolated. Leaf insertion angle was assumed to follow a normal distribution according to the average leaf angle and standard deviation of all replicates in each treatments. For plants with a flower bud, a red sphere with the measured flower diameter was added on top of the 3D plant representation to mimic the similar shading from the flower.

(ii) The radiation model. The light environment was modelled using both a diffuse light dome with moderate gradation towards zenith and azimuthal uniformity and a direct light source spread over the solar path (Evers *et al.*, 2010). To eliminate the border effects in the light environment, each plot of a simulated plant population was replicated 10 times in the x and y directions for the light model calculations, resulting in averaged light conditions that were experienced by 100 copies of each individual plant population (de Vries *et al.*, 2018). The amount of light reaching the 3D objects (e.g., internode and leaf) was simulated using a Monte-Carlo ray tracer embedded in GroIMP (Hemmerling *et al.*, 2008). The light absorption of an individual organ was calculated based on the amount of light reaching that organ and the optical properties of that organ (Evers *et al.*, 2010; Buck-Sorlin *et al.*, 2011).

(iii) The photosynthesis model. Plant net photosynthesis was calculated as the sum of net photosynthesis of each individual leaf. Leaf net photosynthesis was calculated using Eq. 3.1 based on the photosynthetic parameters and light absorption of that leaf. Each leaf had its own photosynthetic parameters. A_{max} and R_d of each individual leaf were calculated using Eq. 3.2 and Eq. 3.3 based on the input parameter values of coefficient a, b and $A_{max,top}$, and the relative light intensity reaching that leaf. $\Phi_{CO2LL(inc)}$ and θ were assumed to be constant in all leaves since we did not find any substantial difference between leaves at different canopy levels. Average $\Phi_{CO2LL(inc)}$ and θ values of the top, middle and low leaves were used in the model.

Model evaluation. The simulated fraction of light intercepted by the plants, plant height and plant total leaf area in each plot were compared with the measurements by calculating the coefficient of determination (r^2) and the relative root-mean-square error (r*RMSE*,

$= \frac{1}{\bar{x}} \sqrt{\frac{\sum_{i=1}^{n}(y_i - x_i)^2}{n}}$, where y_i is the simulated value, x_i is the measured value, n is the number of data points, and $\bar{x}$ is the mean of the measured values).

Model simulation design. Essentially in the simulations we created situations in which our target plants experience different levels of canopy shading. Plants were simulated at the stage when all leaves were fully developed. Distance between plants was kept the same as in the experiment (0.15 m) and a plant population on 1 m^2 soil area was simulated. The background incoming light intensity (i.e., at non-shaded condition) was assumed to be 500 μmol m^{-2} s^{-1}, which represented the average light level during the experiment. The reduction of PAR by canopy shading was calculated according to the Beer-Lambert equation using a value of 0.6 for the light extinction coefficient (Yin & Struik, 2015). The reduction of R:FR by canopy shading was calculated based on the fraction of reduced PAR according to Eq. 3.4 (Evers *et al.*, 2006):

$$R{:}FR = 0.87 \times \exp(-2.32 \times f_{PAR\ intercepted}) \quad (3.4)$$

where $f_{\text{PAR intercepted}}$ is the fraction of PAR intercepted by the canopy. Based on these calculations, our medium PAR treatment and low PAR treatment represent shading by a canopy with a leaf area index (LAI_C) of 1.2 and 2.3 m^2 m^{-2} respectively. The medium R:FR treatment and low R:FR treatment represent shading by a LAI_C of 1 and 1.6 m^2 m^{-2} respectively. Therefore, in the simulation studies, we simulated four levels of canopy shading that represent shading by a LAI_C of 0.5, 1, 2 or 3 m^2 m^{-2}, which were reasonably bracketed by our treatments.

Virtual plant phenotypes under each level of canopy shading were created based on the assumption that plant parameters were linearly related with the PAR and R:FR levels. The linear relationships between plant parameters and the PAR and R:FR levels were quantified using the values obtained in the experiment. By including one single plastic trait response or the response of one plastic trait combination at a time, we estimated the effect of individual plastic responses on the fraction of light interception and plant photosynthesis using Eq. 3.5:

$$E = (Y_{plastic} - Y)/Y \quad (3.5)$$

where E is the relative effect of plastic trait responses on the fraction of light interception or plant photosynthesis; $Y_{plastic}$ is the fraction of light interception or plant photosynthesis calculated under the reduced incoming light intensity by LAI_C, using the target plastic trait values that are changed according to the PAR and R:FR levels under LAI_C, while keeping all other trait values the same as values of non-shaded plant phenotype; Y is the fraction of light interception or plant photosynthesis calculated under the reduced incoming light intensity by LAI_C, using the non-shaded plant phenotype.

The interaction between trait effects on plant photosynthesis was estimated using Eq. 3.6:

$$I = E_{total} - E_{additive} \quad (3.6)$$

where E_{total} is the E (in Eq. 3.5) of which $Y_{plastic}$ is calculated by changing all target plastic traits simultaneously; $E_{additive}$ is the sum of E values estimated for each individual target trait.

Statistical analysis

The effects of reductions in PAR and R:FR on plant architectural traits were analysed using a simple linear regression model ($P < 0.05$) of R (R Core Team) with PAR and R:FR levels considered as continuous factors. The effects of PAR and R:FR levels on leaf photosynthetic parameters were analysed using an one-way ANOVA ($P < 0.05$) of R with PAR and R:FR levels considered as independent fixed factors. The effects of PAR and R:FR levels on coefficients a and b were tested by comparing whether or not the same regression model can be used in different treatments using an F-test ($P < 0.05$) of SAS (SAS Institute Inc., Cary, NC, USA).

Results

Plant responses to reductions in PAR and R:FR

Reductions in PAR decreased plant height, total leaf area, number of leaves and area of individual leaves while it did not significantly affect other architectural traits (Table 3.1, Figure S3.1). Reductions in PAR decreased the maximum leaf photosynthetic rate (A_{max}) and dark respiration rate (R_d) while it did not significantly affect other photosynthetic parameters (Figure 3.1A-D, Table S3.2). The coefficient a (in Eq. 3.2), representing the R_d to A_{max} ratio,

was decreased by reductions in PAR (Figure 3.1E). The coefficient b (in Eq. 3.3), describing the relationship between light gradient and A_{max} gradient in the canopy, was only slightly increased by reductions in PAR (Figure 3.1F).

Reductions in R:FR increased plant height, internode length and leaf inclination angle while it did not significantly affect total leaf area, number of leaves and area of individual leaves (Table 3.1, Figure S3.2). The curvature of light response curve (θ) was decreased by reductions in R:FR under high PAR, and reductions in R:FR also tended to decrease θ at medium PAR, albeit not significantly (Figure 3.1D, Table S3.2). All other leaf photosynthetic parameters were not significantly affected by R:FR (Figure 3.1A-C, Table S3.2). Reductions in R:FR tended to increase b (Figure 3.1F), indicating that the decline in A_{max} from more illuminated leaves in the top of the canopy to the more shaded ones lower down might be steeper in low R:FR plants than in high R:FR plants. Reductions in R:FR did not significantly affect a (Figure 3.1E).

Evaluation of the FSP model of rose

The plant total leaf areas and plant heights simulated with our model were closely aligned with the measured values (Figure 3.2A, B), i.e., the regression lines were very close to the line of 1:1 correspondence. The regression line for simulated values vs. measured values of the fraction of light intercepted by the plants was also very close to the line of 1:1 correspondence, indicating that on average the model gave a good estimate of the fraction of light interception (Figure 3.2C). However, the r^2 of the regression line was relatively low, indicating a fair amount of scatter around the line; indeed in individual cases simulated values deviated up to 15% from measured values. Overall we conclude that the model gave a representation of plant architecture sufficient for the purpose of this study, as also illustrated in Figure 3.3, and gave a reasonable prediction of the fraction of light interception.

Table 3.1. Measured effects of reductions in photosynthetically active radiation (PAR) and red to far-red ratio (R:FR) on architectural traits at plant level and organ level (an example of internode and leaf at rank 6). Values are mean ± SE from three statistical replicates, each of which includes five plants. *ns* indicates a non-significant effect, + indicates a significantly positive effect, and – indicates a significantly negative effect according to the statistical test using a simple linear regression model ($P < 0.05$).

Treatment		Plant level			Organ level (rank 6)		
PAR	R:FR	Plant height (cm)	Total leaf area (cm^2)	Number of leaves	Internode length (cm)	Leaf area (cm^2)	Leaf inclination angle (°)
High	High	62.6±0.4	778±24	12.0±0.2	5.0±0.1	86.9±3.3	28.9±2.1
High	Medium	66.7±1.8	781±46	11.7±0.1	5.4±0.1	87.8±3.4	37.8±3.4
High	Low	66.0±1.1	740±22	11.1±0.3	5.3±0.2	90.2±0.5	39.9±2.9
Medium	High	60.0±1.5	714±8	11.4±0.2	5.0±0.1	76.8±0.7	32.5±5.0
Low	High	52.9±2.0	629±24	11.2±0.1	4.7±0.2	69.8±1.7	31.5±3.4
Reduction of R:FR		+	*ns*	*ns*	+	*ns*	+
Reduction of PAR		–	–	–	*ns*	–	*ns*

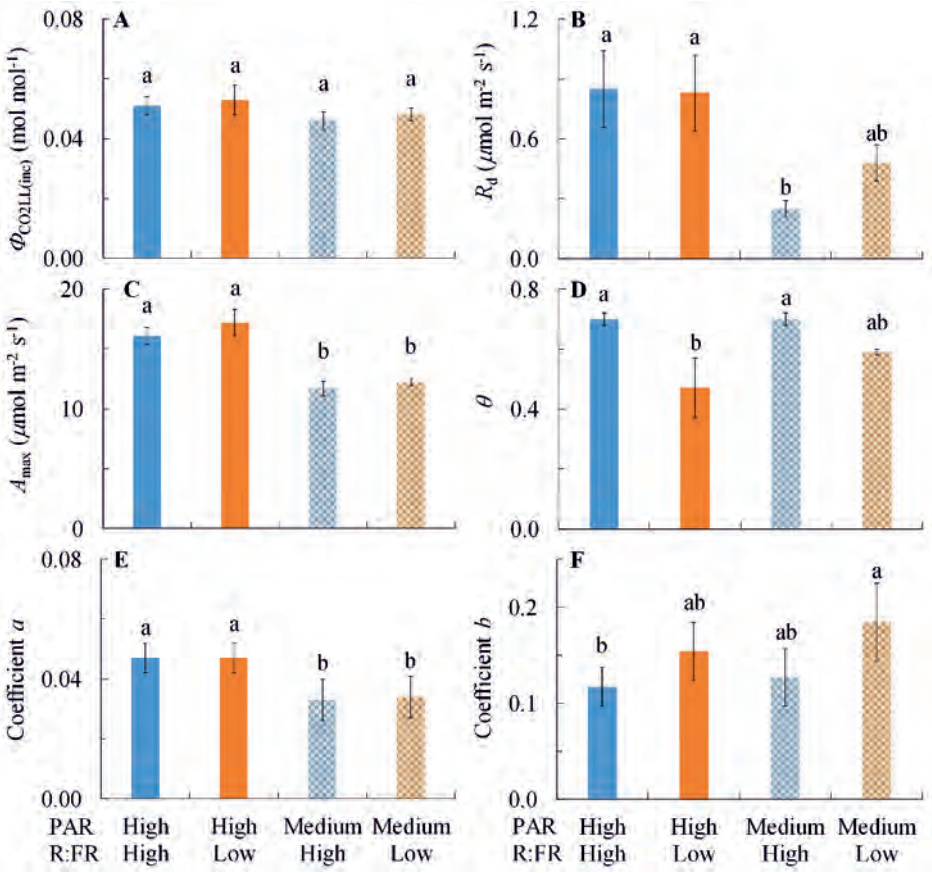

Figure 3.1. Measured effects of photosynthetically active radiation (PAR) and red to far-red ratio (R:FR) on photosynthetic parameters of top leaves in the canopy: (A) quantum efficiency ($\Phi_{CO2LL(inc)}$), (B) dark respiration rate (R_d), (C) maximum leaf photosynthetic rate (A_{max}) and (D) the curvature of the light response curve (θ), and effects of reductions in PAR and R:FR on (E) coefficient a, describing the relationship between A_{max} and R_d in Eq. 3.2: $R_d = a \times A_{max}$ and (F) coefficient b, describing the relationship between light gradient and A_{max} gradient in the canopy in Eq. 3.3: $A_{max,0}/A_{max,top} = (Q_0/Q_{top})^b$. The error bars denote 1SE of means (A-D) or estimations (E, F). Different letters indicate significant difference ($P < 0.05$) according to one-way ANOVA (A-D) or F-test (E, F).

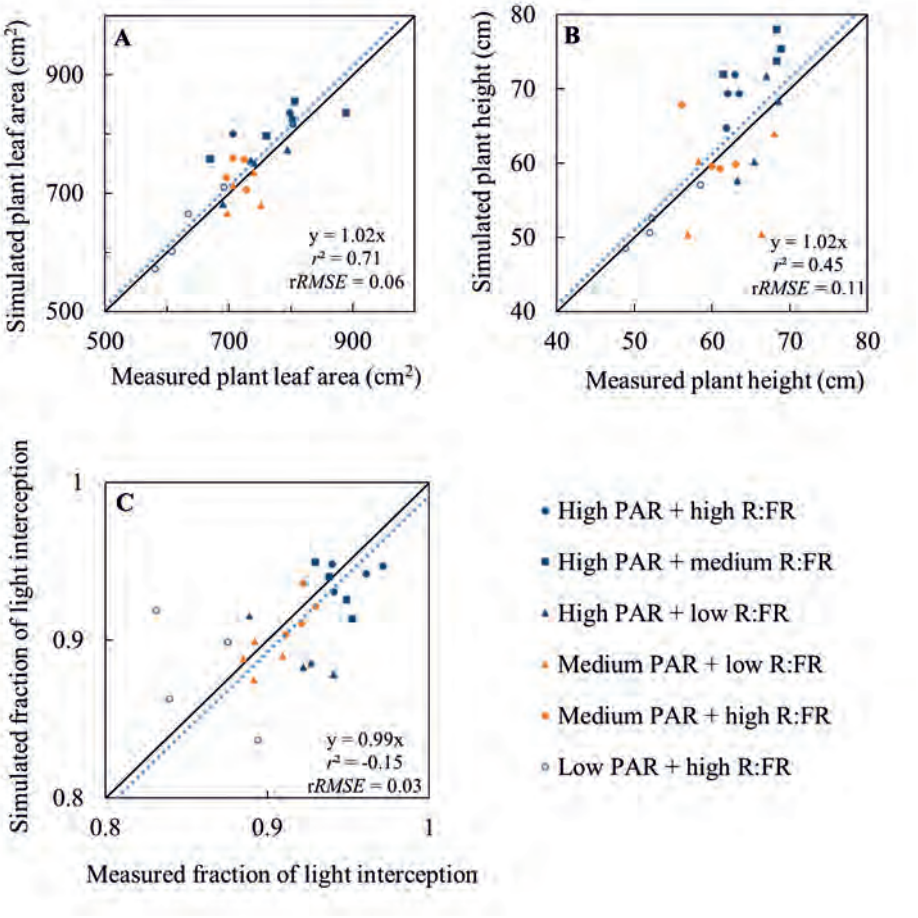

Figure 3.2. The comparisons between measured and simulated results in different photosynthetically active radiation (PAR) and red to far-red ratio (R:FR) treatments. The comparisons were conducted for (A) plant total leaf area, (B) plant height, and (C) the fraction of light intercepted by the plants. Each symbol represents the measured and simulated value for one treatment plot. The equation in each panel represents the linear regression of simulated (y) vs. measured (x) values by forcing the line through the origin, r^2 is the determination coefficient of the regression, and r*RMSE* is the relative root-mean-square error.

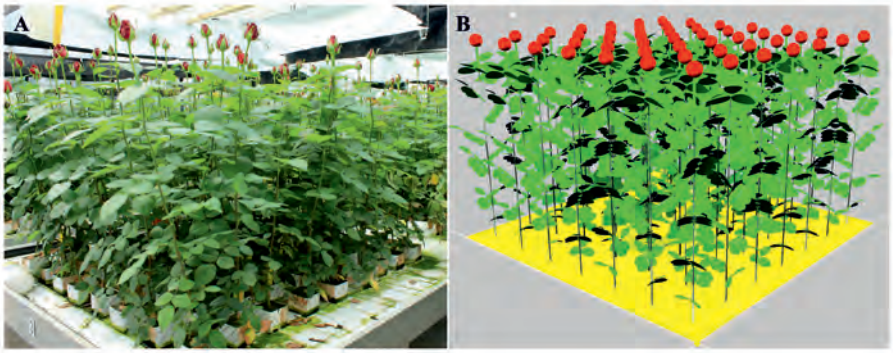

Figure 3.3. A comparison of real and virtual rose plants. (A) A rose plant population in the experiment at flowering stage. (B) A simulated rose population at flowering stage.

Effects of plant plasticity to reductions in PAR and R:FR on light interception and plant photosynthesis

Under simulated canopy shading, reductions in R:FR happened earlier than reductions in PAR (Figure 3.4). By using the simulation model, it was shown that plasticity in plant architecture as a whole (i.e., introducing the combined effects of R:FR and PAR on internode length, leaf angle and leaf area) decreased the fraction of light interception, and this effect (i.e., E calculated with Eq. 3.5) increased with canopy shading from –2% at an LAI_C of 0.5 m^2 m^{-2} to –10% at an LAI_C of 3 m^2 m^{-2} (Figure 3.5). Decreased leaf area by reductions in PAR had the largest effect on the fraction of light interception (–1% to –8%), followed by increased leaf inclination angle by reductions in R:FR that slightly decreased the fraction of light interception (–1% to –2%), while increased internode length hardly affected the fraction of light interception (Figure 3.5).

Plant plasticity as a whole (i.e., 'Full phenotype'; the combination of all plastic trait responses to the combination of reduced PAR and reduced R:FR) decreased plant net photosynthesis by –7% to –8% at mild shade levels (LAI_C = 0.5 and 1 m^2 m^{-2}) but increased net photosynthesis by 10% to 83% at heavy shade levels (LAI_C = 2 and 3 m^2 m^{-2}) (Figure 3.6A). The relative contribution to these effects by the plastic responses to the two shading factors (i.e., reduced

PAR and reduced R:FR) tended to be in the opposite direction and depended on the level of shading. At mild shade levels, the reduction in photosynthesis was mainly caused by plasticity to reduced R:FR. Conversely, at heavy shade levels, the increase in photosynthesis was mainly caused by plasticity to reduced PAR (Figure 3.6A).

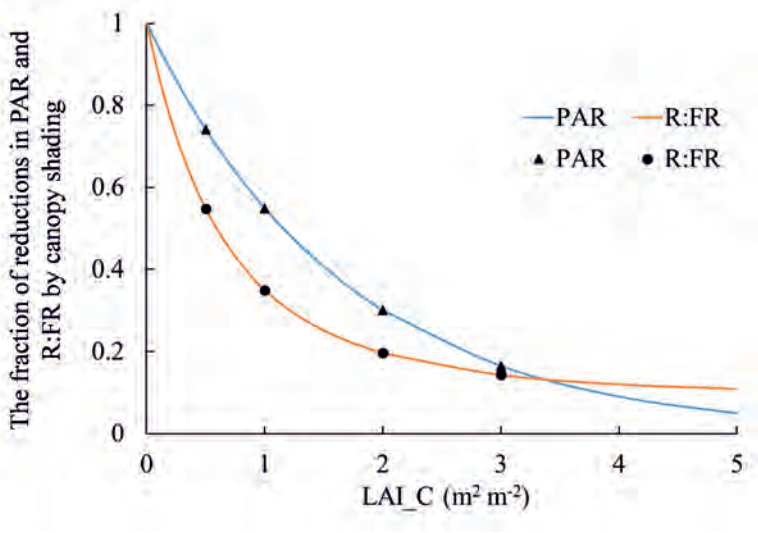

Figure 3.4. The fraction of reductions in photosynthetically active radiation (PAR) and red to far-red ratio (R:FR) by canopy shading of leaf area index (LAI_C) at different levels. Lines are simulated results. Triangles and circles are the relative PAR and R:FR levels at LAI_C = 0.5, 1, 2 and 3 m^2 m^{-2}.

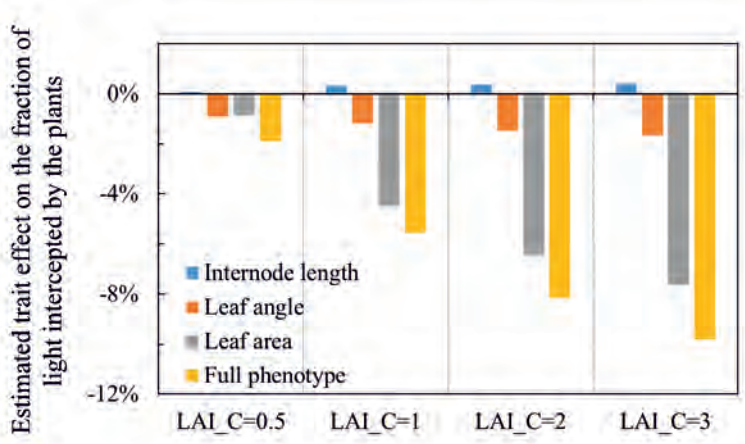

Figure 3.5. Estimated trait effects on the fraction of light intercepted by the plants. Trait effects were estimated for plant architectural trait responses to reduced photosynthetically active radiation (PAR) (i.e., leaf area), to reduced red to far-red ratio (R:FR) (i.e., internode length and leaf angle), and to the combination of the two (i.e., 'Full phenotype') on the fraction of light intercepted by the plants under canopy shading caused by a leaf area index (LAI_C) of 0.5, 1, 2 and 3 m^2 m^{-2}. Trait effects were calculated as the relative changes of light intercepted by plants caused by changing targeted traits compared with light intercepted by the non-shaded plant phenotype (see Eq. 3.5 for the calculation). 'Full phenotype' represents the phenotype that plastic trait responses to both reduced PAR and reduced R:FR are changed simultaneously.

Among all plastic traits, plasticity in leaf photosynthetic characteristics (i.e., changes in θ and b by reduced R:FR, changes in A_{max} and a by reduced PAR) had a larger effect on plant photosynthesis than plasticity in plant architecture (i.e., changes in internode length and leaf inclination angle by reduced R:FR, changes in leaf area by reduced PAR) (Figure 3.6B). Among all plastic trait responses to reduced PAR, changes in a had the largest effects on plant photosynthesis (4% to 94%) at all shade levels, followed by changes in A_{max} (–3% to 72%; note that the effect of A_{max} was both direct through changes in A_{max} itself and indirect through changes in R_d, see Eq. 3.2) and leaf area (–2% to 13%). With the increased shading, all trait responses to reduced PAR tended to more positively affect photosynthesis (Figure 3.6B).

Among all plastic trait responses to reduced R:FR, the relative effect of changes in b on plant photosynthesis increased (1% to 14%) while the relative effect of plasticity in θ became more negative (−7% to −9%) with increasing shade. Changes in internode length and leaf inclination angle only slightly affected plant photosynthesis compared with other trait effects (Figure 3.6B).

Interactions between effects of trait responses to reductions in PAR and R:FR on plant photosynthesis

Effects of individual plastic trait responses to reduced PAR on plant photosynthesis negatively interacted with each other (Figure 3.7A), in that effects of combined trait responses on plant photosynthesis were less positive than when effects of individual trait responses were added. This negative interaction was mainly caused by the negative interaction between the effect of changing A_{max} and the effect of changing a on plant photosynthesis (Figure 3.7B); i.e., the marginal effect of lowering R_d by reducing a (Eq. 3.2) became less when R_d had already been reduced by lowering A_{max}. In addition, effects of changing A_{max} and a on plant photosynthesis became less when leaf area was also reduced (Figure 3.7B). Conversely, there was hardly any interaction between effects of trait responses to reduced R:FR (Figure 3.7A). Further analysis showed that interactions between each low-R:FR response were very small and occurred in both positive and negative directions (Figure S3.3), possibly compensating each other leading to overall no interaction between the effects of individual low-R:FR responses.

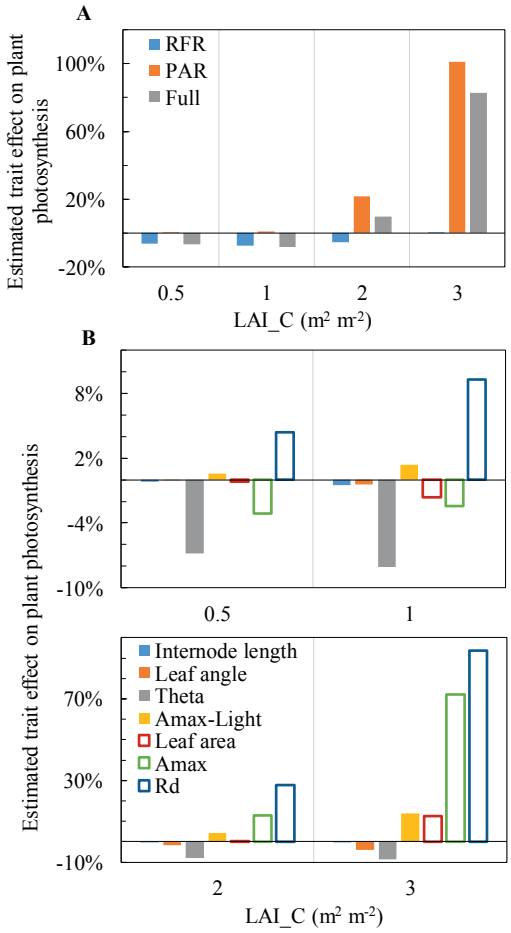

Figure 3.6. Estimated effects of (A) the combination of plastic traits and (B) individual plastic traits on plant photosynthesis under canopy shading caused by a leaf area index (LAI_C) of 0.5, 1, 2 and 3 m^2 m^{-2}. Trait effects are calculated as the relative changes of plant photosynthesis by changing targeted traits compared with plant photosynthesis of non-shaded plant phenotype (see Eq. 3.5 for the calculation). In panel (A), 'RFR' represents the phenotype that all plastic trait responses to reduced red to far-red ratio (R:FR) are changed simultaneously; 'PAR' represents the phenotype that all plastic trait responses to reduced photosynthetically active radiation (PAR) are changed simultaneously; 'Full' represents the phenotype that all plastic trait responses to both reduced R:FR and reduced PAR are changed simultaneously. In panel (B), solid bars are plastic trait responses to reduced R:FR; open bars are plastic trait responses to reduced PAR; Theta' is the curvature factor θ of light response curve; 'Amax' is the maximum leaf photosynthetic rate A_{max}; 'Amax-Light' is the coefficient b describing the correlation between light gradient and A_{max} gradient in the canopy; 'Rd' is the coefficient a describing the relationship between A_{max} and dark respiration rate.

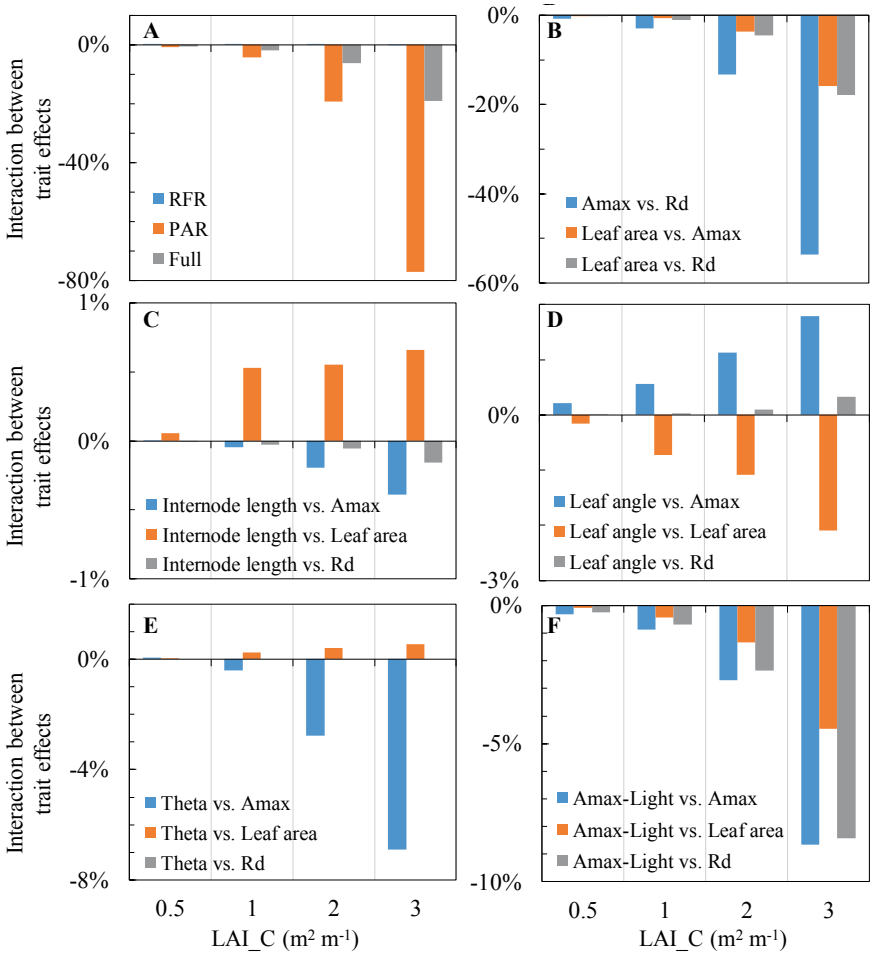

Figure 3.7. Estimated interaction between effects of plastic trait responses on plant photosynthesis under canopy shading caused by a leaf area index (LAI_C) of 0.5, 1, 2 and 3 m^2 m^{-2}. Interactions of trait effects are calculated as the differences between the combined effects of changing all targeted traits on plants photosynthesis and the additive effects of separately changing individual targeted traits on plant photosynthesis (see Eq. 3.6 for the calculation). In panel (A), 'RFR' represents the interaction between effects of all plastic trait responses to reduced red to far-red ratio (R:FR); 'PAR' represents the interaction between effects of all plastic trait responses to reduced photosynthetically active radiation (PAR); 'Full' represents the interaction between effects of all trait combination to reduced R:FR and all trait combination to reduced PAR. In panel (B), each bar represents the interaction between the effects of two individual low-PAR responses. In panel (C)-(F), each bar represents the interaction between the effect of an individual low-R:FR response and the effect of an individual low-PAR response. Detailed descriptions of trait names can be found in Figure 3.6.

The negative interaction also existed between the effect of 'PAR' phenotype (i.e., the combination of all plastic trait responses to reduced PAR) and the effect of 'RFR' phenotype (i.e., the combination of all plastic trait responses to reduced R:FR) on plant photosynthesis (Figure 3.7A). This indicates that the effects of 'Full' phenotype on plant photosynthesis were more negative under mild shade levels and were less positive under heavy shade levels than when the effects of 'PAR' phenotype and 'RFR' phenotype were added (as also shown in Figure 3.6A). The negative interaction between the effects of 'PAR' phenotype and 'RFR' phenotype on plant photosynthesis was mainly caused by the interaction between θ and A_{max} (i.e., the effect of changing A_{max} is smaller when θ is reduced; Figure 3.7E) and the interaction between b and all low-PAR trait responses (changes in A_{max}, leaf area and a) (i.e., the effect of changing the distribution of A_{max} in the canopy is smaller when A_{max} itself is lower, when leaf area is reduced, and when R_d to A_{max} ratio is lower; Figure 3.7F). Some trait effects (e.g., those of internode length and leaf area) interacted positively with each other, but these interactive effects were small (< 2%, Figure 3.7C-E).

Discussion

The relative importance of individual shade responses for plant photosynthesis changes with shade level

Understanding the adaptive significance of plastic trait responses to canopy shading involves quantifying how responses to the individual shading factors interact in determining plant functions such as plant photosynthesis. Here, we showed that plastic responses to reduced PAR and reduced R:FR involve different traits, and that effects of plastic responses to these two shading factors on plant photosynthesis are different and can operate in opposite directions. In addition, the directions of individual trait effects and their relative importance changed with the level of canopy shading itself, being that effects of responses to low R:FR were more dominant at mild shading while effects of responses to low PAR dominated at heavy shading (Figure 3.6A, Figure 3.8). This is in line with the common view that reductions in R:FR operate as an early warning signal for future shading, in contrast to drops in PAR which are only occurring while shading is occurring (Ballaré, 1999).

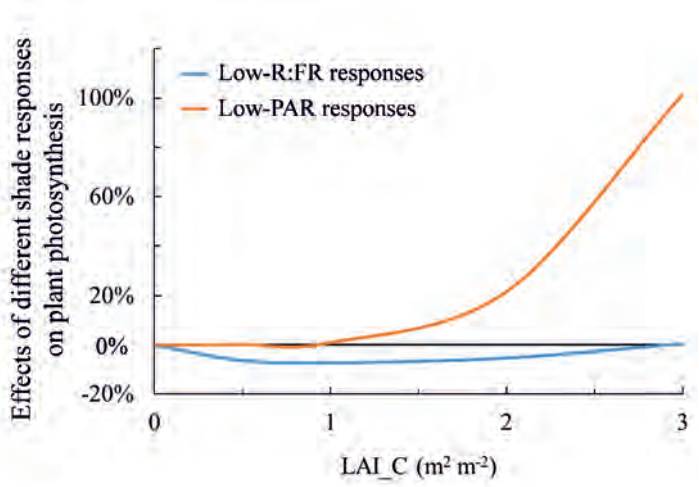

Figure 3.8. Concept figure of changing dominant factor that affects plant photosynthesis with the increasing level of canopy shading (LAI_C).

In early stages of canopy development, plants could immediately experience significant reductions in R:FR when reductions in PAR are still absent or relatively minor (Ballaré, 1999), as also found in our simulations (Figure 3.4). Therefore, low R:FR is widely considered as an early warning signal for plants about proximity of neighbours, and the subsequent shade avoidance responses are considered to improve plant performance by preventing plants from becoming shaded (Ballaré, 1999; Vandenbussche *et al.*, 2005). However, in our simulations in which constant shade was considered, effects of these low-R:FR responses on plant photosynthesis were negative, and these effects were also larger than the effects of low-PAR responses at mild shade levels (Figure 3.6A, Figure 3.8). Moreover, leaf physiological changes induced by low R:FR (i.e., changes in curvature of light response curves and the correlation between light gradient and A_{max} gradient in the canopy) had a relatively large impact on plant photosynthesis compared to typically observed shade avoidance responses in plant architecture (i.e., internode elongation and leaf hyponasty) (Figure 3.6B). These results suggest that apart from the well-observed architectural responses to reduced R:FR, leaf physiological responses to reduced R:FR also substantially affect plant performance. When plant architectural

responses do not lead to a higher light acquisition, overall responses to low R:FR are not beneficial to plant photosynthesis.

With the canopy fully developing, plants experience continuing reductions in PAR while the R:FR ratios stay at constantly low levels (Figure 3.4). Under heavy shading, effects of plasticity to low PAR on plant photosynthesis became larger than effects of plasticity to low R:FR (Figure 3.6A, Figure 3.8), indicating that plasticity to low PAR is high under heavy shading. In contrast to the negative effect of low-R:FR responses on plant photosynthesis, plastic trait responses to low PAR had a positive effect on plant photosynthesis (Figure 3.6A). This indicates that under canopy shading, it is the plant response to low PAR rather than the response to low R:FR, which helps maintaining a positive carbon balance. The positive effect of trait responses to low PAR on plant photosynthesis was mainly caused by responses that reduce respiration costs (Figure 3.6B). In our simulations, lower R_d associated with the decreases in both A_{max} and the R_d to A_{max} ratio (= a) (Figure 3.6B). Under low light, both A_{max} and R_d have been found to decrease (Sims & Pearcy, 1991; Walters *et al.*, 1993), as also found in our experiment (Figure 3.1B, C). Furthermore, R_d has been found to decrease more strongly than A_{max} (Sims & Pearcy, 1991), as also suggested by our result that R_d to A_{max} ratio decreased by reductions in PAR (Figure 3.1E). Although the lower leaf area and lower A_{max} hardly affected net plant photosynthesis at mild shading, the reduction in respiration associated with lower leaf area and A_{max} positively affected net plant photosynthesis (Figure 3.6B). Further analysis indicates that if A_{max} and R_d were not correlated, the lower A_{max} itself would reduce plant photosynthesis (Figure S3.4). Walters & Reich (2000) showed that under low light conditions, minimizing carbon loss is more beneficial to plants than maximizing carbon gain. This result is in concert with ours showing that under canopy shading, plant plasticity to low PAR is beneficial to plant carbon balance due to reduced respiration costs.

Effects of low-R:FR responses and low-PAR responses on plant photosynthesis negatively interact

Interactions occurred between effects of low-R:FR responses and effects of low-PAR responses on plant photosynthesis (Figure 3.7A). The effect of shade responses as a whole on plant photosynthesis was more negative at mild shading and less positive at heavy shading than if effects of low-R:FR responses and low-PAR responses of individual traits would be added (Figure 3.6A). This negative interaction was mainly caused by interactions between

effects of individual low-PAR responses and the effect of low R:FR induced changes in the correlation between light gradient and A_{max} gradient (Figure 3.7F). A steeper decline of this correlation (i.e., a higher *b* value) means the heavy shaded leaves lower in the canopy have less photosynthetic capacity, resulting in less respiration costs in these leaves. This could potentially improve photosynthesis of the whole plant especially at heavy shading (Figure 3.6B) when leaves in the lower canopy hardly receive any light resource for photosynthesis and these leaves are mainly consuming rather than producing assimilates. When R_d to A_{max} ratio and leaf area decreases, reductions in respiration costs resulted from the decreased photosynthetic capacity of shaded leaves would become less due to the negative interactions of A_{max} vs. R_d to A_{max} ratio and A_{max} vs. leaf area (Figure 3.7B). However, when A_{max} itself decreases, the more illuminated leaves at upper canopy have less capacity for photosynthesis as well, resulting in the interactive effect of *b* and A_{max} on plant photosynthesis in a negative direction (Figure 3.7F).

More generally these results show that effects of low-PAR responses on plant photosynthesis depend on effects of low-R:FR responses and vice versa. This suggests that if there is genetic variation in plant plasticity to different shading factors (reduced PAR and reduced R:FR), selection for plasticity to one shading factor depends on the level of plasticity to the other factor. This result further connects to the broader literature on divergent evolution of shade responses, which has shown differentiation in plasticity to low R:FR between ecotypes from different shade habitats. Typically ecotypes e.g. in the annuals *Impatiens capensis* from forest habits experiencing shading from taller plants show much reduced low-R:FR responses compared with grassland ecotypes experiencing from more similar sized plants (Dudley & Schmitt, 1995; Donohue & Schmitt, 1999; Donohue *et al.*, 2000; Huber *et al.*, 2004; Anten *et al.*, 2009). The question arising from our work is whether this divergence also involved a different balance between responses to low R:FR and low PAR.

Limitations of this study and future perspectives

Essentially, our simulations mimic the situation whereby target plants are shaded by an overhead canopy. This situation is commonly found in forest understory, or in certain intercropping and agro-forestry systems. However, as noted, plants also often experience canopy shading caused by crowding of similar-sized neighbours (e.g., high plant density), which, while not necessarily taller than target plants, still cause reductions in R:FR and the amount of PAR available for individual plants. In those situations, responses to low R:FR

maybe be relatively more important than those to low PAR. We did not simulate those situations because our experiments did not allow us to make reasonable assumptions to create reliable virtual phenotypes in crowding populations. However, if combined with appropriate experiments, the modelling approach presented in our study could account for those situations too.

We quantified the effects of all plastic trait responses observed under canopy shading and compared their relative importance by using a combination of experiments and modelling. To our knowledge, this has not been done before. The relative importance of plastic responses to low PAR and low R:FR changed with the increasing level of canopy shading, being that low-R:FR responses had a dominant effect on plant photosynthesis at mild shading whereas low-PAR responses became dominating at heavy shading. Moreover, low-R:FR responses and low-PAR responses interacted functionally with each other, mostly in negative directions, indicating that the adaptive significance of- and thus selection for- plasticity to one shading factor is dependent on the plasticity to the other factor. Like canopy shading, other environmental changes may involve multiple factors, e.g., wind involves both mechanical stress and micro-climatic changes (Anten *et al.*, 2010). A combination of experiments that can separate individual environmental factors and FSP modelling is a useful tool to disentangle the effects of individual plastic architectural and physiological trait responses to these factors on plant performance and to investigate the interactions between trait effects.

Conclusions

Phenotypic plasticity to shading in vegetation stands entails both physiological and architectural responses to reduced PAR and R:FR. The effects of these responses on plant photosynthesis can operate in opposite directions and can be strongly inter-dependent. The relative importance of these responses on plant photosynthesis also changes with the level of shade. Our results indicate that environmental changes entail multiple factors that induce plasticity in different traits, and the effects of plasticity in one trait on plant performance strongly depend on the level of plasticity in another.

Supporting information

Table S3.1. Information on the actual reductions in photosynthetically active radiation (PAR) and red to far-red ratio (R:FR) achieved in different light treatments.

Treatments		Actual levels	
PAR	R:FR	PAR	R:FR
High	High	100%	1.05
Medium	High	60%	0.94
Low	High	29%	0.93
High	Medium	100%	0.36
High	Low	100%	0.25
Medium	Low	70%	0.16

Table S3.2. Measured effects of reductions in photosynthetically active radiation (PAR) and red to far-red ratio (R:FR) on photosynthetic parameters of leaves at up, middle and low levels in the canopy ($\Phi_{CO2LL(inc)}$, quantum efficiency; R_d, respiration rate; A_{max}, maximum leaf photosynthetic rate; θ, the curvature of the light response curve). Values are mean±1SE. *ns* indicates a non-significant effect and – indicates a significantly negative effect according to ANOVA ($P<0.05$).

Treatment		$\Phi_{CO2LL(inc)}$ (mol CO_2 mol^{-1} photon)			R_d (μmol m^{-2} s^{-1})			A_{max} (μmol m^{-2} s^{-1})			θ		
PAR	R:FR	Up leaf	Middle leaf	Low leaf	Up leaf	Middle leaf	Low leaf	Up leaf	Middle leaf	Low leaf	Up leaf	Middle leaf	Low leaf
High	High	0.051 ±0.003	0.052 ±0.004	0.048 ±0.003	0.85 ±0.19	0.53 ±0.19	0.45 ±0.09	16.1 ±0.7	14.0 ±1.2	10.7 ±1.1	0.70 ±0.02	0.71 ±0.03	0.71 ±0.03
High	Low	0.053 ±0.005	0.056 ±0.003	0.047 ±0.004	0.83 ±0.19	0.77 ±0.14	0.35 ±0.09	17.2 ±1.1	16.1 ±1.2	10.0 ±0.5	0.47 ±0.10	0.56 ±0.05	0.46 ±0.05
Medium	High	0.046 ±0.003	0.053 ±0.003	0.041 ±0.004	0.25 ±0.04	0.50 ±0.21	0.19 ±0.16	11.7 ±0.6	10.8 ±0.8	7.9 ±0.6	0.70 ±0.02	0.76 ±0.02	0.72 ±0.04
Medium	Low	0.048 ±0.002	0.052 ±0.005	0.045 ±0.002	0.48 ±0.09	0.25 ±0.09	0.28 ±0.04	12.2 ±0.3	10.0 ±0.6	8.2 ±0.8	0.59 ±0.01	0.61 ±0.04	0.58 ±0.06
Reduced PAR		*ns*	*ns*	*ns*	–	*ns*	*ns*	–	–	–	*ns*	*ns*	*ns*
Reduced R:FR		*ns*	*ns*	*ns*	*ns*	*ns*	*ns*	*ns*	*ns*	*ns*	–	–	–
Reduced PAR × reduced R:FR		*ns*	*ns*	*ns*	*ns*	*ns*	*ns*	*ns*	–	*ns*	*ns*	*ns*	*ns*

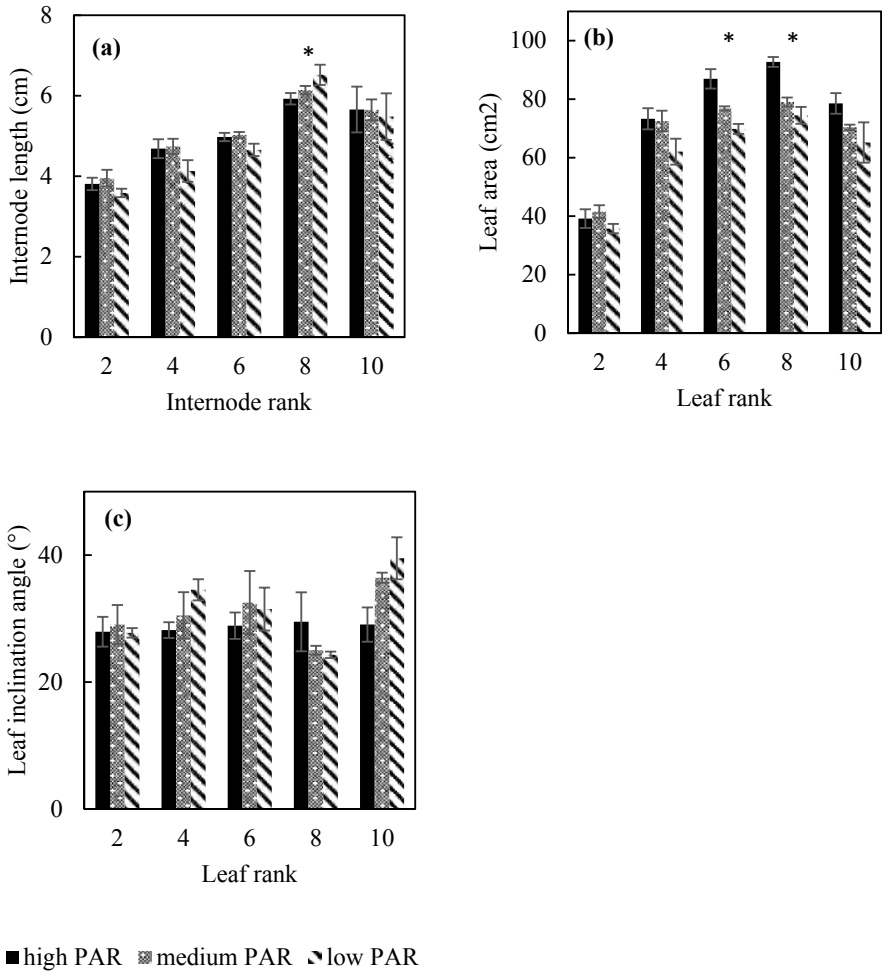

Figure S3.1. Measured effects of reductions in photosynthetically active radiation (PAR) under high red to far-red ratio on plant architectural traits. Measurements were conducted on internode length (a), leaf area (b), and leaf inclination angle (c) for the even numbered leaf ranks (counted from the base) of rose stems. Error bars represent 1SE. * indicates a significant effect according to a simple linear regression model ($P<0.05$).

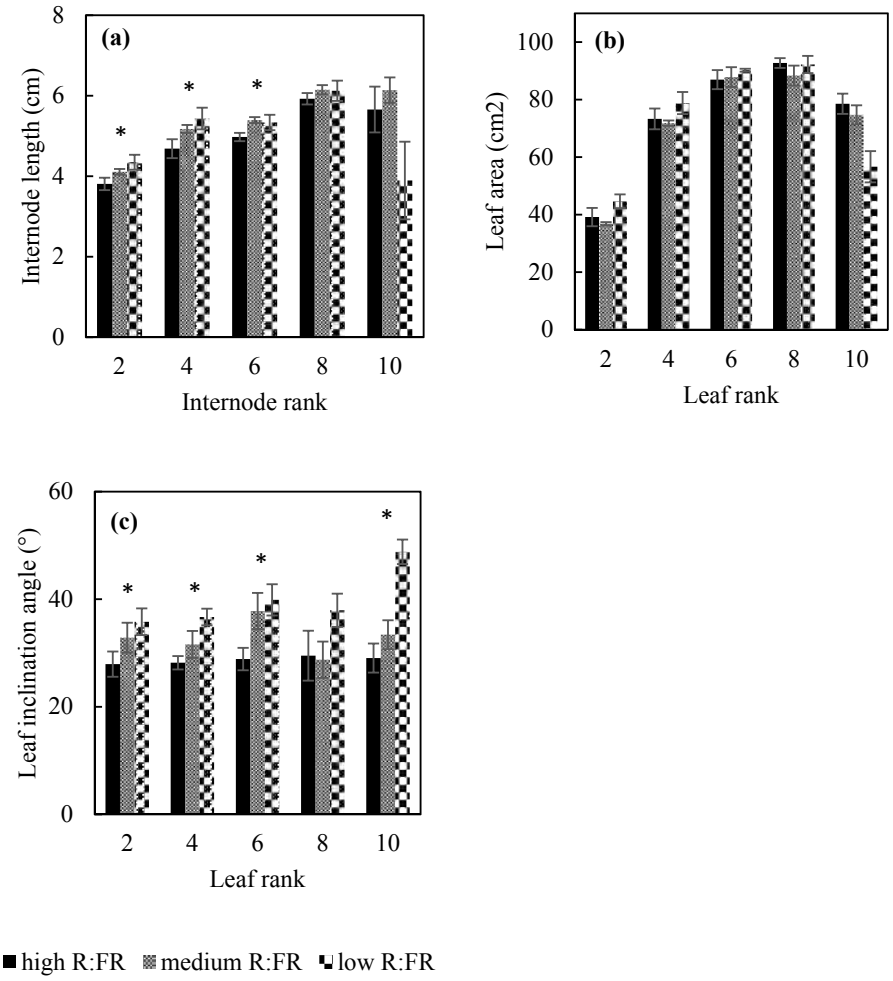

Figure S3.2. Measured effects of reductions in red to far-red ratio (R:FR) under high photosynthetically active radiation on plant architectural traits. Measurements were conducted on internode length (a), leaf area (b), and leaf inclination angle (c) for the even numbered leaf ranks (counted from the base) of rose stems. Error bars represent 1SE. * indicates a significant effect according to a simple linear regression model ($P<0.05$).

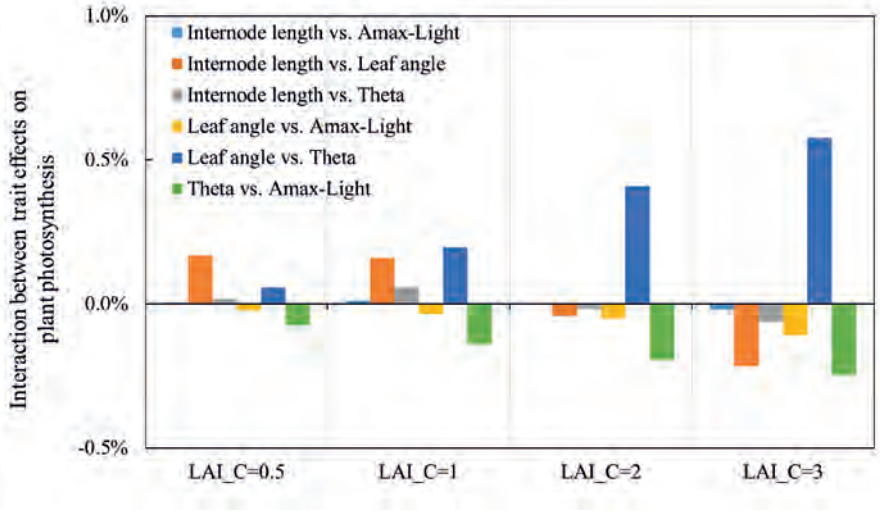

Figure S3.3. Estimated interactions between trait effects on plant photosynthesis. The interactions were estimated between effects of individual trait responses to low red to far-red ratio on plant photosynthesis under canopy shading caused by a leaf area index (LAI_C) of 0.5, 1, 2 and 3 m^2 m^{-2}. Each bar represents the interaction between two individual traits. 'Theta' is the curvature factor θ of light response curve; 'Amax-Light' is the coefficient b describing the correlation between light gradient and the gradient of leaf photosynthetic capacity in the canopy.

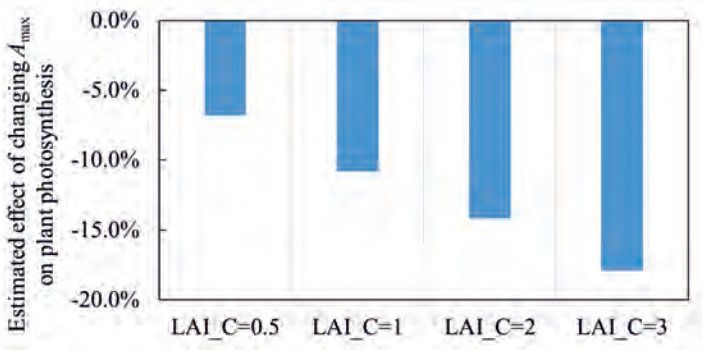

Figure S3.4. Estimated effect of plasticity in leaf photosynthetic capacity (A_{max}) on plant photosynthesis. The estimations were calculated at shade levels caused by a leaf area index (LAI_C) of 0.5, 1, 2 and 3 m^2 m^{-2}, without considering the correlation between changing A_{max} and the dark respiration rate.

Method S3.1. Estimating leaf photosynthetic parameters

The combined measurement of gas exchange and chlorophyll fluorescence was used to determine a set of photosynthetic parameters as reported in the main text, using the method as described by Yin *et al* (2009, 2014). Compared with conventional photosynthetic parameter estimations, this method explores the decrease of the operating photosystem II photochemical efficiency with increasing irradiance, which is likely more relevant to crops grown in relatively low light environment such as in the greenhouse.

The operating efficiency of photosystem II (PSII) photochemistry (Φ_2) at each irradiance level was measured from fluorescence signals, according to Genty *et al* (1989), as:

$$\Phi_2 = 1 - F_s/F'_m \quad \text{(S3.1)}$$

where F_s is the steady-state fluorescence and F_m' is the maximum fluorescence. F_s and F_m' were obtained directly from the combined gas exchange and chlorophyll fluorescence measurements.

First, according to Yin *et al* (2009), the decrease of Φ_2 with increasing irradiance can be fitted to the equation below:

$$\Phi_2 = (\alpha_{2LL} I_{abs} + J_{2max} - \sqrt{(\alpha_{2LL} I_{abs} + J_{2max})^2 - 4\beta J_{2max} \alpha_{2LL} I_{abs}})/(2\beta\rho_2 I_{abs}) \quad \text{(S3.2)}$$

in which $\rho_2 = \alpha_{2LL}/\Phi_{2LL}$ (S3.3)

$$\alpha_{2LL} = \Phi_{2LL} \times (1 - f_{cyc})/(\frac{\Phi_{2LL}}{\Phi_{1LL}} + (1 - f_{cyc})) \quad \text{(S3.4)}$$

where I_{abs} is the irradiance absorbed by the leaf, which is calculated as I_{inc} multiplied by leaf absorbance; J_{2max} (μmol m^{-2} s^{-1}) is the total rate of electron transport passing PSII under saturating irradiance; β is the curvature factor; ρ_2 is the factor of excitation partitioning to PSII; α_{2LL} (mol e$^-$ mol^{-1} photon) is the PSII photochemical efficiency under strictly limiting light on the basis of light absorbed by both PSI and PSII; Φ_{1LL} (mol e$^-$ mol^{-1} photon) is the photochemical efficiency of PSI and a value of 1.0 can be used for C_3 species; f_{cyc} is the fraction of cyclic electron transport in the total electron flux passing PSI and a value of 0.05 can be

used for C_3 species (Yin *et al.*, 2014). The estimated from Φ_{2LL} from this fitting does not depend on the pre-set values of Φ_{1LL} and f_{cyc}.

Next, using the combined measurements of net rate of photosynthesis (A, mol CO_2 m^{-2} s^{-1}) and Φ_2 at different incident irradiance levels (I_{inc}, μmol m^{-2} s^{-1}), a lumped parameter s' and the respiration rate in the light or called day respiration (R_d, μmol CO_2 m^{-2} s^{-1}) were estimated, based on the linear regression equation (Yin *et al.*, 2014):

$$A = s'\left(\frac{I_{inc}\Phi_2}{4}\right) - R_d \tag{S3.5}$$

Thirdly, according to Yin *et al* (2014), the quantum yield of CO_2 assimilation on the basis of incident light ($\Phi_{CO2LL(inc)}$, mol CO_2 mol^{-1} photon) was calculated as:

$$\Phi_{CO2LL(inc)} = s'\Phi_{2LL}/4 \tag{S3.6}$$

where Φ_{2LL} (mol e^- mol^{-1} photon) and the lumped parameters s' were estimated in the preceding steps.

Finally, with the $\Phi_{CO2LL(inc)}$ and R_d estimated above, the maximum leaf photosynthetic rate at the saturating incident irradiance level (A_{max}, μmol CO_2 m^{-2} s^{-1}) and the curvature factor of the light response curve (θ) were estimated by fitting the gas exchange measurements to the non-hyperbola rectangular equation below:

$$A = \frac{\Phi_{CO2LL(inc)}I_{inc}+A_{max}-\sqrt{(\Phi_{CO2LL(inc)}I_{inc}+A_{max})^2-4\theta A_{max}\Phi_{CO2LL(inc)}I_{inc}}}{2\theta} - R_d \tag{S3.7}$$

Chapter 4

Quantifying the contribution of bent shoots to plant photosynthesis and biomass production of rose flower shoots

Ningyi Zhang[1,2], Arian van Westreenen[1,2], Jochem B. Evers[2], Niels P.R. Anten[2], Leo F.M. Marcelis[1]

[1] Horticulture and Product Physiology Group, Wageningen University, Wageningen, The Netherlands

[2] Centre for Crop Systems Analysis, Wageningen University, Wageningen, The Netherlands

Abstract

Background and Aims The success of using bent shoots in cut-rose (*Rosa hybrida*) production to improve flower shoot quality has been attributed to bent shoots capturing more light and thus providing more assimilates for flower shoot growth. We aimed at quantifying this contribution of photosynthesis by bent shoots to flower shoot growth.

Methods Rose plants were grown with four upright flower shoots and with 0, 1 or 3 bent shoots per plant. Plant architectural traits, leaf photosynthetic parameters and organ dry weight were measured. A three-dimensional simulation model of rose was used to calculate photosynthesis of upright shoots and bent shoots separately.

Key Results We found that plant traits relevant to flower shoot quality (e.g., stem length and shoot fresh weight) were all increased by the presence of bent shoots. Bent shoots contributed to 43% to 53% of cumulative plant photosynthesis. The cumulative plant photosynthesis increased by 73% and 117% in plants with, respectively, 1 and 3 bent shoots compared with plants without bent shoots. Upright shoot dry weight increased by 35% and 59% in plants with, respectively, 1 and 3 bent shoots compared to plants without bent shoots. The increased upright shoot dry weight was entirely due to the contribution of extra photosynthesis by bent shoots, as the cumulative upright shoot photosynthesis itself was not affected by the presence of bent shoots. At least 47% to 51% of the photosynthesis by bent shoots was translocated to upright shoots to support their biomass increase.

Conclusions We conclude that the positive effect of shoot bending on flower shoot growth and quality in cut-rose production system can entirely be attributed to assimilate supply from bent shoots. Functional-structural plant modelling is a useful tool to quantify the contributions of photosynthesis by different parts of heterogeneous canopies.

Keywords: bent shoots; biomass allocation; functional-structural plant model; heterogeneous canopy; light absorption; photosynthesis; rose (*Rosa hybrida*)

Introduction

Rose (*Rosa hybrida*) is one of the most popular ornamental crops worldwide. In cut-rose production, weak and non-flowering shoots are usually bent downwards (the so-called bent shoots) to intercept light not captured by the upright shoots, which are the economically valuable flower shoots (Ohkawa & Suematsu, 1997). Bending part of the shoots in rose plants increases stem length, flower size and dry weight of upright shoots, resulting in high commercial quality of harvestable flower shoots (Kool & Lenssen, 1997; Warner & Erwin, 2002; Särkkä & Eriksson, 2003; Kim & Lieth, 2004). The advantages of bent shoots in cut-rose production have been attributed to the extra assimilates produced by bent shoots from which growth of the upright flower shoots benefits (Kim & Lieth, 2004). However, bent shoots are down in the canopy and only receive limited amount of light. Keeping too many bent shoots may lead to a negative carbon balance especially in the lower layers of bent shoots (Pien *et al.*, 2001), resulting in competition between bent shoots and upright shoots for assimilates produced by the whole plant canopy. To optimize the number of bent shoots and to maintain upright shoot quality, it is imperative to quantify to what extent photosynthesis by bent shoots may contribute to upright shoot photosynthesis and biomass production. No studies have ever quantified such contributions.

Bent shoots can contribute to upright shoot growth both directly and indirectly. The assimilates produced by bent shoots can directly contribute to upright shoot growth when they are translocated to the upright shoots (Baille *et al.*, 2006; Kajihara *et al.*, 2009). Photosynthesis of upright shoots themselves can also be indirectly affected by bent shoots. Upright shoot photosynthesis is determined by both upright shoot light interception and leaf photosynthetic characteristics. Although leaf photosynthetic characteristics of upright shoots is unlikely affected by bent shoots (Kim *et al.*, 2004; González-Real *et al.*, 2007), upright shoot light interception may be affected by the presence of bent shoots. The assimilate supply from bent shoots may enhance the establishment of leaf area in upright shoots and result in an increased light interception and photosynthesis.

To quantify the direct and indirect contributions of bent shoots to upright shoot growth, a crucial step is to separately quantify both contributions to plant photosynthesis in the canopy, as photosynthesis drives growth. This contribution is difficult to derive experimentally, but can be done using simulation models. However, most canopy photosynthesis models (e.g.,

multi-layer, big-leaf, or sun-shade models) assume an even light distribution in the canopy (Hikosaka *et al.*, 2016b). Since the rose plants consist of vertically growing upright shoots and horizontally growing bent shoots, they constitute a spatially heterogeneous canopy, which cannot be represented in conventional canopy photosynthesis models to calculate canopy photosynthesis. This issue can be solved by using functional-structural plant (FSP) models. In FSP models, individual plants and their architecture and functioning in a canopy are represented in three dimensions (Vos *et al.*, 2010), which has been applied to rose before (Buck-Sorlin *et al.*, 2011). This approach can therefore be applied to calculate photosynthesis of a heterogeneous rose crop at the leaf level.

The objective of this study was to quantify the relative contributions of bent shoots and upright shoots to photosynthesis of the whole plant. To this end, first a greenhouse experiment with rose plants was conducted to investigate the effects of bent shoots on upright shoot architectural development, leaf photosynthesis and biomass production. The plants were subjected to bending treatments whereby different numbers of bent shoots (0, 1 or 3 shoots) were retained on the plant and four shoots were retained to grow vertically (the so-called upright shoots). Upright shoot morphology, leaf photosynthesis and organ biomass were measured. Then, an FSP model of rose was developed based on morphology and photosynthesis measurements and was used to calculate photosynthesis of bent shoots and upright shoots for plants in the different bending treatments.

Materials and methods

Experimentation

Plant growth conditions. Rose plants (*Rosa hybrida* cv. 'Red Naomi!') were grown in a compartment (12 m × 12 m × 4 m) of a Venlo-type glasshouse located in Wageningen, the Netherlands (52° N, 6° E). The compartment contained six growth beds each consisting of two gutters. On these gutters, rooted rose-cuttings bearing a shoot (the primary shoot) were planted on 4 January 2017 at a plant density of 7.5 plants m^{-2} to closely resemble a realistic commercial cultivation set-up. On 24 January 2017 when all primary shoots had formed a flower bud, the flower buds were removed. On 6 February 2017 when all primary shoots had developed side shoots on the top, these primary shoots were bent downwards (primary bent shoots, hereafter). This mimics the primary bending done in practice. After bending the primary shoots, on

average two axillary buds per plant sprouted. These newly sprouted shoots were harvested on 9 March 2017 because they were too thick to bend. After the harvest, on average four axillary buds per plant sprouted, with two axillary buds on each parent stem. When these axillary buds had developed into mature shoots, two of these shoots were bent downwards (secondary bent shoots, hereafter) on 5 April 2017. The other two shoots were harvested on 12 April 2017. After this harvest, four axillary buds sprouted on most plants. For plants which had more than four axillary buds, only four axillary buds were kept on the plant and the excessive ones were removed. For a few plants which had less than four axillary buds, these plants were not used for measurements. All axillary buds left on the plants were allowed to grow upwards (upright shoots, hereafter) to become the economically valuable cut-flower products.

High-pressure sodium (HPS) lamps (600W, Philips, Eindhoven, The Netherlands) were used between 2:00 and 21:00 hours, only when global radiation outside the greenhouse dropped below 200 W m^{-2} and were switched off when outside global radiation increased to values higher than 300 W m^{-2}. Light intensity from the HPS lamps when they were on was ca 150 μmol m^{-2} s^{-1} at canopy level. Shading screen (HARMONY 4215 O FR, Ludvig Svensson, Hellevoetsluis, The Netherlands) was closed when outside global radiation increased to values higher than 600 W m^{-2} and was opened when outside global radiation dropped below 500 W m^{-2}. CO_2 was supplied when CO_2 concentration inside the greenhouse was lower than 700 ppm, which is similar to the commercial greenhouse settings. However, when windows were opened, CO_2 supply stopped. The average light intensity (photosynthetically active radiation, i.e. PAR, from both sun and lamps) during photoperiod (2:00-21:00 hours) inside the greenhouse during the experiment (from 24 April to 31 May 2017) was 360 μmol m^{-2} s^{-1}. The average daily temperature, relative humidity and CO_2 concentration inside the greenhouse during the experiment were 21.6 °C, 72% and 524 ppm, respectively. Plants were irrigated hourly between 7:00 and 19:00 with standard nutrient solution (EC = 2.2 mS cm^{-1}; pH = 5.8) for rose crop used in practice.

Treatments. On 24 April 2017, treatments started. At that point, each plant had four axillary buds and three bent shoots (including one primary bent shoot and two secondary bent shoots). In total three treatments were established: (i) all bent shoots were removed from the plants (0B), (ii) the secondary bent shoots were removed from the plants and the primary bent shoots were kept on the plants, resulting in one bent shoot per plant (1B), and (iii) all bent shoots were

kept on the plants, resulting in three bent shoots per plant (3B). In all treatments, four axillary buds were kept, resulting in four upright flower shoots per plant. On 1 June 2017, all upright shoots were harvested when they were blooming, and the experiment ended.

Plant architecture and biomass measurements. Six plants per plot were randomly chosen and one upright shoot on each plant was used to measure architectural traits and biomass production. Shoot architectural traits were measured non-destructively on day 6, 9, 14, 19 and 25 after start of treatments. The non-destructive measurements included the number of leaves on the shoot, length and width of all individual leaves on the shoot, stem length, length of all internodes on the shoot, and flower width. On 31 May 2017, all upright shoots used for non-destructive measurements were harvested for destructive measurements. The destructive measurements included shoot fresh weight, stem length, length and diameter of all internodes on the shoot, length, width, leaflet number, area and inclination angle of all individual leaves on the shoot, and flower width. An allometric relationship between leaf area and the product of leaf length and width was derived from the destructive measurements (r^2 = 0.92; relative root-mean-square error = 0.13), and was used to calculate leaf areas on days when non-destructive measurements on leaf length and width were performed. Length of the compound rose leaf was measured from the tip of the terminal leaflet to the end of the petiole that the leaf attached with the stem, and leaf width was measured at the widest part of the leaf. After the destructive measurements, individual organs were put in the oven for 48 hours at 105 °C to measure organ dry weight. Stem length was measured using a measuring tape. Leaf length and width, internode length and flower width were measured using a ruler. Internode diameter was measured using a pair of callipers. Leaf area was measured using a leaf area meter (LICOR-3100, Lincoln, NE, USA). Leaf inclination angle was measured as the insertion angle of the leaf with the horizontal level using a protractor. Shoot fresh weight was measured using a common electronic balance. Organ dry weight was measured using an analytic balance.

Light measurements. On day 13 and 30 after start of treatments (both were overcast days), light measurements were performed using a line quantum sensor (Li-Cor BioScience, Lincoln, NE, USA). In each plot, measurements were performed at three locations (at the front, middle and back of the plot; the distance between front and middle and between middle and back was 60 cm). At each location, light intensities were measured above, in the middle of and at the bottom of upright shoots, and above and below bent shoots.

Leaf gas exchange measurements. At flowering stage, two plants per plot were chosen from the six plants used for architecture and biomass measurements. One shoot per plant was chosen to perform a combined measurement of leaf gas exchange and chlorophyll fluorescence using the LI-6400XT Portable Photosynthesis System (Li-Cor BioScience, Lincoln, NE, USA). The measurements were performed on terminal leaflets of leaves at upper, middle and lower level of the upright shoots and leaves on the bent shoots. Light response curves of photosynthesis were made by decreasing incident light in the leaf cuvette in the series of 1500, 1100, 700, 400, 200, 150, 100, 75 and 50 μmol m^{-2} s^{-1}, while keeping ambient CO_2 at 400 μmol mol^{-1}, O_2 at 21%, leaf temperature at 25 °C, and leaf-to-air vapour pressure difference at 1~1.6 kPa. The steady-state fluorescence (F_s) was measured simultaneously with the gas exchange measurement after 3 to 5 minutes light adaptation. The maximum fluorescence F_m' was measured using the multiphase flash method. The flash intensity (I_{flash}) was increased from the background light level in the leaf cuvette to ca 6300 μmol m^{-2} s^{-1} in phase 1, and I_{flash} maintained at ca 6300 μmol m^{-2} s^{-1} for 300 ms; then I_{flash} was decreased by 35% and maintained at this level for 300 ms in phase 2; in phase 3, I_{flash} was back to the level of phase 1 and maintained at this level for 300 ms. The intercept of linear regression of fluorescence yields during phase 2 against $1/I_{flash}$ gives the estimate of F_m' from the multiphase flash method (Loriaux *et al.*, 2013).

Estimating leaf photosynthetic parameters. Leaf photosynthetic parameters were estimated by stepwise fitting the combined measurements of gas exchange and chlorophyll fluorescence to a non-rectangular hyperbola (Eq. 4.1) (Marshall & Biscoe, 1980):

$$A = \frac{\Phi_{CO2LL(inc)} I_{inc} + A_{max} - \sqrt{(\Phi_{CO2LL(inc)} I_{inc} + A_{max})^2 - 4\theta A_{max} \Phi_{CO2LL(inc)} I_{inc}}}{2\theta} - R_d \quad (4.1)$$

where A (μmol CO_2 m^{-2} s^{-1}) is the net leaf photosynthetic rate; $\Phi_{CO2LL(inc)}$ (mol CO_2 mol^{-1} photon) is the quantum yield of CO_2 assimilation on the basis of incident light; I_{inc} (μmol m^{-2} s^{-1}) is the incident light; A_{max} (μmol CO_2 m^{-2} s^{-1}) is the maximum leaf photosynthetic rate at saturating incident light; θ is the curvature factor of the light response curve and was kept at 0.8 (Yin & Struik, 2015); R_d (μmol CO_2 m^{-2} s^{-1}) is the dark respiration rate. Details on the procedure of estimating $\Phi_{CO2LL(inc)}$, A_{max} and R_d can be found in the supporting information in Chapter 3 (Method S3.1).

The relationships between light gradient and A_{max} gradient in upright shoots and bent shoots were described using Eq. 4.2 (Niinemets & Anten, 2009):

$$A_{max} = A_0 \times (Q/Q_0)^k \quad (4.2)$$

where A_{max} (μmol CO_2 m^{-2} s^{-1}) is the estimated A_{max} for a leaf; A_0 (μmol CO_2 m^{-2} s^{-1}) is the photosynthetic capacity of the highest most illuminated leaves in upright shoots ($A_{0,upright}$) or in bent shoots ($A_{0,bent}$); Q (μmol m^{-2} s^{-1}) is the measured light intensity at the level of photosynthesis measurements for estimating A_{max}; Q_0 (μmol m^{-2} s^{-1}) is the measured light intensity above the plants; k is a coefficient. Taking logarithm of both sides of Eq. 4.2 gives a linear equation (Eq. 4.3):

$$\log A_{max} = \log A_0 + k \times \log(Q/Q_0) \quad (4.3)$$

By curve fitting Eq. 4.3 with values of A_{max} and Q/Q_0 obtained from measurements on top, middle and lower leaves of upright shoots, $A_{0,upright}$ and k were derived. Assuming that the same k holds for bent shoots, $A_{0,bent}$ was derived by fitting the intercept of Eq. 4.3 with values of A_{max} and Q/Q_0 obtained from leaves of bent shoots.

Statistical analysis. The treatments were established with a randomized block design, with three blocks and 72 plants per plot. In the analysis, the treatments were considered as independent fixed factors. The treatment effects on upright shoot architectural traits, upright shoot fresh weight, upright shoot and organ dry weight, upright shoot biomass allocation, and leaf photosynthetic parameters were analysed using a one-way ANOVA ($P < 0.05$) of R (version R 3.3.3, R Core Team).

Simulation

Model development. A three-dimensional (3D) rose model was constructed in the plant modelling software GroIMP (Hemmerling *et al.*, 2008). The model includes (i) a 3D representation of rose plant architecture that changes every three days, (ii) a radiation and photosynthesis model to calculate plant light absorption and photosynthesis, and (iii) virtual sensors to measure light intensities in the canopy analogous to the measurements done in the experiment.

(i) 3D rose plants. Three-dimensional representations of rose plants were constructed for the three treatments. Each plant was composed of four upright shoots, and 0, 1 or 3 bent shoots. Upright shoots were constructed using phytomers consisting of a internode and a compound rose leaf, that together make up the shoot. Architectural parameters used for constructing each individual upright shoot included length and width of all internodes, length, width, leaflet number and inclination angle of all leaves, and flower width. Architectural measurements (measured every 3-5 days) were used to build a database which contains sets of individual architectural parameters. Each parameter set was obtained from architectural measurements of one shoot. In simulations, architecture of individual shoots was changed every three days (from day 1 to 25 after start of treatments) according to the parameter sets that were randomly selected from the database. In case architectural measurements were not performed on that day, parameters were derived from linear interpolations of parameter values measured on two closest days. From day 25, the architectural parameters did not change anymore, as parameter values measured on day 25 were similar to the final measurements on day 35. Due to the architectural complexity of bent shoots, they were constructed by randomly distributing a number of leaves in the area occupied by bent shoots. Total leaf areas of bent shoots used for treatments with one (1B) and three (3B) bent shoots were obtained from the experiment. For the treatment with no bent shoots (0B), simulations were performed without bent shoots. Plant density was set to the same values as in the experiment to mimic the actual plant arrangements in the experiment.

(ii) The radiation and photosynthesis model. The light environment was modelled using a dome of light sources representing diffuse light emitted by an overcast sky with moderate gradation towards zenith and azimuthal uniformity (Evers *et al.*, 2010). To eliminate the border effects in the light environment, the simulated plant population (in total 18 plants were simulated, with two rows and nine plants in each row) was replicated 10 times in the x and y directions, resulting in average light conditions as experienced by 100 copies of each individual plant population (1800 plants in total) (de Vries *et al.*, 2018). The amount of light reaching the plant organs was simulated using a Monte-Carlo ray tracer embedded in GroIMP (Hemmerling *et al.*, 2008). The light reflectance (= 0.08) and transmittance (= 0.06) values of rose leaves were obtained from spectrophotometric measurements on rose leaves of the same cultivar in another experiment; stems were assumed to have the same reflectance as leaves but with no transmission. Plant net photosynthesis was calculated as the sum of net photosynthesis

of individual leaves, which was in turn calculated based on the light absorption and photosynthetic parameters of individual leaves (see Eq. 4.1). A_{max} of individual leaves in upright shoots and bent shoots was derived based on the relative light intensity (Q/Q_0 in Eq. 4.2) experienced by that leaf and parameter values of $A_{0,upright}$, $A_{0,bent}$ and k. R_d of individual leaves was assumed to be proportional to A_{max} of that leaf (Hikosaka *et al.*, 2016b). All leaves were assumed to have the same quantum efficiency ($\Phi_{CO2LL(inc)}$) as we found that neither the treatments nor the positions of the leaves in the canopy affected this parameter.

(iii) Virtual sensors. Virtual light sensors were constructed such that the light intensity could be monitored similar to the line quantum sensor used in the experiment. Virtual sensors were placed at the same locations as where actual light measurements were performed in the experiment.

Model evaluation. Light measurements by virtual sensors were performed for the three treatments using 3D representations of plant architecture on day 14 and 25 after start of treatments. The incoming light intensity in the model was kept at 360 μmol m^{-2} s^{-1}, which represented the average light intensity (including light from both sun and lamps) inside the greenhouse during the experiment. Light measurements by virtual sensors were compared with the actual light measurements on day 13 and 30 after start of treatments. Since the incoming light intensity varied during the actual measurements, light intensities relative to that above upright shoots were used for model evaluation. Relative light intensities obtained in the experiment were compared with simulations by calculating the coefficient of determination (r^2) and the relative root-mean-square error (r*RMSE*):

$$rRMSE = \frac{1}{\bar{x}}\sqrt{\frac{\sum_{i=1}^{n}(y_i - x_i)^2}{n}} \quad (4.4)$$

where y_i is the simulated value, x_i is the measured value, n is the number of data points, and $\bar{x}$ is the mean of the measured values.

Calculating plant daily photosynthesis. Plant daily net photosynthesis (inducing photosynthesis of upright shoots and bent shoots) was calculated for the three treatments over the growth cycle. Photosynthesis was calculated from the first day after start of treatments until the day of destructive measurements of upright shoots (in total 35 days). Light conditions

(including the global radiation outside the greenhouse, and the applications of shading screen and the assimilation lighting inside the greenhouse) were documented every day at a five-minute interval. Based on these measurements, the hourly light intensity inside the greenhouse during the light period was calculated and was used to calculate the hourly net photosynthetic rate of individual leaves. Daily photosynthesis of individual leaves was then calculated by summing up their hourly photosynthesis during the light period in each day. Daily photosynthesis of bent shoots and upright shoots were calculated as the sum of the daily photosynthesis of individual leaves attached on bent shoots and upright shoots. Daily whole plant photosynthesis was then calculated as the sum of daily photosynthesis of bent shoots and upright shoots.

Two additional simulations were performed. First, in the commercial greenhouse, leaf area index (LAI, m^2 leaf m^{-2} floor) of bent shoots can be higher than in our experiment. Thus we further calculated daily photosynthesis for 3B treatment using an LAI of 5 for bent shoots. The calculation was done for the whole growth period (35 days) according to the approach described previously. Second, a common situation in practise is that the rose flower shoots at different developmental stages are coexisting on the plants all year round, with harvestable shoots being pruned every day. Thus we further calculated daily photosynthesis for 3B treatment with upright shoots consisting of shoots at different developmental stages. The phenotypes of individual upright shoots on the plants were randomly obtained from the non-destructive measurements (on day 6, 9, 14, 19 and 25) in 3B treatment, resulting in a mixed developmental stages of upright shoots on the same plant. In this simulation, plant net photosynthetic rate was calculated for once, with the incoming light intensity being kept at the average level during the experiment (= 360 μmol m^{-2} s^{-1}). Number of upright shoots was respectively kept at 4, 6 and 8 shoots per plant in the calculation, and bent shoot LAI was kept at the same level of 3B treatment (= 3.6).

Results

Effects of bent shoots on upright shoot morphology and biomass

Plants with bent shoots (1B and 3B plants) had longer and thicker upright shoots than plants without bent shoots (0B plants) (Table 4.1). Stem biomass per unit of length was also higher in 1B and 3B upright shoots than in 0B upright shoots (Table 4.1), indicating that plants with

bent shoots had stronger flower stems than plants without bent shoots. Individual internode length, mostly for internodes located in the middle of upright shoots, and individual internode diameter at harvest were increased when number of bent shoots increased (Figure 4.1A,B). Bent shoots did not affect the number of leaves on upright shoots (Table 4.1), but increased shoot total leaf area by increasing areas of individual leaves located in the middle of upright shoots (Table 4.1; Figure 4.1C). This resulted in higher upright shoot LAIs of plants with bent shoots (Figure S4.1). Leaf mass per area was not affected by bent shoots (Table 4.1), nor was leaflet number of individual leaves (Figure 4.1D). Flower width at harvest was not affected by bent shoots (Table 4.1).

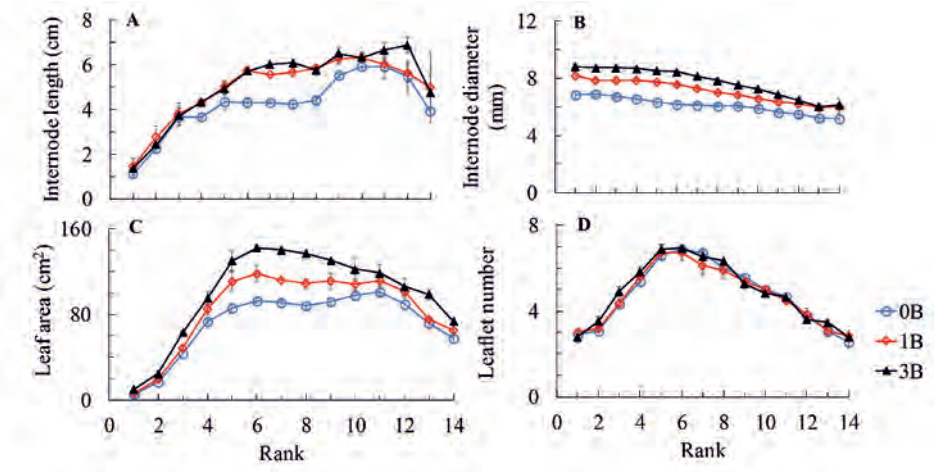

Figure 4.1. Measurements of internode length (A), internode diameter (B), leaf area (C), and leaflet number (D) at harvest. Rank numbers are counted from the base towards the flower on the shoot. Error bars are standard errors of means. 0B, 1B and 3B represent no, one or three bent shoots per plant.

Upright shoot fresh weight was 28% higher in 1B and was 47% higher in 3B than in 0B plants (Table 4.1). Upright shoot dry weight was higher in 1B and 3B plants than in 0B plants, as well as individual organ (stem, leaf and flower) dry weight of upright shoots (Figure 4.2A). The fraction of biomass allocated to stem was higher in 1B and 3B upright shoots than in 0B shoots, which was at the expense of the fractions of biomass allocated to leaf and flower (Figure 4.2B).

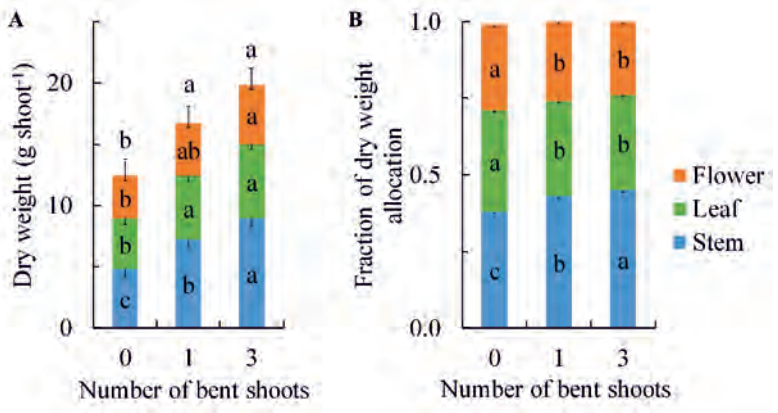

Figure 4.2. Organ dry weight (A) and the fraction of dry weight allocated to different organs of upright shoot (B) at harvest. Letters in columns indicate significant differences when comparing the same organ between treatments with different numbers (0,1,3) of bent shoots per plant (columns in the same colour) ($P < 0.05$). Letters above columns indicate significant differences when comparing shoot dry weight between treatments ($P < 0.05$). Negative error bars are standard errors of means for leaf, stem and flower. Positive error bars are standard errors of means for the whole shoot.

Effects of bent shoots on leaf photosynthetic parameters

Leaf photosynthetic parameters of upright shoots, including the maximum leaf photosynthetic rate (A_{max}) (Figure 4.3A-C), dark respiration rate (R_d) (Figure 4.3E-G) and quantum efficiency ($\Phi_{CO2LL(inc)}$) (Figure 4.3I-K), were hardly affected by the presence of bent shoots, except that A_{max} of lower leaves was higher in 0B upright shoots than in 1B and 3B upright shoots (Figure 4.3C). The number of bent shoots hardly affected photosynthetic parameters of leaves in bent shoots (Figure 4.3D,H,L). The distribution of A_{max} for leaves in upright shoots was correlated with the relative light intensity experienced by that leaf (Q/Q_0 in Eqs. 4.2 and 4.3). By curve fitting Eq. 4.3, leaf photosynthetic capacity of the most illuminated leaf in upright shoots ($A_{0,upright}$) was quantified as 21.0 μmol CO_2 m^{-2} s^{-1} and the slope k of Eq. 4.3 (the same as the curvature factor k of Eq. 4.2) was determined as 0.09 (Figure 4.4). Assuming that the same correlation between A_{max} and Q/Q_0 holds for leaves in bent shoots (i.e., same k value for bent shoots), leaf photosynthetic capacity of the most illuminated leaf in bent shoots ($A_{0,bent}$) was

quantified as 16.9 μmol CO_2 m^{-2} s^{-1} (Figure 4.4), indicating that bending of a shoot decreased photosynthetic capacity of its leaves.

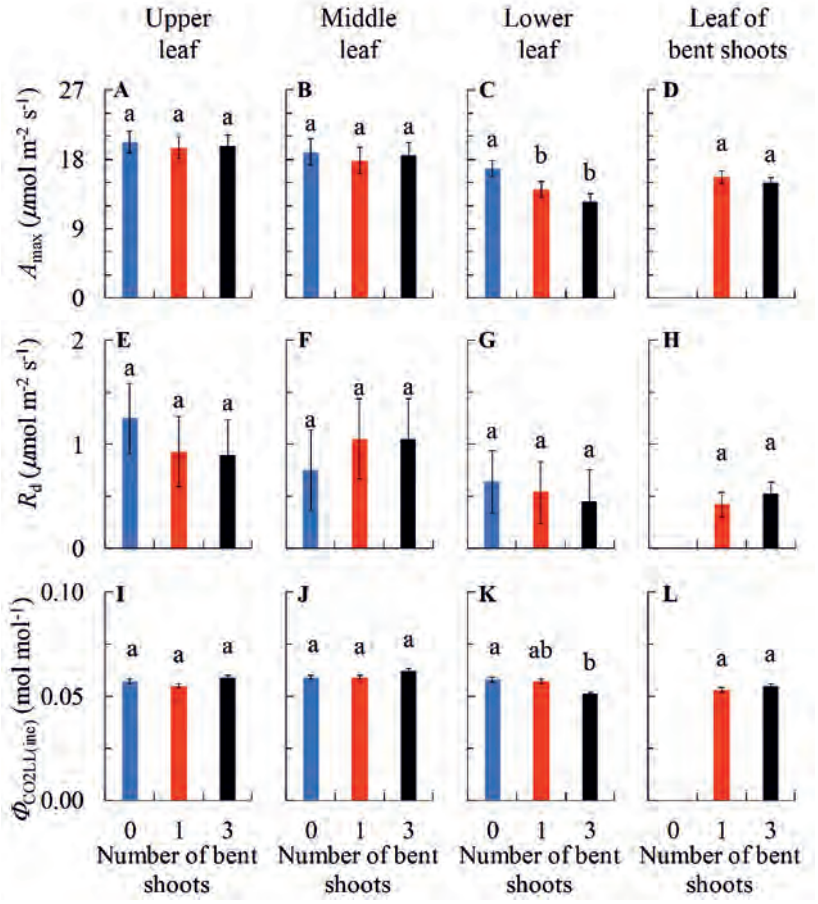

Figure 4.3. Leaf photosynthetic parameters of leaves at upper (A,E,I), middle (B,F,J) and lower (C,G,K) levels of upright shoots and leaves of bent shoots (D,H,L). A_{max} (A-D) is the maximum leaf photosynthetic rate. R_d (E-H) is the dark respiration rate. $\Phi_{CO2LL(inc)}$ (I-L) is the quantum efficiency. Letters above columns indicate significant difference ($P < 0.05$). Error bars are standard errors of means.

Table 4.1. Architectural traits and fresh weight of individual upright shoots at harvest (35 days after start of treatments). Letters following the numbers in each column indicate significant differences when comparing between treatments ($P < 0.05$). Stem diameter is the average diameter of all internodes on a shoot. SEM is the standard error of means. Data were based on 18 replicate plants distributed over 3 blocks (n=3).

Number of bent shoots per plant	Stem length (cm)	Stem diameter (mm)	Stem biomass per unit of length (g cm^{-1})	Leaf number	Shoot leaf area (cm^2)	Leaf mass per unit of area (g m^{-2})	Flower width (cm)	Shoot fresh weight (g)
0	76 b	6.09 c	0.063 b	14 a	1000 c	41.4 a	11.9 a	58 b
1	85 a	7.03 b	0.084 a	14 a	1198 b	43.6 a	12.5 a	74 a
3	88 a	7.67 a	0.101 a	14 a	1412 a	42.9 a	12.6 a	85 a
SEM	1.82	0.19	0.01	0.44	44.10	2.46	6.57	4.73

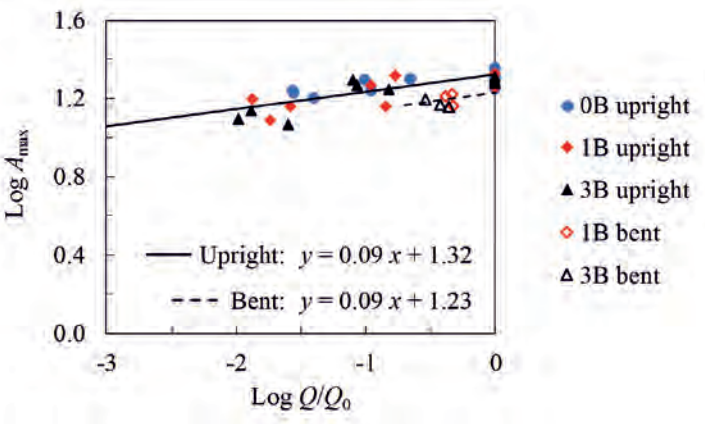

Figure 4.4. The relationships between the logarithm of the maximum leaf photosynthetic rate (A_{max}) of upper, middle and lower leaves in upright shoots and leaves in bent shoots and the logarithm of the relative light intensity (Q/Q_0) experienced by that leaf (see Eq. 4.3: $\log A_{max} = k \times \log Q/Q_0 + \log A_0$). Closed symbols are upright shoots. Open symbols are bent shoots. Solid line is the fitted curve for leaves in upright shoots in the three treatments. Dashed line is the fitted curve for leaves in bent shoots in 1B and 3B treatments, obtained by only fitting the intercept, but keeping the slope the same as for the upright shoots. Intercepts of the solid line and dashed line with y axis represent the logarithm of A_{max} of the most illuminated leaf in upright shoots (Log $A_{0,upright}$) and in bent shoots (Log $A_{0,bent}$) respectively. Slope of the solid line and dashed line represents the k value used for both upright shoots and bent shoots. 0B, 1B and 3B represent no, one or three bent shoots per plant.

Calculations of daily plant net photosynthesis during the whole growth period

The FSP model sufficiently captured the fraction of light interception in both upright shoots and bent shoots, being that the r^2 and r*RMSE* between the measured and simulated relative light intensities (Q/Q_0) were 0.84 and 0.31 respectively (Figure S4.2). This indicates the 3D representation in the model sufficiently represented the rose plants (both with and without bent shoots) for simulations of light absorption and photosynthesis.

Simulated PAR absorption and net photosynthesis of the upright shoots were hardly different between plants with and without bent shoots during the whole growth period (Figure 4.5). When upright shoots were at their early developmental stages, daily PAR absorption of the whole plant was respectively three and five times higher in 1B and 3B plants than in 0B plants

(Figure 4.5A), due to the additional leaf area of bent shoots. This results in that daily photosynthesis was respectively four and seven times higher in 1B and 3B plants than in 0B plants (Figure 4.5C). When upright shoots were fully developed, plant daily PAR absorption was respectively 57% and 82% higher in 1B and 3B plants than in 0B plants (Figure 4.5A). This results in that plant photosynthesis was respectively 51% and 83% higher in 1B and 3B plants than in 0B plants (Figure 4.5C). At harvest, the cumulative plant PAR absorption was 76% and 111% higher, and cumulative plant photosynthesis was 73% and 117% higher respectively in 1B and 3B plants than in 0B plants (Figure 4.5B,D). The cumulative PAR absorption by bent shoots in 3B plants was 40% higher than that in 1B plants, resulting in 54% higher bent shoot photosynthesis (Figure 4.5B,D). At early stages of upright shoots, the relative contribution of bent shoots to daily PAR absorption of the whole plant was 76% in 1B and 81% in 3B plants (Figure 4.6A). This results in that the relative contribution of bent shoots to plant photosynthesis was 78% in 1B and 85% in 3B plants (Figure 4.6C). With the growing of upright shoots, the relative contributions of bent shoots to daily plant PAR absorption and photosynthesis decreased (Figure 4.6A,C). At harvest, bent shoots contributed 43% cumulative PAR absorption and photosynthesis of 1B plants and 51% PAR absorption and 53% photosynthesis of 3B plants (Figure 4.6B,D).

To compare the differences of upright shoot photosynthesis and biomass production between treatments, we normalized these values in all treatments to values obtained in 0B (resulting in all values in 0B = 1). Upright shoot dry weight at harvest was 35% higher in 1B and 59% higher in 3B than in 0B plants (Figure 4.7A). However, cumulative upright shoot photosynthesis at harvest was not different between treatments (Figure 4.7B), indicating that the higher dry weight in 1B and 3B upright shoots did not come from photosynthesis of upright shoots themselves, thus should come from their bent shoots. In addition, owning to the contribution of bent shoots, cumulative whole-plant photosynthesis at harvest was 73% higher in 1B and was 17% higher in 3B than in 0B plants (Figure 4.7C). These fractions were even higher than the fractions of dry weight increases in upright shoots of 1B (35%) and 3B (59%) plants (Figure 4.7A), indicating that their bent shoots produced more assimilates than the amount that had been contributed to upright shoot dry weight increase.

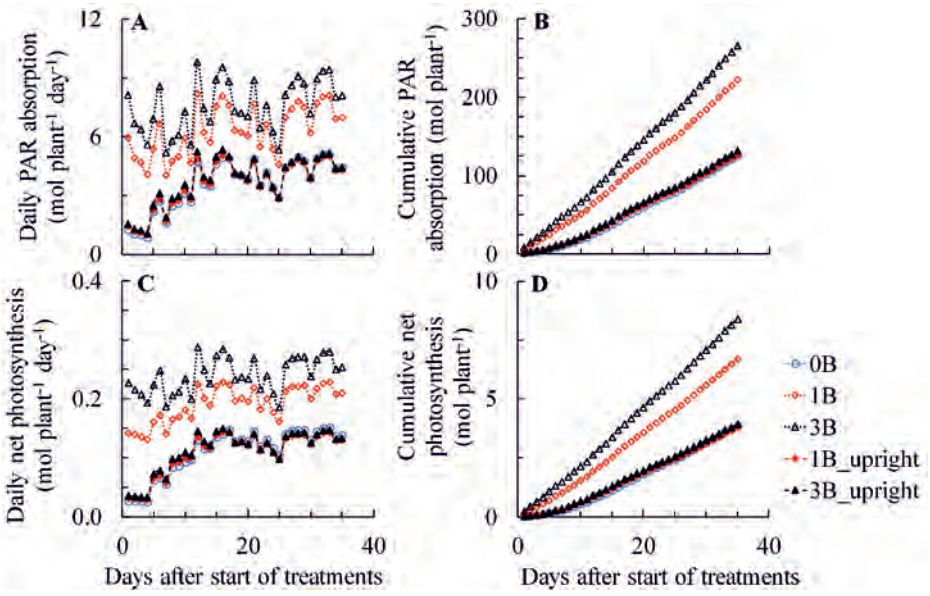

Figure 4.5. Simulated daily (A,C) and cumulative (B,D) photosynthetically active radiation (PAR) absorption (A,B) and net photosynthesis (C,D). Closed symbols with dashed lines are simulated results of upright shoots. Open symbols with dotted lines are simulated results of the whole plant. 0B, 1B and 3B represent no, one or three bent shoots per plant. PAR absorption and photosynthesis of upright shoots equal to that of the whole plant in 0B treatment.

As in the commercial rose greenhouse, LAI of bent shoots is often higher than in our experiment (bent shoot LAI in the experiment was given in Figure S4.1), we calculated the effect of increasing bent shoot LAI to 5 on photosynthesis in 3B plants. Increasing bent shoot LAI led only to a 6% increase in cumulative photosynthesis of bent shoots and a 3% increase in cumulative plant photosynthesis at harvest when compared with a LAI of 3.6 in 3B plants in the experiment (Figure 4.8A). The relative contribution of bent shoots to plant photosynthesis was slightly (2%) higher at a bent shoot LAI of 5 than a LAI of 3.6 (Figure 4.8B). Furthermore, we tested if the contributions from the bent shoots would change if more upright shoots would have been retained on the plant and if these shoots were in different developmental stages instead of all being in the same developmental stage. These scenarios are also common situations in the commercial greenhouse. When upright shoots were

consisting of shoots at different developmental stages, bent shoot photosynthesis decreased with the increasing number of upright shoots (Figure 4.9A). At the presence of 4 upright shoots per plant, bent shoots contributed 48% of plant photosynthesis, and this contribution decreased to 43% at the presence of 6 and 8 upright shoots per plant (Figure 4.9B).

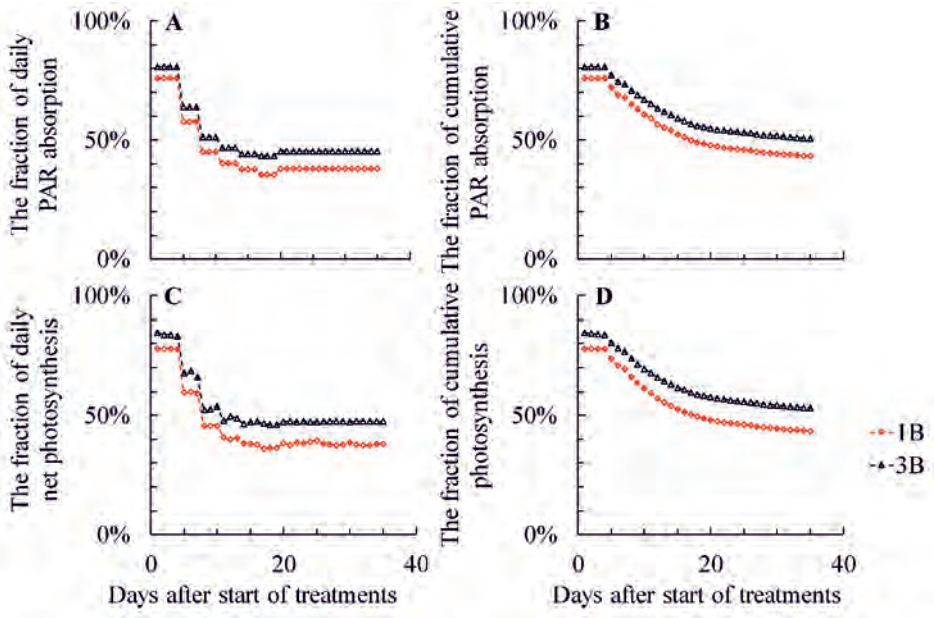

Figure 4.6. Simulated photosynthetically active radiation (PAR) absorption (A,B) and net photosynthesis (C,D) by bent shoots as a fraction of the whole plant. (A,C) Simulated daily PAR absorption and photosynthesis. (B,D) Simulated cumulative PAR absorption and photosynthesis. 1B and 3B represent respectively one and three bent shoots per plant.

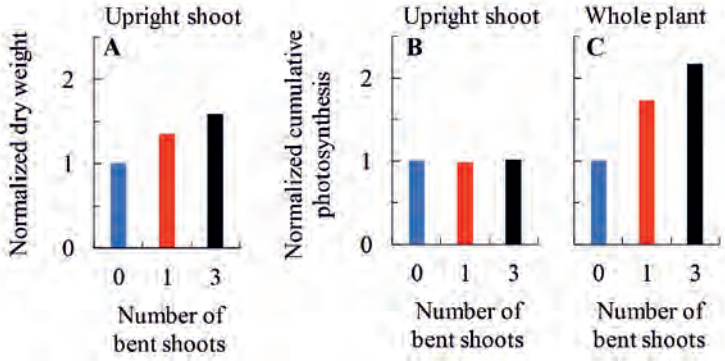

Figure 4.7. Comparisons between shoot dry weight and plant photosynthesis. Upright shoot dry weight at harvest (A). Cumulative upright shoot (B) and plant (C) photosynthesis from bud break until harvest. All data were calculated relative to the data for plants with zero bent shoot.

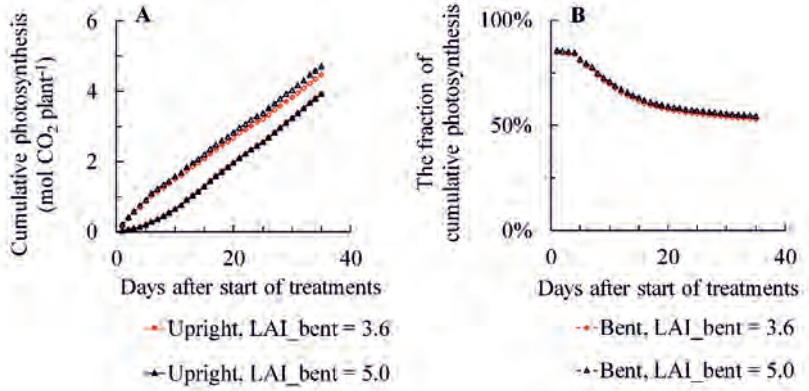

Figure 4.8. Simulated cumulative photosynthesis (A) and the cumulative photosynthesis by bent shoots as a fraction of the whole plant (B). Closed symbols with solid lines are simulated results of upright shoots; open symbols with dashed lines are simulated results of bent shoots. Simulations were conducted for treatment with three bent shoots per plant (3B treatment, with a leaf area index LAI of bent shoots being 3.6, in red colour) and for the situation in which LAI of 3B plants increased to 5 (in black colour).

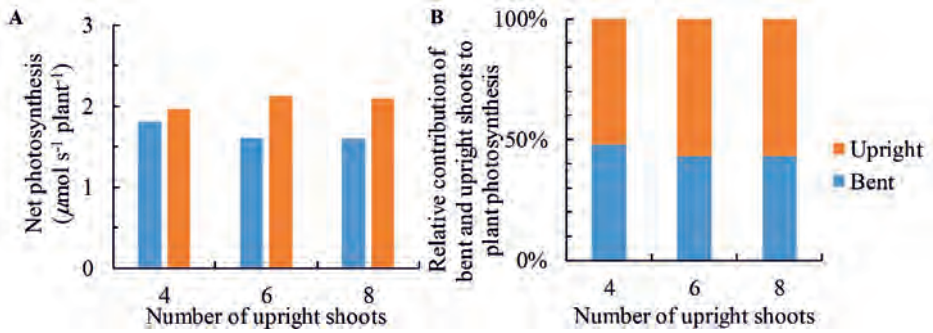

Figure 4.9. Simulated net photosynthesis (A) and the relative contribution to whole-plant photosynthesis (B) by bent shoots and upright shoots. Simulations were done using 3B plants (in treatment with three bent shoots per plant) consisting of 4, 6 or 8 upright shoots at different developmental stages.

Discussion

Bent shoots increased upright shoot biomass due to the contribution of additional photosynthesis by bent shoots

In cut-rose production, bent shoots are normally considered as an extra source of assimilates for the growth of upright flower shoots (Kim & Lieth, 2004). We found that upright shoot dry weight was increased by 35% in plants with one bent shoot and by 59% in plants with three bent shoots than in plants with no bent shoots (Figure 4.7A). The benefit of applying bent shoots in cut-rose production to increase upright shoot dry weight is also found by Kim and Lieth (2004). However, the contribution of photosynthesis by bent shoots to upright shoot biomass production has never been quantified. Here, we quantified such a contribution using a 3D modelling approach. The increased upright shoot dry weight could either come from higher upright shoot photosynthesis in plants with bent shoots, or from assimilate translocation from bent shoots, or from both. Our model simulations clearly indicate that all the increased upright shoot dry weight was from additional photosynthesis by bent shoots, which may entail direct assimilate translocation to upright shoots, since net photosynthesis of upright shoots themselves was hardly affected by the presence of bent shoots. Mor and Halevy (1979) applied labelled carbon and showed that the growth of rose flower shoots, from axillary bud breaking

until the appearance of flower bud, is largely dependent on the supply of assimilates by the foliage of the previous growth cycles. Thus the additional photosynthesis by bent shoots may increase the assimilate supply during this period, resulting in an increase of assimilate translocation to upright shoots and a higher shoot dry weight. At flowering stage, the assimilates produced by bent shoots are mainly translocating to the roots and basal part of the plant (Kajihara *et al.*, 2009).

Interestingly, the cumulative whole-plant photosynthesis was increased by 73% to 117% in plants with bent shoots compared to plants without bent shoots (Figure 4.7C). These fractions were higher than the fractions of increases in upright shoot dry weight in plants with bent shoots (Figure 4.7A,C), indicating that bent shoots produced relatively more amount of assimilates than the relative increase in upright shoot biomass. Assuming that the assimilates in upright shoots increased with the same fraction (35% to 59%) as the biomass increase of upright shoots in plants with bent shoots, the amount of increased assimilates in upright shoots accounted for 47% to 51% of the cumulative assimilates produced by bent shoots during the growth period. However, to properly convert photosynthates to biomass growth, also the respiration cost and the conversion cost from photosynthates to biomass needs to be considered. Thus, to support upright shoot biomass increase, the fraction of assimilates produced by bent shoots that are translocated to upright shoots should be higher than 47% to 51%. Measured bent shoot dry weight at the end of treatments did not significantly differ from that at the start (Figure S4.3), indicating that none of the assimilates produced by bent shoots were remained in bent shoots. These assimilates may be used for plant respiration and conversion cost between photosynthates and biomass, or they may be translocated to other parts (e.g., roots) of the plant (Kajihara *et al.*, 2009).

Bent shoots increased morphological quality traits of upright shoots

The benefits of applying bent shoots in cut-rose production, e.g., increasing shoot fresh weight and stem length, has been demonstrated in previous studies (Warner & Erwin, 2002; Kim & Lieth, 2004) as well as in ours (Table 4.1; Figure 4.1). Longer stems and larger shoot leaf areas of upright shoots in plants with bent shoots were resulting from longer internodes and larger leaves located in the middle of the shoot, whereas internode length and leaf area at lower and higher ranks of upright shoots were hardly affected by bent shoots (Figure 4.1A,C). This is likely because at early developmental stages, sink demand is relatively low and upright shoots

could use assimilates stored in basal part of the plant, while at later developmental stages, upright shoots could produce enough assimilates by themselves (Baille *et al.*, 2006), resulting in less pronounced effects of assimilate supply from bent shoots on growth of organs appeared at early or late developmental stages. However, diameters of all individual internodes in upright shoots were larger in plants with bent shoots than in plants without bent shoots (Figure 4.1B), indicating that positive effects of assimilate supply from bent shoots on upright shoot organ size exists during the whole shoot growth period. This is in line with Marcelis-van Acker (1994) who found strong positive effects of assimilate supply on stem length and diameter and leaf area in rose. The effects of bent shoots on flower size and dry weight were less pronounced compared with the effects on the stem and leaf (Table 4.1; Figure 4.2A), as also found by Kim and Lieth (2004).

Although upright shoot leaf area was increased by 20% to 40% in plants with bent shoots compared to plants without bent shoots, this hardly affected upright shoot light absorption and photosynthesis (Table 4.1; Figure 4.5). This may be caused by the fact that upright shoots in plants without bent shoots received additional light reflected from the ground. When bent shoots were present, this reflected light was mostly absorbed by the bent shoots rather than by the upright shoots. When we ran a simulation assuming that the ground does not reflect any light, upright shoots in plants that had bent shoots increased their light absorption by 6% to 11% compared with upright shoots in plants without bent shoots (Figure S4.4A). This lead to an increase of upright shoot photosynthesis by 5% to 9% (Figure S4.4B). In the case of 100% light reflection by the ground, upright shoot light absorption and photosynthesis were even lower in plants with bent shoots than in plants without bent shoots, because the latter received more light reflected from the ground (Figure S4.4). However, even in the case of a zero ground reflectance, the increase of upright shoot light absorption (6%-11%) and photosynthesis (5%-9%) in plants with bent shoots were not proportional to the increase in upright shoot leaf area (20%-40%) (Table 4.1; Figure S4.4). This may be caused by the fact that upright shoot LAI reached relatively high levels soon after start of treatments (Figure S4.1). Thus, a further increase in upright shoot LAI did not result in a proportional increase in light capture and photosynthesis by upright shoots. Note that due to the patchy distribution of leaves in a heterogeneous canopy (e.g., the rose canopy), a same LAI value could indicate much more dense leaves occupying part of the area compared with a homogeneous canopy. LAI of bent shoots was found to be ca 3.8 in practice (Warner & Erwin, 2002), which is similar to our

treatment with three bent shoots per plant (Figure S4.1). This level of LAI for bent shoots is possibly a reasonable level to keep in practice as our simulations showed that increasing LAI to a higher level (= 5) hardly increased photosynthesis of bent shoots and the whole plants (Figure 4.8A).

Calculating photosynthesis of a heterogeneous canopy

Previously, Baille *et al*. (2006) quantified the biomass import and export in rose flower shoots, under the assumption of a spatially uniform light environment around the growing flower shoots. This assumption, however, does not hold for a rose canopy with both vertically grown upright shoots and horizontally grown bent shoots, in which the light conditions can be quite heterogeneous. We represented the heterogeneous rose canopy in 3D using an FSP modelling approach, which allowed us to simulate light absorption and photosynthesis at individual leaf level without assuming a homogeneous canopy.

It is worthwhile to notice that the approach we used to derive the distribution of leaf photosynthetic capacity in upright shoots and bent shoots is originally proposed in homogeneous canopies. The principle behind this approach is largely based on the premise that light distribution in the canopy drives leaf nitrogen distribution, which in turn determines the distribution of leaf photosynthetic capacity in the canopy (Hirose & Werger, 1987a; Hikosaka, 2014). Although some studies argue that plants could also potentially distribute their leaf nitrogen according to the gradient of red to far-red ratio in the canopy (Pons *et al.*, 1993; Pons & De Jong-Van Berkel, 2004). Our results indicate that this approach cannot be used for the entire heterogeneous rose canopy, since we found that A_{max} of leaves in bent shoots was apparently lower than A_{max} of leaves in upright shoots at the same relative light intensity (Figure 4.4). However, we can use this approach to derive the distribution of leaf photosynthetic capacity in upright shoots and bent shoots separately, since the gradient of A_{max} was found in both upright shoots and bent shoots (Gonzalez-Real & Baille, 2000; González-Real *et al.*, 2007). The coefficient of the relationship between light distribution and A_{max} distribution (k in Eqs. 4.2 and 4.3) in upright shoots of rose plants was determined as 0.09 (Figure 4.4), which is lower than the average value (ca 0.37) found across different species but is still within the range of woody species (Hikosaka *et al.*, 2016a). We assumed the same k also holds for bent shoots (Figure 4.4), based on the fact that extinction coefficients of leaf nitrogen distribution in upright shoots and in bent shoots are similar (González-Real *et al.*,

2007). However, A_{max} of the most illuminated leaf in upright shoots ($A_{0,upright}$) was higher than in bent shoots ($A_{0,bent}$) (Figure 4.4), indicating that shoot bending may decrease leaf photosynthetic capacity of leaves in bent shoots, which is also found by others and in other crops (Schubert *et al.*, 1995; Kim *et al.*, 2004).

Several explanations are proposed to explain the lower photosynthesis of leaves in bent shoots. Kim *et al*. (2004) found that the xylem tissue of rose bent shoots was damaged due to bending, and this could reduce hydraulic conductivity of bent shoots and decrease photosynthesis. The damage of xylem tissues, however, could recover over time under the possible involvement of the phytohormone ethylene (Mitchell, 1996; Liu & Chang, 2011). Even when xylem conductivity is not affected by shoot bending, it induces a transient variation in the hydraulic pressure within the xylem of bent shoot (Lopez *et al.*, 2014). This transient increase in the xylem pressure could be rapidly propagated along the vascular system and such hydraulic signals could be converted into chemical signal abiscisic acid (ABA), which is relevant to stomatal closure in leaves (Christmann *et al.*, 2013; Huber & Bauerle, 2016). In addition, a decrease in Rubisco is found in leaves of downward bending shoots of grapevine (Schubert *et al.*, 1995). Given that there is no consensus on the mechanism of the effect of shoot bending on photosynthesis of its leaves, while shoot bending is a common practise used in woody crops (e.g. rose) and fruit trees (e.g. pear) (Schubert *et al.*, 1995; Ito *et al.*, 1999; Kim *et al.*, 2004; Liu & Chang, 2011), further studies on the mechanisms are worthwhile.

Conclusions

Bent shoots increased upright shoot fresh and dry weight, and improved shoot morphological quality (e.g., longer and thicker stems). The increased upright shoot dry weight (by 35% to 59%) in plants with bent shoots was entirely resulting from the contribution of additional photosynthesis by bent shoots, as upright shoot photosynthesis was not affected by the presence of bent shoots. At least 47% to 51% of the assimilates produced by bent shoots was translocated to upright shoots to support their dry weight increase. The remaining assimilates, however, did not remain in bent shoots, but may be used for maintenance respiration and energy cost during the conversion of photosynthates to biomass, or may be translocated to other parts (e.g., roots) of the plant. We conclude that in cut-rose production, the increased flower shoot dry weight and quality can be entirely attributed to the assimilate supply from bent shoots. Functional-structural plant models can be very useful to quantify the relative

contributions of upright shoots and bent shoots to photosynthesis of the heterogeneous rose canopy, and thus to balance between the number of harvestable flower shoots and shoot quality.

Supporting information

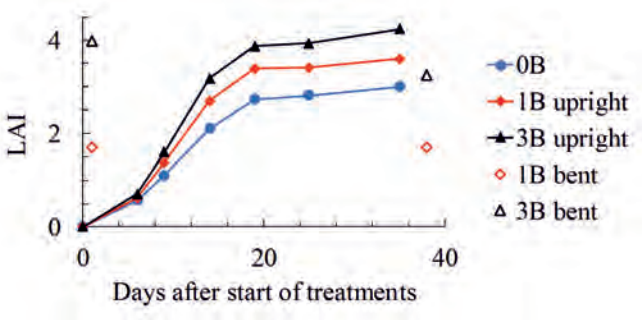

Figure S4.1. Leaf area index (LAI, m^2 leaf m^{-2} floor) of upright shoots and bent shoots. Upright shoot LAI was measured during the experiment (closed symbols and solid lines). Bent shoot LAI was measured at the start and end of the experiment (open symbols). 0B, 1B and 3B represent no, one or three bent shoots per plant.

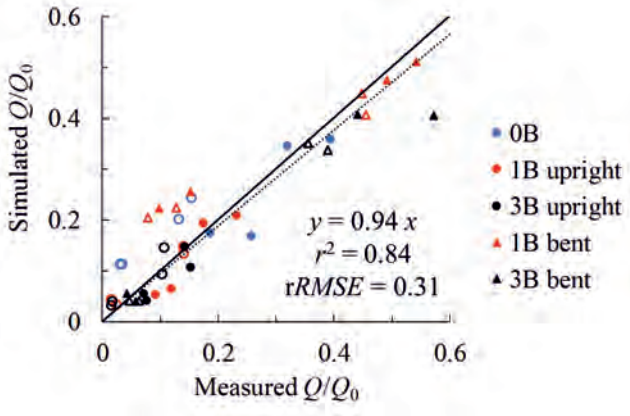

Figure S4.2. Measured and simulated relative light intensities, i.e. Q/Q_0. Q is light intensity at middle or bottom of upright shoots (circles) or above or below bent shoots (triangles), and Q_0 is light intensity above upright shoots. Measurements were conducted on day 13 (closed symbols) and 30 (open symbols) after start of treatments. Solid line is the 1:1 line. Dotted line is the fitted curve for all data points by forcing the line goes through the origin. r*RMSE* is the relative root-mean-square error. 0B, 1B and 3B represent no, one or three bent shoots per plant.

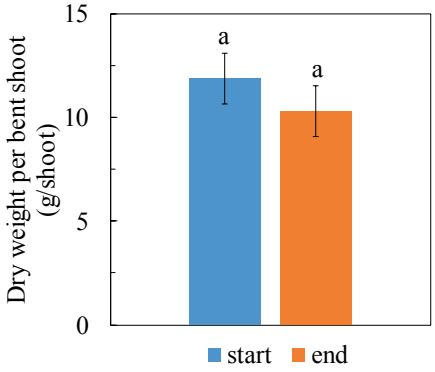

Figure S4.3. Individual bent shoot dry weight measured at the start and end of experiment. Letters above each bar indicate significant difference. Error bars are standard errors of means.

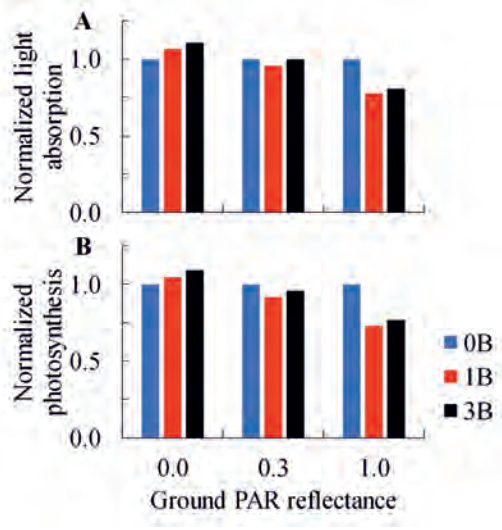

Figure S4.4. Simulated light absorption (A) and photosynthesis (B) by upright shoots with the reflectance of photosynthetically active radiation (PAR) by the ground is 0.0, 0.3 or 1.0. 0.3 is the value used in the simulations. In the simulations, incoming light intensity was kept at the average value during the experiment (=360 μmol m^{-2} s^{-1}). 0B, 1B and 3B represent no, one or three bent shoots per plant. All data were calculated relative to the data for 0B plants.

Chapter 5

Light from below matters: quantifying the responses to far-red light reflected upwards, and the consequences for plant performance in heterogeneous canopies

Ningyi Zhang[1,2], Arian van Westreenen[1,2], Lizhong He[1,3], Jochem B. Evers[2], Niels P.R. Anten[2], Leo F.M. Marcelis[1]

[1] Horticulture and Product Physiology Group, Wageningen University, Wageningen, The Netherlands

[2] Centre for Crop Systems Analysis, Wageningen University, Wageningen, The Netherlands

[3] Shanghai Key Lab of Protected Horticulture Technology, Shanghai Academy of Agricultural Science, Shanghai, China

Abstract

In vegetation stands, plants receive red to far-red ratio (R:FR) signals of varying strength from all directions. However, plant responses to R:FR reflected from below have been largely ignored despite their potential consequences for plant performance.

A heterogeneous rose canopy, consisting of bent shoots down in the canopy and vertically growing upright shoots, was used to quantify the relationship between far-red reflected by bent shoots and upright shoot architectural responses. Using a three-dimensional plant model, we assessed the consequences of these responses to R:FR from below for plant light absorption and photosynthesis.

Bent shoots reflected a substantial amount of far-red and lowered the R:FR ratios in the light reflected upwards. Leaf inclination angle increased in upright shoots which received low R:FR reflected by bent shoots, irrespective of whether these bent shoots belonged to the same plant or neighbour plants. Simulated plant light absorption and photosynthesis were increased by responses to R:FR from below when plants had bent shoots themselves.

Plant response to R:FR from below is an under-explored phenomenon which may induce contrasting consequences for plant performance depending on the type of crop system. The responses are beneficial for performance only when R:FR is reflected by lower foliage of the same plants.

Keywords: heterogeneous canopy; light absorption; photosynthesis; red to far-red ratio; reflection; shade avoidance; rose (*Rosa hybrida*); three-dimensional plant modelling

Introduction

Plants have limited options to escape competitive environments during their lifetime. To optimize competitiveness to ensure survival and reproduction, plants growing in vegetation stands need to show appropriate growth responses to neighbour presence by perceiving and interpreting environmental signals. Among all environmental signals perceived by plants, the low red to far-red ratio (R:FR) of light reflected by neighbouring vegetation is well-known to be recognized by plants as an early warning signal of neighbour proximity (Casal, 2013; Pierik & De Wit, 2014; Ballaré & Pierik, 2017). The R:FR is perceived through phytochrome photoreceptor activity that convert between the active (Pfr) and inactive (Pr) form upon absorption of red and far-red light, respectively (Smith, 2000). The phytochrome photoequilibrium, defined as the fraction of Pfr in the total phytochrome pool, then drives changes in plant traits to avoid competition for light, the so-called shade avoidance responses (Holmes & Smith, 1977; Smith, 2000; Casal, 2013).

Although the actual amounts of red and far-red light determine the photoequilibrium, the directions that the R:FR ratios come from could also potentially contain competitive information. In vegetation stands, a plant receives R:FR signals coming from all directions (i.e., from above, the side and below). These signals are transmitted or reflected by surrounding foliage that can belong either to neighbouring plants or the plant itself. This origin of the R:FR signal may be embedded in the direction that R:FR signals come from. In general, vertically propagating R:FR signals are more likely to originate from foliage of the same plant (self-signalling), whereas horizontally propagating R:FR signals are more likely to come from neighbours (nonself-signalling). For nonself-signals, the directions of R:FR may to some extent indicate the type of the neighbour, as the angle of the incoming signal is likely to be correlated to the size difference between the neighbour and the target plant. Competitiveness and size of the neighbour are linked, as for instance small neighbours may not pose a direct threat, but similar-sized neighbours might. Therefore, plants may need to respond differently according to the origin of the R:FR signals (Dudley & Schmitt, 1995). Many studies focused on plant responses to R:FR signals in incident light or horizontally reflected light, as R:FR ratios from these directions are likely coming from large or similar-sized neighbours (Smith *et al.*, 1990; Van Hinsberg & Van Tienderen, 1997; Héraut-Bron *et al.*, 2001; Evers *et al.*, 2006). However, plant responses to R:FR reflected from below have been largely ignored.

Although low R:FR induced shade avoidance responses are largely confirmed to be beneficial for plant performance when growing in dense canopies (Dudley & Schmitt, 1996; Bell & Galloway, 2007; Keuskamp *et al.*, 2010), low R:FR may not always be a reliable indicator of the competitive strength of neighbours. Coloured (e.g., red and green) soil mulches and small weeds were found to increase shoot-root ratio and stem length and decrease biomass allocated to reproductive organs in crop plants, indicating that low R:FR in the light reflected from below by soil mulches and weeds also induces shade avoidance responses (Hunt *et al.*, 1989; Kasperbauer, 1994; Rajcan *et al.*, 2004; Page *et al.*, 2010; Green-Tracewicz *et al.*, 2012). However, R:FR signals coming from below are unlikely to be reliable signals for light competition, as these can be nonself-signals generated by low vegetation of small neighbours. Additionally, R:FR signals from below could be self-signals, generated by foliage of the same plant. In either case, light competition is unlikely to happen. No studies have investigated the consequences of responses to R:FR signals reflected from below for plant performance.

In this study, we choose a rose crop (*Rosa hybrida*), which has a heterogeneous canopy with distinctly different crop parts, as our study system. In rose production, weak and non-flowering shoots are bent such that they point slightly downwards (the 'bent shoots', see Figure 5.1), which contributes to the growth of upright flower shoots as a source of assimilates to improve their commercial quality (Kim & Lieth, 2004). The heterogeneous structure of a rose canopy consisting of alternating strips of bent shoots and upright shoots makes it possible to generate R:FR signals in light reflected upwards by the lower part of the canopy, i.e., the bent shoots. The objective of this study was to quantify upright shoot responses to low R:FR reflected from below and their consequences for plant performance. First, a greenhouse experiment was conducted, in which focal plants with or without bent shoots were grown with neighbour plants with or without bent shoots. The experiment was used (i) to investigate the effects of bent shoots on the distribution of R:FR ratios as perceived by the upright shoots and (ii) to quantify the relationship between upright shoot architectural responses and the R:FR ratio reflected by the bent shoots. Subsequently, to quantify the consequences of upright shoot architectural responses to R:FR from below for performance of upright shoots themselves, the bent shoots and the whole plant in terms of light absorption and photosynthesis, a three-dimensional (3D) plant simulation analysis was done.

Materials and Methods

Experimentation

Plant growth conditions. Rose plants (*Rosa hybrida* cv. 'Red Naomi!') were grown in a compartment (12 m × 12 m) of a Venlo-type glasshouse located in Wageningen, the Netherlands (52° N, 6° E). On January 4th 2017, one-node cuttings bearing a shoot grown in rockwool cubes were transplanted in the compartment at a density of 7.5 plants m^{-2} (Figure S5.1). Plants were first grown for four growth cycles (one growth cycle is defined as the time duration from one harvest of flowering shoots to the next, approximately six to eight weeks) to allow the basal part growing thick enough to support multiple axillary buds growing simultaneously on the plant. Then plants were pruned to keep four axillary buds sprouting on each plant. When 80% of the shoots were flowering, the flower buds were removed and the shoots were bent downwards, resulting in four bent shoots on each plant. When new axillary buds sprouted on all plants after the bending, the plants were pruned to keep four axillary buds on each plant. Treatments started on September 1st, 2017 (the next day after the pruning) and lasted for four weeks.

During the experiment, assimilation lighting (600W high-pressure sodium lamps, Philips, Eindhoven, The Netherlands) was turned on for approximately 13 hours per day with a light intensity of ca. 150 μmol m^{-2} s^{-1} at the canopy level. Average day and night temperatures during the experiment were 21.7°C and 18.6°C respectively. Average day and night relative humidities during the experiment were 75% and 86% respectively. Average CO_2 concentration at light period during the experiment was 461 ppm. Plants were irrigated hourly between 7:00 and 19:00 with standard nutrient solution (EC = 2.2 mS cm^{-1}; pH = 5.8) for rose crop used in practice.

Treatments. In total four treatments were established. In each treatment, plants chosen for measurements were considered as focal plants. All other plants were considered as neighbour plants. Four focal plants per plot were randomly chosen on condition that at least three neighbour plants were in between two focal plants. The four treatments were (i) focal plants (F) without bent shoots (–; all bent shoots were removed from the plant) and neighbour plants (N) with bent shoots (+; all bent shoots were kept on the plant) (F–N+), (ii) focal plants with bent shoots and neighbour plants with bent shoots (F+N+), (iii) focal plants without bent shoots

and neighbour plants without bent shoots (F−N−), and (iv) focal plants with bent shoots and neighbour plants without bent shoots (F+N−) (Figure S5.2). The four treatments were established in a randomized block design with three blocks, four plots (treatments) per block and 72 plants in each plot (Figure S5.1).

R:FR measurements. The R:FR ratios (red: 660±20 nm, far-red: 730±20 nm) were measured using a spectrometer (SpectroSense2 system, Skye Instruments Ltd, UK) on day 4 (early developmental stage), day 13 (shoot elongation stage) and day 21 (flowering stage) after start of treatments. Measurements were conducted at three locations (front, middle and back) in each plot (Figure S5.1). At each location, R:FR ratios were measured at three heights: above, in the middle of and at the bottom of upright shoots but still being above the bent shoots (Figure 5.1). At each height, R:FR ratios were measured at seven positions: the middle point of the plot (M) and 20 cm, 40 cm and 60 cm from the middle point to the right (R20, R40 and R60) and left (L20, L40 and L60) (Figure 5.1). R:FR measurements inside the upright shoots (at M, R20 and L20) were done with the sensor facing up, down, right (facing the right path) and left (facing the left path) (Figure 5.1). R:FR measurements outside the upright shoots (at R40, R60, L40 and L60) were done with the sensor facing all the aforementioned directions except for the directions facing the upright shoots (Figure 5.1), as light from such directions was propagating away instead of towards upright shoots, rendering those signals irrelevant for focal plant responses.

Plant architecture measurements. Length of every internode and leaf of focal plants was measured non-destructively at day 6 and 12 after start of treatments. When flower buds started to open (day 25), focal plants were destructively harvested to measure length and diameter of all internodes, leaf length, width, area, leaflet number and leaf inclination angle of all leaves, peduncle length and diameter, and flower bud diameter. Length and width measurements were conducted using a ruler. Diameter was measured using a calliper. Leaf area was measured using a leaf area meter (LICOR-3100, Lincoln, NE, USA). Leaf inclination angle was measured as the insertion angle of the leaf relative to the horizontal level using a protractor.

Statistical analysis. The effects of the four treatments on R:FR ratios from each direction (upward, downward, left and right), and on plant architectural traits were analysed using a one-way ANOVA ($P < 0.05$) of R (version R 3.3.3, R Core Team).

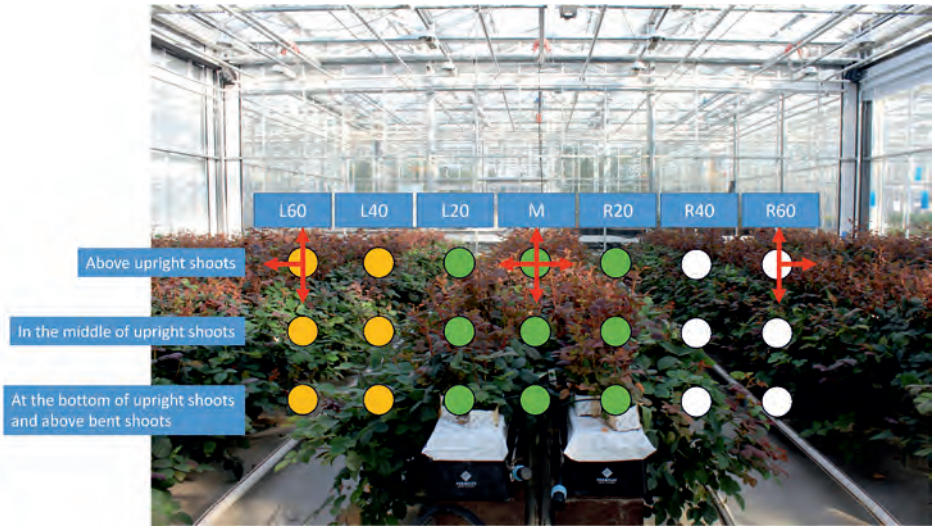

Figure 5.1. The red to far-red ratio (R:FR) measurement plan. Measurements were conducted at three heights (above, in the middle of, and at the bottom of upright shoots but still above bent shoots) and seven positions (L60, L40, L20, M, R20, R40 and R60) with spectrometer sensor facing up, down, right and left. M represents the middle point of the plot; R20, R40 and R60 respectively represent the positions at 20 cm, 40 cm and 60 cm from the middle point to the right; L20, L40 and L60 respectively represent the positions at 20 cm, 40 cm and 60 cm from the middle point to the left. Arrows represent the directions that the spectrometer sensor was facing. In all yellow circles (positions L40 and L60) three measurements were taken, with the spectrometer sensor facing up, down and left; in all green circles (positions L20, M and R20) four measurements were taken, with the sensor facing up, down, right and left; finally in all white circles (positions R40 and R60), again three measurements were taken, now with the sensor facing up, down and right.

Model simulations

Model development. A 3D rose model was constructed in the plant modelling software GroIMP (Hemmerling *et al.*, 2008). The model includes (i) a 3D representation of rose plants at flowering stage, (ii) a radiation and photosynthesis model to simulate light absorption and photosynthesis of rose plants and R:FR distribution in the canopy, and (iii) virtual sensors to measure R:FR in the canopy.

(i) 3D rose plants. Each plant included four upright shoots, and either with or without bent shoots. Upright shoots were constructed using basic plant units representing internodes with compound rose leaves that together make up the shoot. Architectural parameters used for constructing an individual upright shoot included length and diameter of all internodes, length, width, area and leaflet number of all leaves, peduncle length and diameter, and flower width. Architectural measurements of focal plants (measured on day 25) were used to build a database for each treatment. The database contains sets of individual architectural parameters. Each parameter set was obtained from architectural measurements of one shoot. In simulations, architecture parameters of individual upright shoots were randomly selected from the database. Due to the architectural complexity of bent shoots, they were constructed by randomly distributing a number of leaves in the area occupied by bent shoots. Total leaf area of bent shoots was obtained from the experiment. The model was set up such that bent shoot presence could be switched on or off according to the type of treatment to be simulated. Row distance and plant density were set to the same values as in the experiment.

(ii) The radiation and photosynthesis model. The light environment was modelled using a diffuse light dome with moderate gradation towards zenith and azimuthal uniformity (Evers *et al.*, 2010). The light dome started at 60° above the horizontal plane taking into account that most of the light inside the glasshouse compartment (including sunlight and light from the assimilation lamps) comes from the top. Incoming light intensity was kept at 200 μmol m^{-2} s^{-1} and incoming R:FR was kept at 1.4, which represented the average light intensity and R:FR (from both sun and assimilation lamps) inside the glasshouse compartment during the experiment. In each simulation, two rows were simulated, with nine plants in each row. To eliminate the border effects in the light environment, the simulated plant population (18 plants in total) was replicated 10 times in the *x* and *y* directions, resulting in average light conditions as experienced by 100 copies of each individual plant population (1800 plants in total) (de Vries *et al.*, 2018). The amount of photosynthetically active radiation (PAR), red and far-red light reaching the plant organs was simulated using a Monte-Carlo ray tracer embedded in the GroIMP (Hemmerling *et al.*, 2008). Leaf reflectance and transmittance of PAR, red and far-red were obtained from spectrophotometric measurements on rose leaves. Internodes were assumed to have the same reflectance of PAR, red and far-red as leaves, but without transmission. Plant net photosynthesis was calculated as the sum of net photosynthesis of individual leaves, which was in turn calculated based on the light absorption and

photosynthetic parameters (including leaf photosynthetic capacity, dark respiration rate and quantum efficiency) of individual leaves. Photosynthetic parameters of rose leaves were obtained from another experiment with the same rose genotype in the same growth conditions (see Chapter 4). Photosynthetic capacity of individual leaves in upright shoots and bent shoots was assumed to be proportional to the fraction of light intercepted by that leaf (Niinemets & Anten, 2009). Dark respiration rate of individual leaves was assumed to be proportional to photosynthetic capacity of that leaf (Hikosaka *et al.*, 2016b). All leaves were assumed to have the same quantum efficiency.

(iii) Virtual sensors. The virtual sensors were constructed such that the amount of red and far-red light coming from different directions within 180° was measured, similar to the spectrometer used in the experiment. The virtual sensors were rotated and located to mimic the actual measurement plan used in the experiment (Figure 5.1; Figure S5.3).

Model evaluation. The simulated distributions of R:FR ratios in the canopy at flowering stage were compared with the measurements for the four treatments. Virtual sensors were put at the same virtual locations as where the actual R:FR measurements were performed, with sensor facing up, down, right and left. The R:FR ratios measured by virtual sensors were compared with R:FR ratios measured by the spectrometer in the experiment by calculating the coefficient of determination (r^2) and the relative root-mean-square error (r*RMSE*):

$$rRMSE = \frac{1}{\bar{x}}\sqrt{\frac{\sum_{i=1}^{n}(y_i - x_i)^2}{n}} \quad (5.1)$$

where y_i is the simulated value, x_i is the measured value, n is the number of data points, and $\bar{x}$ is the mean of the measured values.

Scenarios. The model simulations were conducted to quantify changes in plant light absorption and photosynthesis resulting from upright shoot architectural responses to the low R:FR ratio reflected from below. Since we found that leaf inclination angle in the upright shoots increased when R:FR from below decreased by the presence of bent shoots, we specifically evaluated the consequences of increasing leaf angle for light absorption and photosynthesis of the upright shoots, the bent shoots and the whole plant. In all simulations, canopies contained both upright shoots and bent shoots (Table 5.1). The bent shoots were always there to generate R:FR signals. In scenarios (i), (iii) and (v), upright shoots and bent shoots together made up the whole plant

(Table 5.1). In scenarios (ii), (iv) and (vi), bent shoots were considered independent foliage that did not belong to the plant, and thus the focal plants were only consisting of upright shoots (Table 5.1). The measurements of the phenotypes of the upright shoots from the four treatments were used to build the upright canopy in the model. First, in scenarios (i) and (ii), we constructed upright shoots using phenotypes obtained from treatments in which neighbour plants did not have bent shoots, i.e., experimental treatments F+N– (i) and F–N– (ii) (Table 5.1). Thus, simulations combining such upright shoot phenotypes in the presence of bent shoots represented the case that upright shoots receive low R:FR from below but do not show any responses to the presence of bent shoots. Then, in scenarios (iii) and (iv), leaf angle in upright shoots was progressively increased by 10%, 20%, 30% and finally 40%, to test situations in which upright shoot leaf angles respond with different strengths to low R:FR signalling from below. The percentages chosen covered the range of changes in leaf angle between treatments observed in the experiment Finally, in scenarios (v) and (vi), we constructed upright shoots using phenotypes obtained from treatments in which neighbour plants had bent shoots, i.e., experimental treatments F+N+ (v) and F–N+ (vi), which represented a full phenotype including all measured architectural responses to low R:FR from below. In scenarios (i), (iii) and (v) in which plants had both upright and bent shoots, whole plant light absorption and photosynthesis were calculated as the sum of upright shoots and bent shoots. In scenarios (ii), (iv) and (vi) in which bent shoots were independent foliage, plant light absorption and photosynthesis equalled to that of upright shoots. The relative changes of light absorption and photosynthesis (ϕ) were calculated (Eq. 5.2) to evaluate the consequences of responses to R:FR from below for plant performance.

$$\phi = (Y - Y_{ref})/Y_{ref} \tag{5.2}$$

where Y_{ref} is the light absorption or photosynthesis calculated in simulation scenarios (i) or (ii); Y is the light absorption or photosynthesis calculated in simulation scenarios (iii)-(vi). ϕ is calculated either between scenarios (i), (iii) and (v) (F+ phenotype) or between scenarios (ii), (iv) and (vi) (F– phenotype). Note that the differences between scenarios (i) vs. (v) and (ii) vs. (vi) could result from not only the differences in architectural traits, but also in shoot arrangements and leaf area distribution. The former may due to random selection of individual shoot phenotype from a different treatment database and the latter may be caused by simultaneous changes of individual internode length and leaf area.

Table 5.1. Descriptions for the simulation scenarios. The scenarios were conducted to study the effects of upright shoot responses to the red to far-red ratio (R:FR) reflected from below on light absorption and photosynthesis of bent shoots and upright shoots. Phenotypes of upright shoots were taken as measured in four treatments of the experiment (scenarios i, ii, v, vi). In Scenario iii and iv the leaf angles of the phenotypes obtained from the experiment were respectively increased by 10%, 20%, 30% and 40%. The column "Experimental treatment used for upright shoot phenotype" gives the treatment from which the phenotype was simulated in each scenario. "F" represents focal plant. "N" represents neighbour plant. – indicates plant with no bent shoots. + indicates plant with bent shoots.

Scenario type	Experimental treatment used for upright shoot phenotype	Attribute of the bent shoots
(i)	F+N–	Part of the focal plants
(ii)	F–N–	Independent foliage
(iii)	F+N–, leaf angles increase by 10% to 40%	Part of the focal plants
(iv)	F–N–, leaf angles increase by 10% to 40%	Independent foliage
(v)	F+N+	Part of the focal plants
(vi)	F–N+	Independent foliage

Results

The presence of neighbour bent shoots decreased R:FR reflected from below

At all three developmental stages of the upright shoots, measured R:FR ratios reflected from below (with sensor facing down) were lower when neighbour plants had bent shoots (F–N+ and F+N+) than when neighbour plants did not (F–N– and F+N–), especially for ratios measured in the middle and at bottom of upright shoots (Figures 5.2, S5.5, S5.6). Such trends were not affected by the presence of bent shoots in focal plants (Figures 5.2, S5.5, S5.6). The R:FR from below, especially at the bottom of the upright shoots, were slightly lower in F+N– than in F–N– due to the scattering of far-red by bent shoots of focal plants (Figures 5.2, S5.5, S5.6). The R:FR of the incident light (measured with sensor facing up) and of horizontally travelling light (with sensor facing right and left) were hardly affected by treatments at all developmental stages (Figures S5.4, S5.5, S5.6).

Leaf inclination angle increased in upright shoots that experienced low R:FR from below

At all developmental stages, internode and leaf length of upright shoots were larger when focal plants had bent shoots (F+N+ and F+N–) than when focal plants did not (F–N+ and F–N–) (Figures 5.3A-D, S5.7). These trends were not affected by the presence of bent shoots in neighbour plants (Figures 5.3A-D, S5.7), suggesting that internode length and leaf length were determined by the assimilates produced by their own bent shoots while their lengths were not affected by R:FR from below. In addition, leaf areas were also larger when focal plants had bent shoots, while the presence of neighbour bent shoots hardly affected leaf area (Figure S5.8). The inclination angles of individual leaves and the average leaf angle in upright shoots were increased in treatments in which neighbour plants had bent shoots (F–N+ and F+N+), regardless of whether or not shoots on the focal plant had been bent (Figure 5.3E,F). This suggested that leaf angle was affected by R:FR from below. Other light signals (e.g., blue and green light) were unlikely to play a role here as we found that the most pronounced effect of neighbour bent shoots on light spectrum in upright shoots was within the range of red and far-red wavelength (Figure S5.9).

The consequences of responding to R:FR from below depended on the type of plants (i.e., with or without bent shoots)

Our model gave sufficiently accurate simulations of R:FR ratios from different directions (up, horizontal and down) and at different heights (above, middle and bottom) in upright shoots (Figure S5.10). The overall *r*RMSE between measured and simulated R:FR values from all directions and at all heights was 0.23, and the overall r^2 was 0.88. This result indicates that the 3D architecture of rose plants both with and without bent shoots was accurately represented in the model, which allowed us to do simulations to explore the consequences of responding to low R:FR from below for plant performance.

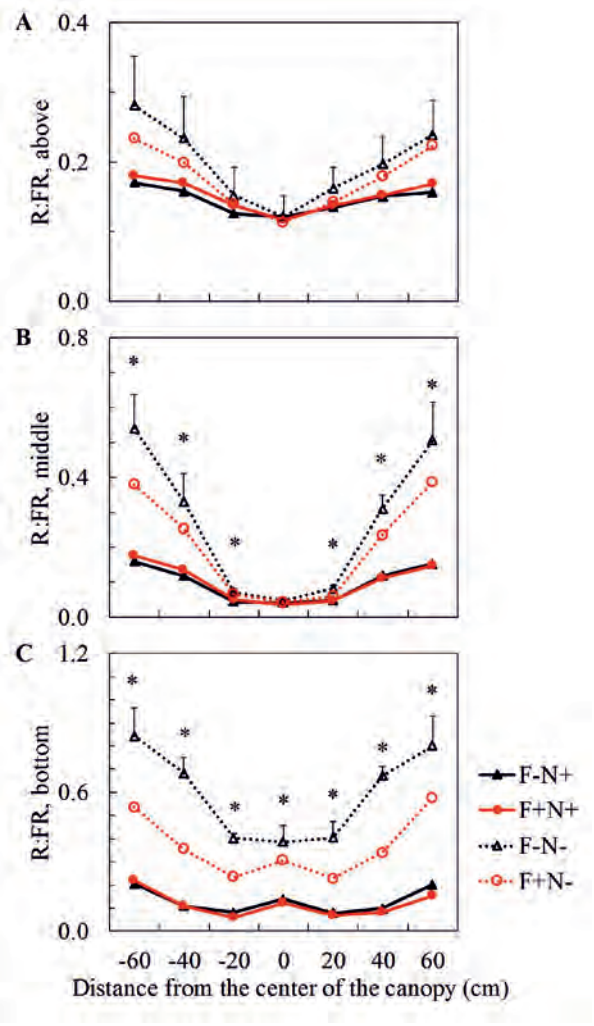

Figure 5.2. Measured red to far-red (R:FR) ratios above (A), in the middle of (B) and at the bottom of (C) upright shoots at flowering stage (day 21 after start of treatments) with spectrometer sensor facing down. In *x*-axis, positive and negative values are distances from the center of the canopy respectively to the right and to the left of the canopy. Details on measurement positions can be found in Figure 5.1. Positive error bars (only given in the highest line in each panel) are standard errors of means. * indicates significant treatment effects when comparing at the same measurement positions ($P < 0.05$). Triangles indicate focal plants (F) without bent shoots (−). Circles indicate focal plants with bent shoots (+). Closed symbols with solid lines indicate neighbour plants (N) with bent shoots. Open symbols with dotted lines indicate neighbour plants without bent shoots.

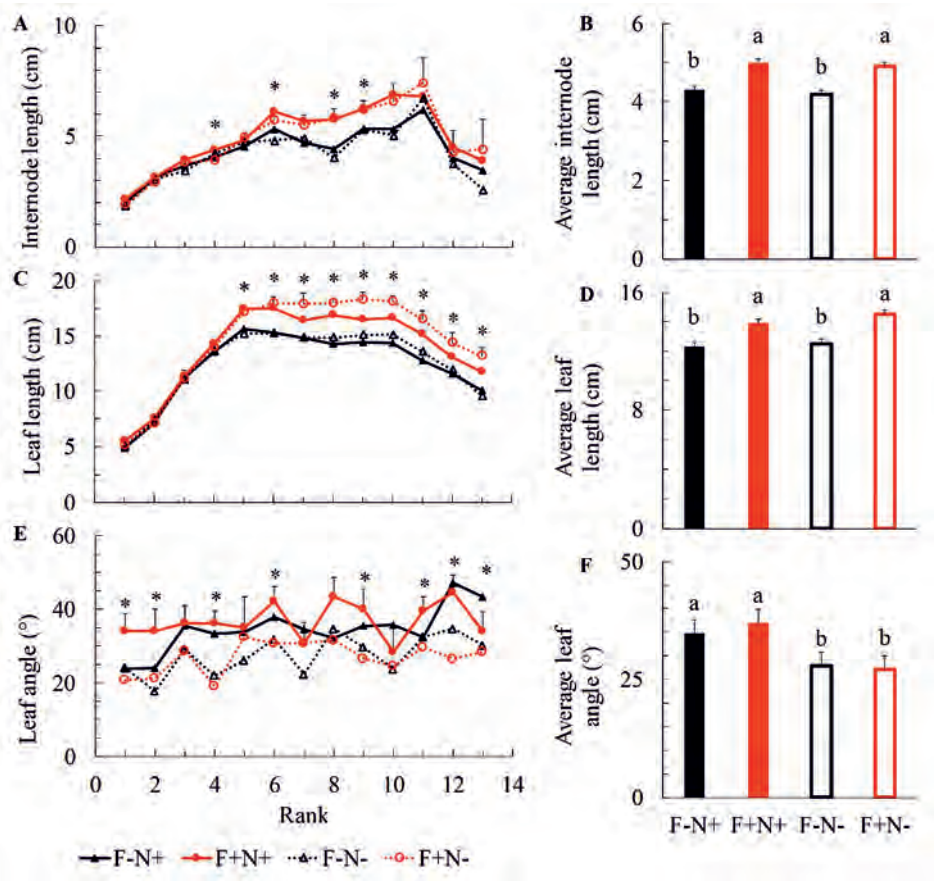

Figure 5.3. Measurements of upright shoot architectural traits. Measurements were conducted on individual organ length at each rank and the average organ length for internodes (A,B) and leaves (C,D), leaf inclination angle at each rank (E), and the average leaf angle (F) in upright shoots at final harvest (day 25 after start of treatments). Positive error bars are standard errors of means (only given in the highest line in panels A,C,E). * (in panels A,C,E) and different letters (in panels B,D,F) indicate significant difference when comparing different treatments at the same rank and for the same trait ($P < 0.05$). "F" represents focal plant. "N" represents neighbour plant. – indicates plant without bent shoots. + indicates plant with bent shoots.

When plants respond to low R:FR by increasing the leaf angle of upright shoots, the simulated light absorption and photosynthesis of upright shoots decreased (Figure 5.4). This occurred in

plants both with and without bent shoots (Figure 5.4). Light absorption and photosynthesis of bent shoots increased due to increasing leaf angle in upright shoots (Figure 5.4). For plants with bent shoots, responses to R:FR from below in upright shoots resulted in an unchanged whole-plant light absorption (Figure 5.4A), as the light not intercepted by upright shoots had been intercepted by bent shoots. Whole-plant photosynthesis was increased by allowing more light to penetrate to bent shoots (Figure 5.4C). When full responses to R:FR from below (including leaf angle and other trait responses that were not statistically significant) were considered, plants with bent shoots increased light absorption and photosynthesis in their bent shoots and the whole plant (Figure 5.5A). However, upright shoot light absorption and photosynthesis were also increased when upright shoots showed full responses to R:FR from below (Figure 5.5A). For plants without bent shoots, full responses to R:FR from below slightly decreased plant light absorption, while plant photosynthesis was not affected (Figure 5.5B).

Discussion

A "bottom-up" effect of far-red on shoot architecture in heterogeneous canopies

Leaves preferentially absorb red light and transmit and reflect a large fraction of far-red light. As a result the R:FR ratio in a plant canopy shows a gradient with the lowest values at the bottom (Holmes & Smith, 1977). Here, we showed that in a heterogeneous canopy, the lower part of a canopy also reflects a substantial amount of far-red to the upper part of the canopy and by consequence the upper canopy perceives low R:FR from below (Figures 5.2, S5.5, S5.6). The decrease in R:FR from below caused by the presence of a lower canopy is the likely cause of an increase of leaf inclination angle in upper shoots (Figure 5.3E,F), as low R:FR is known to induce shade avoidance responses such as leaf hyponasty (Ballaré & Pierik, 2017). In previous studies, the low R:FR reflected from green mulches or weeds below the plants induced longer stems and higher shoot-root ratio in plants (Kasperbauer, 1994; Rajcan *et al.*, 2004). Although we did not find longer internodes in upright shoots that experienced low R:FR from below (Figure 5.3A,B), their internode length per dry weight was higher (Figure S5.8), indicating that these shoots may invest relatively more assimilates into their length growth. Our results together with previous studies indicate that lower vegetation may substantially affect R:FR perception in higher layers, eliciting shade avoidance responses.

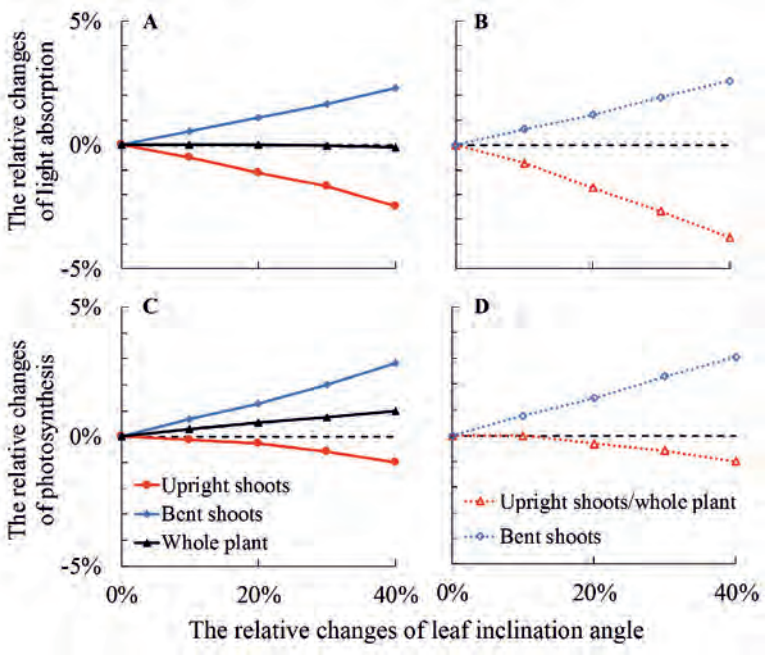

Figure 5.4. The relative changes of simulated plant light absorption (A,B) and photosynthesis (C,D) with increasing leaf angle of upright shoots by 10% to 40%, compared with the case that leaf angle did not respond to low red to far-red ratio from below. In panels (A) and (C), upright shoot phenotype was obtained from the treatment in which focal plants had bent shoots and neighbour plants did not have bent shoots (closed symbols with solid lines). In panels (B) and (D), shoot phenotype was obtained from the treatment in which both focal and neighbours plants did not have bent shoots (open symbols with dotted lines), and upright shoot light absorption and photosynthesis equalled to that of the whole plant. The black dashed line in each panel indicates the level of 0%.

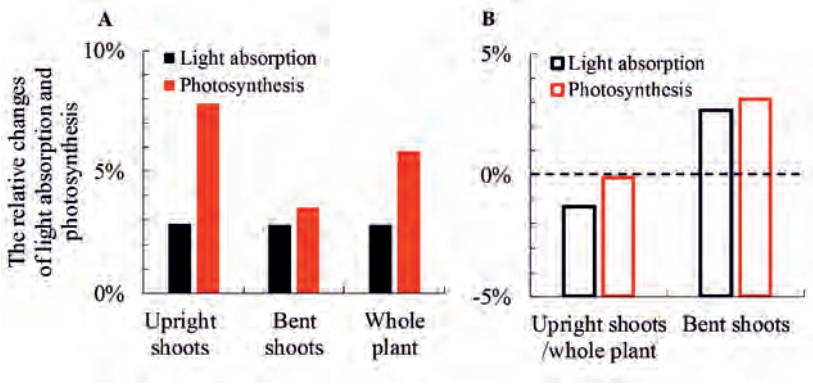

Figure 5.5. The relative changes of simulated plant light absorption and photosynthesis when the full phenotype of upright shoots that did not respond to far-red from below was replaced by the full phenotype that responded to far-red from below. In panel (A), upright shoot phenotypes were obtained from the treatments in which focal plants had bent shoots and neighbour plants either had or did not have bent shoots. In panel (B), upright shoot phenotypes were obtained from the treatments in which focal plants did not have bent shoots and neighbour plants either had or did not have bent shoots; upright shoot light absorption and photosynthesis equalled to that of the whole plant; the black dashed line indicates the level of 0%.

In addition to inducing shade avoidance responses, R:FR could also potentially function as a signal for optimizing canopy performance. Plant canopies are characterized by dramatic gradients of light within the canopy, resulting in leaves in the upper canopy experiencing saturating light conditions whereas leaves in the lower canopy being heavily shaded (Niinemets, 2007). To optimize canopy photosynthesis, plants could (i) distribute their leaf photosynthetic capacities according to the light gradient in the canopy by regulating photosynthetic nitrogen distribution among individual leaves and (ii) optimize light distribution within the canopy by altering canopy structure (Gutschick & Wiegel, 1988; Anten *et al.*, 1995). Although the former has been extensively studied, there is still a debate on what exactly drives leaf nitrogen distribution in the canopy. Light gradient in the canopy either or not through an induction in a transpiration gradient has been proposed as an important mechanism (Boonman *et al.*, 2007). However, plants could also potentially distribute their leaf nitrogen according to the top-down R:FR gradient in the canopy (Pons *et al.*, 1993; Pons & De Jong-Van Berkel, 2004). Here, we showed that the R:FR reflected from the lower canopy (a "bottom-up" R:FR gradient) may also function as a signal to optimize canopy structure, as a

steeper leaf angle in the upper canopy (likely induced by the low R:FR from below) allows more light to penetrate to the lower canopy (Figure 5.4A). Nevertheless, the increase of leaf angle in the upper canopy only led to a marginal increase (1% to 2%) in plant photosynthesis (Figure 5.4C).

The "bottom-up" R:FR effect, however, has been ignored in both shade avoidance studies and canopy performance optimizations. Most shade avoidance studies have focussed on horizontal or top-down light gradient thus implicitly assuming that only R:FR signals from similarly-sized or larger neighbours matter (Evers *et al.*, 2006; Weijschedé *et al.*, 2006; Liu *et al.*, 2007; Bongers *et al.*, 2018). Similarly, only the top-down R:FR gradient has received some attentions in studies on optimizing canopy photosynthesis (Pons *et al.*, 1993; Pons & De Jong-Van Berkel, 2004). However, in most natural systems and some crop production systems that feature spatially heterogeneous canopies, such as the rose crop in our experiment but also strip intercropping systems (Brooker *et al.*, 2015), far-red light is transmitted or reflected not only from above and the side, but also from below. Since such signals may elicit plant responses affecting their performance, the relevance of R:FR signals coming from below should not be ignored.

R:FR from below: to respond or not?

Both lower leaves of a plant canopy or lower vegetation of neighbours located below the plants could induce low R:FR reflection from below. Our simulations showed that the consequences of responding to R:FR from below in terms of leaf angles depend on the type of the signal (Figure 5.4). The responses are only beneficial when R:FR from below is reflected by the lower part of the same plant canopy, as responses in the upper canopy to R:FR from below increase whole-plant photosynthesis by allowing more light to penetrate to the lower canopy, at the expense of light absorption of upper shoots (Figure 5.4A,C). This result suggests that for a heterogeneous plant canopy consisting of distinctly different parts, responses of the upper canopy to R:FR from below decrease the level of competition within the plant, being that the upper canopy "gives away" part of its light absorption to the lower canopy, and such responses increase whole-plant performance. When low R:FR is reflecting from lower canopy of independent foliage, responses to R:FR from below decrease plant light absorption and photosynthesis (Figure 5.4B,D). This result suggests that for plants growing with independent lower vegetation, responses to R:FR from below decrease plant performance, as such

responses are unnecessary competitive responses to unthreatening neighbours. Our results support the idea that plants need to avoid wasteful competition, including self-competition with other parts of the same plant and unnecessary competition with non-competitive neighbours, to optimize performance (Novoplansky, 2009; Pierik *et al.*, 2013). As far as we know, we are the first to exemplify this idea with results in light absorption and photosynthesis of shoots aboveground. While in previous studies, this idea is mostly exemplified by results in roots belowground (Falik *et al.*, 2003, 2006).

To avoid such wasteful competition aboveground, ideally, plants should only respond to R:FR signals from below when such signal comes from lower canopy of the same plant. This requires plants to be able to discriminate between R:FR neighbour signals and self-signals. Evidence on self- and nonself-recognition is mostly documented for belowground signals. Several species are found to be able to discriminate between roots of themselves and roots of neighbours, thus to reduce self-competition in roots and allow more assimilates being allocated to aboveground for competition for other resources such as light (Falik *et al.*, 2003, 2006; Gruntman & Novoplansky, 2004; Chen *et al.*, 2012). Further studies are needed to investigate whether or not plants can discriminate between self- and nonself-signals aboveground and how do plants use self-signals aboveground to optimize canopy structure to increase plant performance.

Future perspectives

Understanding the mechanisms of plant responses to far-red reflected from below may provide new insights in breeding of ideotypes for different crop systems. In mixed-species systems, shade avoidance responses of the large crop induced by R:FR signals reflected by the small crop may allow more light to penetrate to the small crop, reducing the competition for light by the large crop and thus increase productivity of the whole system. In such a case, R:FR signals from below can be regarded as a "self-signal" for the system as a whole, and responses to this signal could reduce "self-competition" within the system and may improve overall light capture and productivity (similar to our simulation results in Figure 5.4A,C). Therefore, if possible, trait selection could focus on crop phenotypes with responses in some traits (e.g., increasing leaf angle) to R:FR from below. In contrast, in crop-weed systems, shade avoidance responses of the crop plants induced by the low R:FR reflected by weeds, especially in early crop developmental stages, could be relevant to crop yield loss (Page *et al.*, 2010). This is

possibly because low R:FR reflected by weeds (i) induces an increase of biomass allocation to stem at the expense of other organs and decreases leaf area and harvest index of the crop and (ii) increases the shoot-root ratio of the crop and may hamper the belowground competition for water and nutrients with weeds (Ballaré & Casal, 2000; Rajcan & Swanton, 2001; Page *et al.*, 2010). Our simulations also suggested that responses to R:FR from independent foliage below the plants decreased plant light absorption and photosynthesis (Figure 5.4B,D). Hence, for higher crop productivity in weed-infested systems, crop genotypes with less or no shade avoidance responses to R:FR signals from below could be selected for. These two examples show the relevance of further research on how and by which plant parts R:FR signals are perceived (Pantazopoulou *et al.*, 2017) and how this information can be used to optimize plant responses through breeding.

Concluding remarks

A "bottom-up" effect of far-red on the architecture of upper shoots in terms of increasing leaf inclination angle was observed in a heterogeneous canopy, indicating that lower vegetation could affect higher parts of the canopy through R:FR signalling. The consequences of responding to R:FR signals from below depend on the origin of the signal. Responses to R:FR from below are beneficial for plant performance when this signal is reflecting from lower part of the same plant canopy. However, such responses are not beneficial for plant performance when R:FR is reflected by independent foliage. We propose that more attention should be paid on plant responses to light signals coming from below to understand plant performance in heterogeneous canopies and guide breeding of ideotypes for different crop systems.

Supporting information

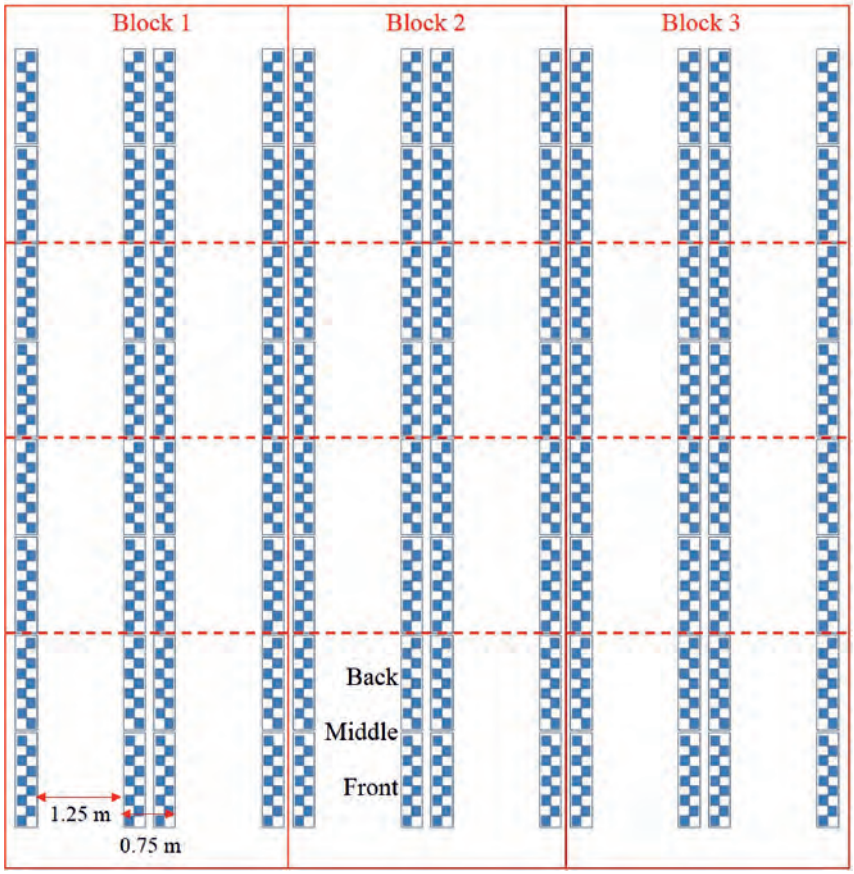

Figure S5.1. Block design in the glasshouse compartment. Each solid blue square represents a rose plant. The solid red lines separate the blocks. The dashed red lines separate the treatments.

Figure S5.2. Pictures of the four treatments in the experiment. (a) F–N+: focal plants (F; marked with red crosses) without bent shoots (–) and neighbour plants (N) with bent shoots (+); (b) F+N+: focal plants with bent shoots and neighbour plants with bent shoots; (c) F–N–: focal plants without bent shoots and neighbour plants without bent shoots; (d) F+N–: focal plants with bent shoots and neighbour plants without bent shoots.

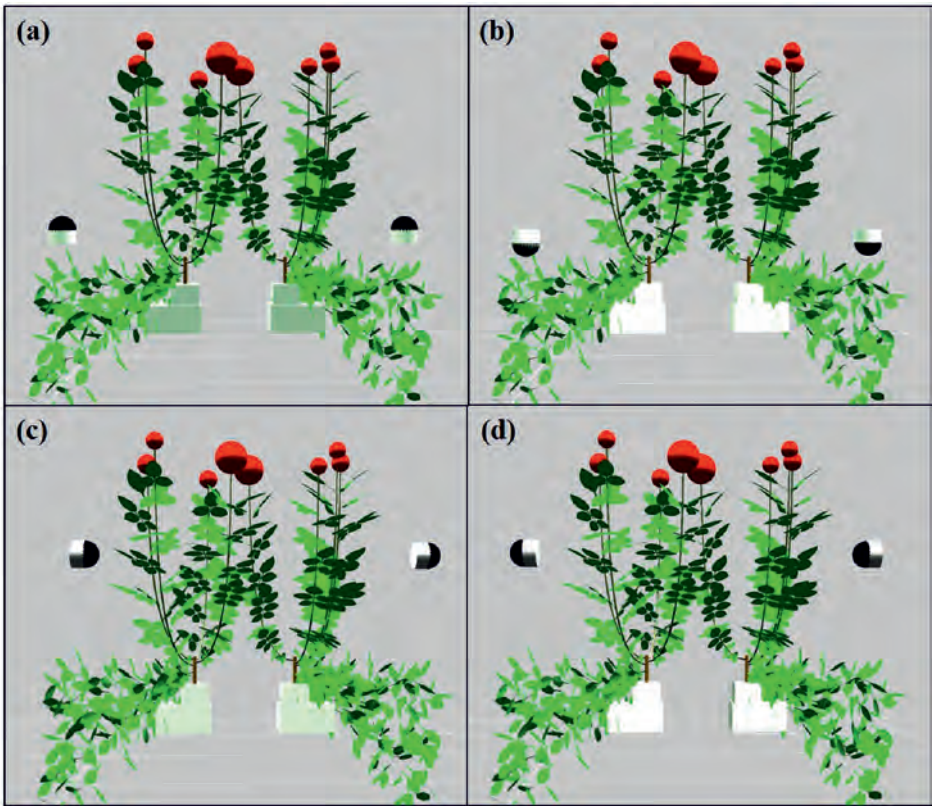

Figure S5.3. Examples of simulated rose plants with bent shoots and virtual sensors. Virtual sensors are located at the bottom (a,b) and in the middle (c,d) of upright shoots, and facing up (a), down (b), right (c) and left (d).

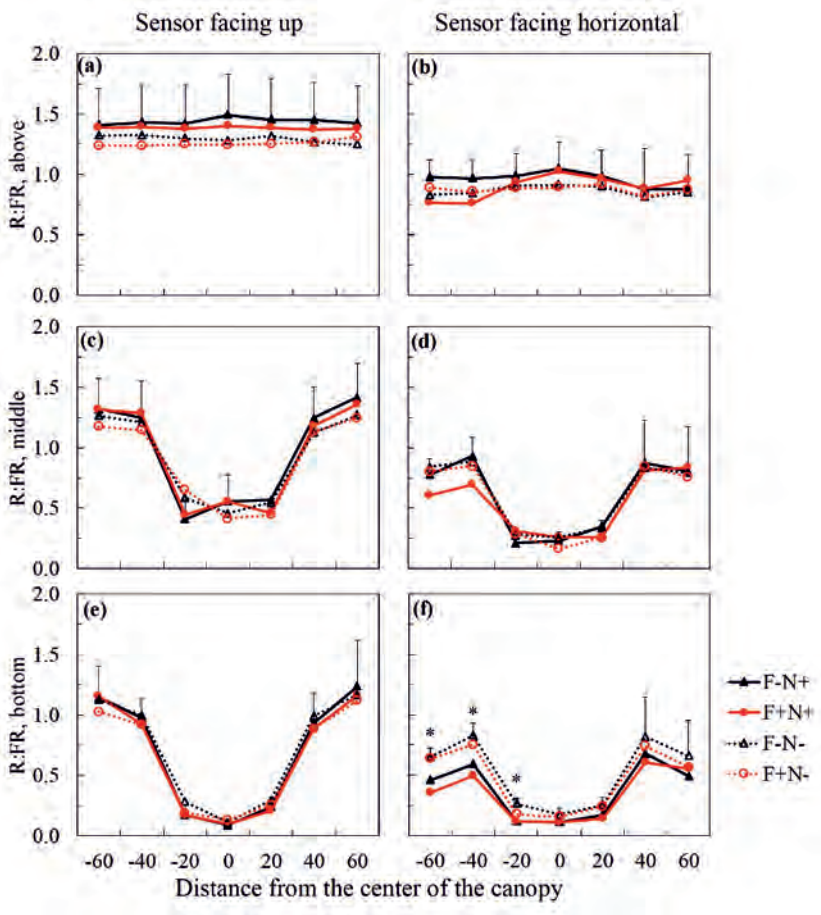

Figure S5.4. Measured red to far-red (R:FR) ratios above (a,b), in the middle of (c,d) and at the bottom of (e,f) upright shoots on day 21 after start of treatments with spectrometer sensor facing up (a,c,e) and horizontal (b,d,f). In *x*-axis, positive and negative values are distances from the center of the canopy respectively to the right and to the left of the canopy. Results of spectrometer sensor facing horizontal are the R:FR ratios measured with sensor facing left at -60 and -40 cm to the center of the canopy, the R:FR ratios measured with sensor facing right at 60 cm and 40 cm to the center of the canopy, and the average values of R:FR ratios measured with sensor facing right and left at -20, 0 and 20 cm to the center of the canopy. Positive error bars (only given in the highest line in each panel) are standard errors of means. * indicates significant treatment effects when comparing at the same measurement positions ($P < 0.05$). Triangles indicate focal plants (F) without bent shoots (−). Circles indicate focal plants with bent shoots (+). Closed symbols with solid lines indicate neighbour plants (N) with bent shoots. Open symbols with dotted lines indicate neighbour plants without bent shoots.

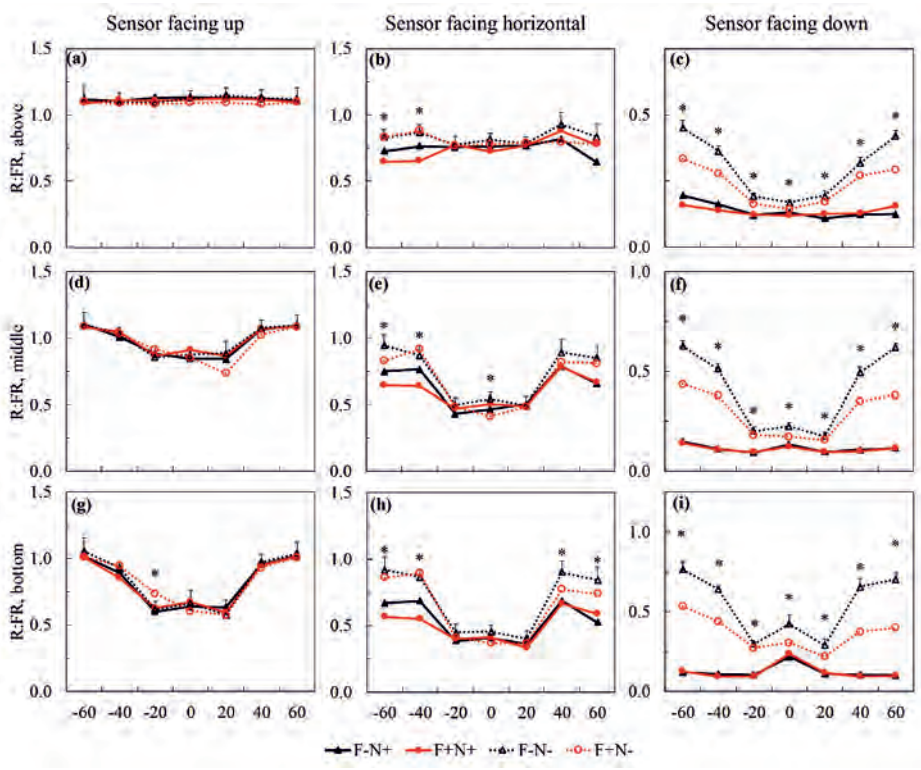

Figure S5.5. Measured red to far-red (R:FR) ratios above (a-c), in the middle of (d-f) and at the bottom of (g-i) upright shoots on day 4 after start of treatments with spectrometer sensor facing up (a,d,g), horizontal (b,e,h) and down (c,f,i). In *x*-axis, positive and negative values are distances from the center of the canopy respectively to the right and to the left of the canopy. Details on measurements with sensor facing horizontal can be found in Figure S5.4. Positive error bars (only given in the highest line in each panel) are standard errors of means. * indicates significant treatment effects when comparing at the same measurement positions ($P < 0.05$). Triangles indicate focal plants (F) without bent shoots (–). Circles indicate focal plants with bent shoots (+). Closed symbols with solid lines indicate neighbour plants (N) with bent shoots. Open symbols with dotted lines indicate neighbour plants without bent shoots.

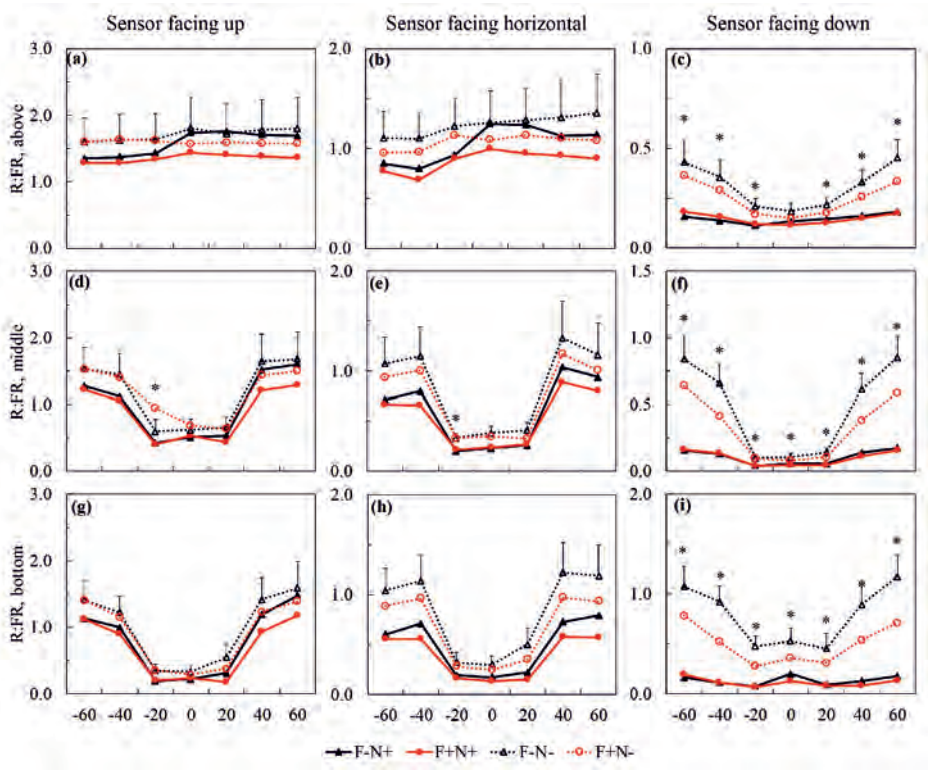

Figure S5.6. Measured red to far-red (R:FR) ratios above (a-c), in the middle of (d-f) and at the bottom of (g-i) upright shoots on day 13 after start of treatments with spectrometer sensor facing up (a,d,g), horizontal (b,e,h) and down (c,f,i). In *x*-axis, positive and negative values are distances from the center of the canopy respectively to the right and to the left of the canopy. Details on measurements with sensor facing horizontal can be found in Figure S5.4. Positive error bars (only given in the highest line in each panel) are standard errors of means. * indicates significant treatment effects when comparing at the same measurement positions ($P < 0.05$). Triangles indicate focal plants (F) without bent shoots (–). Circles indicate focal plants with bent shoots (+). Closed symbols with solid lines indicate neighbour plants (N) with bent shoots. Open symbols with dotted lines indicate neighbour plants without bent shoots.

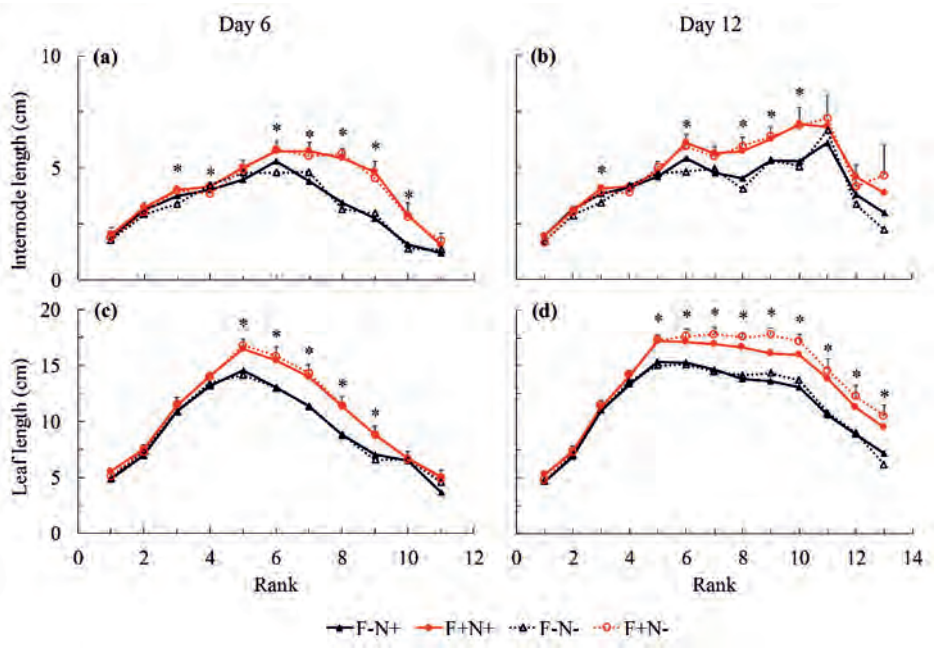

Figure S5.7. Measurements of internode length (a,b) and leaf length (c,d) at each rank of upright shoots on day 6 (a,c) and 12 (b,d) after start of treatments. Positive error bars (only given in the highest line in each panel) are standard errors of means. * indicates significant treatment effects when comparing at the same rank ($P < 0.05$). Triangles indicate focal plants (F) without bent shoots (–). Circles indicate focal plants with bent shoots (+). Closed symbols with solid lines indicate neighbour plants (N) with bent shoots. Open symbols with dotted lines indicate neighbour plants without bent shoots.

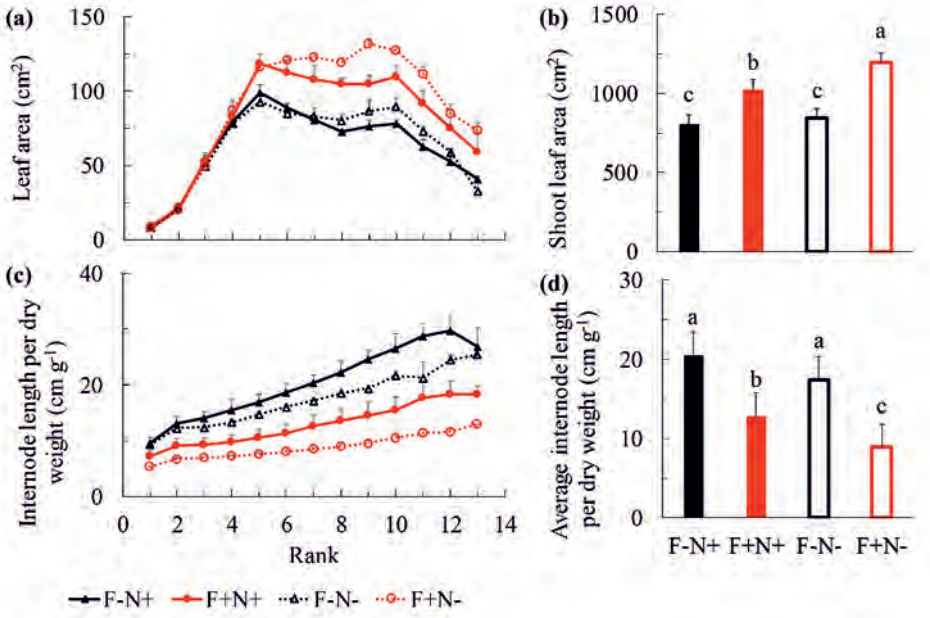

Figure S5.8. Measurements of upright shoot architectural traits. Measurements were conducted on individual leaf area at each rank (a), shoot total leaf area (b), individual internode length per dry weight at each rank (c), and average internode length per dry weight (d) in upright shoots at final harvest (day 25 after start of treatments). Positive error bars are standard errors of means. Different letters (in panels b,d) indicate significant difference ($P < 0.05$). "F" represents focal plant. "N" represents neighbour plant. − indicates plant without bent shoots. + indicates plant with bent shoots.

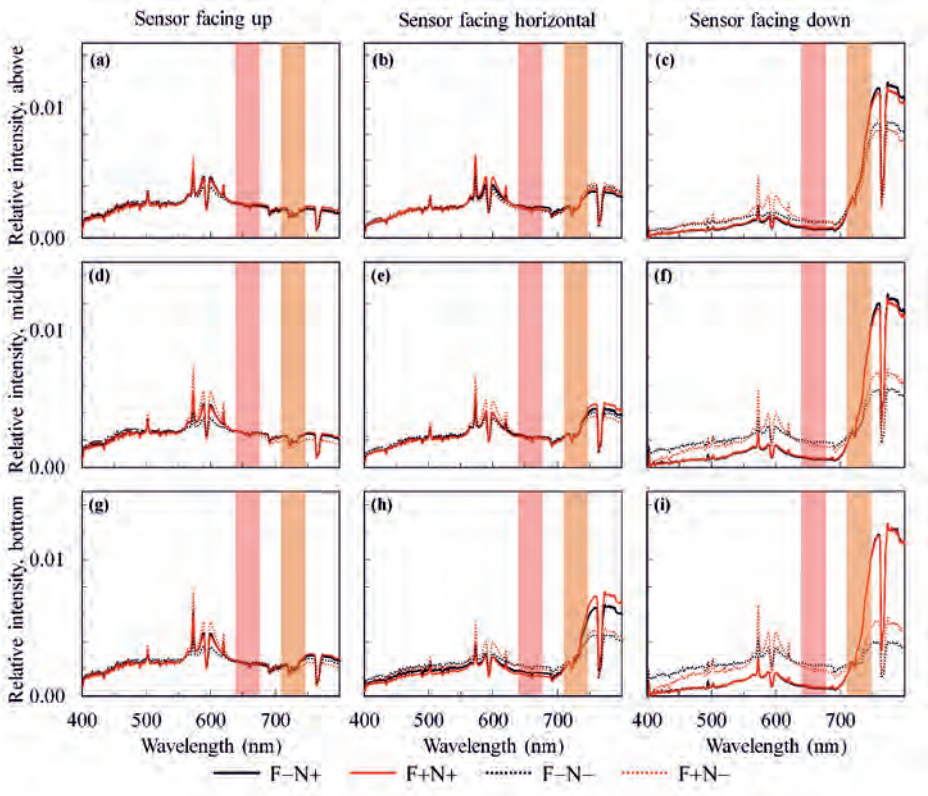

Figure S5.9. Light spectral measured above (a-c), in the middle of (d-f) and at the bottom of (g-i) the upright shoots at flowering stage with sensor facing up (a,d,g), horizontal (b,e,h) and down (c,f,i). The presented results are the light spectrum outside the upright shoots, which is calculated as the average of measurements at 40 cm and 60 cm from the middle to the right and left respectively. These results represent the spectrum composition of light propagating towards (thus can be received by) upright shoots. The red and orange areas in each panel respectively indicate the range of red (660±20 nm) and far-red (730±20 nm) wavelength that corresponds with the ranges of the spectrometer sensor used to measure red to far-red ratio in the experiment. "F" represents focal plants. "N" represents neighbour plants. − indicates plants without bent shoots. + indicates plants with bent shoots.

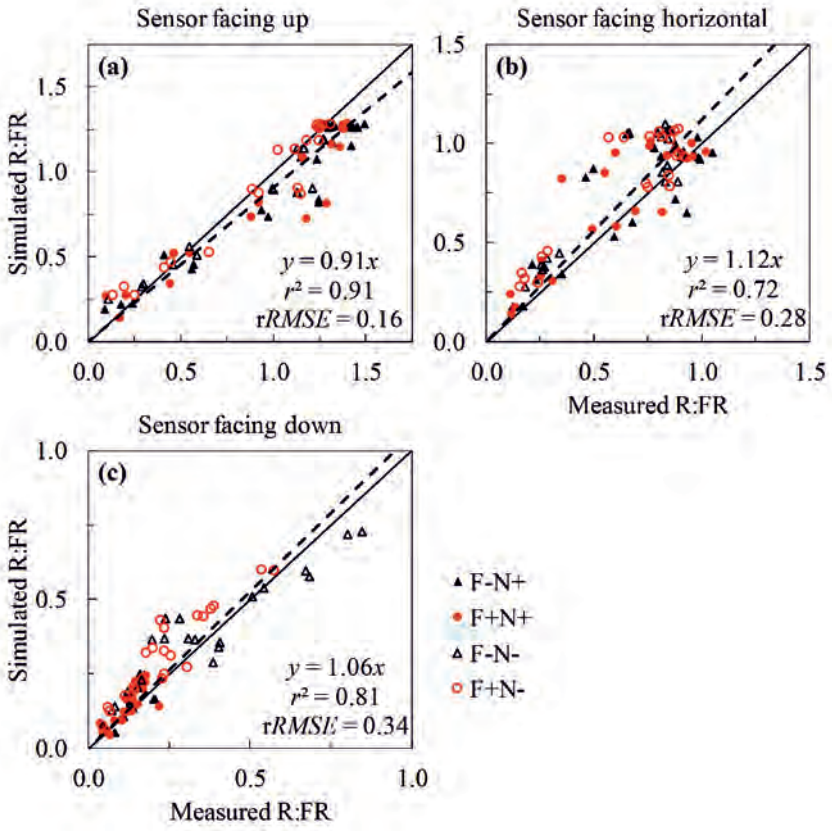

Figure S5.10. Comparisons between measured and simulated red to far-red (R:FR) ratios at flowering stage with sensor facing up (a), horizontal (b) and down (c). Each panel contains measured and simulated R:FR ratios above, in the middle and at bottom of upright shoots. Solid lines are 1:1 line. Dashed lines are fitted curve by forcing the line through the origin. r*RMSE* is the relative root-mean-square error. "F" represents focal plants. "N" represents neighbour plants. – indicates plants without bent shoots. + indicates plants with bent shoots.

Chapter 6

General discussion

In my thesis, I aimed to quantify photosynthesis responses to multiple environmental factors and changes in crop structure linking leaf, plant and crop levels. I did this taking lily and rose crops growing in the greenhouse as examples. First, I quantified photosynthesis responses to water and nitrogen stress combinations at leaf level in lily (Chapter 2). Second, I quantified the consequences of functional trait responses to the combination of low photosynthetically active radiation (PAR) and low red to far-red ratio (R:FR) for photosynthesis at leaf and plant level in rose (Chapter 3). Third, I studied the effects of bent shoots on flower shoot photosynthesis and growth in rose production. In rose, non-flowering shoots are bent downwards (the so-called bent shoots) to support growth of upright flower shoots. (i) I analysed the extent to which photosynthesis by bent shoots contributes to upright shoot growth and thus increases upright shoot biomass and morphological quality traits (Chapter 4). (ii) I studied whether and how reflection of far-red light by bent shoots induces responses in upright shoots and how this in turn indirectly affects plant photosynthesis (Chapter 5).

There are three main themes which flow through my thesis. First, as plants are frequently exposed to simultaneous changes of multiple environmental factors and cues, the combination of multiple factors that affect plant photosynthesis is embedded in my thesis. In all research chapters of my thesis, plants are subjected to simultaneous variations of two factors, e.g., water and nitrogen stress combinations (Chapter 2) and low PAR and low R:FR combinations (Chapter 3). In Chapters 4 and 5, shoot bending entails a combined effect of extra assimilate supply and the far-red reflection on upright flower shoots. Second, an important factor that determines crop performance is canopy photosynthesis rather than photosynthesis of one single leaf or an individual plant. Thus upscaling photosynthesis from leaf to plant and crop level is an important topic in my thesis. Third, computational models are useful tools for quantitative analyses in my thesis. In Chapter 2, I applied the Farquhar, von Caemmerer and Berry (FvCB) model to quantify photosynthesis responses at leaf level. In Chapters 3-5, I applied a functional-structural plant (FSP) model to quantify photosynthesis responses at plant and crop level.

In this general discussion, I will place the three main themes of my thesis in the broader perspective of crop production and provide some thoughts for future studies. First, I will discuss the importance of studying plant responses to the combinations of multiple environmental factors. Then I will discuss the relevance of upscaling from responses of

individual functional traits to performance at plant and crop levels. Following this part, I will discuss how an FSP model can be a useful tool to do the upscaling, and discuss the potential strength of combining the FSP model with other modelling approaches. Finally, I will discuss the implications for crop breeding and cultivation in the greenhouse and field.

Plant responses to simultaneous changes in multiple environmental factors

The complex growth conditions for plants

Plants deal with variations in multiple environmental factors during their life cycle. In natural conditions, plants can hardly achieve potential growth due to the occurrence of growth reducing factors (i.e., stresses). The main abiotic stresses frequently occurring in the field include drought, salinity, heat, chilling and excessive radiation, and the main biotic stresses include pathogens, viruses, nematodes and herbivore pests (Suzuki *et al.*, 2014). The effects of individual stresses on plant growth and reproduction have been extensively studied under controlled conditions in the laboratory where these effects can be studied in isolation (reviews by Mittler, 2006; Mittler & Blumwald, 2010; Atkinson & Urwin, 2012; Suzuki *et al.*, 2014). However, in natural field conditions, variations of multiple environmental factors generally occur simultaneously. For instances, in semi-arid regions, plants not only suffer from drought stress but also may experience excess heat and radiation that often interact with drought (Carvalho *et al.*, 2016). Drought in turn may be accompanied by low nutrient availability in the soil. In Chapter 2, I showed that even plants growing in protected cultivation conditions (in this case low-tech greenhouses) may suffer from water and nitrogen stress combinations. Plants growing in vegetation stands normally experience simultaneous changes in light intensity and spectral composition. These two factors may also change simultaneously in the greenhouse due to the use of artificial lighting. Next to abiotic factors, plants are affected by multiple biotic stresses such as pathogens and pests (Atkinson & Urwin, 2012). This entails that plants need to cope with simultaneous changes of multiple factors during their growth.

The frequency and intensity of stresses may be strongly modified by global climate change. The average surface temperature is predicted to increase by 3–5 °C in the next 50–100 years, with the concurrent increases in the frequency of extreme weather conditions which lead to drought, flood and heat waves (IPCC, 2014). The changes in climate factors in combination will not only affect growth and reproduction of crop plants but also possibly change the habitat

range and behaviour of pests and pathogens, which in turn affects crop production (Gregory *et al.*, 2009). Under such circumstances, agricultural production could be significantly reduced. In the meantime, the global population is expected to reach 9.5 billion by 2050, which requires increases in productions of all crop types (e.g., food crops and ornamental crops) in both field and greenhouse to meet global needs. This leads to a great demand for crop management strategies that optimize crop production, as well as crop varieties that are tolerant to stress combinations (Newton *et al.*, 2011). Understanding the mechanisms underlying plant responses to simultaneous changes of multiple factors is crucial for developing such multi-stress tolerant crop varieties (Mittler & Blumwald, 2010; Atkinson & Urwin, 2012).

Quantifying the consequences of responses to multiple factors for plant performance under environmental variations

Currently there is a consensus that plant responses to stress combinations are unique and cannot be directly derived from responses to individual stresses (Rizhsky *et al.*, 2002, 2004; Hewezi *et al.*, 2008; Atkinson *et al.*, 2013; Suzuki *et al.*, 2014). The unique responses are caused by the fact that (i) the expressions of some genes are only up- or down-regulated under stress combinations but not by individual stresses (Rizhsky *et al.*, 2004; Atkinson *et al.*, 2013) and (ii) hormone signalling pathways that control plant responses to individual stresses interact with each other (both antagonistically or synergistically) when multiple pathways are induced simultaneously under stress combinations (Anderson *et al.*, 2004; Melotto *et al.*, 2006; Atkinson & Urwin, 2012). The identification of specific genes and the interactions between signalling pathways associated with different stresses has received ample attention in the past decades (reviews by Mittler & Blumwald, 2010; Atkinson & Urwin, 2012; Suzuki *et al.*, 2014). Such studies are crucial for understanding the mechanisms that underlie plant responses to stress combinations. However, the ultimate goal of developing new varieties that are tolerant to stress combinations is to increase or at least maintain crop yield production in current and future adverse growth conditions. To achieve this goal, the consequences of plant responses to stress combinations for crop performance need to be understood in detail. This requires upscaling from responses at cellular or organ level to the performance at plant and crop level. This further entails: (i) separately quantifying the consequences of individual functional traits for plant performance to identify which traits are beneficial and which are not and (ii)

quantifying how these functional traits interact in determining plant performance under stress combinations. Such studies are difficult to be done using conventional experiments alone.

In my thesis, I showed that a combination of experimentation and modelling makes it possible to quantify the consequences of individual trait responses to combinations of environmental factors for plant performance. In Chapter 3, I showed an example of quantifying the interactive effects of individual functional trait responses to a combination of low PAR and low R:FR on plant performance in terms of plant photosynthesis. To this end, I applied a combined approach of a light experiment and an FSP model. The light experiment allowed me to separately study the effects of low PAR and low R:FR on leaf photosynthetic and plant architectural traits. In the experiment, R:FR was manipulated by adding additional far-red light emitting diodes (LED) above the plants without changing the PAR level, and PAR was manipulated by adding neutral shading screen above the plants without changing the R:FR. While under natural canopy shade, R:FR reduced with the lowering of PAR. This makes that the plant phenotype under canopy shade is an integrated result of multiple responses to both low PAR and low R:FR. From this experiment, I found that plant responses to low PAR (e.g., decreased leaf photosynthetic capacity) were clearly different from responses to low R:FR (e.g., increased internode length an leaf angle). The plant data that I collected in the light experiment were then used to develop an FSP model. Using the FSP model, I was able to separately quantify the effects of individual trait responses on plant photosynthesis by only changing one trait parameter at a time while keeping all other parameters at the unshaded level. This would be very difficult to do by experiments alone, as we then need to have mutants that only show responses in one specific trait when exposing to changes of an environmental factor. Whereas using the FSP model, any phenotype of interest, including ones that do not exist in reality, can be created virtually. From the simulations, I found that the relative importance of individual trait responses for plant photosynthesis changed with shade levels. Moreover, the consequence of one trait response for plant photosynthesis under shade depended on responses in other traits. For example, lower respiration rate was found under low light and this response was beneficial for plant photosynthesis under shade. However, the positive effect of lower respiration rate was mitigated by the fact that leaf area was also reduced under shade (Chapter 3, Figure 3.7). My results thus suggest the need of considering the interactions between the consequences of multiple plant trait responses to environmental factors for plant performance (i.e., the trait response syndrome). Otherwise, we may overestimate or underestimate the effect of each

individual trait response for plant performance. The approach presented in Chapter 3 (combining experimentation with modelling) can be further extended to other study systems which entail simultaneous changes of multiple factors, to quantify the interactive consequences of individual trait responses to multiple factors for plant performance.

The dynamically changing environments

Natural environments are never constant. Thus plants need to cope with dynamically changing environments during their growth period. Fast responses of functional traits to changes in environmental factors can be induced by chemical signalling. For example, fast stomatal closure can be induced by abscisic acid (ABA) signalling within seconds or a few minutes under drought (Geiger *et al.*, 2011). The fast stomatal closure may increase plant fitness under drought through increasing water use efficiency (Jakab *et al.*, 2005). In general, such a response is almost fully reversible, i.e., plants can open stomates again once water availability improves. However, many other traits, especially architectural and resource allocation traits, need time to adapt to the environment and can be at least to some extent irreversible. For example, plants may respond to low water availability by increasing biomass allocation to roots at the expense of leaves (Li *et al.*, 2000). This helps to maintain a balance between water uptake and loss, and helps the plant to maintain its water status (Sperry *et al.*, 1998). However, once water availability improves, the low leaf area hampers plant light absorption and photosynthesis and associated growth. Thus, when plants suddenly experience a new environment, trait responses that increased plant performance in the previous environment may no longer increase it in the new environment. In other words, plastic adjustments to conditions early in life may compromise performance later in life when conditions change.

The example I showed in Chapter 3 can roughly be extrapolated to agroforestry systems in which small woody species are shaded by overstory tree foliage (the so-called canopy shade). However, it is possible that woody plants suddenly receive high light due to the removal of overstory layers, which may be caused by harvest of timber or when overstory trees lose branches or fall over. This raises the question, how would a plant that plastically adjusts its functional traits to shade conditions perform when the plant is suddenly exposed to high light? Using the same approach as in Chapter 3, I further assessed the consequences of functional trait responses to shade for plant photosynthesis at high light. To this end, I used the simulated shaded phenotype at a shading leaf area index (LAI) of 3 as an extreme case, which was the

most heavy shade simulated in Chapter 3. All plant trait parameters used in this shaded phenotype were directly adopted from parameters used in Chapter 3. The high light intensity was set to 1000 μmol m^{-2} s^{-1}, which represented more than 10-fold increase in light intensity compared to the simulated light level (= 85 μmol m^{-2} s^{-1}) under a canopy with LAI = 3 (Chapter 3). The simulation results showed that most of the trait responses induced by low PAR that increased plant photosynthesis under shade were not beneficial anymore at high light (Chapter 3, Figure 3.6; Figure 6.1A). For example, the lower A_{max} increased plant photosynthesis by up to 70% under shade due to the concomitant reduction in respiration cost (Chapter 3, Figure 3.6B); however, once the plants were suddenly exposed to high light, this reduced A_{max} had a negative effect (40%) on plant photosynthesis (Figure 6.1A). Thus a plastic adjustment to low PAR can at least to some extent compromise performance if light suddenly increases, as it will take time for the plant to readjust its photosynthesis to high light. There are two ways for plants to readjust their A_{max}. First, plants could produce new leaves that develop in and thus adapt to high light environment. This will take time before the leaves are mature and able to contribute to plant photosynthesis. Second, plants could readjust A_{max} in existing leaves by enlarging their chloroplasts. This process, however, can be limited by the thickness of shaded leaves which determines the open palisade cell wall space to accommodate the enlargement of chloroplasts (Oguchi *et al.*, 2003, 2005). Overall, the full phenotype obtained under shade had a 50% lower photosynthesis at high light compared with the unshaded phenotype (Figure 6.1B). These results emphasize the need of taking into account the dynamically changing environments when assessing the consequences of trait responses for plant performance. FSP models can be useful in this regard as they can realistically simulate consequences of plastic trait responses for plant performance.

Upscaling from individual trait responses to performance at plant and crop levels

Yield production is dependent on crop performance rather than performance of one individual plant or photosynthesis of one single leaf (Donald, 1968; Anten & Vermeulen, 2016). Therefore, maximizing crop performance is generally an objective in agricultural production systems. Crop performance is strongly determined by the way individual plants in the crop interact (Hirose & Werger, 1987a; Anten & Hirose, 2001; Anten, 2005). Plant performance in turn is an integrated result of responses of individual functional traits to multiple environmental factors. As noted I found strong interactions between the consequences of

individual trait responses for plant photosynthesis (Chapter 3). This makes that understanding crop performance under changes of multiple environmental factors requires quantifying how responses at organ or plant level interact in determining crop performance, which entails (i) separately quantifying the consequences of individual trait responses to each environmental factor for plant performance and (ii) upscaling from these individual trait responses and their interactions to performance at plant and crop levels.

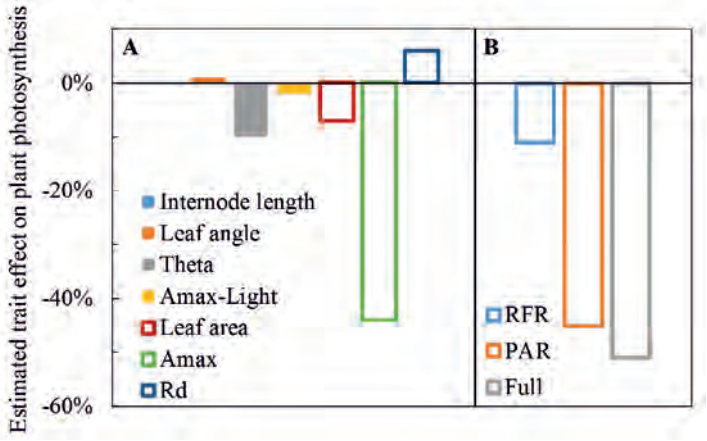

Figure 6.1. The effects of responses of individual functional traits (A) and the combination of traits (B) to canopy shade on plant photosynthesis at high light (= 1000 μmol m^{-2} s^{-1}). Trait parameters of the shaded phenotype are directly adopted from the parameters used in the simulated shaded phenotype under a shading leaf area index of 3 in Chapter 3. Trait effects are calculated as the relative changes of plant photosynthesis caused by changing an individual trait or a combination of traits compared with plant photosynthesis of non-shaded phenotype (Chapter 3, Eq. 3.5). In panel (A), solid bars are trait responses induced by low red to far-red ratio (R:FR); open bars are trait responses induced by low photosynthetically active radiation (PAR); Theta' is the curvature factor of light response curve; 'Amax' is the maximum leaf photosynthetic rate A_{max}; 'Amax-Light' is the coefficient describing the correlation between light gradient and A_{max} gradient in the canopy; 'Rd' is the coefficient describing the relationship between A_{max} and dark respiration rate. In panel (B), 'RFR' represents the phenotype for which all trait responses to low R:FR are changed simultaneously; 'PAR' represents the phenotype for which all trait responses to low PAR are changed simultaneously; 'Full' represents the phenotype for which all trait responses to both low R:FR and low PAR are changed simultaneously.

Trait responses that decrease performance at organ or plant level may be beneficial for crop performance. In Chapter 5, I showed that shoot bending in cut-rose production system entailed a substantial amount of far-red reflected by the bent shoots towards the upright flower shoots (Chapter 5, Figure 5.2). This induced an increase of leaf inclination angle in upright shoots (Chapter 5, Figure 5.3E,F), which decreased light absorption and photosynthesis of upright shoots (Chapter 5, Figure 5.4). The steeper leaf angle, however, allowed more light to penetrate to the bent shoots, which increased photosynthesis of the whole plant canopy (Chapter 5, Figure 5.4). Conversely, trait responses that are beneficial for individual plant performance may decrease performance at the crop level (Anten & Vermeulen, 2016). For instances, a taller plant could capture more light in crop stands, thus the increase of plant height is beneficial for individual plant performance (Falster & Westoby, 2003). However, the increase of plant height also entails costs such as biomass investment in the stem for support and maintenance costs for the stems and vasculature (Givnish, 1982; Midgley, 2003). These costs otherwise may be used to increase seed biomass, which is normally of interest to grain crop production. Thus the increase of plant height may decrease crop performance.

In addition, the consequences of trait responses for crop performance may differ in different types of crop systems. The results shown in Chapter 5 generally indicate that responses of the upper canopy to the R:FR of light reflected by the lower canopy are beneficial for performance of the crop that features a heterogeneous canopy structure. Similarly, such responses may also be beneficial for performance of the strip or mixed intercropping system, where responses of the large crop (occupying the upper canopy of the whole system) to R:FR reflected by the small crop (occupying the lower canopy) may increase photosynthesis of the whole system. However, responses to R:FR from below may not be beneficial when a crop is interacting with a smaller weed, as responses to R:FR reflects off weeds may decrease light absorption and photosynthesis of the crop plants.

Therefore, to avoid any biased evaluations of the benefits of individual traits for crop production, the consequences of trait responses for crop performance, should be assessed at both organ, plant and crop levels and specified for different types of crop systems.

Functional-structural plant model as a tool

The upscaling from individual trait responses to performance at plant and crop level cannot be done by experiments alone, but needs a combination of dedicated experimentation and modelling. Photosynthesis at the canopy level is a crucial factor that drives crop performance. An essential step towards understanding crop performance is properly modelling canopy photosynthesis, which generally involves modelling (i) light distribution and leaf light absorption, (ii) the distribution of leaf photosynthetic parameters, and (iii) the distribution of other environmental factors that are relevant to the photosynthetic process (e.g., temperature and relative humidity) in the canopy. In conventional canopy photosynthesis models, canopy light distribution is normally modelled using the Beer-Lambert equation (Monsi & Saeki, 2005). Some approaches further consider the distributions of direct and diffuse light, solar angle, and leaf angle (de Wit, 1965; Goudriaan, 1977). The distribution of leaf photosynthetic capacity is modelled according to the leaf nitrogen distribution in the canopy, or modelled according to the fraction of light intercepted by the leaf assuming that light distribution in the canopy drives the distribution of leaf nitrogen (Hirose & Werger, 1987b; Niinemets & Anten, 2009). These assumptions are largely used in modelling canopy photosynthesis of the monoculture crop system that consists of the same plant species. In such a system, the strong light gradient exists in the vertical direction in the canopy whereas the horizontal light distribution in the canopy is assumed to be uniform. The distributions of environmental factors other than light, however, are generally assumed to be uniform (in both vertical and horizontal directions) in these canopy photosynthesis models.

Next to the strong gradient of light in the canopy, the distributions of other environmental factors can also be quite heterogeneous. For example, the ambient air temperature differs with the temperature at the leaf or meristem level (Kichah *et al.*, 2012; Savvides *et al.*, 2013). Also, there were strong gradients of temperature and relative humidity in the rose canopy (van Westreenen, unpublished). Furthermore, many natural or agroforestry and intercropping systems consist of mixed stands with species having distinct differences in their architecture (Bellow & Nair, 2003; Brooker *et al.*, 2015). In some crop systems, such as the rose production system with bent shoots used in this study (Chapters 4 and 5), plant architecture is tailored to favour crop management (e.g., reducing the work load of harvesting fruits) or the production of harvestable plant parts (fruits and flower production) (Schubert *et al.*, 1995; Ito *et al.*, 1999;

Kim & Lieth, 2004; Han *et al.*, 2007; Lopez *et al.*, 2014). In these situations, canopy structure can be spatially heterogeneous in the horizontal direction, resulting in strong light gradients in both vertical and horizontal directions in the canopy. Thus, the assumptions in the conventional canopy photosynthesis models do not hold for such heterogeneous situations.

A further key point in upscaling from individual plant performance to the crop level is to consider the interactions between individual plants (described in the previous section). Individual plants in a vegetation stand (including both mono and mixed species vegetation, and especially the natural ones) are not identical, due to intra- and inter-specific variations. Understanding how the performance of a given individual plant affects its neighbours, either by competition or facilitation, is an important topic in ecological research (Brooker, 2006; Aschehoug *et al.*, 2016). This requires a modelling approach that can quantify differences between individuals to investigate the consequences of plant-plant interactions for plant performance.

The FSP model explicitly simulates plant architecture in three-dimensions (3D) taking into account the physiological processes (e.g., photosynthesis and transpiration) and the local environments at the individual organ level (Vos *et al.*, 2010). An FSP model, thus can take into account the variations of environmental factors (not only light, but also other factors like temperature and humidity) in the canopy, including both ones with homogeneous and heterogeneous canopy structures. As FSP models can specifically simulate the 3D architecture of each individual plant in the canopy taking into account the differences between individual plants, they are suitable for simulation studies on crop performance in mixed stands (Zhu *et al.*, 2015; Evers *et al.*, 2018), photosynthesis of heterogeneous canopies (Buck-Sorlin *et al.*, 2011; also see Chapters 4 and 5) and local responses induced by plant-plant interactions (de Wit *et al.*, 2012; Pantazopoulou *et al.*, 2017). Moreover, the FSP model can be further combined with other modelling approaches.

As FSP models explicitly simulate plant 3D architecture and the local light environment at organ level, these models are frequently combined with detailed leaf photosynthesis models, e.g., to simulate plant growth and biomass allocation at the detailed level (Evers *et al.*, 2010) and to analyse limiting factors for photosynthesis in different canopy layers (Chen *et al.*, 2014a). Combing these two types of models results in a useful tool to upscale from leaf photosynthesis to plant and canopy photosynthesis, when plant responses to environmental

variations occur at different levels (e.g., leaf, plant and crop level). For example, in Chapter 2, I quantified responses of photosynthesis and CO_2 diffusional processes to water and nitrogen stress combinations at the leaf level, using the FvCB model (Farquhar *et al.*, 1980) and the Ball, Woodrow and Berry (BWB) (Ball *et al.*, 1987) model which is revised by Leuning (1995) and Yin & Struik (2009a). Plant architecture, however, can also be affected by drought and nitrogen stresses. For instances, leaf folding and changes in leaf inclination angles and leaf orientations are found under drought (Comstock & Mahall, 1985; Kusaka *et al.*, 2005). These changes may reduce the leaf area that is directly irradiated by sunlight. A reduction in leaf area may result in a low light absorption, which will lead to both less transpiration and less photosynthesis. The combination of an FSP model and a leaf photosynthesis and stomatal conductance model can then be applied to analyse how changes in plant architecture affect local light environment, and together with changes in leaf photosynthetic and transpirational processes, affect plant and canopy photosynthesis and water use efficiencies under stress conditions. In addition, there is currently an increasing attention on dynamic photosynthesis, and how to increase yield through manipulating processes that are relevant to photoprotection at the fluctuating light environment (Kaiser *et al.*, 2015; Kromdijk *et al.*, 2016). Light in plant canopies is very dynamic, resulting in leaves frequently experiencing sharp fluctuations of irradiance. When light increases very fast, leaf photosynthetic rate cannot immediately increase to the level of steady-state. Similarly when light suddenly goes from high to low levels, relaxation of photoprotection processes is normally delayed, resulting in losses of photosynthesis at low light (Zhu *et al.*, 2004; Kaiser *et al.*, 2015). This makes that steady-state photosynthesis models tend to overestimate photosynthesis in fluctuating light environments (Naumburg & Ellsworth, 2002). Detailed dynamic photosynthesis models have been developed to take the fluctuating situations into account (Thornley, 1998; Morales *et al.*, 2018). By combining a dynamic photosynthesis model with an FSP model, the consequences of dynamic photosynthesis can be up-scaled from leaf to canopy level, to assess the impact of dynamic photosynthesis on yield production.

An FSP model can also be combined with a phylloclimate model, as many physiological processes (e.g., photosynthesis) and disease and pathogen development (e.g., fungal diseases) are driven by local environmental conditions. Phylloclimate models calculate the distribution of light, temperature, and humidity around each organ (Chelle, 2005). A combination of these two types of models can be used to investigate the feedbacks between local climate conditions

and physiological and disease processes at organ level. Subsequently, these organ-level responses can be up-scaled to performance at plant and crop level using the combined model. For example, stomatal opening, on the one hand, affects local humidity and temperature levels by regulating water vapour exchange between leaf and ambient air (Collatz *et al.*, 1991); the local humidity and temperature levels then affect the development and activity of disease and pests (Boulard *et al.*, 2002). In addition, stomatal closure can be a defence strategy of plants to prevent bacterial invasion through open stomates (Melotto *et al.*, 2006). On the other hand, stomatal opening affects the CO_2 diffusion from ambient air into the leaf, which affects leaf photosynthesis (Farquhar & Sharkey, 1982). These processes in concert cause a trade-off between local disease development or defence processes and local photosynthesis (or growth). For instance, stomatal closure may lower the chance of bacterial invasion (i.e., increase the level of defence), while it also reduces leaf CO_2 uptake and photosynthesis (i.e., decrease growth). However, whether or not the trade-off at local level affects growth at plant level, is dependent on processes at other parts of the plant, e.g., whether or not the decrease of growth at this location can be compensated by growth of other plant parts. Using a combination of an FSP model and a phylloclimate model, these processes can be simulated and their feedbacks can be quantified (Figure 6.2). A parallel project next to my thesis is working on quantifying the distribution of microclimate factors in a rose canopy, and then combining the phylloclimate model with an FSP model to simulate the development of fungal diseases (van Westreenen, on-going PhD project).

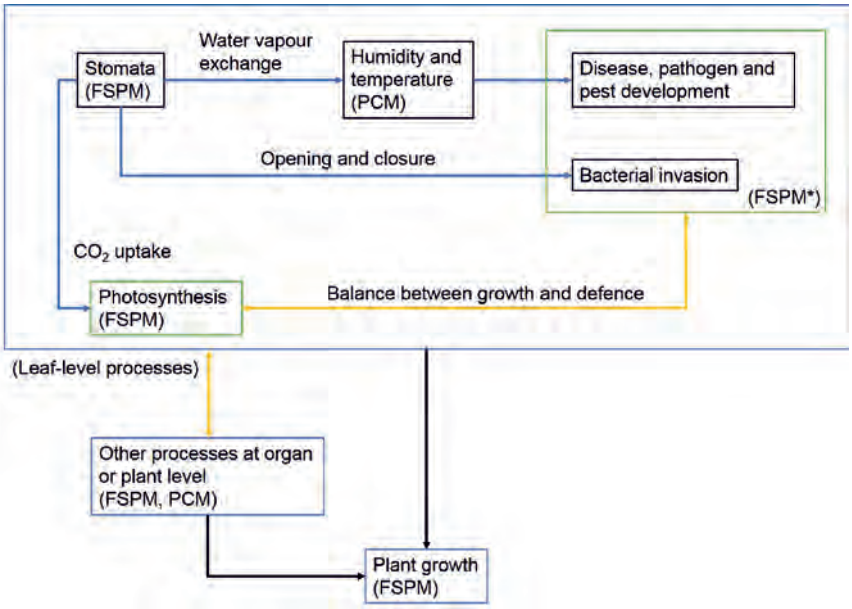

Figure 6.2. An example of combining a functional-structural plant model (FSPM) and a phylloclimate model (PCM). The concept map shows how stomatal opening affects phylloclimate factors, plant physiological processes and disease development, and how these processes and their feedbacks can be simulated by an FSPM and a PCM. *Modelling disease development or bacterial invasion using an FSPM requires the incorporation of specific sub-models to simulate these processes in the FSPM.

Implications for crop breeding and cultivation in the greenhouse and field

The next generation of crop varieties is expected to have a higher yield potential and to be able to tolerate multiple stress combinations (Newton *et al.*, 2011; Long *et al.*, 2015). In the greenhouse where stress levels tend to be lower than in the open field, crops also need to deal with the combination of multiple factors due to intense human interference (e.g., the use of supplementary lighting and manipulations of crop structure). Understanding the mechanisms underlying plant responses to simultaneous changes of environmental factors is a crucial step towards developing new crop varieties for both field and greenhouse conditions (Mittler & Blumwald, 2010; Atkinson & Urwin, 2012). However, achieving a complete overview of these mechanisms is difficult, as plant responses are governed by expressions of many genes and

signalling pathways which interact with each other. Therefore, to speed up crop breeding, it is important to narrow down research and direct it to the specific traits that are relevant to yield production. Crop performance is an end result of multiple plant responses to environmental variations, which are in turn induced by regulations of gene expression and signalling processes (i.e., from genes to plant traits to crop performance). However, with the application of modelling tools, trait selection for crop breeding can go the other way around, i.e., from crop performance to plant traits to genes. Plant traits that are most relevant to crop performance in a specific environment can be identified through model scenario studies (Sarlikioti *et al.*, 2011; also see Chapter 3). The benefits of these trait responses can be tested across a range of environments using models, noting that environmental conditions dynamically change in the field (Sambatti & Caylor, 2007). These results can then guide studies on the mechanisms underlying specific plant trait responses.

In greenhouse production systems, growth conditions can be highly controlled and optimized for crop yield and quality all year round. This increases land use efficiency, resulting in a promising avenue to cope with the decreasing availability in arable land together with the increasing demand for crop production. The greenhouse system allows the environmental factors to be fine-tuned for crop growth and development. However, managements of greenhouse conditions also entail complex effects on plants. For example, the use of artificial lighting (e.g., high-pressure sodium lamps and LEDs) simultaneously change light intensity and spectrum. In addition, assimilation lamps can be put in different positions in the greenhouse (e.g., inter lighting) to optimize light distribution in the canopy (Hovi-Pekkanen & Tahvonen, 2008; Hao *et al.*, 2012). This entails that light in the greenhouse not only comes from the top of the canopy, but also from the middle and even bottom of the canopy, which makes that some leaves may receive relatively more light from abaxial side than adaxial side of leaves. As the leaf photosynthetic rate is generally higher when the leaf receives light from the adaxial side compared to the abaxial side (Paradiso & Marcelis, 2012), changes of the light directions could affect crop photosynthesis. The FSP models (in Chapters 3-5) that include the simulations of photosynthesis and plant morphogenesis responses to light spectrum and directions can be helpful in designing the optimal light recipe for greenhouse crop production. Studies have been done to investigate responses of plant photosynthesis efficiency and morphogenesis to different light spectrum (e.g., red, blue and far-red) and directions (Evans & Vogelmann, 2003; Hogewoning *et al.*, 2010, 2012; Trouwborst *et al.*, 2010; also see Chapters

3 and 5). It is worthwhile to put further effort in modelling these responses, and incorporating these processes in FSP models to facilitate designing light recipe for crop production and ideotype for crop breeding in the greenhouse.

Concluding remarks

Plants generally are exposed to simultaneous changes of multiple abiotic and biotic factors. Plant responses to the combination of multiple environmental factors are unique and cannot be derived from responses to individual factors. Understanding plant responses to simultaneous changes of multiple factors requires not only to understand the mechanisms underlying these unique responses, but also to quantify the consequences of these responses for plant performance under environmental variations. For the latter purpose, the interactions between the consequences of individual trait responses for plant performance need to be considered, as well as the upscaling of trait effects from organ level to plant and crop levels. An FSP model is a very useful tool to quantify the interactive effects of individual trait responses on plant performance and to do the upscaling. Further combining the FSP model with detailed leaf photosynthesis models (for both steady-state and dynamic photosynthesis) and phylloclimate models can be used to quantify the feedbacks between environmental factors, plant responses and biotic processes and the effects of these feedbacks on plant performance. Moreover, the FSP model can be used to identify promising traits for crop breeding to guide research on the underlying mechanisms, and to design optimal growth conditions for greenhouse crops.

References

Adam M, Van Bussel LGJ, Leffelaar PA, Van Keulen H, Ewert F. **2011**. Effects of modelling detail on simulated potential crop yields under a wide range of climatic conditions. *Ecological Modelling* **222**: 131–143.

Alton PB, North PR, Los SO. **2007**. The impact of diffuse sunlight on canopy light-use efficiency, gross photosynthetic product and net ecosystem exchange in three forest biomes. *Global Change Biology* **13**: 776–787.

Anderson JP, Badruzsaufari E, Schenk PM, Manners JM, Desmond OJ, Ehlert C, Maclean DJ, Ebert PR, Kazan K. **2004**. Antagonistic interaction between abscisic acid and jasmonate-ethylene signaling pathways modulates defense gene expression and disease resistance in Arabidopsis. *The Plant Cell* **16**: 3460–3479.

Anten NPR. **2005**. Optimal photosynthetic characteristics of individual plants in vegetation stands and implications for species coexistence. *Annals of Botany* **95**: 495–506.

Anten NPR, Ackerly DD. **2001**. A new method of growth analysis for plants that experience periodic losses of leaf mass. *Functional Ecology* **15**: 804–811.

Anten NPR, Alcala-Herrera R, Schieving F, Onoda Y. **2010**. Wind and mechanical stimuli differentially affect leaf traits in Plantago major. *New Phytologist* **188**: 554–564.

Anten NP, Hirose T. **2001**. Limitations on photosynthesis of competing individuals in stands and the consequences for canopy structure. *Oecologia* **129**: 186–196.

Anten NPR, Martínez-Ramos M, Ackerly DD. **2003**. Defoliation and growth in an understory palm: Quantifying the contributions of compensatory responses. *Ecology* **84**: 2905–2918.

Anten NPR, Schieving F, Werger MJA. **1995**. Patterns of light and nitrogen distribution in relation to whole canopy carbon gain in Cs and C4 mono- and dicotyledonous species. *Oecologia* **101**: 504–513.

Anten NPR, Vermeulen PJ. **2016**. Tragedies and crops: Understanding natural selection to improve cropping systems. *Trends in Ecology and Evolution* **31**: 429–439.

Anten NPR, von Wettberg EJ, Pawlowski M, Huber H. **2009**. Interactive effects of spectral shading and mechanical stress on the expression and costs of shade avoidance. *The American Naturalist* **173**: 241–255.

Archontoulis SV, Yin X, Vos J, Danalatos NG, Struik PC. **2012**. Leaf photosynthesis and respiration of three bioenergy crops in relation to temperature and leaf nitrogen: How conserved are biochemical model parameters among crop species? *Journal of Experimental Botany* **63**: 895–911.

Aschehoug ET, Brooker R, Atwater DZ, Maron JL, Callaway RM. **2016**. The mechanisms and consequences of interspecific competition among plants. *Annual Review of Ecology, Evolution, and Systematics* **47**: 263–281.

Atkinson NJ, Lilley CJ, Urwin PE. **2013**. Identification of genes involved in the response of Arabidopsis to simultaneous biotic and abiotic stresses. *Plant Physiology* **162**: 2028–2041.

Atkinson NJ, Urwin PE. **2012**. The interaction of plant biotic and abiotic stresses: from genes to the field. *Journal of Experimental Botany* **63**: 3523–3544.

Baille A, Gutierrez Colomer RP, Gonzalez-Real MM. **2006**. Analysis of intercepted radiation and dry matter accumulation in rose flower shoots. *Agricultural and Forest Meteorology* **137**: 68–80.

Baird AS, Anderegg LDL, Lacey ME, Hillerislambers J, van Volkenburgh E. **2017**. Comparative leaf growth strategies in response to low-water and low-light availability: variation in leaf physiology

underlies variation in leaf mass per area in Populus tremuloides. *Tree Physiology* **37**: 1140–1150.

Baldocchi D. **1997**. Measuring and modelling carbon dioxide and water vapour exchange over a temperate broad-leaved forest during the 1995 summer drought. *Plant Cell and Environment* **20**: 1108–1122.

Ball JT, Wood IE, Berry JA. **1987**. A model predicting stomatal conductance and its contribution to the control of photosynthesis under different environmental conditions. In: Biggens J, ed. Progress in photosynthesis research. Martinus-Nijhoff Publisher, Dordrecht, The Netherlands, 221–224.

Ballaré CL. **1999**. Keeping up with the neighbors: phytochrome sensing and other signalling mechanisms. *Trends in Plant Science* **4**: 97–102.

Ballaré CL, Casal JJ. **2000**. Light signals perceived by crop and weed plants. *Field Crops Research* **67**: 149–160.

Ballaré CL, Pierik R. **2017**. The shade-avoidance syndrome: Multiple signals and ecological consequences. *Plant Cell and Environment*: 2530–2543.

Bell DL, Galloway LF. **2007**. Plasticity to neighbour shade: Fitness consequences and allometry. *Functional Ecology* **21**: 1146–1153.

Bellow JG, Nair PKR. **2003**. Comparing common methods for assessing understory light availability in shaded-perennial agroforestry systems. *Agricultural and Forest Meteorology* **114**: 197–211.

Bernacchi CJ, Portis AR, Nakano H, von Caemmerer S, Long SP. **2002**. Temperature response of mesophyll conductance. Implications for the determination of rubisco enzyme kinetics and for limitations to photosynthesis in vivo. *Plant Physiology* **130**: 1992–1998.

Bernacchi CJ, Singsaas EL, Pimentel C, Portis AR, Long SP. **2001**. Improved temperature response functions for models of Rubisco-limited photosynthesis. *Plant, Cell and Environment* **24**: 253–259.

Biehler K, Fock H. **1996**. Evidence for the contribution of the Mehler-peroxidase reaction in dissipating excess electrons in drought-stressed wheat. *Plant physiology* **112**: 265–272.

Bongers FJ, Evers JB, Anten NPR, Pierik R. **2014**. From shade avoidance responses to plant performance at vegetation level: using virtual plant modelling as a tool. *New Phytologist* **204**: 268–272.

Bongers FJ, Pierik R, Anten NPR, Evers JB. **2018**. Subtle variation in shade avoidance responses may have profound consequences for plant competitiveness. *Annals of Botany*: 1–11.

Boonman A, Prinsen E, Gilmer F, Schurr U, Peeters AJM, Voesenek LACJ, Pons TL. **2007**. Cytokinin import rate as a signal for photosynthetic acclimation to canopy light gradients. *Plant Physiology* **143**: 1841–1852.

Boulard T, Mermier M, Fargues J, Smits N, Rougier M, Claude Roy J. **2002**. Tomato leaf boundary layer climate: implications for microbiological whitefly control in greenhouses. *Agricultural and Forest Meteorology* **110**: 159–176.

Bradshaw AD. **1965**. Evolutionary significance of phenotypic plasticity in plants. In: Advances in genetics. 115–155.

Braune H, Muller J, Diepenbrock W. **2009**. Integrating effects of leaf nitrogen, age, rank, and growth temperature into the photosynthesis-stomatal conductance model LEAFC3-N parameterised for barley (Hordeum vulgare L.). *Ecological Modelling* **220**: 1599–1612.

Brooker RW. **2006**. Plant – plant interactions and environmental change. *New Phytologist* **171**: 271–284.

Brooker RW, Bennett AE, Cong W, Daniell TJ, George TS, Hallett PD, Hawes C, Iannetta PPM, Jones HG, Karley AJ, *et al.* 2015. Improving intercropping : a synthesis of research in agronomy ,

plant physiology and ecology. *New Phytologist* **206**: 107–117.

Buck-Sorlin G, De Visser PHB, Henke M, Sarlikioti V, Van Der Heijden GWAM, Marcelis LFM, Vos J. **2011**. Towards a functional-structural plant model of cut-rose: Simulation of light environment, light absorption, photosynthesis and interference with the plant structure. *Annals of Botany* **108**: 1121–1134.

von Caemmerer S, Evans J. **1991**. Determination of the average partial pressure of CO_2 in chloroplasts from leaves of several C3 plants. *Australian Journal of Plant Physiology* **18**: 287.

von Caemmerer S, Farquhar G, Berry J. **2009**. Biochemical model of C3 photosynthesis. *Molecules*: 209–230.

Cai T, Flanagan LB, Jassal RS, Black TA. **2008**. Modelling environmental controls on ecosystem photosynthesis and the carbon isotope composition of ecosystem-respired CO2 in a coastal Douglas-fir forest. *Plant, Cell and Environment* **31**: 435–453.

Callaway RM, Pennings SC, Richards CL. **2003**. Phenotypic plasticity and interactions among plants. *Ecology* **84**: 1115–1128.

Carvalho LC, Coito JL, Gonçalves EF, Chaves MM, Amâncio S. **2016**. Differential physiological response of the grapevine varieties Touriga Nacional and Trincadeira to combined heat , drought and light stresses. *Plant Biology* **18**: 101–111.

Carvalho SMP, Heuvelink E. **2003**. Effect of assimilate availability on flower characteristics and plant height of cut chrysanthemum: an integrated study. *The Journal of Horticultural Science and Biotechnology* **78**: 711–720.

Casal JJ. **2012**. Shade avoidance. In: The Arabidopsis Book.

Casal JJ. **2013**. Photoreceptor signaling networks in plant responses to shade. *Annual review of plant biology* **64**: 403–27.

Cechin I, de Fátima Fumis T. **2004**. Effect of nitrogen supply on growth and photosynthesis of sunflower plants grown in the greenhouse. *Plant Science* **166**: 1379–1385.

Centritto M, Lauteri M, Monteverdi MC, Serraj R. **2009**. Leaf gas exchange, carbon isotope discrimination, and grain yield in contrasting rice genotypes subjected to water deficits during the reproductive stage. *Journal of Experimental Botany* **60**: 2325–2339.

Challinor AJ, Ewert F, Arnold S, Simelton E, Fraser E. **2009**. Crops and climate change: Progress, trends, and challenges in simulating impacts and informing adaptation. *Journal of Experimental Botany* **60**: 2775–2789.

Chaves MM, Flexas J, Pinheiro C. **2009**. Photosynthesis under drought and salt stress: Regulation mechanisms from whole plant to cell. *Annals of Botany* **103**: 551–560.

Chaves MM, Pereira JS, Maroco J, Rodrigues ML, Ricardo CPP, Osório ML, Carvalho I, Faria T, Pinheiro C. **2002**. How plants cope with water stress in the field. Photosynthesis and growth. *Annals of Botany* **89**: 907–916.

Chelle M. **2005**. Phylloclimate or the climate perceived by individual plant organs: What is it? How to model it? What for? *New Phytologist* **166**: 781–790.

Chen BJW, During HJ, Anten NPR. **2012**. Detect thy neighbor: Identity recognition at the root level in plants. *Plant Science* **195**: 157–167.

Chen T-W, Henke M, de Visser PHB, Buck-Sorlin G, Wiechers D, Kahlen K, Stützel H. **2014a**. What is the most prominent factor limiting photosynthesis in different layers of a greenhouse cucumber canopy? *Annals of botany*: 677–688.

Chen T-W, Nguyen TMN, Kahlen K, Stutzel H. **2014b**. Quantification of the effects of architectural

traits on dry mass production and light interception of tomato canopy under different temperature regimes using a dynamic functional-structural plant model. *Journal of Experimental Botany* **65**: 6399–6410.

Chow WS, Melis A, Anderson JM. **1990**. Adjustments of photosystem stoichiometry in chloroplasts improve the quantum efficiency of photosynthesis. *Proceedings of the National Academy of Sciences of the United States of America* **87**: 7502–7506.

Christmann A, Grill E, Huang J. **2013**. Hydraulic signals in long-distance signaling. *Current Opinion in Plant Biology* **16**: 293–300.

Collatz GJ, Ball JT, Grivet C, Berry J a. **1991**. Physiological and environmental regulation of stomatal conductance, photosynthesis and transpiration: a model that includes a laminar boundary layer. *Agricultural and Forest Meteorology* **54**: 107–136.

Comstock JP, Mahall BE. **1985**. Drought and changes in leaf orientation for two California chaparral shrubs : Ceanothus megacarpus and Ceanothus crassifolius. *Oecologia* **65**: 531–535.

Cooper SM, Owens MK, Spalinger DE, Ginnett TF. **2003**. The architecture of shrubs after defoliation and the subsequent feeding behavior of browsers. *Oikos* **100**: 387–393.

Cornic G, Briantais JM. **1991**. Partitioning of photosynthetic electron flow between CO_2 and O_2 reduction in a C3 leaf (Phaseolus vulgaris L.) at different CO_2 concentrations and during drought stress. *Planta* **183**: 178–84.

Dai J, Liu S, Zhang W, Xu R, Luo W, Zhang S, Yin X, Han L, Chen W. **2011**. Quantifying the effects of nitrogen on fruit growth and yield of cucumber crop in greenhouses. *Scientia Horticulturae* **130**: 551–561.

Dai Y, Shen Z, Liu Y, Wang L, Hannaway D, Lu H. **2009**. Effects of shade treatments on the photosynthetic capacity, chlorophyll fluorescence, and chlorophyll content of Tetrastigma hemsleyanum Diels et Gilg. *Environmental and Experimental Botany* **65**: 177–182.

Damour G, Vandame M, Urban L. **2008**. Long-term drought modifies the fundamental relationships between light exposure, leaf nitrogen content and photosynthetic capacity in leaves of the lychee tree (Litchi chinensis). *Journal of Plant Physiology* **165**: 1370–1378.

Damour G, Vandame M, Urban L. **2009**. Long-term drought results in a reversible decline in photosynthetic capacity in mango leaves, not just a decrease in stomatal conductance. *Tree physiology* **29**: 675–84.

Demmig-Adams B, Adams WW. **1996**. The role of xanthophyll cycle carotenoids in the protection of photosynthesis. *Trends in plant science* **1**: 21–26.

Díaz-Espejo A, Walcroft AS, Fernández JE, Hafridi B, Palomo MJ, Girón IF. **2006**. Modeling photosynthesis in olive leaves under drought conditions. *Tree physiology* **26**: 1445–1456.

Donald CM. **1968**. The breeding of crop ideotypes. *Euphytica* **17**: 385–403.

Donohue K, Messiqua D, Pyle EH, Heschel MS, Schmitt J. **2000**. Evidence of adaptive divergence in plasticity: density and site dependent selection on shade avoidance responses in Impatiens capensis. *Evolution* **54**: 1956–1968.

Donohue K, Schmitt J. **1999**. The genetic architecture of plasticity to density in Impatiens capensis. *Evolution* **53**: 1377–1386.

Dordas CA, Sioulas C. **2008**. Safflower yield, chlorophyll content, photosynthesis, and water use efficiency response to nitrogen fertilization under rainfed conditions. *Industrial Crops and Products* **27**: 75–85.

Dorn LA, Pyle EH, Schmitt J. **2000**. Plasticity to light cues and resources in Arabidopsis thaliana: testing for adaptive value and costs. *Evolution* **54**: 1982–1994.

Dudley SA, Schmitt J. **1995**. Genetic differentiation in morphological responses to simulated foliage shade between populations of Impatiens capensis from open and woodland sites. *Functional Ecology* **9**: 655–666.

Dudley SA, Schmitt J. **1996**. Testing the adaptive plasticity hypothesis: Density-dependent selection on manipulated stem length in Impatiens capensis. *The American Naturalist* **147**: 445–465.

Egea G, Verhoef A, Vidale PL. **2011**. Towards an improved and more flexible representation of water stress in coupled photosynthesis-stomatal conductance models. *Agricultural and Forest Meteorology* **151**: 1370–1384.

Evans JR. **1989**. Photosynthesis and nitrogen relationships in leaves of C3 plants. *Oecologia* **78**: 9–19.

Evans J, von Caemmerer S, Setchell B, Hudson G. **1994**. Transfer conductance and leaf anatomy in transgenic tobacco with a reduced content of Rubisco. *Australian Journal of Plant Physiology* **21**: 475.

Evans JR, Poorter H. **2001**. Photosynthetic acclimation of plants to growth irradiance: The relative importance of specific leaf area and nitrogen partitioning in maximizing carbon gain. *Plant, Cell and Environment* **24**: 755–767.

Evans J, Terashima I. **1987**. Effects of nitrogen nutrition on electron transport components and photosynthesis in Spinach. *Australian Journal of Plant Physiology* **14**: 59.

Evans JR, Vogelmann TC. **2003**. Profiles of 14C fixation through spinach leaves in relation to light absorption and photosynthetic capacity. *Plant Cell and Environment* **26**: 547–560.

Evers JB, Vos J, Andrieu B, Struik PC. **2006**. Cessation of tillering in spring wheat in relation to light interception and red:far-red ratio. *Annals of Botany* **97**: 649–658.

Evers JB, Vos J, Yin X, Romero P, Van Der Putten PEL, Struik PC. **2010**. Simulation of wheat growth and development based on organ-level photosynthesis and assimilate allocation. *Journal of Experimental Botany* **61**: 2203–2216.

Evers JB, van der Werf W, Stomph TJ, Bastiaans L, Anten NPR. **2018**. Understanding and optimizing species mixtures using functional–structural plant modelling. *Journal of Experimental Botany*.

Eyles A, Pinkard EA, Davies NW, Corkrey R, Churchill K, O'Grady AP, Sands P, Mohammed C. **2013**. Whole-plant versus leaf-level regulation of photosynthetic responses after partial defoliation in Eucalyptus globulus saplings. *Journal of Experimental Botany* **64**: 1625–1636.

Eyles A, Pinkard EA, Mohammed C. **2009**. Shifts in biomass and resource allocation patterns following defoliation in Eucalyptus globulus growing with varying water and nutrient supplies. *Tree Physiology* **29**: 753–764.

Falik O, de Kroon H, Novoplansky A. **2006**. Physiologically-mediated self / nonself root discrimination. *Plant Signaling & Behavior* **1**: 116–121.

Falik O, Reides P, Gersani M, Novoplansky A. **2003**. Self/non-self discrimination in roots. *Journal of Ecology* **91**: 525–531.

Falster DS, Westoby M. **2003**. Plant height and evolutionary games. *Trends in Ecology and Evolution* **18**: 337–343.

Farquhar GD, von Caemmerer S, Berry JA. **1980**. A biochemical model of photosynthetic CO2 assimilation in leaves of C3 species. *Planta* **149**: 78–90.

Farquhar GD, Sharkey TD. **1982**. Stomatal conductance and photosynthesis. *Annual review of plant physiology* **33**: 317–345.

Field CH, Mooney HA. **1986**. Photosynthesis--nitrogen relationship in wild plants. *In On the Economy of Plant Form and Function: Proceedings of the Sixth Maria Moors Cabot Symposium, Evolutionary*

Constraints on Primary Productivity, Adaptive Patterns of Energy Capture in Plants, Harvard Forest, August 1983. Cambridge [Cambridgeshire].

Flexas J, Bota J, Escalona JM, Sampol B, Medrano H. **2002**. Effects of drought on photosynthesis in grapevines under field conditions: an evaluation of stomatal and mesophyll limitations. *Functional Plant Biology* **29**: 461.

Flexas J, Bota J, Loreto F, Cornic G, Sharkey TD. **2004**. Diffusive and metabolic limitations to photosynthesis under drought and salinity in C3 Plants. *Plant Biology* **6**: 269–279.

Flexas J, Ribas-Carbó M, Bota J, Galmés J, Henkle M, Martínez-Cañellas S, Medrano H. **2006**. Decreased Rubisco activity during water stress is not induced by decreased relative water content but related to conditions of low stomatal conductance and chloroplast CO2 concentration. *New Phytologist* **172**: 73–82.

Flexas J, Ribas-Carbó M, Diaz-Espejo A, Galmés J, Medrano H. **2008**. Mesophyll conductance to CO_2 : current knowledge and future prospects. *Plant, Cell & Environment* **31**: 602–621.

Forseth AIN, Ehleringer JR. **1983**. Ecophysiology of two solar tracking desert winter annuals. III . Gas exchange responses to light, CO_2 and VPD in relation to long-term drought. **57**: 344–351.

Franklin KA. **2008**. Shade avoidance. *New Phytologist* **179**: 930–944.

Galmés J, Medrano H, Flexas J. **2007a**. Photosynthetic limitations in response to water stress and recovery in Mediterranean plants with different growth forms. *New phytologist* **175**: 81–93.

Galmés J, Ribas-Carbó M, Medrano H, Flexas J. **2007b**. Response of leaf respiration to water stress in Mediterranean species with different growth forms. *Journal of Arid Environments* **68**: 206–222.

García-Plazaola JI, Hernández A, Olano JM, Becerril JM. **2003**. The operation of the lutein epoxide cycle correlates with energy dissipation. *Functional Plant Biology* **30**: 319–324.

Geiger D, Maierhofer T, Al-rasheid KAS, Scherzer S, Mumm P, Liese A, Ache P, Wellmann C, Marten I, Grill E, *et al.* 2011. Stomatal closure by fast abscisic acid signaling is mediated by the guard cell anion channel SLAH3 and the receptor RCAR1. *Science Signaling* **4**: 1–13.

Genty B, Briantais J-M, Baker NR. **1989**. The relationship between the quantum yield of photosynthetic electron transport and quenching of chlorophyll fluorescence. *Biochimica et Biophysica Acta* **990**: 87–92.

Genty B, Briantais JM, Da Silva JB. **1987**. Effects of drought on primary photosynthetic processes of cotton leaves. *Plant physiology* **83**: 360–364.

Gimeno TE, Sommerville KE, Valladares F, Atkin OK. **2010**. Homeostasis of respiration under drought and its important consequences for foliar carbon balance in a drier climate: Insights from two contrasting Acacia species. *Functional Plant Biology* **37**: 323–333.

Givnish TJ. **1982**. On the adaptive significance of leaf height in forest herbs. *The American Naturalist* **120**: 353–381.

Gonzalez-dugo V, Durand J-L, Gastal F. **2010**. Water deficit and nitrogen nutrition of crops . A review To cite this version : Review article. *Agronomy for Sustainable Development* **30**: 529–544.

González-Meler MA, Matamala R, Penuelas J. **1997**. Effects of prolonged drought stress and nitrogen deficiency on the respiratory O2 uptake of bean and pepper leaves. *Photosynthetica* **34**: 505–512.

Gonzalez-Real MM, Baille A. **2000**. Changes in leaf photosynthetic parameters with leaf position and nitrogen content within a rose plant canopy (Rosa hybrida). *Plant, Cell and Environment* **23**: 351–363.

González-Real MM, Baille A, Gutiérrez Colomer RP. **2007**. Leaf photosynthetic properties and radiation profiles in a rose canopy (Rosa hybrida L.) with bent shoots. *Scientia Horticulturae* **114**: 177–

187.

Goudriaan J. **1977**. *Crop micrometeorology: a simulation study*. Pudoc, Wageningen.

Grassi G, Meir P, Cromer R, Tompkins D, Jarvis PG. **2002**. Photosynthetic parameters in seedlings of Eucalyptus grandis as affected by rate of nitrogen supply. *Plant, Cell and Environment* **25**: 1677–1688.

Gratani L, Varone L, Bonito A. **2007**. Environmental induced variations in leaf dark respiration and net photosynthesis of Quercus ilex L. *Photosynthetica* **45**: 633–636.

Green-Tracewicz E, Page ER, Swanton CJ. **2012**. Light quality and the critical period for weed control in soybean. *Weed Science* **60**: 86–91.

Green TH, Mitchell RJ. **1992**. Effects of nitrogen on the response of loblolly pine to water stress. I. Photosynthesis and stomatal conductance. *New Phytologist* **122**: 627–633.

Gregory PJ, Johnson SN, Newton AC, Ingram JSI. **2009**. Integrating pests and pathogens into the climate change / food security debate. *Journal of Experimental Botany* **60**: 2827–2838.

Gruntman M, Novoplansky A. **2004**. Physiologically mediated self/non-self discrimination in roots. *Proceedings of the National Academy of Sciences* **101**: 3863–3867.

Gu J, Yin X, Stomph T-J, Wang H, Struik PC. **2012**. Physiological basis of genetic variation in leaf photosynthesis methylation and chromatin patterning among rice (Oryza sativa L.) introgression lines under drought and well-watered conditions. *Journal of Experimental Botany* **63**: 5137–5153.

Gulmon SL, Chu CC. **1981**. The effects of light and nitrogen on photosynthesis, leaf characteristics, and dry matter allocation in the chaparral shrub, Diplacus aurantiacus. *Oecologia* **49**: 207–212.

Gutierrez Colomer RP, Gonzalez-Real MM, Baille A. **2006**. Dry matter production and partitioning in rose (Rosa hybrida) flower shoots. *Scientia Horticulturae* **107**: 284–291.

Gutschick VP, Wiegel FW. 1988. Optimizing the canopy photosynthetic rate by patterns of investment in specific leaf mass. *The American Naturalist* **132**: 67–86.

Han HH, Coutand C, Cochard H, Trottier C, Lauri PÉ. **2007**. Effects of shoot bending on lateral fate and hydraulics: Invariant and changing traits across five apple genotypes. *Journal of Experimental Botany* **58**: 3537–3547.

Hao X, Zheng J, Little C, Khosla S. **2012**. LED inter-lighting in year-round greenhouse mini-cucumber production. *Acta Horticulturae* **956**: 335–340.

Harley PC, Thomas RB, Reynolds JF, Strain BR. **1992**. Modeling photosynthesis of cotton grown in elevated CO_2. *Plant Cell and Environment* **15**: 271–282.

Harper J. **1984**. Uptake of nitrogen forms by roots and leaves. In: Hauck R, ed. Nitrogen in crop production. American Society of Agronomy, 165−170.

Hemmerling R, Kniemeyer O, Lanwert D, Kurth W, Buck-Sorlin G. **2008**. The rule-based language XL and the modelling environment GroIMP illustrated with simulated tree competition. *Functional Plant Biology* **35**: 739–750.

Hemming S, Mohammadkhani V, Dueck T. **2008**. Diffuse greenhouse covering materials – material technology, measurements and evaluation of optical properties. *Acta Horticulturae* **797**: 469–476.

Héraut-Bron V, Robin C, Varlet-Grancher C, Guckert A. **2001**. Phytochrome mediated effects on leaves of white clover: consequences for light interception by the plant under competition for light. *Annals of Botany* **88**: 737–743.

Héroult A, Lin YS, Bourne A, Medlyn BE, Ellsworth DS. **2013**. Optimal stomatal conductance in relation to photosynthesis in climatically contrasting Eucalyptus species under drought. *Plant, Cell and Environment* **36**: 262–274.

Hewezi T, Léger M, Gentzbittel L. **2008**. A comprehensive analysis of the combined effects of high light and high temperature stresses on gene expression in sunflower. *Annals of Botany* **102**: 127–140.

Hikosaka K. **2004**. Interspecific difference in the photosynthesis–nitrogen relationship: patterns, physiological causes, and ecological importance. *Journal of Plant Research* **117**: 481–494.

Hikosaka K. **2014**. Optimal nitrogen distribution within a leaf canopy under direct and diffuse light. *Plant, Cell and Environment* **37**: 2077–2085.

Hikosaka K, Anten NPR, Borjigidai A, Kamiyama C, Sakai H, Hasegawa T, Oikawa S, Iio A, Watanabe M, Koike T, *et al.* 2016a. A meta-analysis of leaf nitrogen distribution within plant canopies. *Annals of Botany* **118**: 239–247.

Hikosaka K, Kumagai T, Ito A. **2016b**. Modeling canopy photosynthesis. In: Canopy photosynthesis: from basics to applications. Dordrecht, The Netherlands: Springer, 239–268.

Van Hinsberg A, Van Tienderen P. **1997**. Variation in growth form in relation to spectral light quality (red/far-red ratio) in Plantago lanceolata L. in sun and shade populations. *Oecologia* **111**: 452–459.

Hirose T, Werger MJA. **1987a**. Maximizing daily canopy photosynthesis with respect to the leaf nitrogen allocation pattern in the canopy. *Oecologia* **72**: 520–526.

Hirose T, Werger MJA. **1987b**. Nitrogen use efficiency in instantaneous and daily photosynthesis of leaves in the canopy of a Solidago altissima stand. *Physiologia Plantarum* **70**: 215–222.

Hogewoning SW, Trouwborst G, Maljaars H, Poorter H, van Ieperen W, Harbinson J. **2010**. Blue light dose-responses of leaf photosynthesis, morphology, and chemical composition of Cucumis sativus grown under different combinations of red and blue light. *Journal of experimental botany* **61**: 3107–3117.

Hogewoning SW, Wientjes E, Douwstra P, Trouwborst G, van Ieperen W, Croce R, Harbinson J. **2012**. Photosynthetic quantum yield dynamics: from photosystems to leaves. *The Plant Cell* **24**: 1921–1935.

Holmes MG, Smith H. **1977**. The function of phytochrome in the natural environment—II. The influence of vegetation canopies on the spectral energy distribution of natural daylight. *Photochemistry and Photobiology* **25**: 539–545.

Hovi-Pekkanen T, Tahvonen R. **2008**. Effects of interlighting on yield and external fruit quality in year-round cultivated cucumber. *Scientia Horticulturae* **116**: 152–161.

Huang B, Fu J. **2000**. Photosynthesis, respiration, and carbon allocation of two cool-season perennial grasses in response to surface soil drying. *Plant and Soil* **227**: 17–26.

Huber AE, Bauerle TL. **2016**. Long-distance plant signaling pathways in response to multiple stressors : the gap in knowledge. *Journal of Experimental Botany* **67**: 2063–2079.

Huber H, Kane NC, Heschel MS, von Wettberg EJ, Banta J, Leuck A, Schmitt J. **2004**. Frequency and microenvironmental pattern of selection on plastic shade-avoidance traits in a natural population of *Impatiens capensis*. *The American Naturalist* **163**: 548–563.

Hunt PG, Kasperbauer MJ, Matheny TA. **1989**. Soybean Seedling Growth Responses to Light Reflected From Different Colored Soil Surfaces. *Crop Science* **29**: 130.

van Ieperen W. **2012**. Plant morphological and developmental responses to light quality in a horticultural context. *Acta Horticulturae* **956**: 131–139.

IPCC. **2014**. *Climate Change 2014: Synthesis Report. Contribution of Working Groups I, II and III to the Fifth Assessment Report of the Intergovernmental Panel on Climate Change [Core Writing Team, R.K. Pachauri and L.A. Meyer (eds.)]*. IPCC, Geneva, Switzerland, 151 pp.

Ito A, Yaegaki H, Hayama H, Kusaba S, Yamaguchi I, Yoshioka H. **1999**. Bending shoots stimulates flowering and influences hormone levels in lateral buds of Japanese pear. *HortScience* **34**: 1224–1228.

Jakab G, Ton J, Flors V, Zimmerli L, Me J, Mauch-mani B. **2005**. Enhancing Arabidopsis salt and drought stress tolerance by chemical priming for its abscisic acid responses. *Plant Physiology* **139**: 267–274.

Jamieson PD, Porter JR, Goudriaan J, Ritchie JT, Van Keulen H, Stol W. **1998**. A comparison of the models AFRCWHEAT2, CERES-Wheat, Sirius, SUCROS2 and SWHEAT with measurements from wheat grown under drought. *Field Crops Research* **55**: 23–44.

Jarillo JA, Gabrys H, Capel J, Alonso JM, Ecker JR, Cashmore AR. **2001**. Phototropin-related NPL1 controls chloroplast relocation induced by blue light. *Nature* **410**: 952–954.

Kaiser E, Morales A, Harbinson J, Kromdijk J, Heuvelink E, Marcelis LFM. **2015**. Dynamic photosynthesis in different environmental conditions. *Journal of Experimental Botany* **66**: 2415–2426.

Kajihara S, Itou J, Katsutani N, Goto T, Shimaji H. **2009**. Partitioning of photosynthates originating from bent shoots in the arching and high-rack culture systems of cut rose production. *Scientia Horticulturae* **121**: 485–489.

Kakani VG, Reddy KR, Zhao D, Mohammed AR. **2003**. Effects of ultraviolet-B radiation on cotton (Gossypium hirsutum L.) morphology and anatomy. *Annals of Botany* **91**: 817–826.

Kasperbauer MJ. **1994**. Cotton plant size and fiber developmental responses to FR/R ratio reflected from the soil surface. *Physiologia Plantarum* **91**: 317–321.

Keenan T, Sabate S, Gracia C. **2010**. Soil water stress and coupled photosynthesis-conductance models: Bridging the gap between conflicting reports on the relative roles of stomatal, mesophyll conductance and biochemical limitations to photosynthesis. *Agricultural and Forest Meteorology* **150**: 443–453.

Kempkes FLK, Stanghellini C, Victoria NG, Bruins M. **2012**. Effect of diffuse glass on climate and plant environment: first results from an experiment on roses. *Acta Horticulturae* **952**: 255–262.

Keuskamp DH, Sasidharan R, Pierik R. **2010**. Physiological regulation and functional significance of shade avoidance responses to neighbors. *Plant Signaling & Behavior* **5**: 655–662.

Kichah A, Bournet P, Migeon C, Boulard T, Antipolis S. **2012**. Measurement and CFD simulation of microclimate characteristics and transpiration of an Impatiens pot plant crop in a greenhouse. *Biosystems Engineering* **112**: 22–34.

Kim SH, Lieth JH. **2004**. Effect of shoot-bending on productivity and economic value estimation of cut-flower roses grown in Coir and UC Mix. *Scientia Horticulturae* **99**: 331–343.

Kim SH, Shackel KA, Lieth JH. **2004**. Bending alters water balance and reduces photosynthesis of rose shoots. *J. Amer. Soc. Hort. Sci.* **129**: 896–901.

Kitajima K, Hogan KP. **2003**. Increases of chlorophyll a/b ratios during acclimation of tropical woody seedlings to nitrogen limitation and high light. *Plant Cell and Environment* **26**: 857–865.

van Kleunen M, Fischer M. **2005**. Constraints on the evolution of adaptive phenotypic plasticity in plants. *New phytologist* **166**: 49–60.

Kohzuma K, Cruz JA, Akashi K, Hoshiyasu S, Munekage YN, Yokota A, Kramer DM. **2009**. The long-term responses of the photosynthetic proton circuit to drought. *Plant, Cell and Environment* **32**: 209–219.

Kool MTN, Lenssen EFA. **1997**. Basal-shoot formation in young rose plants: effects of bending practices and plant density. *Journal of Horticultural Science* **72**: 635–644.

Kosugi Y, Shibata S, Kobashi S. **2003**. Parameterization of the CO_2 and H_2O gas exchange of several temperate deciduous broad-leaved trees at the leaf scale considering seasonal changes. *Plant Cell and Environment* **26**: 285–301.

Kromdijk J, Głowacka K, Leonelli L, Gabilly ST, Iwai M, Niyogi KK, Long SP. **2016**. Improving photosynthesis and crop productivity by accelerating recovery from photoprotection. *Science* **354**: 857–862.

Kusaka M, Ohta M, Fujimura T. **2005**. Contribution of inorganic components to osmotic adjustment and leaf folding for drought tolerance in pearl millet. *Physiologia Plantarum* **125**: 474–489.

Lauteri M, Scartazza A, Guido MC, Brugnoli E. **1997**. Genetic variation in photosynthetic capacity, carbon isotope discrimination and mesophyll conductance in provenances of Castanea sativa adapted to different environments. *Functional Ecology* **11**: 675–683.

Lavigne MB, Little CH, Major JE. **2001**. Increasing the sink:source balance enhances photosynthetic rate of 1-year-old balsam fir foliage by increasing allocation of mineral nutrients. *Tree physiology* **21**: 417–26.

Lawlor DW, Cornic G. **2002**. Photosynthetic carbon assimilation and associated metabolism in relation to water deficits in higher plants. *Plant, Cell and Environment* **25**: 275–294.

Leuning R. **1995**. A critical appraisal of a combined stomatal-photosynthesis model for C3 plants. *Plant, Cell and Environment* **18**: 339–355.

Leuning R. **1997**. Scaling to a common temperature improves the correlation between the photosynthesis parameters J max and V cmax. *Journal of Experimental Botany* **48**: 345–347.

Li C, Berninger F, Koskela J, Sonninen E. **2000**. Drought responses of Eucalyptus microtheca provenances depend on seasonality of rainfall in their place of origin. *Functional Plant Biology* **27**: 231–238.

Li G, Lin L, Dong Y, An D, Li Y, Luo W, Yin X, Li W, Shao J, Zhou Y, *et al.* 2012. Testing two models for the estimation of leaf stomatal conductance in four greenhouse crops cucumber, chrysanthemum, tulip and lilium. *Agricultural and Forest Meteorology* **165**: 92–103.

Lichtenthaler HK, Buschmann C, Döll M, Fietz HJ, Bach T, Kozel U, Meier D, Rahmsdorf U. **1981**. Photosynthetic activity, chloroplast ultrastructure, and leaf characteristics of high-light and low-light plants and of sun and shade leaves. *Photosynthesis Research* **2**: 115–141.

Lin L, Li W, Shao J, Luo W, Dai J, Yin X, Zhou Y, Zhao C. **2011**. Modelling the effects of soil water potential on growth and quality of cut chrysanthemum (Chrysanthemum morifolium). *Scientia Horticulturae* **130**: 275–288.

Liu FY, Chang Y Sen. **2011**. Effects of shoot bending on ACC content, ethylene production, growth and flowering of bougainvillea. *Plant Growth Regulation* **63**: 37–44.

Liu Y, Dawson W, Prati D, Haeuser E, Feng Y, Van Kleunen M. **2016**. Does greater specific leaf area plasticity help plants to maintain a high performance when shaded? *Annals of Botany* **118**: 1329–1336.

Liu Z, Dickmann DI. **1996**. Effects of water and nitrogen interaction on net photosynthesis, stomatal conductance, and water-use efficiency in two hybrid poplar clones. *Physiologia Plantarum* **97**: 507–512.

Liu Y, Schieving F, Stuefer JF, Anten NPR. **2007**. The effects of mechanical stress and spectral shading on the growth and allocation of ten genotypes of a stoloniferous plant. *Annals of Botany* **99**: 121–130.

Long SP, Marshall-Colon A, Zhu XG. **2015**. Meeting the global food demand of the future by engineering crop photosynthesis and yield potential. *Cell* **161**: 56–66.

Lopez R, Badel E, Peraudeau S, Leblanc-Fournier N, Beaujard F, Julien J-L, Cochard H, Moulia B. **2014**. Tree shoot bending generates hydraulic pressure pulses : a new long-distance signal? *Journal of Experimental Botany* **65**: 1997–2008.

Loriaux SD, Avenson TJ, Welles JM, Mcdermitt DK, Eckles RD, Riensche B, Genty B. **2013**. Closing in on maximum yield of chlorophyll fluorescence using a single multiphase flash of sub-saturating intensity. *Plant, Cell and Environment* **36**: 1755–1770.

Makino A, Osmond B. **1991**. Effects of nitrogen nutrition on nitrogen partitioning between chloroplasts and mitochondria in pea and wheat. *Plant Physiology* **96**: 355–362.

Makino A, Sakashita H, Hidema J, Mae T, Ojima K, Osmond B. **1992**. Distinctive responses of ribulose-1,5-bisphosphate carboxylase and carbonic anhydrase in wheat leaves to nitrogen nutrition and their possible relationships to CO_2-transfer resistance. *Plant physiology* **100**: 1737–43.

Marcelis-van Acker CAM. **1994**. Effect of Assimilate Supply on Development and Growth Potential of Axillary Buds in Roses. *Annals of Botany* **73**: 415–420.

Marshall B, Biscoe P. **1980**. A model for C3 leaves describing the dependence of net photosynthesis on irradiance. *Journal of Experimental Botany* **31**: 29–39.

Maseyk KS, Lin T, Rotenberg E, Grünzweig JM, Schwartz A, Yakir D. **2008**. Physiology-phenology interactions in a productive semi-arid pine forest. *New Phytologist* **178**: 603–616.

Mc Naughton SJ. **1983**. Compensatory plant growth as a response to herbivory. *Oikos* **40**: 329–336.

Medhurst JL, Pinkard EA, Beadle CL, Worledge D. **2003**. Growth and stem form responses of plantation-grown Acacia melanoxylon (R. Br.) to form pruning and nurse-crop thinning. *Forest Ecology and Management* **179**: 183–193.

Medlyn BE, Dreyer E, Ellsworth D, Forstreuter M, Harley PC, Kirschbaum MUF, Le Roux X, Montpied P, Strassemeyer J, Walcroft A, *et al.* 2002. Temperature response of parameters of a biochemically based model of photosynthesis. II. A review of experimental data. *Plant, Cell and Environment* **25**: 1167–1179.

Meir P, Kruijt B, Broadmeadow M, Barbosa E, Kull O, Carswell F, Nobre A, Jarvis PG. **2002**. Acclimation of photosynthetic capacity to irradiance in tree canopies in relation to leaf nitrogen concentration and leaf mass per unit area. *Plant, Cell and Environment* **25**: 343–357.

Melotto M, Underwood W, Koczan J, Nomura K, He SY. **2006**. Plant Stomata Function in Innate Immunity against Bacterial Invasion. *Cell* **126**: 969–980.

Van der Meulen-Muisers JJM, Van Oeveren JC, Van der Plas LHW, Van Tuyl JM. **2001**. Postharvest flower development in Asiatic hybrid lilies as related to tepal carbohydrate status. *Postharvest Biology and Technology* **21**: 201–211.

Midgley JJ. **2003**. Is bigger better in plants? The hydraulic costs of increasing size in trees. *Trends in Ecology & Evolution* **18**: 2002–2003.

Misson L, Panek JA, Goldstein AH. **2004**. A comparison of three approaches to modeling leaf gas exchange in annually drought-stressed ponderosa pine forests. *Tree physiology* **24**: 529–541.

Misson L, Rasse DP, Vincke C, Aubinet M, François L. **2002**. Predicting transpiration from forest stands in Belgium for the 21st century. *Agricultural and Forest Meteorology* **111**: 265–282.

Mitchell CA. **1996**. Recent advances in plant response to mechanical stress: theory and application. *HortScience* **31**: 31–35.

Mittler R. **2006**. Abiotic stress, the field environment and stress combination. *Trends in plant science* **11**: 15–9.

Mittler R, Blumwald E. **2010**. Genetic engineering for modern agriculture: challenges and

perspectives. *Annual Review of Plant Biology* **61**: 443–462.

Monsi M, Saeki T. **2005**. On the factor light in plant communities and its importance for matter production. *Annals of Botany* **95**: 549–567.

Monti A. **2006**. The effect of transient and continuous drought on yield, photosynthesis and carbon isotope discrimination in sugar beet (Beta vulgaris L.). *Journal of Experimental Botany* **57**: 1253–1262.

Mor Y, Halevy AH. **1979**. Translocation of 14C-assimilates in roses: I. The effect of the age of the shoot and the location of the source leaf. *Physiologia Plantarum* **45**: 177–182.

Morales A, Kaiser E, Yin X, Harbinson J, Molenaar J, Driever SM, Struik PC. **2018**. Dynamic modelling of limitations on improving leaf CO_2 assimilation under fluctuating irradiance. *Plant Cell and Environment* **41**: 589–604.

Morison JIL, Lawson T, Cornic G. **2007**. Lateral CO_2 diffusion inside dicotyledonous leaves can be substantial: quantification in different light intensities. *Plant Physiology* **145**: 680–690.

Müller J, Eschenröder A, Christen O. **2014**. LEAFC3-N photosynthesis, stomatal conductance, transpiration and energy balance model: Finite mesophyll conductance, drought stress, stomata ratio, optimized solution algorithms, and code. *Ecological Modelling* **290**: 134–145.

Müller J, Wernecke P, Diepenbrock W. **2005**. LEAFC3-N: a nitrogen-sensitive extension of the CO_2 and H_2O gas exchange model LEAFC3 parameterised and tested for winter wheat (Triticum aestivum L.). *Ecological Modelling* **183**: 183–210.

Murchie EH, Horton P. **1997**. Acclimation of photosynthesis to irradiance and spectral quality in British plant species: chlorophyll content, photosynthetic capacity and habitat preference. *Plant, Cell & Environment* **20**: 438–448.

National Bureau of Statistics of China. **2017**. Data bulletin of the third agricultural census (No.2), http://www.stats.gov.cn/tjsj/tjgb/nypcgb/qgnypcgb.

Naumburg E, Ellsworth DS. **2002**. Short-term light and leaf photosynthetic dynamics affect estimates of daily understory photosynthesis in four tree species. *Tree Physiology* **22**: 393–401.

Newton AC, Johnson SN, Gregory PJ. **2011**. Implications of climate change for diseases , crop yields and food security. *Euphytica* **179**: 3–18.

Niinemets Ü. **2007**. Photosynthesis and resource distribution through plant canopies. *Plant, Cell and Environment* **30**: 1052–1071.

Niinemets Ü, Anten NPR. **2009**. Packing the photosynthetic machinery: from leaf to canopy. In: Photosynthesis in silico. Netherland: Springer, 363–399.

Niinemets Ü, Díaz-Espejo A, Flexas J, Galmés J, Warren CR. **2009**. Importance of mesophyll diffusion conductance in estimation of plant photosynthesis in the field. *Journal of Experimental Botany* **60**: 2271–2282.

Niinemets Ü, Kull O, Tenhunen JD. **1998**. An analysis of light effects on foliar morphology, physiology, and light interception in temperate deciduous woody species of contrasting shade tolerance. *Tree Physiology* **18**: 681–696.

Novoplansky A. **2009**. Picking battles wisely: Plant behaviour under competition. *Plant, Cell and Environment* **32**: 726–741.

Nowak RS, Caldwell MM. **1984**. A test of compensatory photosynthesis in the field: Implications for herbivory tolerance. *Oecologia* **61**: 311–318.

Oguchi R, Hikosaka K, Hirose T. **2003**. Does the photosynthetic light-acclimation need change in leaf anatomy? *Plant, Cell and Environment* **26**: 505–512.

Oguchi R, Hikosaka K, Hirose T. **2005**. Leaf anatomy as a constraint for photosynthetic acclimation:

Differential responses in leaf anatomy to increasing growth irradiance among three deciduous trees. *Plant, Cell and Environment* **28**: 916–927.

Ohkawa K, Suematsu M. **1997**. Arching cultivation techniques for growing cut-roses. *Acta Horticulturae* **482**: 47–52.

Ohsumi A, Hamasaki A, Nakagawa H, Yoshida H, Shiraiwa T, Horie T. **2007**. A model explaining genotypic and ontogenetic variation of leaf photosynthetic rate in rice (Oryza sativa) based on leaf nitrogen content and stomatal conductance. *Annals of Botany* **99**: 265–273.

Ozaki K, Saito H, Yamamuro K. **2004**. Compensatory photosynthesis as a response to partial debudding in ezo spruce, Picea jezoensis seedlings. *Ecological Research* **19**: 225–231.

Page ER, Tollenaar M, Lee EA, Lukens L, Swanton CJ. **2010**. Shade avoidance: An integral component of crop-weed competition. *Weed Research* **50**: 281–288.

Pallas B, Christophe A, Lecoeur J. **2010**. Are the common assimilate pool and trophic relationships appropriate for dealing with the observed plasticity of grapevine development? *Annals of Botany* **105**: 233–247.

Palosuo T, Kersebaum KC, Angulo C, Hlavinka P, Moriondo M, Olesen JE, Patil RH, Ruget F, Rumbaur C, Takac J, *et al.* 2011. Simulation of winter wheat yield and its variability in different climates of Europe: A comparison of eight crop growth models. *European Journal of Agronomy* **35**: 103–114.

Pantazopoulou CK, Bongers FJ, Küpers JJ, Reinen E, Das D, Evers JB, Anten NPR, Pierik R. **2017**. Neighbor detection at the leaf tip adaptively regulates upward leaf movement through spatial auxin dynamics. *Proceedings of the National Academy of Sciences* **114**: 7450–7455.

Paradiso R, Marcelis LFM. **2012**. The effect of irradiating adaxial or abaxial side on photosynthesis of rose leaves. *Acta Horticulturae* **956**: 157–164.

Pearcy RW, Muraoka H, Valladares F. **2005**. Crown architecture in sun and shade environments: Assessing function and trade-offs with a three-dimensional simulation model. *New Phytologist* **166**: 791–800.

Perez-Martin A, Flexas J, Ribas-Carbó M, Bota J, Tomás M, Infante JM, Diaz-Espejo A. **2009**. Interactive effects of soil water deficit and air vapour pressure deficit on mesophyll conductance to CO2 in Vitis vinifera and Olea europaea. *Journal of Experimental Botany* **60**: 2391–2405.

Pien H, Bobelyn E, Lemeur R, Van Labeke MC. **2001**. Optimising LAI in bent rose shoots. *Acta Horticulturae* **547**: 319–327.

Pierik R, Mommer L, Voesenek LA. **2013**. Molecular mechanisms of plant competition: Neighbour detection and response strategies. *Functional Ecology* **27**: 841–853.

Pierik R, De Wit M. **2014**. Shade avoidance: Phytochrome signalling and other aboveground neighbour detection cues. *Journal of Experimental Botany* **65**: 2815–2824.

Pinheiro C, Chaves MM. **2011**. Photosynthesis and drought: Can we make metabolic connections from available data? *Journal of Experimental Botany* **62**: 869–882.

Pinkard EA, Beadle CL. **1998**. Aboveground biomass partitioning and crown architecture of Eucalyptus nitens following green pruning. *Canadian Journal of Forest Research* **28**: 1419–1428.

Pons TL, De Jong-Van Berkel YEM. **2004**. Species-specific variation in the importance of the spectral quality gradient in canopies as a signal for photosynthetic resource partitioning. *Annals of Botany* **94**: 725–732.

Pons TL, van Rijnberk H, Scheurwater I, van der Werf A. **1993**. Importance of the gradient in photosynthetically active radiation in a vegetation stand for leaf nitrogen allocation in two monocotyledons. *Oecologia* **95**: 416–424.

Poorter H, Niinemets U, Poorter L, Wright IJ, Villar R. **2009**. Causes and consequences of variation in leaf mass per area (LMA):a meta-analysis. *New Phytologist* **182**: 565–588.

Qian T, Elings A, Dieleman JA, Gort G, Marcelis LFM. **2012**. Estimation of photosynthesis parameters for a modified Farquhar-von Caemmerer-Berry model using simultaneous estimation method and nonlinear mixed effects model. *Environmental and Experimental Botany* **82**: 66–73.

Radin JW, Ackerson RC. **1981**. Water relations of cotton plants under nitrogen deficiency III. Stomatal conductance, photosynthesis, and abscisci adic accumulation during drought. *Plant Physiology* **67**: 115–119.

Rajcan I, Chandler KJ, Swanton CJ. **2004**. Red-far-red ratio of reflected light: A hypothesis of why early-season weed control is important in corn. *Weed Science* **52**: 774–778.

Rajcan I, Swanton CJ. **2001**. Understanding maize-wheat competition: resource competition, light quality and the whole plant. *Field Crops Research* **71**: 139–150.

Reich P, Kloeppel B, Ellsworth D, Walters M. **1995**. Different photosynthesis-nitrogen relations in deciduous hardwood and evergreen coniferous tree species. *Oecologia* **104**: 24–30.

Reich PB, Walters MB, Ellsworth DS, Uhl C. **1994**. Photosynthesis-nitrogen relations in Amazonian tree species - I. Patterns among species and communities. *Oecologia* **97**: 62–72.

Reich PB, Walters M, Tjoelker M, Vanderklein D, Buschena C. **1998**. Photosynthesis and respiration rates depend on leaf and root morphology and nitrogen concentration in nine boreal tree species differing in relative growth rate. *Functional Ecology* **12**: 395–405.

Renou JL, Gerbaud A, Just D, André M. **1990**. Differing substomatal and chloroplastic CO2concentrations in water-stressed wheat. *Planta* **182**: 415–419.

Richards CL, Bossdorf O, Muth NZ, Gurevitch J, Pigliucci M. **2006**. Jack of all trades, master of some? On the role of phenotypic plasticity in plant invasions. *Ecology Letters* **9**: 981–993.

Rizhsky L, Liang H, Mittler R. **2002**. The combined effect of drought stress and heat shock on gene expression in Tobacco. *Plant Physiology* **130**: 1143–1151.

Rizhsky L, Liang H, Shuman J, Shulaev V, Davletova S, Mittler R. **2004**. When defense pathways collide. The response of Arabidopsis to a combination of drought and heat stress. *Plant Physiology* **134**: 1683–1696.

Ryan MG. **1995**. Foliar maintenance respiration of sub-alpine and boreal trees and shrubs in relation to nitrogen-content. *Plant Cell and Environment* **18**: 765–772.

Sala A, Tenhunen JD. **1996**. Simulations of canopy net photosynthesis and transpiration in Quercus ilex L. under the influence of seasonal drought. *Agricultural and Forest Meteorology* **78**: 203–222.

Sambatti JBM, Caylor KK. **2007**. When is breeding for drought tolerance optimal if drought is random? *New Phytologist* **175**: 70–80.

Särkkä LE, Eriksson C. **2003**. Effects of bending and harvesting height combinations on cut rose yield in a dense plantation with high intensity lighting. *Scientia Horticulturae* **98**: 433–447.

Sarlikioti V, De Visser PHB, Buck-Sorlin GH, Marcelis LFM. **2011**. How plant architecture affects light absorption and photosynthesis in tomato: Towards an ideotype for plant architecture using a functionalstructural plant model. *Annals of Botany* **108**: 1065–1073.

Savvides A, Van Ieperen W, Dieleman JA, Marcelis LFM. **2013**. Meristem temperature substantially deviates from air temperature even in moderate environments : is the magnitude of this deviation species-specific ? *Plant Cell and Environment* **36**: 1950–1960.

Schachtman DP, Goodger JQD. **2008**. Chemical root to shoot signaling under drought. *Trends in Plant Science* **13**: 281–287.

Schlichting CD. **1986**. The evolution of phenotypic plasticity in plants. *Annual review of ecology and systematics* **17**: 667–693.

Schubert A, Restagno M, Novello V, Peterlunger E. **1995**. Effects of shoot orientation on growth, net photosynthesis, and hydraulic conductivity of Vitis vinifera L. cv. Cortese. *American Journal of Enology and Viticulture* **46**: 324–328.

Schuerger AC, Brown CS, Stryjewski EC. **1997**. Anatomical features of pepper plants (Capsicum annuum L.) grown under red light-emitting diodes supplemented with blue or far-red light. *Annals of botany* **79**: 273–282.

Shangguan ZP, Shao MA, Dyckmans J. **2000**. Nitrogen nutrition and water stress effects on leaf photosynthetic gas exchange and water use efficiency in winter wheat. *Environmental and Experimental Botany* **44**: 141–149.

Sharkey TD, Seemann JR. **1989**. Mild water stress effects on carbon-reduction-cycle intermediates, ribulose bisphosphate carboxylase activity, and spatial homogeneity of photosynthesis in intact leaves. *Plant Physiology* **89**: 1060–1065.

Sharp RE, Matthews MA, Boyer JS. **1984**. Kok effect and the quantum yield of photosynthesis: light partially inhibits dark respiration. *Plant physiology* **75**: 95–101.

Sims DA, Pearcy RW. **1991**. Photosynthesis and respiration in Alocasia macrorrhiza following transfers to high and low light. *Oecologia* **86**: 447–453.

Smith H. **1982**. Light quality, photoperception, and plant strategy. *Annual review of plant physiology* **33**: 481–518.

Smith H. **2000**. Phytochromes and light signal perception by plants - An emerging synthesis. *Nature* **407**: 585–591.

Smith H, Casal JJ, Jackson GM. **1990**. Reflection signals and the perception by phytochrome of the proximity of neighbouring vegetation. *Plant, Cell & Environment* **13**: 73–78.

Sperry JS, Adler FR, Campbell GS, Comstock JP. **1998**. Limitation of plant water use by rhizosphere and xylem conductance : results from a model. *Plant Cell and Environment* **21**: 347–359.

Sultan SE. **2000**. Phenotypic plasticity for plant development, function and life history. *Trends in plant science* **5**: 537–542.

Sun Q. **2013**. Quantifying the effect of nitrogen on external quality of cut lily in greenhouse (in Chinese with English abstract).

Suzuki N, Rivero RM, Shulaev V, Blumwald E, Mittler R. **2014**. Abiotic and biotic stress combinations. *New Phytologist* **203**: 32–43.

Tenhunen JD, Sala Serra A, Harley PC, Dougherty RL, Reynolds JF. **1990**. Factors influencing carbon fixation and water use by mediterranean sclerophyll shurbs during summer drought. *Oecologia.* **82**: 381–393.

Thornley JHM. **1998**. Dynamic model of leaf photosynthesis with acclimation to light and nitrogen. *Annals of Botany* **81**: 421–430.

Trouwborst G, Oosterkamp J, Hogewoning SW, Harbinson J, van Ieperen W. **2010**. The responses of light interception, photosynthesis and fruit yield of cucumber to LED-lighting within the canopy. *Physiologia Plantarum* **138**: 289–300.

Turnbull TL, Adams MA, Warren CR. **2007**. Increased photosynthesis following partial defoliation of field-grown Eucalyptus globulus seedlings is not caused by increased leaf nitrogen. *Tree physiology* **27**: 1481–92.

Tuzet A, Perrier A, Leuning R. **2003**. A coupled model of stomatal conductance , photosynthesis.

Plant, Cell and Environment **26**: 1097–1116.

Vandenbussche F, Pierik R, Millenaar FF, Voesenek LACJ, Van Der Straeten D. **2005**. Reaching out of the shade. *Current Opinion in Plant Biology* **8**: 462–468.

Vermeulen P. **2016**. *Kwantitatieve informatie voor de glastuinbouw 2016-2017: kengetallen voor groenten, snijbloemen, pot en perkplanten teelten (No. 5121). Wageningen UR Glastuinbouw.*

Vos J, Evers JB, Buck-Sorlin GH, Andrieu B, Chelle M, De Visser PHB. **2010**. Functional-structural plant modelling: A new versatile tool in crop science. *Journal of Experimental Botany* **61**: 2101–2115.

de Vries J, Poelman EH, Anten N, Evers JB. **2018**. Elucidating the interaction between light competition and herbivore feeding patterns using functional–structural plant modelling. *Annals of Botany*: 1–13.

Walcroft A, Whitehead D, Silvester W, Kelliher F. **1997**. The response of photosynthetic model parameters to temperature and nitrogen concentration in Pinus radiate D. Don. *Plant, Cell and Environment* **20**: 1338−1348.

Walters RG. **2005**. Towards an understanding of photosynthetic acclimation. *Journal of Experimental Botany* **56**: 435–447.

Walters MB, Kruger EL, Reich PB. **1993**. Growth, biomass distribution and CO_2 exchange of northern hardwood seedlings in high and low light: relationships with successional status and shade tolerance. *Oecologia* **94**: 7–16.

Walters MB, Reich PB. **2000**. Trade-offs in low-light CO_2 exchange: a component of variation in shade tolerance among cold temperate tree seedlings. *Functional Ecology* **14**: 155–165.

Wang YP, Leuning R. **1998**. A two-leaf model for canopy conductance, photosynthesis and partitioning of available energy I: Model description and comparison with a multi-layered model. *Agricultural and Forest Meteorology* **91**: 89–111.

Warner RM, Erwin JE. **2002**. Estimation of total canopy photosynthetic capacity of roses grown under two canopy management systems. *Acta Horticulturae* **580**: 89–93.

Warren CR. **2004**. The photosynthetic limitation posed by internal conductance to CO_2 movement is increased by nutrient supply. *Journal of Experimental Botany* **55**: 2313–2321.

Warren CR. **2008**. Soil water deficits decrease the internal conductance to CO2 transfer but atmospheric water deficits do not. *Journal of Experimental Botany* **59**: 327–334.

Weijschedé J, Martínková J, De Kroon H, Huber H. **2006**. Shade avoidance in Trifolium repens: Costs and benefits of plasticity in petiole length and leaf size. *New Phytologist* **172**: 655–666.

White CS, Moore DI, Craig JA. **2004**. Regional-scale drought increases potential soil fertility in semiarid grasslands. *Biology and Fertility of Soils* **40**: 73–78.

Wilson KB, Baldocchi DD, Hanson PJ. **2000**. Spatial and seasonal variability of photosynthetic parameters and their relationship to leaf nitrogen in a deciduous forest. *Tree Physiology* **20**: 565–578.

de Wit C. **1965**. *Photosynthesis of leaf canopies*. Pudoc, Wageningen.

de Wit M, Kegge W, Evers JB, Vergeer-van Eijk MH, Gankema P, Voesenek LACJ, Pierik R. **2012**. Plant neighbor detection through touching leaf tips precedes phytochrome signals. *Proceedings of the National Academy of Sciences* **109**: 14705–14710.

Wubs AM, Heuvelink E, Marcelis LFM, Okello RCO, Shlyuykova A, Buck-Sorlin GH, Vos J. **2013**. Four hypotheses to explain axillary budbreak after removal of flower shoots in a cut-rose crop. *J. Amer. Soc. Hort. Sci.* **138**: 243–252.

Xu L, Baldocchi DD. **2003**. Seasonal trends in photosynthetic parameters and stomatal conductance of

blue oak (Quercus douglasii) under prolonged summer drought and high temperature. *Tree physiology* **23**: 865–877.

Yin X. **2013**. Improving ecophysiological simulation models to predict the impact of elevated atmospheric CO2 concentration on crop productivity. *Annals of Botany* **112**: 465–475.

Yin X, Belay DW, van der Putten PEL, Struik PC. **2014**. Accounting for the decrease of photosystem photochemical efficiency with increasing irradiance to estimate quantum yield of leaf photosynthesis. *Photosynthesis Research* **122**: 323–335.

Yin X, Struik PC. **2009a**. C3 and C4 photosynthesis models: An overview from the perspective of crop modelling. *NJAS - Wageningen Journal of Life Sciences* **57**: 27–38.

Yin X, Struik PC. **2009b**. Theoretical reconsiderations when estimating the mesophyll conductance to CO_2 diffusion in leaves of C_3 plants by analysis of combined gas exchange and chlorophyll fluorescence measurements. *Plant, Cell & Environment* **32**: 1513–1524.

Yin X, Struik PC. **2015**. Constraints to the potential efficiency of converting solar radiation into phytoenergy in annual crops: From leaf biochemistry to canopy physiology and crop ecology. *Journal of Experimental Botany* **66**: 6535–6549.

Yin X, Struik PC, Romero P, Harbinson J, Evers JB, Van Der Putten PEL, Vos J. **2009**. Using combined measurements of gas exchange and chlorophyll fluorescence to estimate parameters of a biochemical C3 photosynthesis model: A critical appraisal and a new integrated approach applied to leaves in a wheat (Triticum aestivum) canopy. *Plant, Cell and Environment* **32**: 448–464.

Yin X, Sun Z, Struik PC, Gu J. **2011**. Evaluating a new method to estimate the rate of leaf respiration in the light by analysis of combined gas exchange and chlorophyll fluorescence measurements. *Journal of Experimental Botany* **62**: 3489–3499.

Zhou S, Duursma RA, Medlyn BE, Kelly JWG, Prentice IC. **2013**. How should we model plant responses to drought? An analysis of stomatal and non-stomatal responses to water stress. *Agricultural and Forest Meteorology* **182–183**: 204–214.

Zhu GF, Li X, Su YH, Lu L, Huang CL. **2011**. Seasonal fluctuations and temperature dependence in photosynthetic parameters and stomatal conductance at the leaf scale of Populus euphratica Oliv. *Tree Physiology* **31**: 178–195.

Zhu X, Ort DR, Whitmarsh J, Long SP. **2004**. The slow reversibility of photosystem II thermal energy dissipation on transfer from high to low light may cause large losses in carbon gain by crop canopies : a theoretical analysis. *Journal of experimental botany* **55**: 1167–1175.

Zhu J, van der Werf W, Anten NPR, Vos J, Evers JB. **2015**. The contribution of phenotypic plasticity to complementary light capture in plant mixtures. *New Phytologist* **207**: 1213–1222.

Summary

Plant biomass is essential for guaranteeing many quality traits of ornamental crops, which are often grown in a greenhouse. However, variations in greenhouse conditions may occur, which may affect plant biomass production through affecting photosynthesis. First, variations in light intensity and spectrum occur in the greenhouse due to the use of supplementary lighting. Second, fluctuations in water and nutrient supplies could occur in low-tech greenhouses due to suboptimal crop managements. Third, canopy structure is often intensely manipulated in the greenhouse to optimize crop production. Therefore, to optimize crop photosynthesis (i.e., in terms of maximum assimilation or maximum resource use efficiency) in greenhouse conditions, photosynthesis responses at both leaf, plant and crop (i.e., the population of crop plants) level to the aforementioned conditions and their interactions need to be adequately understood. The aim of this thesis was to quantify photosynthesis responses to multiple greenhouse conditions, including the combined changes of photosynthetically active radiation (PAR) and red to far-red ratio (R:FR), water and nitrogen stress combinations, and plant structure manipulations (i.e., shoot bending in cut-rose production). To reach this objective, first experiments in greenhouses with cut-flower crops (lily and rose) were conducted to investigate plant responses (including responses in leaf photosynthetic traits and plant architectural traits) to changes in PAR, R:FR, water and nitrogen levels, and the presence of bent shoots. Then modelling studies were conducted to quantify photosynthesis responses to these conditions at leaf, plant and crop levels.

In the general introduction (Chapter 1), first I justified the importance of quantifying photosynthesis responses to multiple greenhouse conditions for ornamental crop production. Then I reviewed the current knowledge of photosynthesis responses to variations in light intensity, light spectrum, water and nitrogen conditions and changes in plant structure. Finally, I introduced the study approach of combining experimentation and modelling, and outlined the reasoning underlying the choices for the experimental systems and modelling approaches in this thesis.

In Chapter 2, photosynthesis responses to water and nitrogen stress combinations were quantified at leaf level in lily (*Lilium*. *auratum* × *speciosum*), using the photosynthesis model of Farquhar, von Caemmerer and Berry (the FvCB model) and the stomatal conductance model

of Ball, Woodrow and Berry (the BWB model). The changes of the FvCB model parameters due to variations of water and nitrogen conditions were linearly correlated with the changes of leaf nitrogen content per unit leaf area. These linear relationships were incorporated into the FvCB model to accurately simulate net photosynthetic rate in response to different water and nitrogen conditions. Most of the BWB model parameters needed to be adjusted specifically to water conditions (independent with the nitrogen level) to allow the model to accurately predict stomatal conductance.

In Chapter 3, plant functional trait responses to the combined changes in PAR and R:FR were quantified in rose (*Rosa hybrida*), and the consequences of individual trait responses for plant light absorption and photosynthesis under different levels of canopy shade were quantified using a functional-structural plant (FSP) model. At mild shade, functional trait responses to low R:FR were more important for plant photosynthesis, while at heavy shade, trait responses to low PAR became more important. Moreover, the consequences of individual trait responses for plant photosynthesis under shade tended to mitigate each other.

In Chapter 4, the contribution of bent shoots to plant photosynthesis in a heterogeneous rose canopy was quantified using a combination of experimentation and FSP modelling. In cut-rose production, weak and non-flowering shoots are bent downwards (the so-called bent shoots) to support the growth of upright flower shoots. Bent shoots contributed to 43% to 53% of the total assimilated CO_2 by the plant. The presence of bent shoots increased flower shoot dry weight by 35% to 59%, which was entirely due to the contribution of extra photosynthesis by bent shoots. At least 47% to 51% of the bent shoot photosynthesis was translocated to flower shoots to support their biomass increase.

In Chapter 5, the relationship between the presence of bent shoots and the R:FR ratio distribution in upright shoots was quantified, as well as the upright shoot architectural responses. Bent shoots reflected substantial amounts of far-red light and this lowered the R:FR ratio in light reflected upwards. The low R:FR reflected from below was associated with an increase of leaf inclination angle in upright shoots. The consequences of responses to R:FR from below for plant performance in terms of light absorption and photosynthesis were quantified using an FSP model. Responses to R:FR from below were beneficial for plant performance when the low R:FR was reflected by the lower part of the same plant canopy, as in this case, responses in the upper canopy allowed more light to penetrate to the lower canopy,

and thus increased whole-plant photosynthesis. However, when the low R:FR was reflected by independent foliage located below the plants, responses to this signal decreased plant light absorption and photosynthesis.

In Chapter 6, I outlined three main themes in this thesis and discussed the three main themes in the broader perspective of crop production. The three main themes were (i) the combination of multiple environmental factors, (ii) the upscaling of photosynthesis from leaf level to plant and crop level, and (iii) the application of the FSP model to do the upscaling. First I discussed the importance of studying plant responses to multiple environmental factors in combination. In this section, I proposed that understanding those plant responses requires not only understanding the mechanisms underlying those responses, but also quantifying the consequences of those responses for plant performance. Second, I discussed the need of upscaling plant performance from individual trait responses to plant and crop levels. In this section, I highlighted the importance of quantifying the consequences of individual trait responses for performance at both individual organ, plant and crop level, as trait responses that are not beneficial for performance at the organ level may beneficial at the crop level and thus favour yield production, and vice versa. I also discussed how different types of crop systems could lead to opposite directions for traits selections. Third, I introduced the FSP model as a useful tool to do the upscaling, and discussed the potential strength of further combining the FSP model with a detailed leaf photosynthesis model and a phylloclimate model. Finally, I discussed the implications for crop breeding and cultivation in the greenhouse and field.

Acknowledgements

Doing a PhD is not a lonely journey! Therefore, in the last pages of my PhD thesis, I would like to thank everyone who has involved in my four-year research work and accompanied me during my staying in Wageningen. I would like to start with thanking my three supervisors: Leo, Niels and Jochem. You are all great scientists with your own expertise, from which I benefit a lot. You are all very open-minded and give me the freedom to do the things that I am interested in, while in the mean time you guide me and provide suggestions to make sure that I am not doing nonsenses. I still remember that at the beginning of my PhD, you told me that I should be "the driver" and you are all passengers sitting on the back seats. I am happy that with the help of all my passengers, I made to the destination! I hope you can be proud of me, as I am very proud of my supervision team! Leo, you are a very responsible supervisor and always there when I need help. As a group leader, you must be very busy. But you hardly missed my supervision meetings and the meetings with Unifarm staff during my experiment. I really appreciate that a lot. Also thanks for being so patient to me when I was being emotional. Niels, I am really impressed by your knowledge of ecology. Every time after discussion with you, I got some new ideas. Although sometimes those were wild ideas that turned out to be I was thinking too much…… Niels, thanks for taking me to the ecology world as I am really having fun there! Jochem, you are always very supportive and open for a discussion! Your knowledge of functional-structural plant modelling and crop modelling really helps me a lot. Thanks for being so patient to me when I was bothering you about the basic questions on GroIMP and programming. To all of you, I truly hope that we can stay in touch and keep cooperation in the future. Maybe one day we can co-supervise PhD students!

I would like to thank my Chinese supervisor Weihong Luo in Nanjing Agricultural University (NAU). Luo, you supervised my Chinese PhD thesis and part of this thesis was used as Chapter 2 in my WUR thesis. We have known each other since 2010 in the last year of my Bachelor in NAU. I would never think of doing a PhD abroad if you had not encouraged me to do so in the first place. Eight years ago when I started my PhD in NAU, I was even not sure if I could finish my Chinese thesis, let alone write a whole book in English. But look at it now, I made it! I wrote two PhD theses, one in Chinese and one in English! I really appreciate your support

during my eight-year double PhD journey! Also thanks for your nice cooking during your visit in Wageningen!

I would like to thank Xinyou Yin and Yarong Qi. Xinyou, you are officially not my supervisor, but I think I went to your office as often as I went to my supervisor's. You are always there when I have questions on e.g., photosynthesis processes, modelling and plant physiology, or sometimes just questions on life as a scientist in general. You are a coauthor of my first publication. Thanks a lot for all your helps! Yarong, I really enjoyed those afternoons at your place when we had nice tea and chat. We both love reading books, and I especially enjoyed the time when we shared our feelings about books of Stefan Zweig! You and Xinyou have been so generous to me for inviting me to your house and making me feel at home. Thanks a lot!

I would like to thank Ep and Mariko. We first met on 2010 when you two visited Nanjing together. During my staying in Wageningen, you invited me to your farm every summer. Ep, it was a lot of fun to paint the old storage rooms together with you! Mariko, you always prepare very nice food when I was there for dinner! Ep and Mariko, you are a very nice couple with very lovely kids. I had a great time at your house and thanks a lot!

I would like to thank my two paranymphs Xixi and Arian. Xixi, I am so lucky to have you as a good friend. I really enjoyed our coffee breaks in Doppio when we talked about those difficulties we met during our experiments, data analysis or writing, or about life in general. I literally dreamed about the initial idea of writing my Chapter 5 after drinking two cherry beers with you in a bar at Wageningen centre. Arian, we did all the hard work together in the greenhouse. Measuring rose plants, which have lots of annoying thorns, during summer time in the greenhouse was not a very pleasant work. But lucky for us, we can at least think about that there is another guy who is suffering exactly the same thing as I am (just joking). You are the second author in three out of my four research chapters. I think this clearly states how important you are in my PhD project. Xixi and Arian, thanks a lot for standing by my side during my defence.

I would like to thank my Chinese colleagues and friends. 老季，刘老师，金总，忆菲，张雪，波哥，李桦，小寒，朱老师，杨宸尧，玉琪，婉菊师姐，文静姐，芳姐，小顾，旗哥，董蓓，王子申，方亮，昭君，浩子哥，旭哥，培育，薛老板，张怡，林正仪, I

was so lucky to have so many Chinese colleagues and friends around. This really makes me feel not so far away from home and less homesick. 何老师，于佳琪, thanks for helping me with the measurements! 学妹妹，贝勒爷, you are the first and only two master students that I supervised. Thanks a lot for your helps in the experiment. I had a great time working with you in the greenhouse. We are all very funny persons and like to make jokes. We triggered the alarm in Unifarm once, not because we finished our measurements too late, but because we were so happy that we finished our measurements, so we took many photos in our rose compartment and forgot about the time. Every time I think about this, I could not help to laugh! 大哥，阿汤，小师妹, we are from the same research group in NAU, it was so nice to have you around during part of my staying in Wageningen. 大哥, we travelled together to Spain. 阿汤, we travelled together to Paris. 小师妹, we travelled together to Switzerland. Thanks a lot for those nice trips! 一鸣，一丹，小熊玲玲，菜菜, I had a great time with you in those dinner parties, coffee breaks and trips when we all wear nice traditional Chinese cloths! Thanks! To my AiCU team members, 队长，李叔叔，老铁，星哥，白博, the autonomous greenhouse challenge was a new experience for all of us. What I enjoyed the most was the rice noodle every time when we had to drive to Eindhoven for a group discussion. 白博, thanks a lot for your helps with the programming and calculations in the last months of my PhD!

I would like to thank all my HPP colleagues. Faline, Elias, Arian, Priscila, Dorthe, Ana, Sara, Rachel, Evelien, Yutaka, Martina, Cristina, Fahrizal, Alejandro, Sharath and Maarten, because of you guys, the atmosphere of our PhD office is always nice and cozy. I enjoyed a lot for those lunch discussions in the coffee room and “gossips” in our PhD office. Sometimes we also talk about serious topics like our papers or experiments, which reminds us that we are young scientists who work on serious stuff. I really had a great time with you guys. Thanks a lot! Dorthe, thanks for organizing the champagne celebration for me even before the submission of my thesis. I really appreciate that! Menno, Joke, Arjen, Maarten, Jeremy, Wim, Rob, Julian, Sander, Tijmen, Theoharis, Dalia, Habtamu, Aina, Francisca and Pol, thanks a lot for the discussions in seminars or just a chat in the coffee place. Pauline, thanks for arranging my tickets, accommodations and reimbursement for all the conferences and workshops that I went to.

I would like to thank my CSA colleagues. Peter, thanks for helping me with the Licor measurements. Martin, Luuk, Ambra, Paulina, Franca, Jorad, Alejandro, Paul, Tjeerd, Wopke, Bob and Steven, thanks for the nice discussions in seminars, PFF meetings or just a chat in the coffee break. Ambra and Paulina, I had a nice trip with you in Lisbon! Martin, we started our PhD project on the same day, and I am happy that we both defend our thesis on the same year!

I would like to thank Unifarm staff Sean, Ad, Maarten and Geurt, and Bas. Thanks for taking care of my rose plants in the greenhouse. I would like to thank Dick vander Sar. Thanks for visiting Wageningen regularly, to check rose crop growth and greenhouse management, and to discuss my experimental data. Special thanks to Henry. Thanks for checking the English of my propositions just before the submission of my thesis!

I would like to thank my parents. You are very cool parents! You guide me, provide me suggestions, but never force me to do anything. Thanks for bringing me to the world and giving me the freedom to do the things that I want. Thanks for being so supportive! I would like to thank my younger sister. Thanks for accompanying our parents while I am away from home. You are an angel who always brings happiness to our family. I am really happy to have you around! 弟弟, our names and our parents' names are all extremely similar. It was like magic to meet you in Wageningen! It was so nice to have a "family member" here so I can feel free to cry when I was stressed by my thesis. Thanks for always being there for me!

Last but not least, I would like to thank myself. Thanks for never giving up and finally bringing me here. I hope in the future I can keep smiling and keep going! 不忘初心，砥砺前行！

Ningyi Zhang

May 2019, Wageningen

About the author

Ningyi Zhang was born on 17 February 1991 in Yongzhou, Hunan, China. She went to Nanjing Agricultural University (NAU) for Bachelor study on 2007. She obtained Bachelor of Agronomy in NAU on 2011. Due to her outstanding performance, she was directly enrolled in a five-year PhD project in NAU after her Bachelor study. In this PhD project, she focused on the effects of water and nitrogen on lily plants and modelled leaf photosynthesis responses to water and nitrogen stress combinations. On 2012, HortiModel conference was held in NAU and she was the conference secretary. In this conference, she had the opportunity to talk to the world leading scientists in crop modelling and horticulture. This conference triggered her interest to go abroad for further study. Therefore, on 2014, she applied for a scholarship from China Scholarship Council to go to Wageningen University. On March 2015, she arrived at Wageningen and started her second PhD project, which was under the cooperation of Horticulture and Product Physiology Group (HPP) and Centre for Crop System Analysis (CSA). In this PhD project, she focused on rose crop and quantified photosynthesis responses to light conditions and crop structure manipulations from leaf to crop level, using a functional-structural plant model. She defended her NAU PhD thesis on November 2016, and she will defend her WUR thesis on June 2019. At this moment, she is looking for a job that could allow her to stay in academia.

PE&RC Training and Education Statement

With the training and education activities listed below the PhD candidate has complied with the requirements set by the C.T. de Wit Graduate School for Production Ecology and Resource Conservation (PE&RC) which comprises of a minimum total of 32 ECTS (= 22 weeks of activities)

Review of literature (4.5 ECTS)

- Functional-structural modelling of horticultural plants

Writing of project proposal (4.5 ECTS)

- Optimizing canopy structure for improving ornamental crop production in the greenhouse

Post-graduate courses (6 ECTS)

- The art of modelling; PE&RC, SENSE (2015)
- Modelling plant form and function using GroIMP; PE&RC (2016)
- Basic statistics; PE&RC, SENSE (2016)

Invited review of (unpublished) journal manuscript (1 ECTS)

- New phytologist: Relationship between plant morphology and functioning (2018)

Competence strengthening / skills courses (2.8 ECTS)

- Presenting with impact; Wageningen in'to Language
- Scientific writing; Wageningen in'to Language

PE&RC Annual meetings, seminars and the PE&RC weekend (1.8 ECTS)

- PE&RC First year weekend (2015)
- PE&RC Day (2016, 2017, 2018)

Discussion groups / local seminars / other scientific meetings (7.5 ECTS)

- FLOP (Frontier Literature Of Plant Physiology) meeting (2015-2017)
- PFF (Plant Form and Function) meeting (2015-2018)

International symposia, workshops and conferences (9.0 ECTS)

- GroIMP Workshop; Ange, France (2015)
- Model-IT; Wageningen, the Netherlands (2015)
- FSPMA; Qingdao, China (2016)
- PEPG Workshop; Lisbon, Portugal (2018)

Lecturing / Supervision of practical's / tutorials (1.8 ECTS)

- Crop ecology (2015-2017)

Supervision of MSc students

- Rui Yin: the contribution of bent canopy to crop growth in cut rose (*Rosa hybrida L.*)
- Yuqing Huang: compensatory branching and leaf photosynthesis responses to bent-canopy removal in cut rose

The research described in this thesis was financially supported by China Scholarship Council (No. 201406850003), China Natural Science Foundation (No. 31171453), Netherlands Organisation for Scientific Research (No. 870.15.040), Signify and Glastuinbouw Nederland.

Cover design by Xiaodong Li

Printed by Digiforce | Proefschriftmaken.nl